UNCLASSIFIED

AD NUMBER
AD365804
CLASSIFICATION CHANGES
TO: unclassified
FROM: confidential
LIMITATION CHANGES
TO: Approved for public release, distribution unlimited
FROM: Distribution authorized to U.S. Gov't. agencies and their contractors; Critical Technology; MAY 1964. Other requests shall be referred to Office of Naval Research, Arlington, VA.
AUTHORITY
7 Apr 1967, per doc markings; ONR ltr,4 May 1977

THIS PAGE IS UNCLASSIFIED

UNCLASSIFIED

Office of Naval Research
Contract Nonr 4112(00)
Final Report II

365804

CLASSIFICATION CANCELLED UNCLASSIFIED
(OR CHANGED TO ______________)
BY AUTHORITY OF ONR LTR 3/23/67
(INDIVIDUAL OR WRITTEN AUTHORITY)
BY [signature] 4/7/67
(NAME & GRADE OF INDIVIDUAL MAKING CHANGE) (DATE)
RGB 65-11

Geophysics in Warfare

Report II

ANALYSES OF GEOPHYSICAL PHENOMENA

Douglas L. Brooks
Glenn R. Hilst
George H. Milly

May 1964
7862-119C

THE TRAVELERS RESEARCH CENTER, INC.

UNCLASSIFIED

DEPARTMENT OF THE NAVY
OFFICE OF NAVAL RESEARCH
WASHINGTON, D. C. 20360

IN REPLY REFER TO

462:FJK:em
Travelers/Nonr-4112(00)
23 Mar 1967

From: Chief of Naval Research
To: Administrator, Defense Documentation Center
(Data Control Branch - Mr. C. C. Becks)

Subj: Classification and Distribution Statement for the Travelers Research Center, Inc. report "Geophysics in Warfare - Report II: Analyses of Geophysical Phenomena (U)" - AD 365-804L; changes of

Encl: (1) Revised pages vii and viii of subject report

1. It is requested that the following changes be incorporated in the subject report:

A. Reclassify to "UNCLASSIFIED" upon:

1) Substitution of enclosures (1), O/C M Anderson 3 apr 67

2) Deletion of the word "CONFIDENTIAL" on front and back covers and pages v, vi, ix, x, 5 and 6,

3) Deletion on title page of time-phased downgrading statement "Group 3 - Downgraded at 12-year intervals; not automatically declassified."

B. Change item 2a of DD Form 1473 to "Unclassified."

C. Change Availability/Limitation Notice on title page and item 10 of DD Form 1473 to:

"This document is subject to special export controls and each transmittal to foreign governments or foreign nationals may be made only with prior approval of Office of Naval Research (Code 462)."

J R Marvin
J. R. MARVIN
By direction

Copy to: (w/encl)
Travelers Research Center
NRL (Code 4324)
NRL (Code 2020)

UNCLASSIFIED

Copy 40

of 74 copies

Geophysics in Warfare

Report II

ANALYSES OF GEOPHYSICAL PHENOMENA (U)

by

Douglas L. Brooks
Glenn R. Hilst
George H. Milly

This doc. is subject to special export controls & each transmittal to foreign Govts. or foreign nation: is may be made only with prior approval of Office of Naval Research (Code 462)

May 1964
7662-119C

"This document contains information affecting the National Defense of the United States within the meaning of the Espionage Laws, Title 18, U. S. C., Section 793 and 794. Its transmission or the revelation of its contents in any manner to an unauthorized person is prohibited by law."

~~U.S. military agencies may obtain copies of this report directly from DDC. Other qualified users shall request through the Office of Naval Research, Code 493.~~

~~GROUP~~
~~Downgraded at 12-year intervals, not automatically declassified~~

THE TRAVELERS RESEARCH CENTER, INC.
250 Constitution Plaza Hartford, Connecticut 06103

UNCLASSIFIED

ABSTRACT

This report presents the results of a scientific analysis conducted as part of a one-year survey of geophysics in naval warfare conducted for the Office of Naval Research by The Travelers Research Center, Inc. In the main study, reported separately and entitled Geophysics in Warfare, Report I—Geophysical Factors in Naval Warfare (U), the scientific feasibility and military significance to the Navy and Marine Corps of exploiting a large range of possibilities for either geophysical prediction or control are systematically explored and recommendations for the most fruitful follow-on programs are provided. In this report, (Report II), details of the scientific analysis of feasibility of control of a number of geophysical phenomena are presented. In addition, there are presented the theoretical aspects of evaluating the utility of prediction and control in operations affected.

FOREWORD

Because the scope and findings of this study have implications for many users, the study has been documented in two reports; these reports have separate security classifications, distribution lists, and applications. Following the Table of Contents of each report there is a list of sections and appendixes that appear in the complementary report. Note especially that Sections 3.0 and 4.0 of Report I - Geophysical Factors in Naval Warfare (U) comprise the entire basic text of Report II - Analyses of Geophysical Phenomena. (U).

TABLE OF CONTENTS*

*This is Report II of a two-report series. For an explanation of its contents and format, see the Foreword, page iv.

SUMMARY

This is Report II of a two-report series which summarizes the results of a one-year study of the possibilities for exploiting the prediction or control of geophysical phenomena in naval and marine warfare.

More than two hundred fifty geophysical factors were considered capable of affecting in some degree about thirty-four major Navy and Marine Corps missions. Many of these factors exhibited several distinct facets or stages, each of which had its own unique military significance. Practical limitations in time and funds required that detailed feasibility studies be limited to those factors of highest potential military importance and technological promise. Although a quasi-objective methodology was developed for this selection process, budget limitations again precluded its use and a qualitative judgmental procedure, which included ONR review, was used instead.

The thirty-four geophysical phenomena and situations selected as of greatest potential military significance were examined in detail for scientific and technological feasibility both of prediction and control. The energy budgets and conversion processes associated with each were studied quantitatively, and the most likely modification opportunities identified, considering the kinds of energy resources available to technology during the next five to fifteen years.

Similarly, the predictability of each phenomenon by both statistical and analogue, or dynamic, techniques was assessed, and the extent to which present techniques have succeeded in exploiting this predictability were reviewed. Considerable scope for extending and improving present methods was revealed and the most promising avenues for advance were specified.

Since the conclusions of the study with regard to military importance depend so strongly on qualitative reasoning and judgment, care has been taken to document both the geophysical analyses which served as inputs and detailed descriptions of the evaluation methods used. It is believed the geophysical analyses represent a more comprehensive survey of the scientific considerations underlying prediction and control than is available elsewhere in the literature and

will support continuing evaluation of novel geophysics-in-warfare concepts that may materialize in the future. The detailed analyses supporting prediction and control potentialities are presented in this report.

UNCLASSIFIED

3.0 ANALYSES OF GEOPHYSICAL PHENOMENA

Since the dawn of time, man has had to contend with the variabilities of the environment of earth, air and water which is his natural endowment and the source and sustenance of his existence. On balance, he has contended very successfully, but generally by an adaptive and protective technique, the control of these phenomena being ascribable only to omnipotent dieties and therefore beyond the considered manipulation of mere mortals. Earthquakes, floods, coastal inundations, hurricanes, tornadoes, thunderstorms, droughts, these things happen, and there's not much one can do but protect oneself and one's property, or move on to more benign surroundings.

This attitude is literally the result of millenia of experience, observation and action—and in point of fact, is appropriate in a very large measure to the world in which we live today. Significant as man's efforts are to control floods, redistribute water for agricultural purposes, and construct earthquake, wind, water, and temperature proof buildings and shelters, he has now only the slightest influence on the geophysical processes which plague and sustain him.

But what about the future? Are significant geophysical phenomena beyond man's control? Are they so complex, large and energetic as to defy any manipulative techniques man may be able to control and afford? The answers to these questions are not available for the vast majority of those geophysical phenomena which are significant to man's survival and advancement. But, more important, we are now reaching the point where these questions can be asked with candor, and objective answers can be sought. The feasibility of control (and by feasibility we mean successful control by means within the resources available to men) can only be assessed when an objective, quantitative evaluation of the mechanisms which produce, sustain and destroy these environmental events is at hand. The desirability of control is a

social, economic and operational problem, assessable only in terms of the effects such control ca. produce and the relative worth of these effects compared to the cost of control or alternative methods.

The present study recognizes this whole gamut of interests in the control of geophysical phenomena within the operational context of future naval systems. As has been described previously, the choice of interactions between naval operations and processes within the natural environment in which these operations occur has been deliberately and strongly constrained so that analyses in depth could be performed. Beyond this constraint, the studies reported in summary form in this section (and in detail in Volume III) were conducted without regard for specific applications to naval operations. Their naval implications will be considered in Sections 5.0, 6.0, and 7.0.

3.1 Methods of Analyses

The analyses of geophysical phenomena, which constitute phase II (see Section 1.2.1) of this study, have been designed to systematize information on three major facets of these phenomena as they pertain to feasibility of control or modification:

(a) systematic delineation of the scale (in time and space) of a phenomenon,

(b) detailed descriptions (kinematics) of the phenomenon and, as far as possible, quantitative and rigorous statements of the dynamics and energetics of the phenomenon, and

(c) analyses of the kinematic, dynamic, and energetic descriptions of the phenomenon for potential control or modification techniques and/or improved prediction methods.

Because of the complexity of geophysical phenomena in general, it was recognized from the outset that incomplete descriptions and large uncertainties would be the rule rather than the exception in the results of these studies. However, it was also evident that systematic, knowledgeable appraisals, done with complete candor and integrity, would yield valuable and useful summaries of what is known, and would identify those areas in which the lack of knowledge is critically detrimental

to full exploitation of geophysical phenomena in naval operations.

To assure objectivity and efficiency in these analyses, senior scientists were assigned individual phenomenological analyses in their areas of greatest competence. The general purpose of these analyses was described to them, but the importance of scientific objectivity was emphasized. The following outline of the analysis was given for uniformity of approach and format, but each scientist was given considerable latitude in its use, to assure the clearest presentation consistent with his particular subject assignment.

3.2 Outline for Selected Phenomena Analyses

A. General Description
  1) Phenomena types
  2) Characteristic geographical extent
  3) Characteristic process and property involvement
    (a) Basic forces
    (b) Modifying factors
    (c) Property transports
  4) Characteristic variations (life cycle)

B. Assessment of Geophysical Forces
  1) Basic physical equations
  2) Force analysis
    (a) Order-of-magnitude
    (b) Horizontal-scale
    (c) Vertical-scale
  3) Characteristic structure

C. Assessment of Geophysical Energy
  1) Energy budget
    (a) Storage estimates
    (b) Transformation-rate estimates
    (c) Dissipation-rate estimates

2) Instabilities

D Modification or Control Feasibility

1) Force and/or energy interference

(a) Direct

(b) Indirect

2) Promotion or suppression of critical conditions

3) Survey of simulation and predictive capabilities

(a) Theoretical

4) Research required for further control or modification feasibility assessment

(a) Theoretical

(b) Experimental

(c) Observational

Against this general background of requirements and format, each scientist was given complete freedom to survey the state of knowledge in his assigned problem area, consolidate and quantify this knowledge and assess from an objective, physical basis the feasibility of modification or control of that phenomenon. In addition, and as a natural corollary of these analyses, an assessment was made of the predictability of the phenomenon.

In several instances, control and modification feasibility could be assessed directly on the basis of energy requirements and logistics. However, much more frequently this decision had to be qualified by a recognition of inadequacy of knowledge and the need for further research before any confident statement could be made. This was, of course, one of the purposes of these analyses, namely to pinpoint wherever possible areas of uncertainty and ignorance which must be removed before progress could be made in any deliberate attempt to modify geophysical phenomena.

3.3 Analyses Completed

The following analyses of geophysical phenomena, or important geophysical properties which are alterable by geophysical processes have been completed.

TABLE 3-1

GEOPHYSICAL PHENOMENA ANALYSES

Topic	See Section	Analyzed by
I. Geological environment		
Earthquakes	3.4.1	R.M. Jorden
Surface and ground water	3.4.2	R.M. Jorden
Soil trafficability	3.4.3	R.M. Jorden
II. Atmospheric environment		
Atmospheric turbulence	3.4.4	K.D. Hage
Hurricanes	3.4.5	K.W. Veigas
Thunderstorms	3.4.6	E. Kessler and P. Feteris
Lightning	3.4.7	V.J. Schaefer*
Air mass formation and cyclogenesis	3.4.8	D.L. Cooley and F. Sanders*
Clouds and precipitation	3.4.9	E. Kessler and J. Wilson
Fog	3.4.10	K.D. Hage
Boundary layer winds	3.4.11	J.L. Pandolfo
Ionospheric phenomena	3.4.12	P. Harteck* and J.L. Pandolfo
Ozone	3.4.13	V.J. Schaefer*
Electromagnetic propagation	3.4.14	B.M. Herman*

* Consultants to TRC

TABLE 3-1 (continued)

Topic	See Section	Analyzed by
III. Oceanographic environment		
Surface waves	3.4.15	J.L. Pandolfo
Internal waves	3.4.16	R.G. Harris
Surface currents	3.4.17	W.L. Gates
Internal currents	3.4.18	W.L. Gates
Tsunami	3.4.19	W.L. Gates
Oceanic turbulence	3.4.20	W.L. Gates

In addition to these studies, consultations were held with Drs. Allyn Vine and Arthur Voorhees at the Woods Hole Oceanographic Institution (WHOI) regarding environmental effects on underwater sound propagation. It was apparent from these discussions that very extensive programs of analyses and research are underway at WHOI and elsewhere and any attempt to survey this important problem area in depth in the context of the present program would be redundant.

3.4 Summary of Geophysical Analyses

3.4.1 Earthquakes

Recent technological developments suggest methods for detection of the areas of accumulation of tectonic strain which may be released by overt high-energy inputs, such as the detonation of nuclear devices. Results of underground detonations by the AEC confirm the feasibility of release of tectonic strain by this method, but the "free energy" realized has been quite small.

The feasibility of detecting areas of tectonic strain in unfriendly or alien territories is very marginal and will probably remain so. Offensive use of this technique is equally subject to lack of surreptitious modes of operation. From a defense point of view, further research on the detection of vulnerable areas, so as to isolate or obviate significant damage, appears desirable.

3.4.2 Surface and Ground Water Hydrological Processes

The multiple roles of water, in the ecology of plants and animals, in the energetics of atmospheric motions on all weather-producing scales, in industrial activities of all kinds, in transportation, recreation, and in geological processes of erosion and transport, all point to the importance of consideration of water in the context of the geophysical environment.

Attention is turned here to two important geophysical processes, 1) evaporation of surface waters, and 2) the hydrology and geology of stream bed alteration.

3.4.2.1 Evaporation Suppression

A review of the work done to date shows that following the initial concepts of evaporation suppression by some eight different methods, major attention has been directed toward the use of monomolecular films over open water surfaces. The efficacy of significant reductions of evaporation over small, fresh water surfaces has been clearly demonstrated. Major problems which remain are,

(a) Prevention of disruption of the film by wave action.

(b) Maintenance of the film against the "sweeping" action of surface winds greater than 15-20 mph.

(c) Extrapolation to large areas and to saline water surfaces.

The last problem appears to be the most serious since the one laboratory study which has been completed tends to show an adverse chemical effect due to salt which is at a maximum when salt is at concentrations normally found in sea water.

The effects of waves and surface winds on the disruption and removal of monomolecular films appear soluble at this time. Mixtures of stearyl and cetyl alcohols should provide maximum self-healing and evaporation suppression. In addition, the possibility of simultaneously producing a surface oil film which selectively suppresses small-scale waves can be considered (see Section 3.4.15 for an analysis of wave suppression techniques).

The logistics and technological feasibility of evaporation suppression by monomolecular films can be judged by the estimate of 0.2 to 0.4 lb acre^{-1} day^{-1}, or between 128 and 256 lb mi^{-2} day^{-1}. For small and medium size lakes (10-100 mi^{2}),

no particular problems of practicality arise. Problems arising from attempts to alter evaporation over millions of square miles of ocean surface appear formidable.

3.4.2.2 Stream Bed Alteration

The natural diversion of rivers from one stream bed to another is well established and, in the case of the lower Mississippi, the effects of erosion, siltation and altered flow rates due to such a change (partly man-made) has been well studied. Denial of ports, changes in navigability and ultimately dramatic changes in water supply could be achieved by artificial diversion of rivers. In general, the technological feasibility of such an operation depends upon the pre-existence of an alternate stream bed separated from the present bed by modest land barriers which could be removed by high explosives. It is believed many such situations exist and could be identified from available topographic and hydrologic maps.

3.4.3 Soil Trafficability

Present knowledge of soil trafficability (the ability of a natural soil surface to sustain a compressive load and traction) is highly empirical and incomplete. The resume in Appendix T points clearly to the environmental parameters which affect soil trafficability (principally rainfall or local moisture content) but much more definitive knowledge of the multiple effects of soil parameters is clearly required before optimum modification and control (by other than tried road building techniques) can be developed and assessed.

3.4.4 Atmospheric Turbulence in Relation to Structural Damage

Atmospheric turbulence pervades all facets of geophysical phenomena within the atmosphere and at the earth-air and air-sea interfaces. The importance of turbulent transfer processes can hardly be overestimated, and, without a doubt, man's ability to control and modify atmospheric and interface phenomena will be greatly extended when he understands the subtleties and criticalities of these extremely complex processes.

In order to focus attention (and constrain the very broad range of scales at which turbulent processes operate) the specific effect of atmospheric turbulence

on structures is singled out for consideration here. This permits consideration of the controlling features of the structure and intensity of turbulence in the frequency range from 0.5 to 50 cycles/hr. In keeping with the purpose of this study, however, emphasis is directed to the controlling features of turbulent transfers of momentum exercised by the fluid state rather than the mechanisms of structural damage.

The analysis presented in Appendix K clearly points up the role of vertical motions in sustaining turbulence and the critical role of surface roughness, wind shear, and thermal (or density) stability in turbulent transfer processes. Because of the complexity of the interaction of driving forces (pressure gradients, buoyancy) and turbulence generation by instabilities of fluid flow, obstacle perturbations, etc., present knowledge does not permit a clear definition of how one might significantly alter either the scale of these turbulence elements or their intensity. Yet it is well known that natural variations of only a change in sign of the vertical lapse rate of temperature have a profound effect upon both of these parameters of turbulence and the resultant momentum transfer rates. Modification of stability by surface modification (albedo or direct heating and cooling) will have an effect, but more research is required to specify the extent and optimum methods.

3.4.5 Hurricanes

Studies of the description and dynamics of hurricanes have advanced our knowledge of this important phenomenon steadily, particularly since the advent of radar, aircraft surveillance and penetration. Simultaneously, developments in dynamical and statistical prediction techniques have also made possible better forecasts of the movements and developments of mature hurricanes.

The greatest lack of knowledge, and the most significant from the viewpoint of control or modification, is in the area of hurricane formation. As pointed out in Appendix G, our knowledge here only permits us to define areas where hurricanes will never form. But early detection of successful, imminent hurricane formation (so necessary to successful modification in this crucial period) is not now within our means. These means may develop, however, and the real possibility for prevention of hurricanes by interference in the energy transfers and organization of circu-

lations in the formative stage is a strong motivation for continued intensive observations and research. (As is true of so many geophysical processes and phenomena, one may reasonably ask, "If we shut off hurricanes, what other mode of energy, heat, and material (water vapor) transfer will nature utilize—and will this mode be more or less benign than hurricanes?" At present we can only defer this as a second-generation question!)

Modification of hurricanes by interference with the energy sources, sinks and transfer modes, particularly by interference in the condensation-evaporation processes, is feasible but at present of uncertain effect. Similarly, sea surface temperature alterations, by heating, cooling, or mixing, should have a strong effect but are technologically and logistically staggering operations.

It would appear the significant modification of hurricanes will ultimately be within man's capability but the best path to full assessment of the feasibility and results of such control is through much-improved mathematical analogues of hurricane dynamics and observational studies of their nascent stage.

3.4.6 Thunderstorms

The energy budget of a single cell convective storm has been described by Braham [3] in terms of the following energy sources and sinks.

Energy sources are:

(a) the released heats of condensation and fusion,

(b) forces of gravity acting on cold air in the downdraft during the precipitation stage of the cloud.

Energy sinks are:

(a) increases in internal and potential energy of the environment,

(b) energy expended in lifting water particles,

(c) work done in separating electrical charges which discharge to ground,

(d) friction.

The difference in energy between the sources and sinks, which is an order of magnitude smaller than the total energy involved in either category, appears to be very sensitive to small changes in temperature lapse rate and moisture content of

the environment air. Slow, large-scale vertical motions are also likely to alter profoundly the work done against the environment by a convective cell.

Under some circumstances, a deficit of the released heats of condensation and fusion with respect to the energy sinks can be overcome by adding an amount of sensible heat. Dessens succeeded in triggering a shower in a conditionally unstable atmosphere by producing 9×10^{11} calories over an area of 25×10^{4} m^{2} in 30 minutes. Rapid heating or forcing the air to rise will result in more efficient production of convective clouds and showers than slow heating, since in the latter case the convective condensation level will be much higher than the lifting condensation level in the former.

A more harmless method of triggering convection may be to cool the air in a low level inversion layer by evaporating water into it. In this case, the atmosphere needs to be potentially unstable.

The amount of water required to saturate the lowest 2.5 km of the atmosphere over an area of 2 km diameter in a maritime tropical air mass would have to be of the order of 20 m^{3}. This water would have to be distributed very rapidly over the whole volume in the form of very tiny droplets.

It must be emphasized that these consideration serve only to give an order-of-magnitude estimate of the energies necessary to trigger the development of a large convective cloud in conditionally unstable atmosphere. The dynamical implications and the technical problems involved in starting convective circulations require much further study.

3.4.7 Lightning*

The possibility of manipulating lightning discharges has been considered by many individuals. Until recently, the main interest was speculative. Several industrial concerns, notably General Electric and Westinghouse, have had high-voltage laboratories for the study of protective devices for switchgear power transmission lines and related materials.

Within the past few years, three different efforts have been organized to determine what, if anything, could be done to modify or attract lightning.

---

* Communication from Vincent J. Schaefer, State University of New York, Consultant.

Vonnegut, Moore, and Brook, using a wire carried by a rocket, attempted to "draw down" lightning at the summit of Mt Withington, N. M. This approach was devised after it was found that a stable conductor carried into a thunderstorm would not "attract" lightning. Rather, it was found (using the Van de Graaf high-voltage generator at the Boston Museum of Natural Science) that a discharge could be induced only by the sudden introduction of a grounded wire into the neighborhood of a highly charged sphere. Attempts to do this with a small rocket on Mt. Withington have been made but have been frustrated by problems related to unreeling the grounded wire.

Newman, using the same approach but on shipboard, claimed success at the Montreux, Switzerland, meeting last spring. The papers presented at this meeting are soon to be published under the editorship of Sam Coroniti of AVCO. He has a mobile laboratory on a seagoing vessel and has mounted a very ambitious research program centered about the induction of natural lightning.

The Forest Fire Laboratory developed a field station at Phillipsburg, Montana, to study the possibility of modifying thunderstorms by cloud seeding. To establish statistically significant results, four airborne silver iodide generators fly below clouds moving over the station's network, seeding or not seeding the clouds on a randomized pair-selection basis. Although results showing statistical significance have not been established, the seeded clouds tend to show less cloud-to-ground lightning than the unseeded unit of the pair.

The Nature of Ball Lightning, a book to be published in 1964 by the Plenum Press, available from Consultants Bureau, 227 West 17th Street, New York, N.Y., 10011, may have interesting information. It will include the studies of Kapitsa, Barat and Yutkin and will consider the speculations "on the application of ball lightning to weapons, nuclear power, etc."

3.4.8 Air-mass Formation and Cyclogenesis

Much of the larger scale "weather" which affects man's activities, such as precipitation and cloudiness, wind, and temperature extremes are directly associated with the formation, movement and life history of low- and high-pressure areas. The primary role of these migratory pressure centers is to transport heat and moisture in some optimum fashion between the differentially heated equatorial and polar zones. The resultant patterns of motion, temperature contrasts, and moisture (water vapor) produce the "weather" phenomena mentioned previously.

Analysis of the energy content and transfer, the dynamics of these systems and observational summaries of land-water, mountain and surface effects on preferred regions of pressure center development show quickly that these pressure centers are not isolated, closed systems. Rather, they are interdependent, constantly evolving systems which must be treated in their entirety, i.e., on a global or at least hemispheric basis.

Because atmospheric systems are generally in a quasi-equilibrium stage, major effects (insofar as cyclogenesis is concerned) frequently stem from what appear to be minor perturbations. A considerable theory has been built on this concept and the analyses of instabilities for small perturbations in baroclinic fluids. An analysis of the dependence of the growth of cyclones on the stability and motion stratification of a large volume of the atmosphere, and the inadequacies of present theories of baroclinic instabilities, preclude any definitive promise of control of these processes by interference at a logistically and economically feasible level in the formative stage of incipient cyclones.

Dr. Sanders and Dr. Cooley also point out the considerable freedom nature exercises in her choice of transfer mechanisms and the resultant combinations of motions, only some of which lead to classical pressure-center formations. In common with analysts of other phenomena, they, also, point out that successful interference at one locality or level may induce compensatory developments at another level or place, and that these are not now predictable.

Given successful research on the "triggering" mechanisms for cyclonic development (or accelerated air-mass modification) and understanding of the subsequent fluid motion developments, the feasibility of control during the incipient stage appears probable. Major modification of well-developed synoptic scale systems is not probable, however.

3.4.9 Clouds and Precipitation

The development of the kinematics of clouds and precipitation is reported here (see Appendix F) as the basis for a general survey of the probable points of interference and modification in the natural processes of cloud and precipitation phenomena. Appendix H is, in turn, a survey of various cloud and precipitation modification techniques which have been proposed and, in some cases, experimentally tested.

Because of the significant and all-pervading influence of the transport and phase changes of water substance in the atmosphere and in the hydrosphere, and the strong consequences of precipitation, attention has been strongly focused on the possibilities of significantly altering natural cloud formation and precipitation processes. For this reason, this facet of geophysical control is perhaps more advanced than any other. The effects of local seeding of supercooled stratus clouds has been clearly demonstrated. A significant increase of precipitation in selected regions by similar techniques appears to be conclusively demonstrated. At the same time, however, more general control capabilities, such as thunderstorm suppression, wide-area ($> 10^5$ km^2) modification of precipitation, etc., are openly disputed and must be viewed as open questions of feasibility today.

Dr. Kessler's analysis points clearly to the major processes of cloud formation and precipitation which must be understood and which provide entrees to possible control. These are:

(a) The magnitude and areal extent of the vertical motions of the atmosphere,

(b) The rate of condensation of water vapor,

(c) The size distribution of cloud droplets and their dependence on nuclear and condensation rates,

(d) The growth of cloud or initial precipitation elements by condensation, coagulation, and accretion.

Interference in the basic vertical velocity patterns and the moisture (vapor) content of the air involve large-scale circulations and trajectories discussed in Section 3.4.8 and Appendix E. If attention is focused on the micro-physical parameters, the effects of altering drop size (by nuclei control, for example) and cloud conversion and accretion rates could be significant on several scales. For example, precipitation downwind of major mountain ranges could be increased (at the expense of windward precipitation). Similarly, successful large scale modification of drop size and growth characteristics could have significant effect on latitudinal temperature structure and the resultant global circulations.

The logistics and technological feasibility of cloud and precipitation modification on the micro- and meso-scale are well within the state-of-the-art today when seeding with chemically or thermodynamically active materials is considered. Significant alterations of nuclei or active agents on larger (say, continental) scales are not so obviously feasible and depend largely on better understanding of the critical role of these agents in cloud and precipitation processes. With these reservations, the prospects for significant control appear excellent.

3.4.10 Visibility and Fog

The limiting effect on visibility of suspended particulates or droplets depends upon the number and size of the suspensoids, the wavelength of illumination, the background illumination, and response and resolution of the eye or sensing instrument. Of these, the primary variables subject to control are the number and size of the suspensoids. Various methods of modifying fog droplet concentrations and sizes have been proposed and the feasibility of modifying these very significantly, in a local area such as an airport runway, has been confirmed. Such modification, as by heating, hygroscopic material, or freezing nuclei seed (for supercooled fog) is generally costly or highly restricted in application.

Attention is turned here to another technique; i.e., clearing by accretion on optimum-sized artificial spray droplets. The analysis of this technique (Appendix I) needs experimental verification, but it appears to be technologically feasible, from all points of view except one. This exception is the technology of spray or droplet production, probably through relatively high-capacity nozzles.

Further development of systems for temporary improvement of visibility over areas the size of approach zones and carrier or land-based runways appears to hold significant potential for operational usefulness.

The reduction of visibility near the surface by artificial means has long been an operational capability. Artificially generated aerosols are customarily employed and appear to offer advantages in terms of availability and relative insensitivity to atmospheric conditions.

3.4.11 Boundary Layer Winds

The variability of wind velocity profiles with height, in the zone from the surface to the gradient wind level (1500-2500 ft) has been studied extensively for several decades. Interest in this phenomenon stems primarily from the role such shear zone (and the turbulent exchange it represents) plays in the vertical transfer of momentum, heat, and water vapor between the earth's surface (including the oceans) and the atmosphere. Interest is also generated by the operational consequences of wind shear and turbulence, including hazards to aircraft and the dispersion of extraneous materials.

The systematic analyses of mechanisms of transfer of momentum and the energy storage and transfer rates in Appendix J lead to the conclusion that direct interference in the larger-scale pressure gradients which drive these winds is feasible only to the extent large-scale pressure systems can be modified (see Section 3.4.8). Similarly, "brute force" interference in the turbulent energy content (and thereby the diffusivity) of the boundary layer by heating is largely unfeasible due to large energy source and expenditure requirements (10^4 to 10^5 tons of coal per km^2 per 3 hr).

Indirect interference by way of modification of the surface heat capacity or reflectivity, or by warming or cooling of the atmosphere near the top of the boundary layer may be feasible. These modifications of stability are particularly crucial in vertical exchange processes and are achieved at much smaller expenditures of energy. Alterations of surface albedo appear most promising but require quantitative testing for further information on their effectiveness and their secondary effects or on alternative modes of momentum exchange which the atmosphere might utilize.

3.4.12 Ionospheric Phenomena

For the purposes of the present study, attention has been focused on photoluminescence and partially self-regenerative chemical reactions which might be initiated at will. Professor Paul Harteck, R.P.I., contributed these concepts and analyses, included in Appendix L. The earlier intention of exploring modification of the electrical charge density and distribution in the ionosphere was suppressed when we learned, in consultation with Professor John C. Johnson, Worcester Polytechnic Institute, that a very substantial effort is underway in the U.S. Air Force and that our analyses would be redundant.

The existence of the chemosphere and man's ability to trigger light-producing chemical reactions by introduction of materials into this region has been known for at least eight years. The major concern here is the control of intensity and duration which might be achieved by the use of various materials, introduced into the chemosphere over a sizeable area. Among the materials which produce suitable photon emissions in the visible portion of the spectrum, and are partially regenerative, is aluminum ($Al[CH_3]_3$ is a particularly suitable form). Professor Harteck's estimates indicate that, conservatively, 7.2 tons of $Al[CH_3]_3$ spread uniformly over an area of 10^4 km^2 could produce several hours of illumination at ten times the intensity of moonlight.

The logistics of delivery of this much material to altitudes around 120 km by suborbital, rocket-propelled vehicles appears to be well within the state of the art.

3.4.13 Ozone*

The presence of a zone of ozone within the 24-26 km level is well established and has been the subject of extensive studies for many years. A currently operating network of sounding stations makes weekly ozonesonde ascents. One of these stations is at Colorado State University. These soundings utilize the Regener chemiluminescent ozone detector, which seems to be quite reliable.

In addition to the maximum concentration that occurs in the stratosphere, a secondary peak has been found in the region of 10-15 km. This at times may be of sufficient concentration to pose problems for passengers on jet transports. The problem may become more serious in the supersonic jets, since it may be necessary for them to fly in the higher ozone region.

Dr. Regener's program at the University of New Mexico, Albuquerque, makes routine observations and comparative studies.

Kofsky has given consideration to the effects that might occur at the earth's surface if the natural ozone layer is disrupted by the production of ultraviolet photons emitted from a nuclear burst [4].

The conclusion reached in this study is that the ozone in the 10-40 km (level) reforms so rapidly that only a negligible addition of ultraviolet from the sun would reach the earth under clear sky conditions. At higher levels, however, the O_3 does not reform for several hours. The concentration at these higher levels is not of much consequence except for the role it might play in producing air glow if this is caused by the reaction of ozone and hydrogen atoms.

3.4.14 Electromagnetic Propagation

In traversing the atmosphere, electromagnetic energy is subject to absorption and scattering due to pressure, temperature and humidity variations in the atmosphere. In addition, atmospheric gases also emit electromagnetic energy in selected wavelengths. The primary atmospheric variables are:

* Communication from Vincent J. Schaefer, Consultant.

(a) Particulates or droplets (size and number),

(b) Water vapor distribution,

(c) Temperature distribution,

(d) Density of gases (atmospheric).

In addition, there is a strong dependence, insofar as attenuation and scattering are concerned, on the wavelengths of the electromagnetic energy itself. Ability to alter significantly the propagation of electromagnetic energy, given the source wavelength and intensity, depends upon ability to alter the gaseous constituents of the atmosphere, the density of water, the temperature distribution and the concentration, size and distribution of particulates or droplets.

The volumes of the atmosphere which must be subjected to such alterations depend upon the range of propagation to be affected and the discontinuities or steepness of gradients which can be induced. Generally speaking, however, these volumes are large and techniques such as addition of water vapor or particulates, or large-volume heating and cooling, are technologically infeasible. More subtle alterations due to cloud seeding (for droplet production), surface albedo changes, and evaporation suppression or enhancement will, if successful, have an effect in this area, also.

3.4.15 Surface Waves

The generation of surface waves on the oceans is related to the momentum transfer between the atmosphere and the ocean and the temporal growth and stability of surface waves under prolonged and varying momentum transfer rates. The major energy source for wave development is, of course, the large-scale wind systems considered in Section 3.4.8. Interference or modification on this scale is not feasible.

The momentum transfer mechanisms, or eddy-diffusivity coupling between the atmosphere and the ocean, do offer two potentially feasible means of control or modification on the length scale from tens to thousands of meters. The first of these is through surface-tension modification. Oil slicks or other near-monomolecular films, less dense than sea water and having the important property

of increased surface tension with increased lateral deformation (stretching), are selectively effective for damping small-scale waves. Since the momentum transfer to the sea surface depends upon the slope of the waves, and this slope is greatest for short wavelengths, the slick partially decouples the atmosphere and ocean, reducing the wave build-up rate.

Similarly, debris (logs, mud, ice) dissipates the orbital wave motion and suppresses wave height. Slicks and debris appear to be feasible methods of altering local wave generation and moderate-to-small waves significantly. Neither is apt to be effective in a fully developed sea, generated over long (and uncontrollable) wind fetches.

An indirect method of control, found in common with other phenomena involving turbulent transfer processes, is limitation of the vertical turbulent energy-transfer rate in the atmospheric boundary layer. In the present context, large-area surface temperature and heat storage capable of modifying the thermal stability of the surface layers of the atmosphere could significantly alter surface wave formation. Feasible methods for accomplishing this are not now known but may appear out of future research.

3.4.16 Internal Waves

A summary of existing knowledge of the structure of internal waves, the forces that are believed to generate them, and their dependence on density discontinuities or gradients, ocean depth, and ocean bottom slope is presented in Appendix P. The operational implications of relatively slow moving (0.1-4 knot) waves with amplitudes of up to the order of 100 ft and widely varying wavelengths are pointed out, but the lack of systematic observational data, and realistic theoretical models tested against such data, preclude quantitative assessment of the energy budgets and dynamics of such systems. Areas of potentially fruitful research are delineated, with emphasis on the need for adequate quantitative measurements under varying conditions of tidal and surface-wind stresses, barometric pressure, ocean depth, and bottom contouring.

3.4.17 Surface Currents

Surface ocean currents are a permanent large-scale feature of the world's oceans and are driven by the stress of the large-scale atmospheric wind field. Extending over a few hundred meters' depth, the surface currents' kinetic energy totals approximately 10^{17} cal, with energy transfers of the order of 10^{12} cal sec^{-1} to the kinetic energy of internal currents. Energy dissipation by internal eddy viscosity and by bottom friction are also of the order of 10^{12} cal sec^{-1}. Unestimated are the possibly significant energy transfers between both surface and internal waves.

Direct modification of surface ocean currents is not feasible, and indirect modification by alteration of the surface stress or change of water depth or boundary configuration is feasible only on a local (and transitory) basis. Large-scale stress or topographic modification appears unfeasible not only from an energetic viewpoint, but also because it would doubtless have unforeseen results on both the oceanic and atmospheric circulation. Much further research is needed on the general problem of sea-air interaction and on oceanic dynamics before even an estimate of these effects could be made.

3.4.18 Internal Ocean Currents

The internal ocean currents consist mainly of the thermohaline circulation driven by the large-scale distribution of the heat balance and evaporation-precipitation regime at the sea surface. We may also include the system of equatorial undercurrents, although these appear to be more closely related to the surface stress. The internal currents characteristically occupy the full depth of the ocean, and are a purely internal mode of motion. Their total energy, both potential and kinetic, is of the order of 10^{17} cal, with the most significant energy transformations of the order of 10^{12} cal sec^{-1} for diffusive dissipation into smaller-scale motion and 10^{9} cal sec^{-1} for losses through bottom friction. These currents derive their energy from the surface ocean layer at a rate of approximately 10^{12} cal sec^{-1}, with an estimate of nearly the same order for the energy addition by geothermal heating at the ocean bottom.

Direct modification of the oceanic internal currents is not considered feasible in view of the large amounts of energy involved, the large scale on which

the phenomena is organized, and the uncertainty of correctly indicating the full effects of any proposed modification. The time scale or characteristic response time of the ocean's internal currents is of the order of 10^2–10^3 years; presumably any interference would have to be applied for an appreciable fraction of this period in order to be effective. Much further research on the reaction of the internal ocean currents to the conditions of stress, temperature and water balance at the sea surface is needed in order to assess adequately the possibilities of ultimate modification and/or control.

3.4.19 Tsunami

The tsunami or seismic sea wave is a relatively rare oceanic phenomenon caused by a submarine volcanic eruption, an underwater landslide or earthquake, or a sufficiently large underwater explosion. The tsunami wave travels at about 500 mph along the sea surface, outward from the source area, with the ocean bottom topography serving to refract or focus the wave ray paths. Upon moving into shallow (coastal) water, the waves' large speed causes a sudden increase in amplitude, which strikes the coast as the familiar "tidal wave". The total energy of the larger tsunami wave train is of the order of 10^{15} cal, with most of this energy being dissipated in coastal waves and surf.

Modification of the natural tsunami itself does not appear feasible, although certain measures may obviously be taken to reduce the damage of the tsunami's coastal waves. The erection of off-shore breakwater or submarine barriers may greatly reduce the shore wave heights, or at least cause their effective dissipation in preassigned areas. The creation of tsunami by underwater nuclear explosions is feasible, and the general course of such tsunami may be estimated from a knowledge of the submarine topography. By suitable selection of an explosion site, focusing of tsunami waves only on an exposed shore appears feasible, although the detailed configuration of the water depths immediately off shore evidently causes large variations in wave heights along neighboring shore locations. More detailed studies on the transmission and dissipation of long ocean surface waves in the tsunami energy range are required before a locally significant degree of tsunami wave predictability is possible.

3.4.20 Oceanic Vortices and Turbulence

The oceans display a broad spectrum of behavior, ranging from the organized circulations on the scale of the ocean basins themselves to the fine-grain turbulence produced by surface and internal wave motions. Some of these phenomena display an individual coherence or life-cycle over long periods of time, while others apparently serve as eddies transmitting energy to other portions of the spectrum. The total energy of the oceanic motion spectrum may be estimated as 10^{19} cal; moreover, there appears to be an overall energy distribution roughly according to vortex size, with the largest-scale motions possessing approximately 100-fold more energy than the smallest significant vortex scales. Total or net dissipation may be estimated as 10^{12} cal sec^{-1}, with the energy cascade within the oceanic vortex spectrum corresponding to eddy diffusion coefficients ranging from 10^{10} cm^2 sec^{-1} (for the largest scales) to the order 1–10 cm^2 sec^{-1} (for surface wave eddies).

Modification or control of oceanic vortex phenomena is in general not considered feasible. There is apparently a continuous energy flux among the various scales of phenomena and alteration on a specific scale could conceivably alter other scales as much as the scale over which control was intended. Local or small-scale modification of current eddies by barrier erection, surface wave control by stress reduction, and modification of vertical overturning by interference with the density structure of the surface ocean layer are possible modification measures whose limited application would probably not seriously interfere with the overall oceanic energy budget for the larger scales of motion, although undesired effects may arise on the yet smaller scales of turbulence.

3.5 Technological and Logistic Considerations in the Modification of Geophysical Phenomena

The preceding reviews and the more complete analyses presented in Appendices E to V tend to show in isolated ways the order of magnitude of the dynamics, energetics and kinematics of geophysical phenomena. In order to bring these into better perspective, we may select a few for more detailed consideration.

Figure 3-1 summarizes the area vs. energy content of six phenomena, thunderstorms, hurricanes, tsunami, cyclones, surface waves (oceans), and ocean

currents. For comparison, the total world's electrical energy production for 1962 and the area of the world are indicated on the appropriate ordinates.

In Fig. 3-2, estimates of the energy dissipation rates for the same phenomena are plotted vs. energy content.

Recognizing that the estimates of quantities plotted in Figs. 3-1 and 3-2 may be subject to considerable uncertainty, they are still sufficiently well known to permit several judgments. The first of these, and hardly a new one, is that brute force manipulation of major atmospheric and oceanographic phenomena by controlled expenditure of energy is not now and may very well never be within the capability of man.

Take, for example, cyclones. This phenomenon typically represents an organization of energy (kinetic, potential and internal) of the order of 10^{17} cal over an area of 10^6 km^2. This phenomenon is dissipating energy at a rate 1000 times the world's electrical energy production rate in 1962 (or at the rate of one nominal atomic bomb detonation per ten seconds). Figure 3-2 also indicates that, if the energy source driving a cyclone were abruptly cut off and the dissipation rate were unaltered as the cyclone "died", it would last for approximately twenty minutes. The typical life time of a cyclone is about seven days, a measure of the time period over which the organization of energy input is maintained by nature.

Similar comparisons may be made for ocean currents, surface waves, hurricanes and tsunami. However, isolated thunderstorms admit of the possibility of direct energetic interference. The area of organized motions and energy is small (2-20 km^2), the total energy content is one-tenth the energy of a nominal nuclear detonation, and the period of time over which energy input must be maintained against dissipative forces is brief. From these results, we may again conclude modification and control, perhaps even generation of thunderstorms, is or will be within the realm of technological feasibility, albeit at a substantial price. For example, a thunderstorm "uses" the equivalent of approximately 10^8 kwh of electrical energy. At 5 mills per kwh, this is half a million dollars. [This illustration of brute force, i.e., providing all of the energy, differs

strongly from the "triggering" of latent energy as tried by Desseas (see Appendix F).]

3.5.1 The Subtleties of Modification of Geophysical Phenomena

If we conclude from the foregoing evidence that direct interference with major oceanographic and atmospheric phenomena and processes is beyond human resources, we must return to the basic concept that successful control or modification will depend upon more subtle control of the distribution and utilization of naturally available energy sources. The diminution of turbulent flux rates for (say) water vapor by expenditure of modest amounts of energy to control the hydrostatic stability of the lower atmosphere, local or large-scale alteration of condensation or freezing nuclei, suppression of evaporation by artificial films, construction of dams to prevent exchange of water of varying degrees of salinity and temperature, these and many other ways represent the subtleties of interference and direction of the internal workings of the atmosphere and oceans.

A detailed review of all these methods which have been suggested, including the economic, technological, and logistic aspects, is beyond the scope of the present analysis. Several of these are mentioned in the geophysical analyses, and the detailed analyses of selected methods is anticipated in future work. For the present, we must conclude that the only real hope for significant control resides in these manipulative techniques.

Finally we must reiterate that the very complexity and size of interrelated geophysical phenomena calls for much more complete understanding of their natural workings and the alternatives by which nature may accomplish her basic task of maintaining long-term equilibrium of energy exchange between the polar and equatorial regions in the presence of their differential energy receipt from the sun.

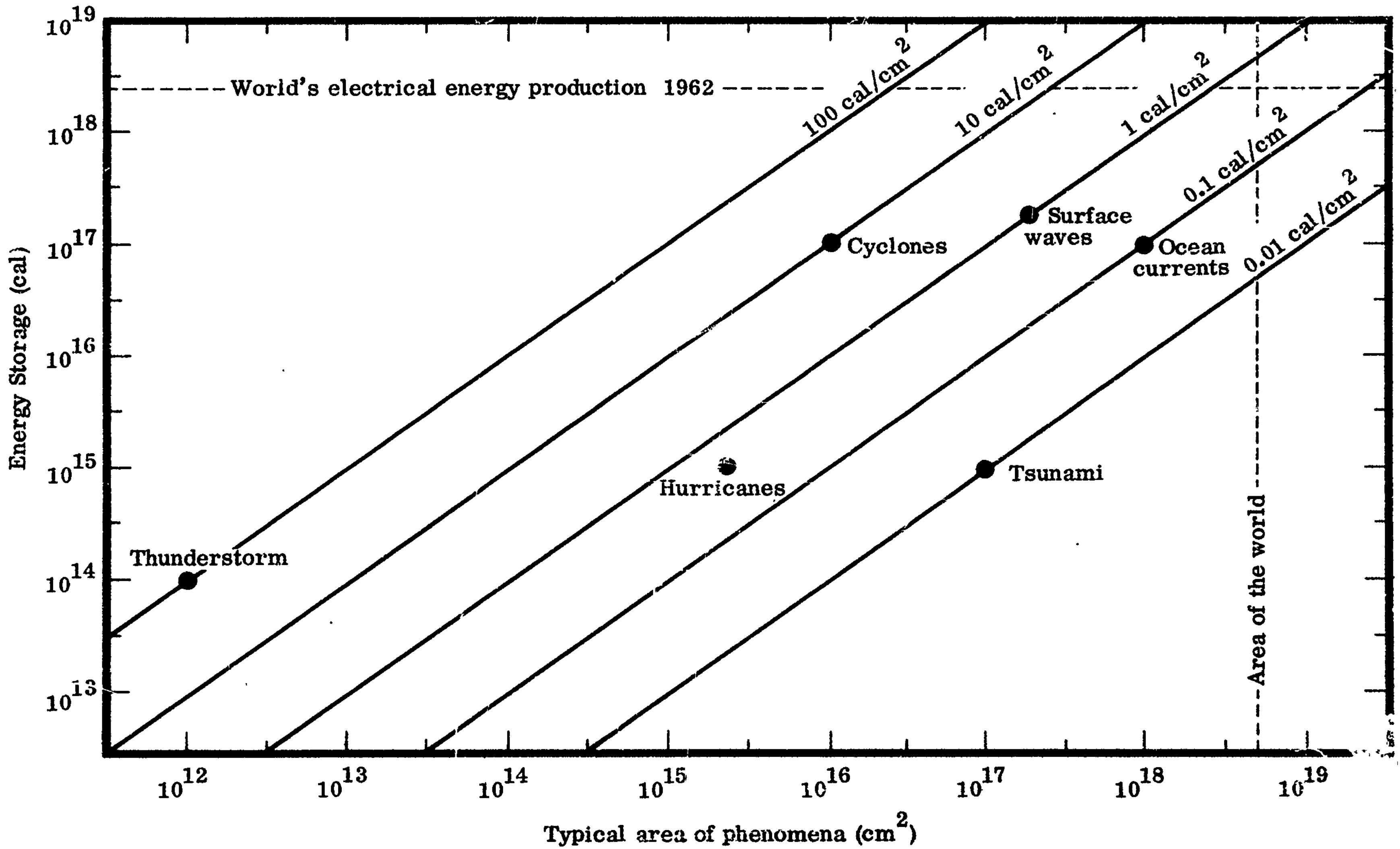

Fig. 3-1. Analysis of geophysical phenomena.

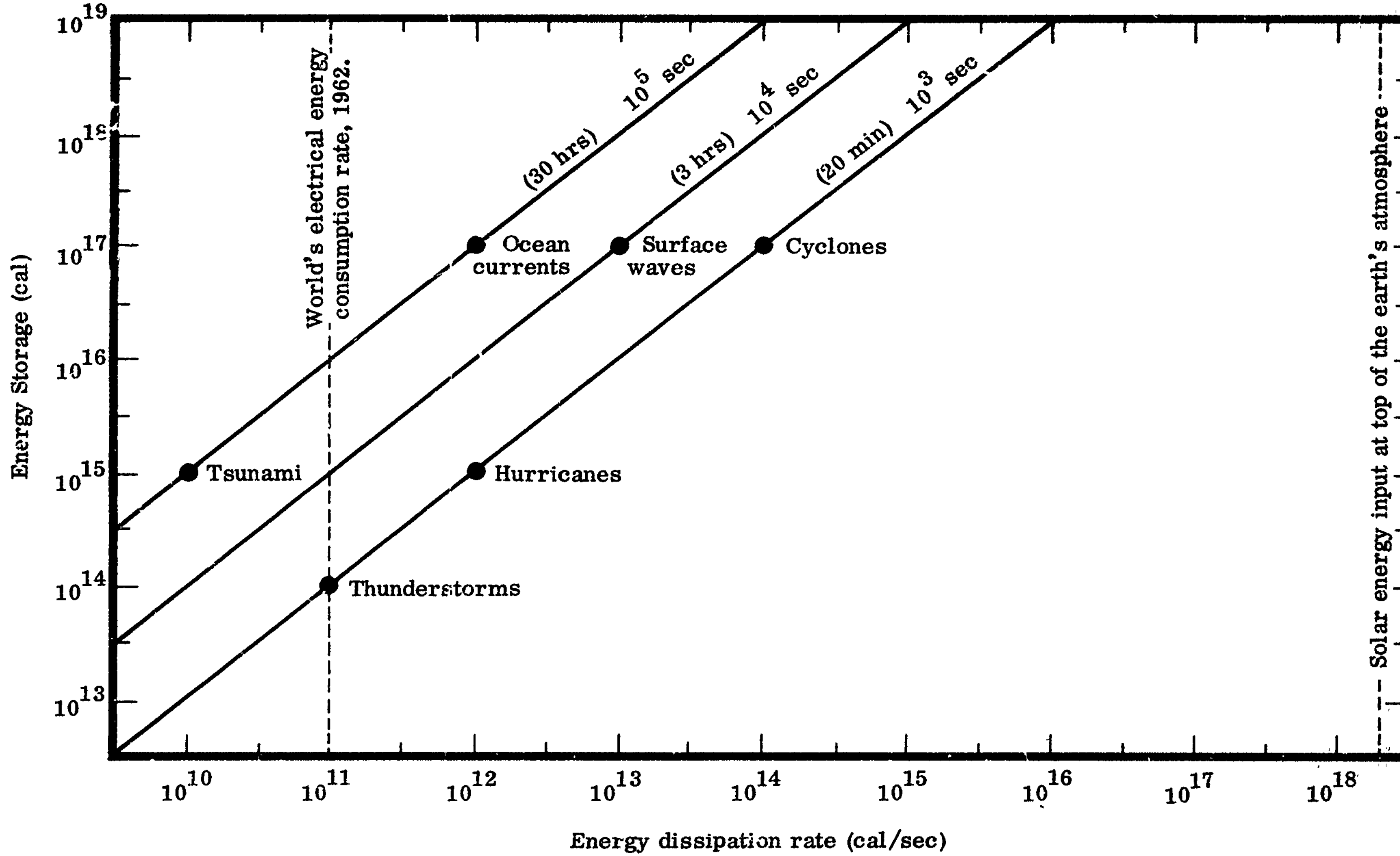

Fig. 3-2. Analysis of geophysical phenomena.

4.0 PREDICTION OF GEOPHYSICAL FACTORS

4.1 Introduction

There seem to be two principal aspects of the prediction of geophysical factors which require particular attention in this study. First, we are obviously concerned with the state of the art, i.e., with our ability to predict various geophysical factors, both at present and in the foreseeable future; a survey of this state of the art consists of a screening process wherein various geophysical factors are identified as elegible candidates for further consideration in relation to military operations. The second aspect is much more subtle, concerns the very nature of a forecast, and must be considered prior to developing an adequate mathematical or conceptual formalism within which the relationship of forecasts to military operations can be viewed and assessed. There is a common misconception among both laymen and professionals that a forecast must be either "right" or "wrong." The notion is not only incorrect but, more seriously, reflects an erroneous conception of what a forecast is and, in consequence, what its properties may be. In order that this be clarified and an adequate understanding of the probabilistic nature of a forecast be developed, this second aspect is discussed first. Then, within this framework, an assessment of the predictability of geophysical factors will be made, and the possible impact of future developments will be considered. The results will provide an input to the consideration of military exploitation of prediction discussed in Sections 5.0 and 6.0.

4.2 The Nature of Geophysical Prediction*

A prediction of a geophysical phenomenon is sometimes a simple statement that a specific event will or will not occur during a specific time interval in the future; for example, "There will be a thunderstorm in Washington this afternoon," or "There will be a volcanic eruption in Hawaii next month." We shall refer to any statement of this sort as a simple prediction.

Often a prediction is a statement of a numerical value of some variable quantity. Such a statement is equivalent to a combination of simple predictions, if the term "event" is interpreted liberally. For example, if the occurrence of

---

*by Edward N. Lorenz, MIT, consultant.

a wind speed of 45 knots is one event, and the occurrence of a wind speed of 46 knots is a second event, the statement, "Tomorrow's maximum wind speed will be 45 knots," is equivalent to the two simple predictions that the first event will occur tomorrow and the second will not.

Whether an anticipated event will actually occur or not depends upon how the state of some physical system will develop from the present state, in accordance with governing physical laws. In the strictest sense, the relevant physical system is the whole universe. However, the effect of all but a small portion of the universe upon most geophysical phenomena is insignificant. Even the sun may be eliminated from the system whose development needs to be considered, and the solar constant may be treated as part of the governing physics, if variations of the solar output do not significantly affect the phenomenon in question. Thus, for example, in predicting a thunderstorm for the coming afternoon, the relevant system is essentially the portion of the atmosphere and the underlying land or water surface within a few hundred miles of the location in question.

The easiest way to determine whether a specific event will occur during a specific future time interval is to wait and see; a procedure which unfortunately is quite impractical for the purpose of obtaining an answer in advance. Nevertheless, many of the most practical methods of prediction may be regarded as attempts to duplicate the wait-and-see procedure in its essentials, while modifying it enough to make it yield an answer before the occurrence or non-occurrence of the event. Predictions by these methods are based upon the development of analogous physical systems, from initial states analogous to the present state.

One method consists of letting the physical system be its own analogue. An analogous initial state is obtained by searching the records of the past behavior of the system. The anticipated event is then predicted to occur, or not to occur, according to whether or not it occurred in the analogous situation.

When the relevant physical system is restricted in size, there is the additional possibility of finding other real geophysical systems as analogues. Sometimes a simple translation in space of the original system will serve as a

substitute system; thus, for example, the prediction of thunderstorms in the Washington area should be aided by studies of thunderstorms in the New York area. The chances of finding suitable initial conditions in the recorded history are thereby considerably improved.

Instead of using real systems as analogues, one may construct artificial systems which are believed to behave like the real geophysical system. These artificial systems may be laboratory models. In this case the model will probably be much smaller than the real system, and its state may evolve much more rapidly. When the appropriate initial conditions are introduced into the model, the prediction may be obtained well in advance of the event. Considerable success has been obtained, for example, in the prediction of floods, with the aid of laboratory models of river basins.

An artificial system need not be as realistic as a model river basin. It is well known, for example, that the behavior of certain mechanical systems may be approximated by that of certain electrical systems, whose governing equations are similar in form. Probably the most widely used artificial systems are systems of mathematical equations, to be solved by high-speed computers. If the equations are made sufficiently simple, while still retaining a fairly close resemblance to the equations which govern the real system, the appropriate initial conditions may be introduced in numerical form, and a prediction may again be obtained in advance of the event. A large share of the recent research in weather forecasting has been devoted to the solution of dynamic equations by numerical processes.

One important class of prediction methods is peculiar in that the methods do not represent attempts to duplicate the wait-and-see procedure. These methods include linear regression and discriminant analysis [5]. They are related to the methods which we first discussed, in that they are based upon the past behavior of a real geophysical system. However, the coefficients in the derived prediction formulas are statistics computed from large numbers of states of the system, most of which bear little or no resemblance to the actual present state. The physical basis for these methods is therefore somewhat in doubt, even though they seem to be on firm ground mathematically. Attempts to fit the data to non-linear formulas of a prechosen form also fall into this class of methods.

All of these procedures, except the wait-and-see procedure itself, require that we observe the present state of the relevant system. Such observations are ordinarily subject to some error, as well as incompleteness, so that generally the most we can do is to specify a collection of possible present states, each possessing a certain probability of being correct. If some but not all of these states lead to the occurrence of a certain event, we can specify a certain probability, other than 0 or 1, that the event will occur. This probability will depend upon the precision with which we have observed the present state. A statement of the probability of occurrence of a specific event, as opposed to a statement that the event will, or will not, occur, will be called a probability prediction.

Unless the prediction procedure makes use of the physical system as its own analogue, there is further uncertainty involved in the choice of an analogous system. The probability of occurrence of an event will the be further affected. Thus, in general, the stated probability in a probability prediction will depend upon the prediction method used.

It is interesting to consider the intrinsic probability of occurrence of an event, as opposed to the probability conditioned by our own capabilities. Any intrinsic probability other than 0 or 1 would imply that the relevant system is not deterministic. Conversely, if a system is not deterministic, at least one event characteristic of the system has a probability other than 0 or 1, although some other event may have probability 0 or 1. We shall not try to settle the philosophical question of determinism; suffice it to say that many geophysical systems are influenced to some extent by human activity, and any assumption that these systems are deterministic would imply that human activity is deterministic.

In a sense, a probability prediction is more realistic than a simple prediction, since our prediction methods do not in general allow us to state with certainty whether a given event will occur. A probability of 0 or 1 implies a virtual impossibility or a virtual certainty, and the event is completely predictable. A probability equal to the a priori probability of the event, i.e., to the probability that a randomly chosen initial state will lead to the event, indicates that the event is completely unpredictable. All other possibilities lie between these extremes.

Thus the predictability of any event is related to the probability of occurrence of the event. It follows that the predictability is dependent upon the method of prediction. An event also has an intrinsic predictability, related to its intrinsic probability of occurrence, but this intrinsic predictability is of somewhat academic interest, since no practical method of prediction will yield intrinsic probabilities.

Let us therefore consider the various methods of prediction, with regard to their relative abilities to predict various types of phenomena. We begin by summarizing some ideas of Wiener [6] concerning predictions based upon past history. Wiener notes that in observing the present state of a system, we are forced by practical considerations to measure only a finite number of physical elements. Each of these elements has a finite range, and its recorded value will be rounded off to a specified number of digits, limited for practical purposes by the accuracy of observation. Hence only a finite number of distinct states are observable. If the recorded past history of the system is infinite, and if the system is statistically stationary, a set of past states observed to be identical to the present state may be found. The fraction of these past states which are followed by the occurrence of a specific event is then the probability of occurrence of the event. No other procedure based upon the same observations of the present state can do better. A deterministic dynamic equation, for example, yielding the same yes-or-no answer every time, is less realistic, since the same thing need not occur every time.

Here we should note that when two given states which are really not identical are observed to be identical, perhaps because the observations do not cover the entire relevant system, the differences between the two given states may sometimes be revealed through observable differences in the states which precede the two given states by a certain time. That is, two states should perhaps not be considered analogous unless their antecedent states, over some finite time interval, are all analogous. If this is the case, the preceding paragraph retains all its truth when the word "state" is replaced by the expression "combination of successive states," whenever it occurs. The antecedent states to two states considered analogous need not be analogous over an infinite time interval; this could not occur anyway unless the process is strictly periodic.

Wiener also observes that the prediction scheme which he has described may be expressed as a linear regression scheme, if the predictors and the predictand are characteristic functions. A characteristic function of an event is a time-variable quantity which simply has the value 1 whenever the event is occurring and 0 whenever the event is not occurring.

Through characteristic functions we can establish an important relation between predictability and periodicity. If F(t) is the characteristic function of a specific observable initial state (or combination of successive states), and G(t) is the characteristic function of an event to be predicted, the means $\overline{F}$ and $\overline{G}$ are the *a priori* probabilities of occurrence of the initial state and the event, while the mean product $\overline{F(t)\ G(t + \gamma)}$ is the probability that the initial state will occur, and be followed after time γ by the event. The probability that, given the initial state, the event will occur after time γ, minus the *a priori* probability of the event, is therefore given by

$$\overline{F}^{-1} \left(\overline{F(t)\ G(t + \gamma)} - \overline{F}\ \overline{G}\right) .$$

In this expression, the factor in parentheses is simply the covariance of F and G, at lag γ. If the event is predictable at arbitrarily long range, the *a posteriori* probability of the event does not approach the *a priori* probability as a limit. It follows that the covariance of F and G does not approach 0 as a limit. as $\gamma \rightarrow \infty$. But this means that F contains a component whose spectrum is not absolutely continuous, i.e., a periodic or almost-periodic component, or else a somewhat pathological component with a non-absolutely continuous spectrum, if such components exist in natural processes. The predictability of a purely nonperiodic process, i.e., one with an absolutely continuous spectrum, must become arbitrarily small as the range of prediction becomes arbitrarily long, if the number of observably different states is finite.

It is important to observe that this result applies even when the prediction is based upon infinite recorded past history, i.e., when it is made by the best possible method. Hence the limitation upon predictability applies to prediction by any method, and is subject only to the restriction that the system is not observed with absolute precision.

Periodic components, however, are predictable at arbitrarily long range, provided that the past history is sufficient to reveal the periodicity. They also yield readily to linear regression procedures.

Knowing that there is an upper limit to the range of predictability of non-periodically occurring events, let us now restrict our attention to predictability at ranges where prediction is possible. Wiener's ideas should not be interpreted as meaning that prediction based upon past history is superior to other methods. Rather, they indicate the conditions under which such a method will be superior. These conditions include the availability of infinite past history. The method seems to be favored, then, when the recorded past history is sufficiently long to include virtually all the different situations which are likely to arise.

Prediction by linear regression becomes equivalent to this method, if the class of allowable predictors is extended to include all characteristic functions. If the allowable predictors are more restricted in nature, the predictability of an event will be limited by any lack of linearity, even when the system is deterministic. But since the linear regression method does not demand that we find past states analogous to the present, it may be favored over prediction based upon analogous past states, if the recorded history of the process is insufficient to yield good analogues.

By analogy with Wiener's ideas, it is tempting to state that prediction by means of laboratory models must be as good or better than prediction by any other means, provided that we can construct models which behave exactly like the original system, and provided that we can introduce the initial conditions with the same accuracy and completeness with which they have been observed. Such a statement may not be justified, however. Common to all those states which are observed to be the same as the present state, even though they really differ, there may be some peculiarity which is not observed. This peculiarity occurs in the past history, but it may not be present in the initial states which are introduced into the model.

Nevertheless, the use of models seems to be favored when good modeling is possible, and the recorded past history of the system is limited.

Likewise, prediction by means of dynamic equations might seem to be as good or better than any other method, provided that the governing equations are known precisely, and provided that methods for solving them exactly are available. Usually, however, the precise equations refer to a completely observed system. We might in theory choose a collection of initial states, each compatible with the observed state, and solve the equations in each instance, thereby obtaining the probability of occurrence of a given event. Again, an unobserved peculiarity common to those real states compatible with the observed initial state might bias the probability.

Nevertheless, when the dynamic equations are known with fair precision, but the recorded history of the system is meager, solution of the equations seems to be a favored method.

In short, each method of prediction demands, for its successful application, that certain conditions be met. These conditions include a long recorded past history if the prediction is based upon past behavior, the possibility of accurate modeling if the prediction is based upon laboratory models, and the ability to formulate and solve the appropriate equations, if the prediction is to be made dynamically. For any given phenomenon, the predictability by any process depends upon the extent to which the corresponding conditions are met by the relevant physical system. In the case of nonperiodic processes, the predictability by any process decays toward complete unpredictability as the range of prediction increases.

Among the phenomena for which prediction methods based upon past records seem preferable, although not altogether satisfactory, are tornadoes. The dynamics of tornadoes are poorly understood, and the condensation processes instrumental in the development of a tornado are difficult to model, even though a mature tornado vortex might be modeled.

As already suggested, laboratory models may afford the preferred method for flood prediction, provided that the heavy rainfall or rapid melting of snow leading to the flood has already occurred. The dynamics are somewhat complicated, and the number of previously recorded floods in a given river basin may be small.

Dynamical equations may afford the best methods for predicting extratropical storms. Here much of the dynamics is understood, while the possible configurations

of storms are so numerous that it is difficult to find truly analogous initial conditions.

Finally, we mention earthquakes. Here it is exceedingly difficult to measure the important features of the present state of the relevant system, such as stresses within the solid earth. Immediate prospects for prediction of earthquakes by any method are therefore rather dim.

4.3 Prediction by Statistical Methods*

4.3.1 Definitions

The term prediction is used here in much the same sense as defined in Section 4.2. It will always mean a statement that an event, or a numerical value of an event, will or will not occur at an instant of time or during an interval of time in the future. A statistical prediction is a prediction made by statistical methods wherein the coefficients in the derived prediction formulas are statistics computed from a large historical sample of data. A statistical prediction procedure is completely objective—everyone using it must obtain the same answer. Such objective procedures are quite amenable to use on high-speed computers.

This definition eliminates many cases wherein statistics play an important role in forecasting but the basic forecasting method is not statistical. Two areas of wide interest thus eliminated are the determination of some important parameters by statistical methods or the development by statistical methods of some guide or aid for a human forecaster. An example of a statistically-derived parameter is in ocean-wave forecasting wherein the statistical method of spectrum analysis is used to define numerically the quantity to be predicted but the actual predictions are not made statistically [7]. A procedure for using spectrum analysis as a statistical prediction method, as defined here, is given in [8]. It turns out that such predictions must be made by linear regression. Easily, the most widely-used examples of aids for human forecasters are the tables or charts of normal values, many of which were obtained by statistical methods.

A case not eliminated by the definition is the two-stage procedure of deriving formulas by statistical methods relating a predictand to some predictors observed simultaneously and then using forecasted values of the predictors. An example is given in [9] wherein some surface variables are related to simultaneous observations of the 500-mb surface by screening regression. In application of the equations, data from the 500-mb prognostic charts prepared

*By Isadore Enger

regularly twice a day by the U.S. Weather Bureau would be used as input to the equations.

The organization of this section will follow the grouping of geophysical phenomena by subject matter presented in Table 3-1 of the first part of this report. There are four major subject areas: geological, atmospheric, oceanographic, and others, but only atmospheric and oceanographic phenomena will be treated in very great detail here because these appear to be most amenable to statistical prediction.

4.3.2 Geological Phenomena

4.3.2.1 Earthquakes and Landslides

The effort devoted to seismology has increased enormously under the impetus of the problem of detecting underground nuclear explosions. Great strides have been made in theory, instrumentation, data collection and processing, location of epicenters by digital computer, and on the central problem of differentiating between seismic disturbances caused by underground nuclear explosives and those due to earthquakes. (See [10] for a review of recent work in seismology; see [11] for a study on the central problem.) However, it is only recently that attention has turned to the problem of predicting earthquakes. Apparently, no work has been done in prediction although there have been several methodologies put forth. A Russian seismologist has suggested that Love waves be examined because as the stress in rocks builds up prior to an earthquake the character of the waves changes*. A magazine article [12] quotes Dean Carder of the U.S. Coast and Geodetic Survey as suggesting that geophones, sensitive instruments to detect vibrations, be buried one or two thousand feet deep near known earthquake faults. Carder, and others, have suggested also the use of several lasers pointing at various angles across faults to detect slight differences in the tilt of the earth on either side of the fault which may precede earthquakes; tiltmeters have been suggested for the same purpose. Stacey [13] reasons that the magnetism of the rock changes with stress and he suggests an investigation of the possibility of forecasting earthquakes on this basis by placing magnetic instruments

*Personal communication from Dean Carder, U.S. Coast and Geodetic Survey.

at fault lines.

No statistical methods have been used for earthquake prediction. In recent years vast amounts of seismic data have been collected and much is available in digitized form from the data center of the U.S. Coast and Geodetic Survey. From the statistical methodology viewpoint, the problem is very much like that faced in the prediction of meteorological events. Time series of observations are available at a number of stations around the country and the problem is to combine these statistically to predict earthquakes. The statistical methods developed in meteorology could be quite useful. Unfortunately, for purposes of prediction (fortunately otherwise) it may be that the number of earthquakes is not sufficient to develop statistical relationships between the seismic time series and the subsequent occurrence of earthquakes. However, it may be worthwhile to devote a small amount of effort to investigate the possibility of statistical prediction.

4.3.2.2 Volcanoes

The ultimate cause of volcanism is the fundamental instability of the crust and upper mantle of the earth. The partial melting of the mantle at about 60 kilometers yields a magma whose density is less than that of the surrounding rock. The magma rises along conduits associated with fractures in the earth and forms a shallow reservoir within the volcanic pile, and, depending on rapidity of filling, volume, and other factors, this may lead to an eruption [14, 15].

The prediction of an eruption can be made because the slow movement of the magma causes tilting of the ground surface around the summit of the volcano and this can be measured by tiltmeters. Eaton and Murata [14] found that in the eruption of Kilavea in Hawaii the tiltmeters were affected more than a year before the actual eruption.

For places where no such instrumentation is possible, such as in the more remote reaches of Alaska, the situation is more difficult. Here, the only evidence is seismological, unless an airplane happens to note smoke. Although the movement of the magma does cause seismic disturbances, Eaton and Murata [14] conclude that such evidence tells little about the likelihood that a particular disturbance will culminate in an eruption. If statistics can be of use in predicting

volcanoes, it is in associating eruptions with seismological records. Volcanic data for many areas of the world are kept at the International Volcanological Association in Naples, Italy and seismological records are available from a number of places. However, it may be that the number of volcanoes is too small to establish a definite statistical relationship.

4.3.3 Atmospheric Phenomena

The use of statistics in meteorology has increased enormously in recent years. Lorenz [16] estimates that in 1960, 56 percent of meteorological articles made some use of statistics. Klein [17] cites over 50 references on the use of screening multiple regression in weather forecasting, almost all appearing in the last 10 years. This growth in statistical prediction is due in large part to the availability of an enormous amount of data on punched cards at The National Weather Records Center in Asheville, North Carolina (see [18] for a brief description). As more and more meteorologists become aware of this gold mine of information and also of the power of statistical methods and high-speed computers, it is anticipated that the growth will accelerate.

As indicated by the number of references cited by Klein [17], the most widely used statistical prediction method at present is screening multiple regression: a description of this method is given by Miller [19]. Briefly, from a large set of possible predictor variables a smaller subset of contributing predictors is selected by an objective statistical procedure. The redundant or noncontributory variables are then eliminated from the analysis and an ordinary multiple regression equation is computed between the selected predictors and the variable to be predicted, usually termed the predictand.

A second statistical procedure which is coming into prominence is screening multiple discriminant analysis (see [19] for a description). Here too a subset of important predictors is selected objectively. The primary difference between the two statistical techniques is that the predictand is a continuous variate in regression but can be discontinuous, or even qualitative, in discriminant analysis. However, there are some examples of regression being applied to discontinuous variables and of discriminant analysis applied to continuous

variables.

A third, and quite old, technique is the contingency table in which counts are made of the subsequent occurrence or nonoccurrence of events when given that a specified event or events have occurred. An example is given in [20].

4.3.3.1 Atmospheric Turbulence

Although scores of articles and several books have been written on turbulence, statistical prediction of turbulence is virtually nonexistent. The main reason appears to be difficulty in obtaining sufficient data in the proper form. For purpose of this study, turbulence is divided into high-level, low-level, and boundary-layer, although the words may not be fully descriptive of the types of turbulence being considered.

4.3.3.1.1 High-Level

The impetus for predicting high-level turbulence comes from its effect on aircraft. The two types affecting aircraft are clear-air and convective turbulence; the latter is usually associated with thunderstorms, and prediction of thunderstorms will be considered later. The only statistical prediction on clear-air turbulence (CAT) that could be found is the work by Ball [21] based on previous work by Clodman, et al. [22]. Ball had five days of pilot reports of CAT over the United States and attempted to relate the severity of turbulence to large-scale features of the upper-air circulation by screening multiple discriminant analysis. He was not successful and attributed this to lack of data, both of occurrences of CAT and of observations of meteorological data on a sufficiently dense network. There does not appear to be much chance of predicting CAT by statistical methods until more and better data become available.

4.3.3.1.2 Low-Level

Low-level turbulence, below 1000 feet, as it affects the design of aircraft has been studied mainly by Lappe and others at New York University (see [23] for an outline of the work and [24] for the latest report). Simultaneous measurements of turbulence were made from an instrumented tower and by aircraft. At present, effort is being expended to relate properties of the spectrum (the

predictands) to predictors such as terrain types, measures of stability and wind speed. Lappe and his group are not developing statistical prediction methods but rather are using a combined physical-empirical approach. Thus, no statistical prediction of low-level turbulence has been attempted. It appears that the amount and condition of the existing data do not warrant any large-scale effort in this direction at the present time.

4.3.3.1.3 Boundary-Layer

A good deal of work in turbulence has been directed toward predicting the concentration of pollutants in the atmosphere. Although much knowledge has been gained and advances have been made, it is fair to say the the existing state of theoretical knowledge (particularly of nonhomogenous, nonsteady state, and nonisotropic turbulence existing at the surface) is such that prediction methods based on theory leave much to be desired. Furthermore, it appears that no statistical prediction methods have been attempted.

The most widely used prediction technique is an equation relating concentration of the pollutant to some measure of the variability of the wind. The problem then is to predict the wind variability. This variability is dependent upon a number of factors, some of which are the features of the terrain (smooth, wooded, grassy, wet, dry, etc.) the stability of the air (in turn this is affected by the time of day, season of the year, amount of clouds, synoptic situation, etc.), and the wind speed averaged over some convenient length of time. It is the opinion here that statistical methods can play a role in prediction of turbulence and that the time is ripe for such a study. A general framework is presented below.

First, the quantities to be predicted, the predictands, must be defined. These could be the amount of energy in various frequency bands of the spectrum, or the variances of the vertical and cross-wind components of the wind, or the concentration of the pollutant, or even the meandering of the plume from a source such as a smoke stack. These, or other predictands, could be defined numerically or even qualitatively in broad groups. The definition of the predictand would depend upon the problem and upon the data available.

The second step is to define the predictor variables. If the statistical prediction technique is of a screening nature (see Section 2.0) then there is no need to keep the number small. For example, in screening regression up to 180 predictors can be handled by existing computer programs [25] and in screening discriminant analysis up to 450 predictors can be analyzed. However, if the prediction problem were sufficiently important the number of predictors could be increased substantially.

The actual meteorological variables chosen as predictors would depend again upon the problem and the availability of the data. However, based on considerable experience in other fields the following remarks may aid in the predictor selection.

(a) Although the relationship between some predictand and a set of predictors may depend upon the hour of the day and the season of the year, it is not necessary to stratify the data into small time-dependent groups and obtain a relationship within each group. In a large-scale effort to develop statistical prediction methods for forecasting cloud heights and visibility [20] it was found that the same statistical prediction formulas could be applied for every hour of the day and every day of the year. This was accomplished by including the hour and the season explicitly as predictor variables. In a somewhat smaller study [26], regression equations were developed in forecasting wind, temperature, and pressure. Again, hour and season were included as predictors and the result was equations which could be applied at any time. The use of these time predictors is almost mandatory if data from different hours and seasons are to be handled simultaneously.

(b) A second type of predictor found valuable is the dummy variable. An example will illustrate this. Suppose observations are made under varying terrain conditions and it is desired to combine these, but to retain terrain as a predictor. This could be done if some numerical value could be assigned to terrain--but the present knowledge of turbulence makes this difficult. The problem can be overcome by generating dummy or zero-one variables. If the terrain for a certain set of observations is a solid canopy of trees, then we

generate a variable, say Z, which takes on a value of 1 for these observations but is set equal to zero for all other observations. If the terrain of another set of observations is grassy then a second dummy variable is generated, say Z_2 where Z_2 is one for all grassy cases but zero for all other cases. It is clear that dummy variables constitute a method for quantifying qualitative data. Such variables are widely used in psychology and sociology [27] as well as meteorology [28].

(c) Variables can be subjected to various transformations. Some of these are given by Miller in Appendix W and in [29] Bryan describes several transformations he found of use in geophysical prediction including optimum subdivision of a variable, calibration, dummy variables, segmented variables, heterofunctions, and normalizing.

Once the predictors and predictands have been defined a sufficiently large sample of data must be collected and pre-processed to produce the variables in the proper form. This would probably be the most expensive and time-consuming portion of any study. At least this has been true in similar studies in meteorological prediction.

Given the sample of data, various statistical prediction techniques could be applied to answer a variety of questions. Particularly valuable would be the screening techniques wherein predictor variables are selected objectively. Although the primary aim of these techniques is to produce prediction methods they often aid in gaining greater insight into the physical nature of the problem.

4.3.3.2 Tornadoes and Thunderstorms

An up-to-date review of the current status of the tornado and severe thunderstorm forecasting is given by House in [30]. Forecasts are made on a regular basis by the Severe Local Forecasting Center (SELS) of the U.S. Weather Bureau. At present, the forecast procedure is much the same as that used by subjective forecasters in day-to-day forecasting of other meteorological elements although the problem is more difficult.

As stated by House:

> "While the procedures utilized in arriving at a particular forecast solution are in general well specified, the success of the prediction depends, in a large part, upon the forecaster's experience and ingenuity in relating the synoptic observations to the tractable physical processes specified by the theory."

The forecasts are categorical statements that a tornado will occur in a 20,000 square mile area in a 6-hr period beginning shortly after forecast time, and 50 percent of such statements are correct. The basic difficulty of the forecasting problem from a physical viewpoint is compounded by the lack of observations on a sufficiently dense spatial and time scale. This latter difficulty is being overcome somewhat by objective analyses of mesoscale observations. The work of Dellert [31] is outstanding in this respect.

At present no statistical prediction methods are available for forecasting thunderstorms and tornadoes. It is strongly recommended that effort be initiated toward developing such methods. The requisite data are now available in sufficient quantity, the problem will not be solved in the near future by dynamic models, and similar problems have been attacked successfully by statistical methods (hurricanes [32], ceiling and visibility [20], and cyclone movement [33]). A proposed outline for such a study follows.

The predictand variable would be the occurrence or nonoccurrence of "activity" in a specified area, probably 20,000 square miles, for specific time intervals, say 6-hr interval beginning three hours after forecast time. An example of "activity" is: no convective activity, nonsevere thunderstorms, severe thunderstorms, and tornadoes. The precise categories would depend on the reliability of the available data. The geographical region of concern would be the area of maximum severe weather occurrence—from east of the Rockies to the Mississippi Valley. Also, the seasonal maximum of March to June would receive emphasis.

The predictor variables would be chosen on the basis of the experience of SELS personnel and might include pressure tendencies, moisture measures,

temperature advection, vorticity, vorticity advection, stability measures, gradients, etc. The moving-coordinate method could be used [33] wherein predictor information is tabulated at locations relative to the prediction area or some other convenient "module."

Approximately three years of carefully analyzed manuscript surface and upper-air maps would be needed. In addition, detailed climatological information concerning severe weather occurrence, such as the SELS log, would be required.

The basic approach would be screening multiple discriminant analysis (see Section 2.0) in a moving coordinate system. It will be recalled that MDA selects from a set of potential predictors a subset that efficiently separates or discriminates between the mutually-exclusive predictand groups. The end product is a statistical prediction method giving the subsequent probability of occurrence of the selected predictors.

4.3.3.3 Hurricanes

Unlike the atmospheric phenomena discussed in the previous two sections, extensive work has been done to develop statistical methods for predicting hurricane movement, mainly by Veigas and a group at The Travelers Research Center, Inc. [32], and such methods are part of the regular forecast routine of the agency responsible for hurricane prediction, The National Hurricane Center (NHC) at Miami. Following Veigas' procedures, Arakawa [34, 35] developed statistical methods for predicting typhoon movement in the Western North Pacific but he extended the work to predict the change in central pressure also. This procedure is being used by the Japan Meteorological Agency.

The procedure followed at the NHC for forecasting hurricane movement is given in Chapter 10 of [36]. A number of objective prediction methods, including Veigas', are used and all serve as input to the duty forecaster who makes the final decision. Tracy [37] of NHC verified several hundred forecasts of 24- and 36-hr movement and found that Veigas' statistical prediction method was the best of several objective forecast procedures. These other procedures included the Riehl-Haggard system [38], a numerical prediction method [39],

and persistence of the previous movement. A brief description of Veigas' work follows.

Veigas considered 12 predictands, E-W and N-S movement at 12, 24, and 36 hours for northern and southern zones. He used from 99 to 154 potential predictors, all of which involved either sea-level pressures, 500-mb heights, or previous movement of the hurricane center. He obtained data for 384 cases. The screening multiple regression technique (see Section 2.0) was applied and a small sub-set of predictors was selected out objectively. The remaining predictors were eliminated from the analysis and 12 regression equations were obtained, relating each predictand to its selected predictors. These equations constitute the statistical prediction method.

Although much work has been done there are two unfinished tasks. Arakawa developed reasonably accurate regression equations for predicting change in central surface pressure for typhoons in the Pacific. Similar equations should be derived for hurricanes in the Atlantic and Gulf of Mexico. Second, the 500-mb prognostic charts for various forecast lengths prepared twice daily by the National Meteorological Center at Suitland should be incorporated into Veigas' regression equations. Data from these charts would be added to the list of potential predictors and the screening procedure would be applied to derive new regression equations. In operational forecasting, these prognostic charts are readily available and pertinent data could be extracted in precisely the same manner as data are extracted from observed charts on the present method.

4.3.3.4 Blizzards

The U.S. Weather Bureau specifies for blizzard a wind of 32 miles per hour or higher, low temperatures, and sufficient snow in the air to reduce visibility to less than 500 ft. From a survey of the literature it appears that there are no specific procedures for forecasting blizzards as there are for tornado, thunderstorm, and hurricane forecasting. The forecasting of wind, snow, and temperature are treated separately and blizzard forecasts are issued when all three elements meet the required conditions. There are no

verification statistics on blizzard forecasting and no statistical prediction methods.

It is felt that development of statistical methods for forecasting blizzards is quite feasible. The suggested method of attack is a two-stage procedure–forecasting of the surface pressure map and upper-level charts and relating the occurrence of blizzards to the maps. The predictand–a blizzard–could be defined to suit some operational requirement; the simultaneous occurrence of specified wind, temperature, and snowfall rate could be used to categorize the predictand into several classes, say, no blizzard, light blizzard, moderate blizzard, and severe blizzard. The predictors would be the location and central pressure of simultaneous surface maps, features of the simultaneous 500-mb charts and any other predictors felt to be pertinent and which would be available at forecast time. The statistical method of screening multiple discriminant analysis would be used to select important predictors and generate forecast relationships. In making the forecasts under operational conditions, the location and central pressure of the surface lows would be forecasted by the method of Veigas and Ostby [33, 40]; the 500-mb prognostic charts put out twice daily by the National Meteorological Center would be available as would other pertinent variables. The predictors selected by the screening procedure would be extracted and inserted into the forecasting relationships and the end product would be a probability forecast.

4.3.3.5 Cyclogenesis

Cyclogenesis is the intensification of existing cyclonic flow or the development of cyclonic circulation where previously it did not exist (commonly, the initial appearance of a low or trough). The major effort in statistical prediction of cyclogenesis has been conducted by Veigas and Ostby and their results are contained in two reports [33, 40]. The reports give a brief resumé of previous work in the field. Briefly, they set up a moving coordinate system in which predictor information is measured at points fixed with respect to the moving cyclone center rather than at points fixed with respect to the earth. They then applied the technique of screening multiple regression to obtain equations for predicting

24-hr displacement, change in central pressure, and change in intensity of existing lows on the surface pressure map. Their procedures have been applied in routine forecasting by the U.S. Navy group at Monterey, California, and have been found to be quite successful.

There are improvements and extensions to other geographic areas that can be made to the Veigas-Ostby technique. However, a more fruitful area is extension of the technique to cases wherein no low exists, i.e., there is need to develop methods for predicting the position, central pressure, and intensity of the initial occurrence of lows or troughs. It is felt that efforts in this direction would be rewarding.

4.3.3.6 Lightning

Not only is statistical prediction of lightning nonexistent but there does not appear to be any research effort at all devoted solely to prediction of lightning by any method. A survey of the literature reveals several hundred articles devoted to the physics of the lightning flash, scores devoted to the effects of lightning, to lightning protection, and to atmospheric electricity in general, but nothing on prediction of lightning. It appears to be tacitly assumed that forecasting the severity and location of a thunderstorm is sufficient information for forecasting lightning. Although this is not true in general, it is the opinion here that thunderstorm forecasting is such a difficult problem that any resources available for developing statistical methods for predicting lightning should be devoted to predicting thunderstorms.

4.3.3.7 Clouds

By far the largest effort in statistical prediction of clouds has been conducted by The Travelers Research Center, Inc. of Hartford, Connecticut. The motivation for the studies is improved forecasting for aviation, both at air terminals and enroute. A brief survey of the effort is given below.

One study involved developing and testing procedures for forecasting ceiling heights for periods from 2-7 hours at terminals where a large amount of historical data are available, and the usual weather variables are currently being transmitted hourly over the weather teletype network in the United States.

The predictand was ceiling height classified into operationally-useful categories (i.e., for aircraft landing and takeoff). The predictors were surface elements observed hourly at a network of stations. A number of statistical prediction procedures were compared with each other and with the subjective forecasts, and it was concluded that the screening multiple discriminant analysis procedure was the best statistical procedure and was slightly better than the subjective forecaster (see [20] and [41] for the verification results).

A second study involved forecasting ceiling height and total cloud amount at terminals where no historical data exist and weather observations are not being made. This is the so-called "no-data" problem—it is particularly useful over ocean areas and over silent areas in wartime. The screening regression procedure is used to develop equations on a simultaneous basis between predictor data from upper-air charts and ceiling and total cloud amount at various terminals where data were observed. By using the "generalized-operator" concept the equations are applicable to other terminals. In making the forecasts, the predictor data are picked off the hemispheric prognostic charts prepared twice daily for 12-, 24-, and 48-hr forecast lengths. Some results are given in [9], and it is concluded therein that "... the technique is feasible and may provide for a useful and economic means 1) for specifying surface conditions over which upper-air analyses are performed but surface data are unavailable, and 2) for incorporating dynamical upper-air prognostic information into long-range (e.g., 12–24-hour forecasts of surface weather conditions)." Although the procedure was tested on a simultaneous basis at stations withheld from the analysis, it has not been tested with prognostic charts. This will be done shortly.

A third study [42, 43] is much the same as the second in concept but the development sample of data and some of the predictors are different. The regression equations derived under this project are now being used by the Air Force in regular day-to-day forecasting of total cloud amount over the United States. However, the evaluation of the accuracy of these forecasts is still going on.

In light of the very considerable activity now going on in statistical prediction of cloud and present plans for continuing this activity, no additional work

is suggested.

4.3.3.8 Precipitation

A great deal of effort has been expended to develop objective methods for predicting precipitation. As far back as 1952 a bibliography of over 100 items was published [44] and many articles have appeared since then. No exhaustive inventory of the work in this field will be presented; instead a brief summary of the current situation follows.

Although hundreds of contributions to the theory of precipitation type, occurrence, and amount have been made the present forecasting procedures are largely empirical-synoptic. It is on the empirical side that objective procedures have been developed to incorporate both the forecaster's experience and ideas based on theoretical results. A variety of graphical correlation techniques have been attempted in which the predictor variables are features of height or pressure patterns observed at or during the predictand period of time. In practice, prognosticated maps of these parameters are used to prepare a forecast. The graphical correlation procedures developed by Brier [45, 46] are often employed to obtain the graphs. (See [47] for a typical example of the use of Brier's technique.) These empirical-type studies are usually of limited scope, applying to only one station or small area, dealing with only one facet of precipitation, such as occurrence vs. nonoccurrence, and able to handle only a few predictor variables. Nevertheless, they are in use at many stations and forecasters feel that they are valuable even though the final precipitation forecast is prepared subjectively.

A notable exception to the type of study described above is the work of Klein [17] and, on a smaller scale, that of Glahn [48]. Klein used screening regression to obtain regression equations for predicting 5-day precipitation amounts, in broad categories, at some 30 areas covering the United States. The predictions are plotted on a map and analyzed subjectively to produce a prediction at every point in the U.S. Such forecasts are now made routinely three times a week and formal verification indicates that these forecasts are quite good. Glahn used screening regression and factor analysis to develop

equations for predicting 24-hr areal coverage of precipitation in an area in Mississippi. His results were poor when tested on independent data. Both studies have in common that they used high-speed computers and, therefore, could handle a very large number of predictor variables; a much more realistic procedure than being forced, by the graphical procedure, to confine attention to as little as two predictors and to small data samples.

There appears to be a great deal of interest among forecasters on development of objective procedures for forecasting precipitation, and it is the opinion here that the time is ripe for a large-scale effort in this direction. Vast amounts of data are readily available, the statistical procedures appropriate to the problem are at hand and have been programmed for high-speed computers, and an enormous backlog of theoretical, synoptic, and empirical "know-how" is available. It is felt that the chances for success are very good indeed.

4.3.3.9 Fog

The situation in statistical prediction of fog is much the same as that in precipitation except on a somewhat smaller scale. There are numerous objective aids to fog forecasting, some are graphical involving the combined effects of two or more predictors, but many are simply tabulations of the subsequent occurrence of various types of fog when given the occurrence of some meteorological element such as wind direction or air-sea temperature difference.

The largest single effort in statistical prediction of fog did not deal with fog directly but with visibility at airports, with no consideration of the causes of the restriction to visibility (see [20]). The screening multiple discriminant analyses procedure was applied to develop methods for predicting visibility ranges in gross categories at seven stations in the United States. The resulting methods were applied to independent data and the forecasts were found to be somewhat better than persistence and slightly better than routine operational forecasts prepared subjectively. This work is being continued (by The Travelers Research Center, Inc.) and, therefore, no additional effort is recommended.

4.3.3.10 Planetary Boundary-Layer Shear

In Appendix J of this report Pandolfo presents a survey of boundary layer

winds. These are winds from the surface to approximately 5000 feet, but eliminating small-scale variations which were considered previously under turbulence. Pandolfo discusses refining the available nonlinear physical-mathematical models to relate the wind profile to simultaneous observations of horizontal pressure gradient forces, radiation, evaporation, clouds, and baroclinicity. Therefore, even if the new models prove realistic there will still exist the problem of predicting the elements affecting the wind profile. Prediction of boundary-layer wind shear by such models appears to be years away.

At present, predictions are made subjectively at U.S. Weather Bureau forecast centers of the wind at 1000-ft intervals up to 5000 feet for stations in the U.S. at which radiosonde observations are made. The wind profile can be obtained by drawing or fitting lines to these predictions.

Little effort has been directed toward statistical forecasting of winds from the surface to 5000 feet. It is felt that the time is ripe for such an effort. In a recent study, in which the author participated [26], the screening regression method was applied to forecasting surface winds at Idlewild Airport. It was found that the statistical forecast errors were 1/3 smaller than the subjective errors. These same procedures could be applied to the 500- and 1000-meter winds because a very large backlog of such wind observations are available at Asheville for rawin and rawinsonde stations in the United States. It would not be necessary to predict the 5000-ft wind because reasonably accurate 850-mb height forecasts are now being made routinely by the National Meteorological Center.

4.3.3.11 Upper-Level Winds

Although statistical methods have been used extensively in the climatology of upper-air winds, very little effort has been devoted to prediction. This is quite understandable because winds can be derived from heights of constant pressure surfaces and fairly accurate prognostic charts of the 850-, 500-, and 200-mb levels are being prepared and widely disseminated twice a day by the National Meteorological Center. The winds can be obtained by the geostrophic or gradient wind equation or by statistical methods. Two examples of such methods are St. John [49] and Spiegler, et al. [50].

For use in flight planning, St. John developed a series of regression equations relating the wind at dependent levels to stream-function forecasts. Spiegler derived regression equations for vertically extrapolating height values from prognostic 500- and 200-mb charts to produce prognostic height charts at stratospheric levels. Both St. John and Spiegler are attempting to refine their equations.

This two-stage procedure of first predicting heights by dynamical methods and then obtaining certain winds by statistical methods is, in our opinion, quite correct. It is highly doubtful that any statistical method could compete with the dynamical method for producing prognostic height charts. The interpolation or extrapolation to heights other than those of the prognostic charts could be done by other than statistical methods. However, both St. John's and Spiegler's work indicates that statistical methods give reasonably accurate predictions and both methods have been programmed for real-time use. In view of the continuing effort by both groups, no further work in statistical prediction of upper-level winds is recommended. This, of course, is subject to change if very special problems arise, such as nuclear fall-out, missile launching, or re-entry of spacecraft.

4.3.3.12 Ionospheric Charge Density and Structure

The amount of effort expended on research on the ion density and structure of the ionosphere is simply enormous. A bibliography of several hundred articles was prepared in June 1962 [51] and it was found necessary to compile a second bibliography only 4 months later [52]. No attempt will be made to cover the entire field, rather attention will be focused on one specific type of prediction.

Radiation from the sun causes ionization of the atmosphere at high altitudes in several distinct ionospheric layers or regions. In order of increasing altitude and increasing ion concentration, they are called the D, E, F_1, and F_2 regions whose approximate heights are 60--85 km, 85–140 km, 140–200 km, and 200–1300 km respectively. There is a generally accepted nomenclature for the properties of the different regions: N_mD, N_mE, N_mF_1, and N_mF_2 denote the maximum electron concentrations; h_mD, h_mE, etc. denote the heights of the peak concentrations, and fD etc. are the lowest radio frequencies which can penetrate

the various regions at normal incidence.

Predictions of these properties are made primarily for use in radio communication. The variation in the values of the properties affects transmission of different frequencies of radio waves in a complicated manner. In the United States, ionospheric prediction is made by the Central Radio Propagation Laboratory (CRPL) of the U.S. Bureau of Standards. Their predictions take the form of hemispheric maps of monthly median values of certain of the ionospheric properties at specific hours of the day. That is, there could be 24 maps, one for each hour, with isolines of $N_m F_1$. The method of prediction is a sort of climatology. It is known that the ionospheric properties have a diurnal, seasonal, and geographical variation and also a variation with the sunspot cycle. The diurnal, seasonal, and solar-cycle variations at any one station can be obtained from historical records, or, if none exist, by interpolation from nearby stations. When a prediction is to be made, the hour and season are known, and the position in the sunspot cycle is estimated by first taking an average cycle, made up from the past 17 cycles, then locating the current month's sunspot number in this average cycle and, finally, extrapolating one month ahead. This description is, of course, grossly oversimplified. For example, the "interpolation from nearby stations" is done by electronic computer using Fourier analysis and global spherical harmonics [53].

The CRPL predictions are monthly median values and do not forecast variations about the medians. These variations can be quite large. It is well-known that severe interference to certain kinds of radio communications, particularly in higher latitudes, is caused by sudden magnetic storms which, in turn, are due to sudden activity on the sun. Unfortunately, there is very little lag between the onset of such activity and the change in ion density. Although effort has been devoted to predict the storms, there has been only limited success. The only predictive information comes from the magnetic storm information itself in the form of some 27- and 54-day periodicity and from persistence of the last observed value.

There is now beginning a concerted effort to predict the time of onset of radiation hazardous to man in space. A good deal of data will be collected

for many indices of solar activity on very short cycling times. The greatest promise, for the near-future, in short-period ionospheric prediction is to relate these data to the values representing the various properties of the ionosphere. There is no doubt that the statistical prediction methods described in previous sections could be used extensively and profitably in developing such relations.

4.3.3.13 Ozone

The research effort devoted to ozone in the upper atmosphere, although not as huge as that devoted to the ionosphere, is quite large. Again, no attempt will be made to cover the field. However, there can be no concentration on any prediction methods because there does not appear to be any direct prediction whatsoever of ozone amounts, heights, or distribution. Research on ozone is motivated primarily by the effects of ozone on radiation. Absorption by atmospheric ozone produces a cut-off for solar radiation spectra at about 3000 angstrom units. The variations in the amount and height of ozone over the globe produce important effects on the radiational balance and heat transfer in the atmosphere; these in turn are of great importance in numerical models of atmospheric circulation.

There does not appear to be any inherent difficulty in predicting ozone amounts and distributions. From theoretical considerations and observational evidence it is know that there are height, latitudinal, seasonal, air mass, diurnal, and synoptic variations in amount of ozone. There have been a number of studies relating ozone amounts to meteorological factors on a contemporaneous basis. For example, in [57] total ozone amount is correlated with temperature, geopotential height, and north-south wind component at 100 mb. Quite respectable correlations are obtained. In [55], significant correlations were obtained between ozone amount and vertical movements, temperature, and vorticity at the 100-mb level. And, as a final example, the relationships between ozone and meteorological-factors, i.e., 250-mb height, tropopause height, 100–30-mb thickness, etc., were analytically investigated in [56]. Thus, by predicting these stratospheric factors and using the proven simultaneous relationships predictions of ozone could be made.

If ozone predictions are ever needed, there is no doubt that the predictions could be made statistically. In fact, at the present time, it is the opinion here that this is undoubtedly the best method. The theory of ozone production by photochemical reaction, the principal cause, is reasonably well-known. But the ozone remains in the atmosphere for considerable lengths of time and is subject to movements, both horizontal and vertical, by the stratospheric and upper-tropospheric winds. So prediction of the winds is required, along with some knowledge of the current distribution of ozone and the relationships between ozone amounts and the wind. All these factors are amenable to statistical analysis.

4.3.4 Oceanographic Phenomena

There is much less statistical prediction in oceanography than in meteorology. There appear to be four main causes: meteorological prediction directly affects many more people and, consequently, a greater effort is devoted to it; oceanographic observations are much more expensive to obtain than atmospheric observations and, therefore, long series of relatively homogeneous data required for development of statistical methods are not available for many parameters and in many areas; until the recent establishment of the National Oceanographic Data Center, the observations were not in a form suitable for use in high-speed computers; and, finally, many oceanographic prediction problems are wholly or partly meteorological in nature (an outstanding example is the prediction of ocean wave heights).

There are some highly sophisticated statistical techniques being used in oceanography today, primarily for describing the state of the sea by spectral analysis. (See [57] for a description of ocean wave spectra.) However, this same degree of sophistication does not carry over to oceanographic prediction except in isolated cases. It is the opinion here that this situation should be corrected and that several oceanographic prediction problems can be solved by statistical methods. Some examples are given in the sections following.

4.3.4.1 Surface Waves

The effort devoted to the prediction of surface waves far exceeds that

devoted to any other prediction problem in oceanography. The reason for this is probably the importance of such forecasts to the Navy, where so many operations conducted at sea are affected by surface wave conditions, to civilian ship operations, to off-shore oil drilling, etc.

By far the best source of information about the present status of research on wind-generated waves is Ocean Wave Spectra, the proceedings of a conference held at Easton, Maryland in 1961 [57]. Some 30 formal papers are presented along with a good deal of formal and informal discussion. Scattered throughout this volume is considerable information on prediction of surface waves. A review article on wind waves is given in [58] and a brief summary of research in 1960-62 is given by Pierson [59].

The theory on wave generation is not sufficiently advanced to have forecasts produced by, say, a set of dynamic equations. In 1956, Ursell stated flatly that, "[knowledge of] the generation of waves by wind and growth of the wave spectrum [is] at the present time with few exceptions either empirical and concerned only in part with hydrodynamics or theoretical and incapable of explaining the facts" [60]. Five years later, Barber and Tucker echoed this sentiment by stating, "The fundamental theory of the generation of waves by wind has not yet reached the stage where it usefully can be applied to practical wave prediction....Though some practical wave predictions are based on formulas derived partly theoretically, the theory is in all cases unsatisfactory, and the formulas can only be relied upon to the extent to which experience has shown them to be reliable" [58].

In any forecast problem the first task is to decide what to forecast and for surface waves this is not as simple as for the meteorological examples discussed in Section 2. A complete description of an observed wave pattern is an extremely complicated affair. The present trend in oceanography is to apply spectral analysis to reduce the number of values needed to describe a chaotic sea and, because of difficulties in observation, most attention has been directed toward one-dimensional spectra wherein the direction of the waves is ignored and all that is measured is the mean square oscillation of the sea height over a

scale of frequency. The spectrum is then taken to be related to the speed, duration, and fetch of the surface wind. Unfortunately, there is considerable disagreement about the form of this relationship. A number of "theoretical" wave spectra have been worked out and published by various authors but when given the same wind characteristics the resulting spectra are different. Walden [61] has discussed some of these differences.

Despite all these difficulties wave forecasts are being made on a routine basis. As would be expected from the above discussion there are differences of opinion about the best way to produce these forecasts with each country using a somewhat different procedure. Here in the United States, the two primary methods are those devised by Pierson, Neumann, and James [7] and the method that evolved from the work of Sverdrup, Munk, and Bretschneider [62].

The day-to-day forecasting operations are carried on in the United States by the U.S. Navy Fleet Numerical Weather Facility at Monterey, California under the direction of Commander Paul M. Wolff. Their procedures are described briefly in three progress reports [63]. They do not predict the spectrum but the "significant wave height" which is defined as the arithmetic mean of the heights of the highest one-third of all waves. They go through a four-stage procedure of first predicting the 500-mb height surface, then the sea-level pressure field, which in turn is converted to a sea-level wind field, and finally this is used to forecast the waves. In a continuing operation such as this one it is dangerous to detail the methods used in each stage because they change so often. Nevertheless, a brief description is presented below in order to aid in understanding a subsequent discussion on the possible role of statistical techniques.

The 500-mb heights are forecasted by a two-level barotropic model. The surface pressure forecast includes part of the 500-mb height change added to a temperature advection term at 850-mb to produce a surface tendency. They have modified this procedure to include better measures of steering and they are using the Veigas-Ostby statistical forecasts of the movement and central pressure of cyclones. The winds are obtained from the surface pressures by taking 75 percent of the geostrophic winds and turning the wind 15 degrees

across the isobars toward lower pressure. The factor of 75 percent is reduced to 60 percent for southerly winds. The sea and swell forecasts are derived from the wind field using the methods of Sverdrup, Munk and Bretschneider. An empirical correction is added to the forecast by comparing the forecasted values to those observed at weather ships. At the end of the month a ratio of the two is obtained and is used to adjust the forecasts in the subsequent month.

Although there are empirical correction factors used in the present procedure, statistical prediction methods are not used at any stage. In the first stage, the 500-mb forecast, it is highly doubtful that any statistical method could do as well. In the second stage, the sea-level pressure forecast, the situation is not so clear-cut. Klein [17] has developed a series of regression equations for obtaining sea-level pressures from upper-air prognostic charts. On a limited scale he has applied the equations and compared his results with similar forecasts made by the National Meteorological Center using the Reed model. His forecasts compare favorably and are particularly good over the oceans. Work similar to Klein's is being pursued at The Travelers Research Center, Inc. and plans are underway to compare these forecasts with both Klein's and the Reed model forecasts. Apparently there have been no comparisons of forecasts by any of these three methods with those produced by the Fleet Facility. This is, in our opinion, an error. As stated by the Fleet Facility, the major sources of error in forecasting waves is in forecasting the winds. At the very least, the work planned to compare the three other methods should include the Fleet Facility's forecasts.

Obtaining winds from pressures is almost a field in itself. That the Fleet Facility has run into difficulties is evident from their use of a different factor for southerly flow. Further, the use of a 15 degree turning and a reduction factor of 70 percent are more or less arbitrary. Statistics could help here by relating the pressure field to observed winds, say at weather ships, by means of regression equations. With the use of screening regression a great many factors could be taken into consideration, such as time of day, season, direction of the wind, curvature of the isobars, latitude, nearness to coasts, etc.

The fourth stage, obtaining sea heights from the wind field, is essentially an empirical procedure involving the relationship between the sea heights and periods as a function of wind speed, duration, and fetch. In August 1963 a new swell-forecast program was being planned by the Fleet Weather Facility to obtain the highest swell which would reach any point by estimating the speed and direction of movement of waves generated in stormy areas. It is not known at this time whether statistical procedures can be of use here.

Two final points are of importance. The first one concerns verification, or the lack thereof, of the forecasts. Although statements are made in the progress reports [63] about the accuracy of the sea-height forecasts there does not appear to be any formal program of verification or, at least, the results are not published. Although such verification is not an easy task because of the errors in observation of wave heights, it is difficult to see how improvements in forecasting can be made if we cannot measure the results of new techniques, and it is also difficult to see how the forecasts can be used if no one knows how good they are. Before any statistical methods can be used in the forecasting procedure it is essential that verification results be published.

The second point is much more radical: why go through the entire forecast procedure at all; why not go directly from the upper-air prognostic charts to sea height forecasts by means of a statistical prediction procedure such as regression or discriminant analysis? Admittedly, this is a large task but, because of the present state of the theory, it may do as well or better than the present procedure. <u>It would be desirable to give some attention to this idea, at least to the point of conducting a feasibility study.</u> The spectra computed by Moskowitz from sea-borne wave-recording equipment aboard British weather ships [64] would provide an excellent source of data for such a study.

4.3.4.2 Internal Waves

No prediction of any kind appears to have been attempted and the data available are far too sparse for development of any statistical prediction methods.

4.3.4.3 Ocean Currents

There is insufficient data to develop any statistical technique for predicting either surface or subsurface ocean currents. For tidal currents the situation is a little different. The astronomic and gravimetric forces that cause tides are quite well-known [65, 9]. These give an equation with tide height expressed as a function of 37 trigonometric terms. The terms have unknown constants which depend on location and these are determined from observations by a least squares procedure. The procedure has recently been programmed for high-speed computers [66]. Since quite accurate estimates of the tide height can be computed for any instant of time, then good estimates of the tidal current can be obtained by examining the physical characteristics of the tidal current area. It is felt that this procedure would probably prove superior to any statistical method.

4.3.4.4 Tsunamis

Tsunamis are long waves in the ocean excited by sudden disturbances in the earth's crust caused by earthquakes, land slides, or submarine volcanic eruptions. The waves traverse the oceans to distant shores where they may cause substantial loss of life and property. Long waves can be generated by underwater nuclear explosions, but such waves contain much less energy than the larger, naturally-caused, waves [67].

There are two parts to the prediction problem, time of arrival of the waves and their height. The U.S. Coast and Geodetic Survey (CGS) maintains a tsunami warning system in the Pacific Ocean area to furnish estimated times of arrival at various islands and coastlines. They use the method devised by Zetler [68] and in real-time forecasting the estimated and actual times of travel of the waves agree within 2-1/2 percent. Some work is being pursued to reduce even this small error by obtaining better measurements of the depth of the ocean bottom and recomputing the path from an earthquake epicenter to the tidal guage. Certainly, no statistical method could do as well.

The situation in predicting the height of the waves is much different. The CGS does not issue height forecasts because of the difficulty of the problem. There have been several attempts to relate seismic measurements to tsunami

activity but Munk concludes that, "The observed fact is that two earthquates which are seismically undistinguishable with regard to location and evergy can generate tsunamis whose amplitudes differ by an order of magnitude" [69]. Another factor is that no one has ever seen or measured a tsunami in the open ocean. Tide guage records represent most of the tsunami data presently available but these are almost all in bays and harbors and are not representative since movements of the gua by even a few hundred yards change the records considerably. Zetler, et al. [70] have outlined some research being carried on to improve the height forecasts and Van Dorn [71] has summarized current research on tsunamis.

It is concluded that at the present time statistical methods have little to offer to improve forecasting of tsunamis.

4.3.4.5 Storm Surges

Surges are abnormally high water levels along the coasts associated with the passage of hurricanes and other severe storms [72]. From the point of view of the spectrum of sea level, surges have dominant periods of 1 to 100 hours, falling between the tsunamis and the lower frequency astronomical tides [73]. The water lefel due to the storm is the deviation of the level from what would have occurred in the absence of the storm or, in practice, the normal level due to tides.

A great deal of effort has been and is being devoted to developing methods for predicting surges, see [73], [74], [75], [76], and [72] for reviews of surge prediction. A few highlights follow.

Numerical-dynamical approaches to surge prediction have led to a better understanding of the surge phenomena, but they have not led to the development of any outstandingly successful prediction system. As far as can be ascertained, none of the countries making surge predictions are using the numerical approach. This is in sharp contrast to Welander's optimism in 1961 [74]. But, as pointed out by Harris, "A unified theory of the hydrodynamic processes involved in storm surge generation has been proffered by Fortak [77] ... but much additional developmental work will be needed before the results can be used in quantitative calculations."

A second approach is essentially statistical. These use direct relations between the wind and pressure and the height of the surge at some specific tide guage. This latter condition eliminates the need for considering the physical characteristics at and near the guage—e.g., bottom bathymetry, size and shape of harbor or bay, orientation of sea coast, flatness of land, etc.—which influence the surge over and beyond the influence of the storm. Articles have appeared describing the development of such relationships at locations in the United States, Japan, Great Britain, Germany and the Netherlands. These relationships are being used by the meteorological services in routine operations at least in the United States [78] and Japan [79] and probably in other countries as well.

Recently, the screening regression technique has been introduced into storm surge forecasting, the work of Pore [80] being an excellent sample. Pore developed multiple regression equations for predicting storm surge at Atlantic City from on-shore and along-shore wind components, and atmospheric pressure at three stations with various time lags. When tested on independent data, the forecast root-mean-square-error was about 0.5 for 6-hour forecasts.

This work of Pore, and other work, particularly by Harris, clearly indicate that the statistical technique of screening regression can be used to develop useful forecasting equations. It is strongly recommended that the method be applied to other stations. Also, the method should be tested with prognostic data as input to the regression equations to measure the forecast accuracy for periods beyond six hours.

4.3.4.6 Oceanic Turbulence

An exposition of the various sized eddies and vortices encompassed in the term "oceanic turbulence" is given by Gates in Appendix S of this report. They range from fine-grain turbulence of less than one meter to wind-driven gyres thousands of kilometers across. Thus, the prediction of any movement of the sea may be considered to be prediction of "oceanic turbulence". It is felt that the discussions of statistical predictability presented here in Section 4.3.4 adequately cover oceanic turbulence. The scales of motion for which statistical predictibility appear to be feasible include tidal vortices (Section 4.3.4.3), and sea-surface wave

eddies (Section 4.3.4.1), including storm surges (Section 4.3.4.5).

4.3.4.7 Submarine Eruptions

Submarine bottom slides and volcanic eruptions are of interest because they may cause tsunamis. See Section 4.3.4.4 on tsunami prediction and Section 4.3.2 on prediction of geological phenomena.

4.3.5 Other Phenomena

4.3.5.1 Visual Phenomena

Included in the term "visual phenomena" are rainbows, sun dogs, St. Elmo's fire, and mirages. Rainbows and mirages do not need to be defined. Sun dogs, also called parhelia, are two colored luminous spots that appear at points 22^{o} (or 46^{o}) on both sides of the sun at the same elevation as the sun. They are produced by refraction in hexagonal crystals falling with principal axes vertical. St. Elmo's fire, also known as coronal discharge, is a luminous and often audible discharge which occurs from objects, especially pointed ones, when the electric field strength near their surfaces attains a value near 1000 volts per cm. St. Elmo's fire sometimes develops on aircraft flying through active electrical storms and on yards and masts of ships at sea during stormy weather [81].

It appears that no prediction whatsoever has been attempted for any of the four visual phenomena. Statistical prediction methods do not appear to be practical at the present time because no historical sample of data is readily available. The best approach to developing prediction methods appears to be a physical one. The meteorological conditions giving rise to the phenomena are reasonably well-known and, therefore, the prediction problem reduces to predicting these meteorological factors.

4.3.5.2 Magnetic Storms

Some remarks on prediction of magnetic storms are given in Section 4.3.3.12. The possible prediction of solar flares, discussed in the following section, is of interest also because magnetic storms are associated with enhanced solar activity.

4.3.5.3 Hazardous Interplanetary Radiation

If operations in the space environment follow the course of operations in the air environment, there will be growing need for prediction of hazardous space environmental conditions. It appears that energetic solar corpuscular radiation is the most serious hazard to manned space flight and that such radiation is associated with the occurrence of large solar flares. Thus, the prediction of flares is important.

Flares, at least large ones, are usually short-lived phenomena, increasing to maximum brightness in 5 to 10 minutes, with a slower decline which typically lasts 20 to 30 minutes. Flares occur only in active solar regions, they vary considerably, both in size and brightness, and their shapes are highly irregular.

A host of solar phenomena, for possible use in flare prediction, are observed either optically, at radio frequencies, or as a consequence of their geophysical effects. Although the mechanisms producing these phenomena, and in particular those that appear to be responsible for energetic particle emission, are not completely understood, a com[illegible]rrangement of partial associations is known to exist among the various pheno[illegible]ecause of the lack of knowledge of the physics, it is felt that the application of statistical techniques would provide a promising avenue for the development of prediction techniques. Some considerations on such an approach follow.

As a first step, the prediction of flare occurrence in a pre-existing active region could be considered. The predictand would be the probability of occurrence of a flare falling into a specified class within a specified time period. The predictors would include, among other variables, those features of sun which provide evidence of the appearance of an active region, including photospheric faculae, chromospheric plages, and sunspot values. For very short periods, 0-24 hr, the past history of solar flare activity would probably prove to be a good predictor. The statistical techniques of autoregression and multiple discriminant analysis appear to be particularly applicable here.

A second step might include the prediction of the development of new active regions, a process requiring several days. While this prediction problem is important, it is extremely difficult because it involves the prediction of both the time and place of occurrence. On a longer time scale, the general level of solar activity might be predicted. Such predictions would be phrased in general terms applicable to one or more solar rotations. In both these problems, the statistical technique of screening multiple discriminant analysis would be applied.

4.4 The Predictability of Geophysical Phenomena by Dynamical Methods*

4.4.1 Introduction

In the present survey, only those geophysical phenomena which are in some respect predictable by dynamical methods are considered. The many interesting phenomena for which there exist only statistical or empirical prediction methods are therefore excluded. Here we shall consider a dynamical method as one based upon a theoretical formulation for the occurrence, development and/or dissolution of the phenomena, or one which theoretically prescribes the phenomena's structure in terms of the primary variables or parameters.

For each meteorological and oceanographical phenomenon for which there exists a significant dynamical predictability, we shall briefly consider the phenomenon's characteristic time and space scales, and present relative estimates of the dynamic predictability of the phenomenon's location, structure and behavior during the occurrence, development and dissolution stages.

These predictability estimates aremade on a subjective basis and the stated accuracy or percentage predictability should be understood as the percentage of the natural variability which is accounted for by prediction. It should also be noted that these estimates are based upon present operational capability as well as the capabilities of presently feasible systems. Some of the developments which appear necessary to attain and even surpass these predictability levels are also briefly discussed.

*By W. L. Gates

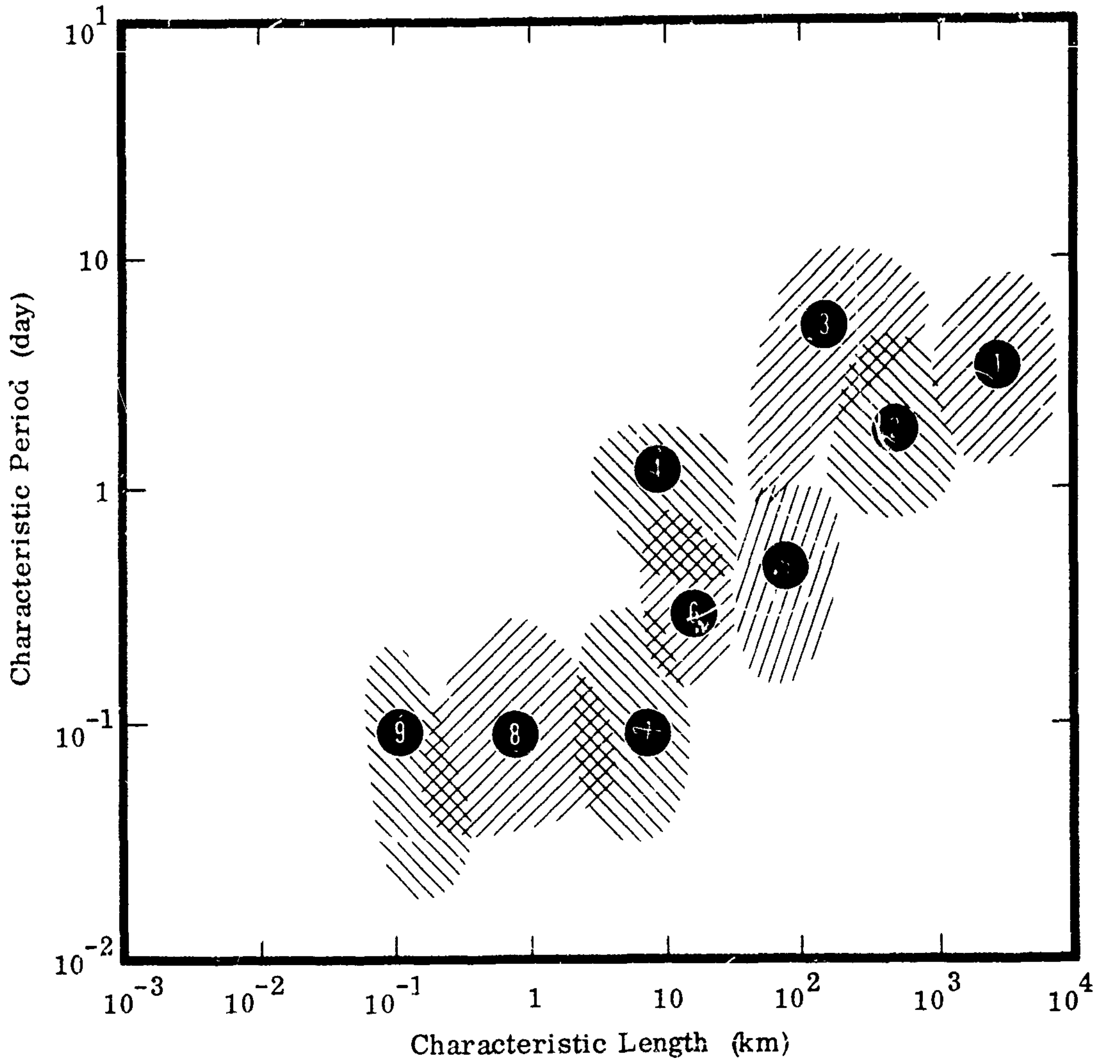

1. Large-scale atmospheric disturbances.
2. Synoptic-scale atmospheric disturbances.
3. Hurricane
4. Internal and orographic waves
5. Squall line
6. Sea breeze
7. Thunderstorm
8. Convective cloud
9. Tornado

Fig. 4-1. Summary of atmospheric phenomena.

4.4.2 Large-scale Atmospheric Disturbances

4.4.2.1 Dynamic Predictability Summary

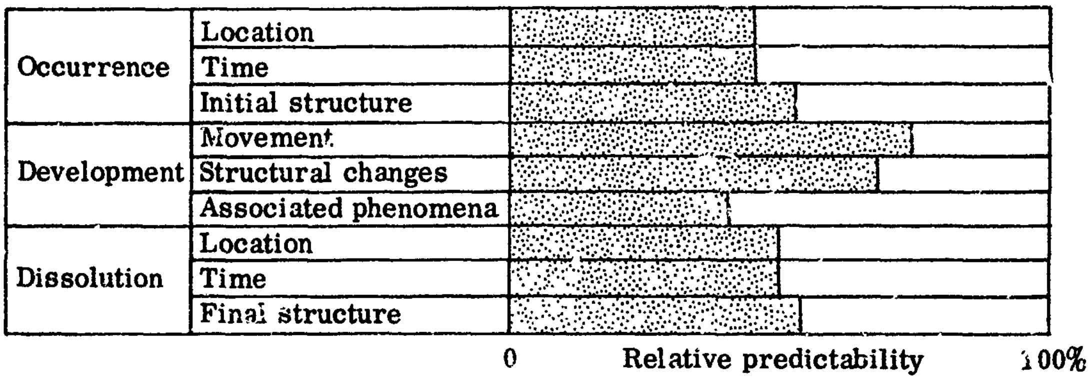

4.4.2.2 Introduction

The large-scale atmospheric disturbances or long atmospheric waves are the major disturbances of the world-wide atmospheric circulation, and are responsible for the bulk of the atmospheric heat and momentum transport. The first practical demonstration of the dynamical predictability of these disturbances was made in 1950 [82], and has subsequently been somewhat extended and developed as the familiar area of numerical weather forecasting. On the basis of the barotropic model [83], the movement and structural changes (intensity and shape) of the large-scale mid-tropospheric disturbances are now routinely forecast over the northern hemisphere [84], with approximately 60% of the observed variance accounted for at 500 mb over periods of a day or two. The use of baroclinic models results in an increased accuracy in the development stage, as well as handling the associated lower-level distrubances more adequately [85]. The use of such models also permits the prediction of certain aspects of the occlusion process.

4.4.2.3 Predictability Survey

4.4.2.3.1 Occurrence

4.4.2.3.1.1 Location

The position of an incipient large-scale disturbance is given by baroclinic models generally in the vicinity of intense wind shear and large horizontal temperature

gradients. An accuracy of about ± 600 km exists for the position of an incipient wave trough on the basis of 3- and 4-level baroclinic models [86, 87].

4.4.2.3.1.2 Time

The time of occurrence of a large-scale disturbance can be predicted with an accuracy of about ± 6 hr with the multi-level baroclinic models [86], but even then a relatively large number of occurrences will probably not be forecast.

4.4.2.3.1.3 Initial Structure

The structure of the incipient disturbance is given with any significant accuracy only by the higher-resolution baroclinic models [85]. A reasonable gross structural representation is also given by the linearized dynamic models for the three-dimensional temperature and wind distrubitons [88]. The initial pattern of large-scale vertical motion is also apparently well-described by even the simpler baroclinic models [89, 90].

4.4.2.3.2 Development

4.4.2.3.2.1 Movement

The movement of large-scale disturbances is perhaps the best forecast of all the phenomenon's characteristics. The mid-tropospheric (500 mb) displacement is forecast for 24–36 hr with an accuracy of approximately 75% by the barotropic and simpler baroclinic models [89, 84]. The correlation coefficients between the predicted and observed 500-mb height changes, for example, are about 0.80, 0.70, and 0.60 for 1-, 2-, and 3-day predictions [86].

4.4.2.3.2.2 Structural Changes

The characteristic structural changes in a developing large-scale disturbance are reasonably well forecast by the baroclinic models [86], although there is a marked tendency for error under certain conditions [85]. The intensity of the disturbance is often overforecast by as much as 100% in 2- or 3-day predictions by the most advanced models, and systematic errors in the temperature and wind fields over coastal and mountainous regions have been noted.

4.4.2.3.2.3 Associated Phenomena

The phenomena associated with a developing disturbance in large-scale flow which can presently be predicted by dynamical methods are the wind speed and the expected large-scale cloudiness and precipitation. Here the overall accuracy in wind prediction represents approximately a 50% relative predictability, or about a 10-knot mean vector error at 500 mb in a 24–36-hr forecast [86]. The large-scale cloudiness has a similar predicability, while precipitation is somewhat less predictable by these methods [91].

4.4.2.3.3 Dissolution

4.4.2.3.3.1 Location

The location of the occlusion of large-scale disturbances cannot at present be predicted dynamically with an accuracy greater than ± 1000 km.

4.4.2.3.3.2 Time

The timing of the disturbance dissolution is probably predictable to within about ± 1 day in most circumstances. Stagnation and/or regeneration of a large-scale disturbance are at present poorly handled by dynamical models [86].

4.4.2.3.3.3 Final Structure

The structure of a dissipating large-scale disturbance may be envisaged in a general fashion from theoretical analyses [88]. These results are only grossly matched by actual dynamical forecasts; the final structure is somewhat less well predicted than is either the initial or developing structure [92].

4.4.2.3.4 Predictability Extension

The basic equations of atmospheric dynamics form the basis of the predictability discussed above, and for the large-scale disturbances the effects of irregular terrain, heating and friction have only been introduced provisionally [93]. The more comprehensive representation of these processes appears as a major problem for the improvement of the predictability of the large-scale flow [94]. In the production of practical numerical forecasts by dynamical methods, the relatively poor synoptic data coverage over large regions of the earth presents a second major problem for predictability improvement. This error, together with those associated

with the numerical computations themselves, may account for about 50% of the present predictability error over periods of 1–2 days [95]. Further refinements in the dynamical models themselves, particularly the use of multi-level primitive equations, should further increase the predictability close to that ultimately attainable with a given data and observational resolution over periods of 2–3 days. It seems likely that significantly accurate dynamical predictions beyond 3 days, however, will require a much more sophisticated treatment of the atmospheric energy sources and sinks on both the large and smaller scales than has heretofore been undertaken. In particular, the processes of energy exchange with the higher atmosphere and with the oceans may largely control the longer-term behavior of the large-scale disturbances.

4.4.3 Synoptic-scale Atmospheric Disturbances

4.4.3.1 Dynamic Predictability Summary

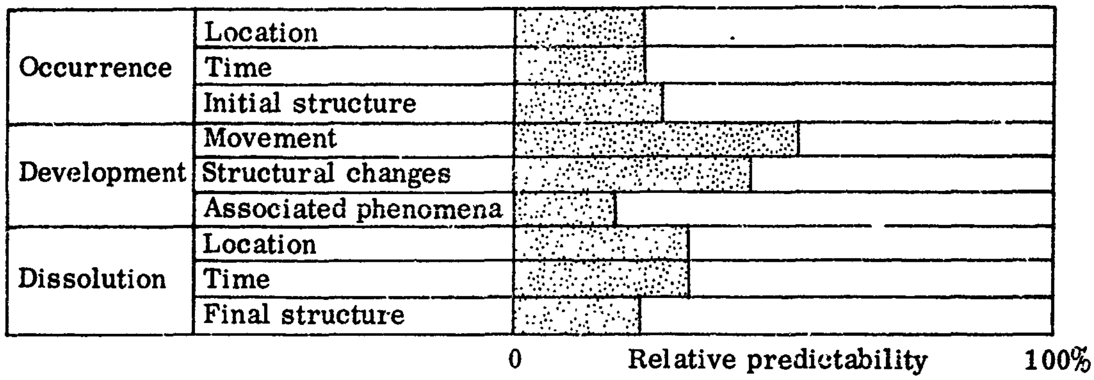

4.4.3.2 Introduction

Synoptic atmospheric disturbances are represented by the synoptic-scale weather systems often found in the lower atmosphere. These disturbances may be associated with frontal waves near the earth's surface, for example, or be waves in the subtropical easterlies. The predictability of these disturbances by dynamical methods is generally somewhat less than that of the larger-scale atmospheric disturbances. This circumstance appears to be due to the relatively more prominent roles played by heating and friction on the smaller scale motions near the earth's surface, and to the generally less adequate data resolution on this scale. The synoptic atmospheric disturbances are consequently somewhat better predicted at the present time by empirical and synoptic methods than they are by dynamical methods as herein defined.

4.4.3.3 Predictability Survey

4.4.3.3.1 Occurrence

4.4.3.3.1.1 Location

Only a relatively low dynamical predictability exists for the location of the occurrence of synoptic-scale disturbances; their location appears to be governed mainly by the lower-level mesoscale wind and temperature fields, which are themselves only poorly predicted. An overall accuracy of about ± 300 km may

be estimated, which is a major fraction of the distrubances' characteristic wavelength.

4.4.3.3.1.2 Time

The time of occurrence of synoptic-scale disturbances is likewise poorly predicted by dynamical methods. Probably an accuracy of ± 1/2 day is attainable, inasmuch as they are more likely to occur in favored portions of the larger-scale disturbances' life cycle.

4.4.3.3.1.3 Initial Structure

Relatively little of the synoptic-scale disturbance's initial structure is predictable by present dynamical methods and with present data coverages. That predictability which is present is due almost entirely to theoretical analyses of the initial structure of idealized synoptic perturbations [87, 88]. These studies describe the initial wind and temperature fields, together with the associated convergence and vertical motion.

4.4.3.3.2 Development

4.4.3.3.2.1 Movement

The synoptic-scale disturbances' movement is perhaps their best dynamically-predicted characteristic; this predictability is closely tied to that of the larger-scale disturbances in the middle and upper troposphere.which frequently guide the movement of the smaller-scale features. The forward speed of the synoptic-scale disturbances is often underestimated by approximately 20% [90], and their movement is seldom predictable beyond that of the large-scale flow, i.e., about 2 days. Hence, the uncertainty in their position during movement and development is about ± 400 km.

4.4.3.3.2.2 Structural Changes

Only the general shape and intensity of the developing synoptic disturbance is at present dynamically predictable [86]. The motion and temperature fields associated with developing frontal waves have been studied, and represent a fair degree of predictability for the steady case.

4.4.3.3.2.3 Associated Phenomena

The occurrence of cloudiness and rain accompanying the developing synoptic disturbance is at present poorly predicted by dynamical methods. This is no doubt due to the dominant effects of small-scale topography and cloud thermodynamics, neither of which are well predicted. The surface and lower-level wind fields are likewise poorly predicted by dynamical methods.

4.4.3.3.3 Dissolution

4.4.3.3.3.1 Location

The dynamical predictability of the location of dissolution of a synoptic-scale disturbance is difficult to assess, although it is probably of an inherently low quality at present. A certain number of synoptic-scale disturbances develop into identifiable large-scale features (including hurricanes); in these cases their dissolution is discussed in Section 4.4.2. Otherwise, an accuracy of approximately ± 500 km appears reasonable.

4.4.3.3.3.2 Time

An accuracy of about ± 1 day seems applicable, and represents in many cases approximately half of the synoptic-scale disturbances' life-time.

4.4.3.3.3.3 Final Structure

The disturbances' final structure is dynamically predictable with about the same accuracy as are the developmental structural changes. Qualitatively this stage represents a relative reduction of wind and temperature gradients. Low-level frictional and non-adiabatic effects are dominant at this stage, and often the synoptic-scale disturbance (i.e., those which do not develop into a larger-scale system) is lost or disappears from the synoptic data network when it is of small or decreasing amplitude.

4.4.3.4 Predictability Extension

Due to the mesoscale character of the synoptic disturbances, an increased data coverage would undoubtedly contribute directly to an increased predictability by dynamical (as well as other) methods. The uncertainties in initial position and structure are such that the later movement and behavior of the disturbances

are rather poorly predicted at present. The dynamical tools appear to be available to treat more adequately these disturbances once they are well documented [90]. In particular need of further improvement, however, are the treatments of frictional and diabatic effects, especially in the lowest 1 km or so. To increase further the synoptic-scale disturbances' dynamical predictability, it would appear to be necessary to consider the energy transfers between this scale and that of the large-scale disturbances, as well as with the yet smaller-scale flow of the sub-synoptic disturbances.

4.4.4 Hurricanes

4.4.4.1 Dynamical Predictability Summary

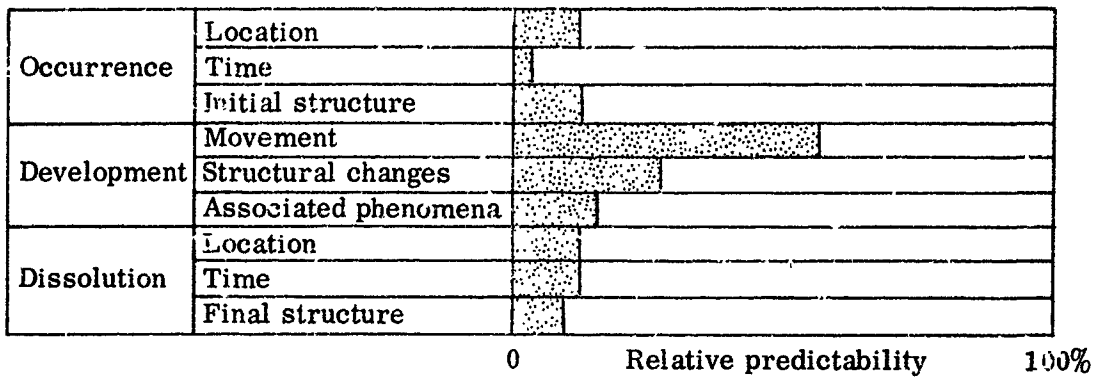

4.4.4.2 Introduction

Hurricanes are perhaps the most violent of the larger-scale disturbances in the atmosphere, and their prediction is a matter of considerable practical importance. It is only recently, however, that a time dynamical predictability has been developed, although the present overall level of accuracy now achieved by these techniques is probably inferior to that attainable with empirical and statistical procedures. The problem of hurricane formations, however, is poorly handled by all methods, and it is here that dynamical methods may make a unique contribution when adequate observational data are available.

4.4.4.3 Predictability Survey

4.4.4.3.1 Occurrence

4.4.4.3.1.1 Location

The location of hurricane genesis cannot at present be dynamically predicted with great accuracy, although the dynamic and/or baroclinic instability of the large-scale circulation may be a useful precursor [96, 97]. Many hurricanes also develop in association with a pre-existing easterly wave. The intensification of such conditions into actual hurricanes, however, can only be regarded as dynamically experimental [98]. An overall accuracy of about ± 1000 km may be estimated.

4.4.4.3.1.2 Time

The timing of hurricane formation is quite poorly predicted by dynamical methods; it could probably even be argued that such a predictability does not now exist. The timing accuracy would therefore certainly be of the order of days.

4.4.4.3.1.3 Initial Structure

The forming hurricane's initial structure is poorly predicted by dynamical methods. Those few attempts which have been made [98] do not reveal convincing skill and the causative dynamical mechanisms are unclear. There is rather general agreement, however, that the latent heat of condensation is a critical factor in the mature hurricane's maintenance and it may be conjectured that it is likewise important in the storm's early stages. The present dynamical models all display a maximum growth rate for cloud-scale systems, rather than for disturbances of hurricane scale [99, 100, 97], so that from this viewpoint the hurricane itself is not actually being predicted.

4.4.4.3.2 Development

4.4.4.3.2.1 Movement

Once the hurricane circulation has assumed a distinct identity, its movement during the growth and development stage is predictable by dynamical methods with a useful accuracy for periods of 1–3 days. Use of a barotropic model for mid-tropospheric flow as a "steering current" for the hurricane vortex gives 1-, 2-, and 3-day displacement forecast errors of the order of 150, 300, and 450 naut. mi., respectively [101, 102, 103, 104]. Such techniques all appear to systematically underestimate the hurricane's forward speed by about 25%, and often show a tendency to deflect the vortex to the right of the downstream steering current [105]. The speed prediction error may be reduced through use of a finer mesh [106], although significant error remains. Some further small improvement in displacement prediction may be possible by using a baroclinic steering model [107].

4.4.4.3.2.2 Structural Changes

Only a part of the structural changes accompanying the intensification

of a hurricane are at present dynamically predictable. The growth of an initially symmetrical circulation has been treated [108, 98, 109], but the intensification is generally much too rapid. The vertical circulation system and the development of descent in the hurricane core have been successfully predicted only for a few hours' time [108], and the hurricane eye is not yet clearly indicated. The critical factor in these dynamical predictions appears to be the release of latent heat of condensation, which strongly favors growth of the cloud-scale motions. Frictional effects may offset this tendency to some extent, but unless very large eddy frictional coefficients are employed the difficulty remains [98, 99].

4.4.4.3.2.3 Associated Phenomena

In view of the relatively limited dynamical predictability of the developing hurricane's structural changes, there is little dynamical predictability of the associated phenomena such as rainfall and surface wind. Both of these phenomena may attain extreme values in the hurricane, and at present their predictability is almost entirely empirical and/or statistical.

4.4.4.3.3 Dissolution

4.4.4.3.3.1 Location

Very little dynamical predictability now exists for the location, time and/or structure of the dissipating hurricane, except in those cases in which the hurricane dissolves after moving over land. In these cases, an estimate of the dissolution stage (assuming an accurate movement prediction) may be made with an accuracy of about $\pm$ 1 day and $\pm$ 500 km. Frictional damping at the ground appears to weaken the circulation rather rapidly. For most hurricanes, however, dissolution occurs after they have been effectively transformed into extra-tropical systems, and this process is somewhat more difficult to predict from the hurricane circulation itself than is the analogous dissipation of an initially large-scale disturbance.

4.4.4.3.3.2 Time

See Section 4.4.4.3.3.1 (above).

4.4.4. 3.3.3 Final Structure

See Section 4.4.4. 3.3.1 (above).

4.4.4. 4 Predictability Extension

The successful prediction of a developing hurricane circulation may be furthered by recent efforts to parametize the cloud-scale motions with respect to the hurricane-scale flow [110]. The release of latent heat on a small scale may drive the larger-scale circulation, which in turn supports the cloud-scale convection through the surface frictional convergence. In this sense friction promotes the hurricane development as long as a water vapor source is available. Further refinement of large-scale dynamical models should also contribute to greater predictability of hurricane displacement. Basic to all such increases in predictability is, of course, the requirement for much more complete measurements of the velocity and temperature fields in and around the hurricane itself; the best present data consist of a few radial penetrations by aircraft, which tends to restrict dynamical considerations to composite and/or axially synmmetrical models.

4.4.5 Internal and Orographic Waves

4.4.5.1 Dynamical Predictability Summary

4

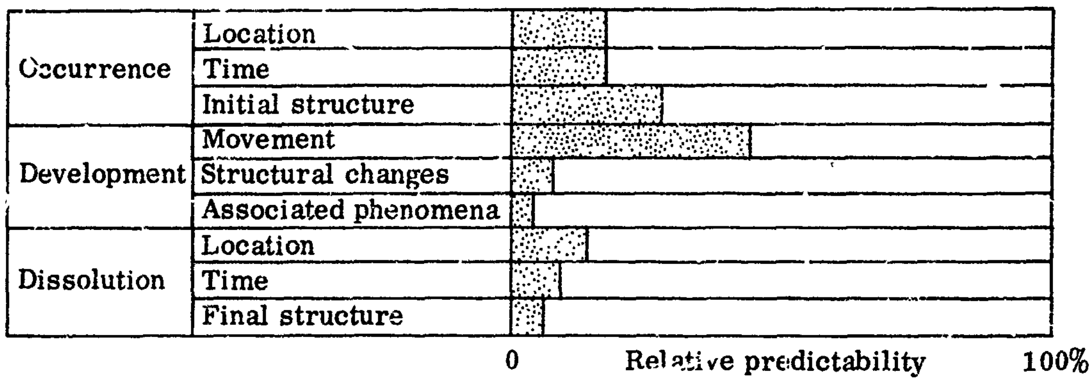

4.4.5.2 Introduction

Internal and orographic waves are of intermediate scale and represent modes of internal atmospheric response to locally large vertical temperature and/or wind speed gradients, or represent modes of forced response to irregular terrain, possibly modified by the internal atmospheric structure. In the case of internal waves, the most favored location seems to be near frontal zones or sharp inversions; for orographic (or mountain) waves, a suitable obstacle in the path of the air flow may result in their formation. This shared dependence upon the internal atmospheric structure provides a logical basis for considering the internal and orographic waves together. These phenomena also display similar characteristic space and time scales.

4.4.5.3 Predictability Survey

4.4.5.3.1 Occurrence

4.4.5.3.1.1 Location

The location of orographic waves can be estimated with perhaps 50% confidence, inasmuch as they are fixed in a general sense to the land forms themselves. The location of free internal waves, on the other hand, is somewhat less accurately predicted by dynamical methods; here an uncertainty of $\pm$ 500 km certainly exists, and in many instances the location is virtually unpredictable by dynamical (or synoptic) means.

4.4.5.3.1.2 Time

For mountain waves, an uncertainty of about ± 1/2 day may be estimated, while for the free internal waves, at least this uncertainty is present. Relatively good agreement, however, is found with the theoretically prescribed conditions for lee wave occurrence once the waves have been initiated [111].

4.4.5.3.1.3 Initial Structure

The size and general shape of the internal or orographic wave is specified in an idealized fashion by dynamical theory [112, 113], although marked variations are often found. The waves' length, amplitude and motion field may be estimated with an accuracy of about 30%; small-scale irregularities restrain the more comprehensive application of dynamical theory.

4.4.5.3.2 Development

4.4.5.3.2.1 Movement

The movement of internal and orographic waves is explicitly considered by dynamical theory, subject to the constraint of not-too-large amplitude [114]. The wave speed depends critically upon the vertical temperature and wind speed distribution, as well as upon the length of the wave. A dynamical predictability of about 50% may be estimated.

4.4.5.3.2.2 Structural Changes

Very little dynamical predictability exists for the waves' structural changes during development. The growth of wave amplitude renders inapplicable most existing wave theory, and the energetic interactions between the wave and the environment are not well understood.

4.4.5.3.2.3 Associated Phenomena

Very little dynamical predictability exists. The development of intense fields of vertical motion and characteristic cloud patterns are almost exclusively predicted by synoptic means.

4.4.5.3.3 Dissolution

4.4.5.3.3.1 Location

The location of dissolution of the orographic wave can be specified with about the same accuracy as can the location of its initiation. The dissipation of the internal wave is somewhat less well specified.

4.4.5.3.3.2 Time

The timing of the dissolution of the waves can be performed reasonably well by non-dynamical methods, but only with low accuracy by present dynamical techniques The life-time of these waves extends from hours (for internal waves) to days (for mountain waves); the dynamical predictability is not capable of a resolution below this.

4.4.5.3.3.3 Final Structure

Very little dynamical predictability.

4.4.5.4 Predictability Extension

Prerequisite to the extension of the dynamical predictability of internal and orographic waves is an increased resolution of the mesoscale structure of the atmosphere. With such information, present dynamical theory will probably be capable of considerably increased prediction of the waves' development. The dissolution stage will still be more difficult, and, it appears, will probably require further research into the waves' energetics and their apparent destruction by turbulence.

4.4.6 Squall Line

4.4.6.1 Dynamical Predictability Summary

5

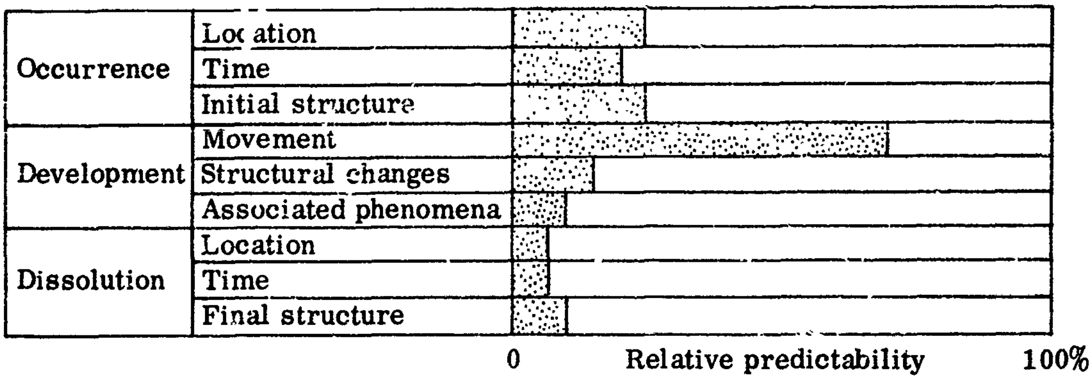

4.4.6.2 Introduction

The squall line is a relatively rare but intense convective-scale disturbance, whose prediction has been attempted most commonly by synoptic means. More recently, however, some advance has been made in dynamical theory aimed more-or-less toward the squall line phenomenon, and a nascent dynamical predictability is appearing. These theoretical developments are geared to the overall growth of a dynamical attack on the several phenomena of the mesoscale; the mechanics of the convection itself, however, is currently receiving more attention than its overall organization, as in the line storm or squall line. Two approaches have been promising for squall line formation; one based upon an analogy with the hydraulic jump phenomenon, initiated by Tepper in 1950, and the other based upon the direct numerical integration of the dynamical equations.

4.4.6.3 Predictability Survey

4.4.6.3.1 Occurrence

4.4.6.3.1.1 Location

From the observed acceleration of a suitable cold front, the location of an incipient squall line may be predicted by the method of characteristics, likening the line to a pressure jump phenomenon [115, 116]. On those occasions in which a squall line actually forms under these conditions, a position accuracy of about $\pm$ 25 km may be assigned.

4.4.6.3.1.2 Time

The hydraulic analogy provides a dynamical prediction of squall line timing concurrent with a location prediction. An accuracy of about ± 6 hr may be estimated for this method, although only on about half of the occasions so predicted does a detectable squall line or pressure jump actually form [116]. This accuracy also seems compatible with the experimental numerical integrations of the dynamical equations [117].

4.4.6.3.1.3 Initial Structure

Aside from indicating the squall line as a region of generally rising motion and an abrupt pressure disturbance, the hydraulic analogy provides relatively little information on the line's initial (or subsequent) structure. Numerical integration of suitable dynamical equations, however, provides some prediction of the velocity field and the associated temperature distribution [117].

4.4.6.3.2 Development

4.4.6.3.2.1 Movement

The squall-line's movement after formation is explicitly predicted by the pressure-jump mechanism and the theory of wave motion in a stratified fluid of known depth [115]. The accuracy may be estimated at about ± 15 mph, which represents a fair degree of predictability. This estimate is compatible with that furnished by the numerical integrations as well.

4.4.6.3.2.2 Structural Changes

The developing squal line's structural changes of increased vertical motion and strengthened temperature gradient are predictable in part by the numerical integration of the governing dynamical equations for period of a few hours. The resolution is not high, however, and the technique is still experimental.

4.4.6.3.2.3 Associated Phenomena

The development of cloudiness, precipitation and wind squalls characteristic of the growing squall line are not significantly predictable by dynamical methods

at present. Empirical and synoptic techniques are probably at their maximum utility in such instances.

4.4.6.3.3 Dissolution

4.4.6.3.3.1 Location

Very little dynamical predictability now exists for the dissipation stage of the squall-line phenomenon, with respect to either location or time.

4.4.6.3.3.2 Time

See Section 4.4.6.3.3.1 (above).

4.4.6.3.3.3 Final Structure

The structure of the dissipating squal line is quite poorly predicted by dynamical methods, if at all. Turbulent and frictional processes are probably dominant at this stage, and these effects are poorly treated in present dynamical considerations.

4.4.6.4 Predictability Extension

As with other mesoscale phenomena, perhaps the greatest increase of predictability would result from greater data coverage. The present dynamical capability probably exceeds that attainable with present data available for squall line studies. The development of new dynamical models suitable for numerical solution would likely effect a substantial increase in the predictability, particularly during the important development stage. Preliminary research in this direction could even proceed prior to the availability of increased synoptic squall-line data.

4.4.7 Sea Breeze

4.4.7.1 Dynamical Predictability Summary

6

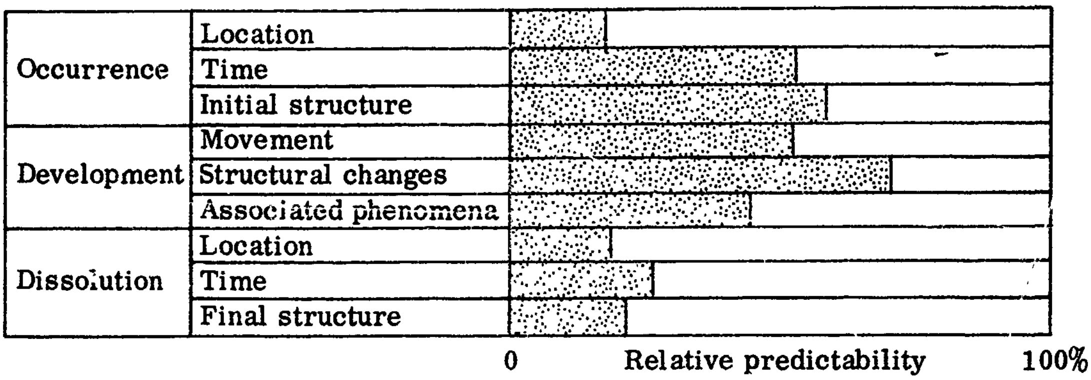

4.4.7.2 Introduction

The sea breeze is perhaps the most familiar example of a truly diurnal thermally-driven atmospheric phenomenon experienced at the earth's surface. Its dynamical role in interaction with the larger-scale motions does not appear to be critical, at least as far as the larger-scale flow is concerned, and it appears to execute its life-cycle in a relatively confined area near the coast. The dynamical predictability of the sea breeze is set within a recently-acquired predictive capability for the atmospheric boundary layer itself [118, 119], with the exception of the driving thermal mechanism itself.

4.4.7.3 Predictability Survey

4.4.7.3.1 Occurrence

4.4.7.3.1.1 Location

The location of sea breeze occurrence is confined to the immediate coastal area, with occasional landward extensions of 100 mi or so. Within this region, the location of specific sea breezes by dynamical methods is at present relatively undeveloped. Preliminary models have indicated, however, a preference for areas of initially offshore winds and large land-sea temperature contrasts [120].

4.4.7.3.1.2 Time

The prediction of the time of sea-breeze onset both at the coast and inland is now feasible by the numerical integration of dynamical equations [121, 120], and an accuracy of approximately $\pm$ 1 hr may be estimated. This appears comparable with that achieved by conventional synoptic methods.

4.4.7.3.1.3 Initial Structure

The distribution of the wind components both parallel and perpendicular to the shoreline and of the air temperature (relative to an ocean of uniform temperature) in the nascent sea-breeze circulation are directly provided by the numerical integration of dynamical models [122]. The accuracy of such predictions has not been thoroughly tested, although the fields bear many of the features observed. An overall accuracy of about $\pm$ 2° and $\pm$ 5 m sec^{-1} may be tentatively estimated.

4.4.7.3.2 Development

4.4.7.3.2.1 Movement

The movement of the sea breeze may be identified with the inland progression of the sea-breeze "front," and as such is directly related to the prediction of the time of occurrence. See Section 4.4.7 3.1.2 (above).

4.4.7.3.2.2 Structural Changes

The integration of dynamical models [120, 121, 123] shows a striking amount of detail in the development and intensification of the sea-breeze circulation, in spite of the possibly crude approximation made with regard to frictional and heating effects. The growth of convective motion at the sea breeze front (including vertical motions), the sharpening of the air temperature contrast at the breeze's leading edge, and the gradual deepening of the overall circulation system are all displayed in recent solutions [120], made with respect to artificial initial data. Although actual verification is necessary, the dynamical predictability here appears to be relatively high, possibly of the order of 70 percent.

4.4.7.3.2.3 Associated Phenomena

The prediction of the cloudiness often associated with the sea-breeze has not yet been accomplished by dynamical methods, although the required distributions of vertical motion and temperature are available. There is some dynamical suggestion, for example, of multiple cloud bands parallel to the coast [120] under certain conditions.

4.4.7.3.3 Dissolution

4.4.7.3.3.1 Location

The decaying sea-breeze's location and timing follows naturally from the cycle of the circulation induced by the sea-air temperature contrast. After approximately 6 hr from inception, the dissolution stage sets in over distances inland of up to 100 km. This phase, however, is not as well treated by the dynamical methods as are the initiation and development stages. Here the effects of frictional and turbulent dissipation probably become more critical.

4.4.7.3.3.2 Time

See Section 4.4.7.3.3.1 (above).

4.4.7.3.3.3 Final Structure

The structure of the decaying sea breeze is certainly suggested by the numerical experiments with the dynamical equations [120], but the predictability is probably not very high. We may estimate, in fact, errors in wind and temperature specification of the same order as those for the sea-breeze's characteristic amplitude itself.

4.4.7.4 Predictability Extension

The relatively significant dynamical predictability of the sea breeze which now exists is due almost entirely to a small number of quite recent experiments [121, 120, 123]. This success suggests that further research with such formulations may well achieve the refinement necessary for an actual operational prediction program. The inclusion of actual initial data and a verification program with even the present models is very much in order. The models themselves should be extended to include the diabatic effects of latent heat release in condensation

and those involved in low-level radiative transfer. The often associated phenomenon of coastal fog may also assume a significant dynamical predictability as a result of such studies; a preliminary effort in this direction has already shown considerable promise [122].

4.4.8 Thunderstorm

4.4.8.1 Dynamical Predictability Summary

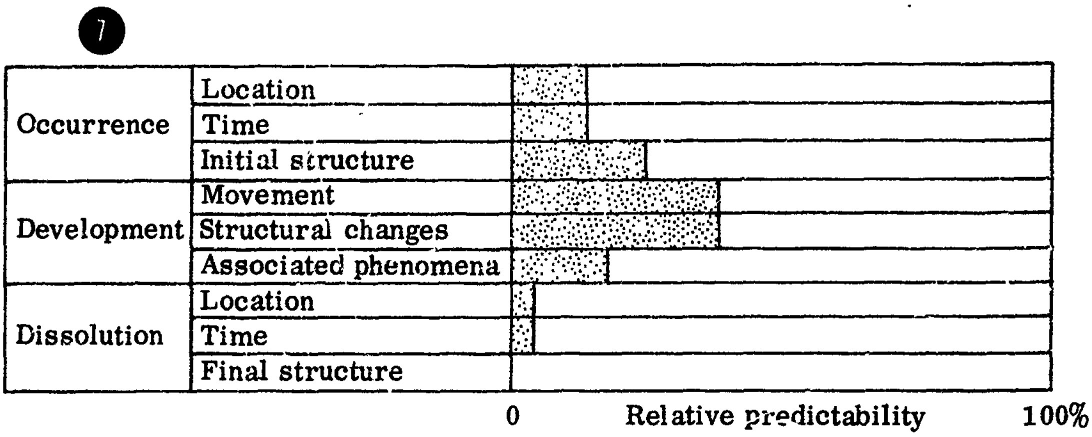

4.4.8.2 Introduction

The thunderstorm is one of the most familiar local "weather-bearing" phenomena, and is responsible for a significant fraction of the total rainfall over large portions of the earth. A large body of synoptic and observational information has been accumulated for thunderstorms [124], and their prediction is usually attempted by methods drawn from this experience. Only relatively recently have adequate dynamical investigations on this scale of convective motions been carried out, and it is on these efforts that a modest dynamical predictability now rests.

4.4.8.3 Predictability Survey

4.4.8.3.1 Occurrence

4.4.8.3.1.1 Location

Assuming that a thunderstorm arises from a locally intense convective element [124], there is at present virtually no dynamical predictability of the storm's location or timing; only, the general area and period of thunderstorm activity is partially predictable.

4.4.8.3.1.2 Time

See Section 4.4.8.3.1.1 (above).

4.4.8.3.1.3 Initial Structure

The thunderstorm's initial structure may be dynamically predicted as an example of a particularly intense convection element. The initial updraft speed and thermal buoyancy given by numerical integrations of the equations for (shallow) convection bear some resemblance to those characteristic of the nascent thunderstorm [125]. The accuracy is undoubtedly significant on a physical basis (in the sense that the upward motion is of the right magnitude and in the generally buoyant portion of the storm), but specific velocity and temperature predictions would be difficult to verify. Marked convergence regions are typical, but are of a diagnostic rather than prognostic nature [126].

4.4.8.3.2 Development

4.4.8.3.2.1 Movement

The thunderstorm generally behaves as though imbedded in the mean tropospheric flow, and movement predictions on this basis have a useful accuracy. Hence the dynamical predictability for the storm's overall motion may be estimated as about 50% accurate, on the basis of the accuracy with which the larger-scale flow may itself be predicted by dynamical methods.

4.4.8.3.2.2 Structural Changes

The growth of the upward convective motion, the development of the characteristic anvil top, and the progressive mixing or dilution of the air near the cloud boundary are all clearly indicated in the results of the numerical-dynamical integrations with both dry and wet convective models [127, 128], although the convection may not be regarded as that of the thunderstorm in other respects.

4.4.8.3.2.3 Associated Phenomena

The rainfall, hail, lightning, and the intense surface wind and temperature changes usually associated with a mature thunderstorm are predictable only indirectly by dynamical methods. The development of the characteristic downdraft is believed to be caused by the evaporative cooling of falling rain, and has not yet been successfully incorporated into a dynamical thunderstorm model [129, 130].

4.4.8.3.3 Dissolution

4.4.8.3.3.1 Location

The location and time of the dissipating thunderstorm is rather poorly predicted by dynamical methods. The considerable roles of turbulent mixing, downdraft formation, and surface frictional dissipation in the storm's dissolution are either absent or rather poorly treated at present.

4.4.8.3.3.2 Time

See Section 4.4.8.3.3.1 (above).

4.4.8.3.3.3 Final Structure

Virtually no dynamical predictability.

4.4.8.4 Predictability Extension

The thunderstorm's interaction with the environment is perhaps the key to a significant extension of the dynamical predictability. Thunderstorm growth appears to be favored by strong vertical shear [131], and the effective protection of the main updraft from the diluting effects of lateral entrainment is possibly the most important consequence of this selectivity. Dynamical thunderstorm studies to date have not considered these effects, and their treatment appears to hold the prospect of attaining at least an improved predictability of the mature thunderstorm's structure. Improved predictability of the dissolution stages may well prove somewhat more difficult, but should be furthered in some measure by continued numerical experimentation with intense convective systems.

4.4.9 Convective Clouds

4.4.9.1 Dynamical Predictability Summary

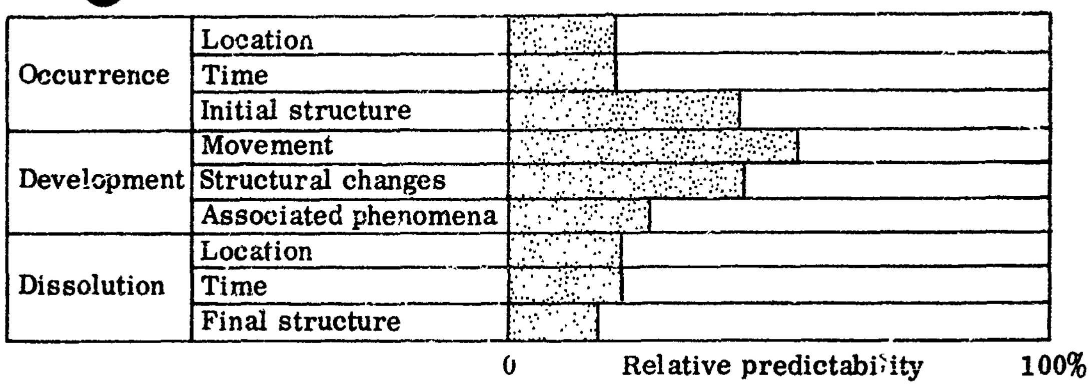

4.4.9.2 Introduction

Small-scale convective motions in the atmosphere represent virtually omnipresent phenomena, and account for the bulk of the vertical transfer of heat and water vapor into the atmosphere from the earth's surface. The formation of clouds might be incidental to these processes were it not for the release of latent heat upon condensation; this internal energy source strongly affects the subsequent cloud development and introduces rather severe complicating factors into the dynamics which are not yet resolved. The comprehensive dynamical investigation of even dry convective cloud phenomena is a relatively recent effort, and a considerable predictability has already been acquired. Previous to these numerical investigations, dynamical theory had only been applied in limited contexts [132], whose most serious defect was perhaps an inability to consider the cloud-environment interactions.

4.4.9.3 Predictability Survey

4.4.9.3.1 Occurrence

4.4.9.3.1.1 Location

The location of convective motions leading to clouds may be identified with areas of high relative low-level temperature (buoyancy) and suitable vertical distribution of both wind and temperature. Such configurations have

served as the initial conditions in most dynamical investigations of convection [125]. The height (and lateral dimensions) of the initial cloud are predictable with an accuracy of about $\pm$ 200 m.

4.4.9.3.1.2 Time

The timing of the cloud occurrence also follows from the numerical solution of the convection models [128]. A predictive accuracy of $\pm$ 5 min may be estimated, although verification with respect to atmospheric conditions has not yet been performed.

4.4.9.3.1.3 Initial Structure

The distribution of temperature and vertical velocity, and sometimes of water vapor and liquid water content as well, is directly predicted by dynamical models of convection [133, 127, 128]. These distributions appear fairly realistic and constitute a significant dynamical predictability.

4.4.9.3.2 Development

4.4.9.3.2.1 Movement

The movement of the developing convective cloud is both laterally in the ambient wind field and vertically as a result of the buoyancy. The former has not yet been treated on an intimate scale, but may be inferred from the dynamical predictability of the larger-scale wind field itself. The vertical movement of the cloud, on the other hand, is directly predictable by dynamical methods with an apparent accuracy of about $\pm$ 1 m sec^{-1}.

4.4.9.3.2.2 Structural Changes

The characteristic columnar or tower-like appearance of the convection element or cloud has been successfully predicted by dynamical methods [133, 134], and there appears reason to estimate that these methods could be applied to actual atmospheric data with a predictive accuracy of about 50 percent. The mushroom-like spread of the mature convection cloud under certain circumstances appears to be similarly predictable.

4.4.9.3.2.3 Associated Phenomena

The most important phenomena associated with convective clouds is doubtless the concentration of liquid water and the possible subsequent production of rain. These effects are now predictable with much accuracy by dynamical methods. The effects of evaporation and of the growth of the cloud droplet size spectrum pose relatively difficult dynamical problems.

4.4.9.3.3 Dissolution

4.4.9.3.3.1 Location

The position of the dissipating convective cloud is predictable by extension of the dynamical solutions to the stage where buoyancy is significantly reduced. At this point, however, the theory's accuracy is somewhat reduced, and the effects of turbulent dissipation, entainment, and evaporation–all poorly treated at present–become dominant. Most attention has been given to the attainment of a convective shape-preservation stage, rather than to the details of actual dissipation [133].

4.4.9.3.3.2 Time

The timing of the dissipation of the convective cloud is also rather poorly specified by present dynamical models. An individual buoyant parcel's life-cyle is reasonably well treated (i.e., about 30 min.), but the tendency for continued and renewed convection to occur in natural convective clouds has not been treated.

4.4.9.3.3.3 Final Structure

Only slight dynamical predictability exists for the cloud's final structure. An adeqaute mechanism for the cessation of the buoyancy forces' operation has apparently not been formulated [128].

4.4.9.4 Predictability Extension

The predictability of dynamical models of convection appears to be most seriously limited by an inadequate treatment of the downdraft mechanism. This feature is probably related to the evaporative cooling from rain, and evidently plays a decisive role in the stabilization and ultimate dissipation of the system. The interaction of the convective system with the environment also needs further attention, as do the mechanism of frictional dissipation.

4.4.10 Tornado

4.4.10.1 Dynamical Predictability Summary

Occurrence	Location	
	Time	
	Initial structure	
Development	Movement	
	Structural changes	
	Associated phenomena	
Dissolution	Location	
	Time	
	Final structure	

0 Relative predictability 100%

4.4.10.2 Introduction

The tornado is the most violent of all atmospheric phenomena, and is one for which there is possibly the least information. Certainly the tornado's predictability by dynamical methods is minimal; almost all of the knowledge of the storm's occurrence and behavior stems from observational and synoptic studies [135], and even here the data is not in abundance. The maximum wind speed and minimum pressure, for example. have not yet been adequately measured. From a dynamical viewpoint the tornado presents a severe problem of resolution of intense wind and pressure gradients, as well as an apparently basic dependence upon an intense mesoscale circulation.

4.4.10.3 Predictability Survey

4.4.10.3.1 Occurrence

4.4.10.3.1.1 Location

A small dynamical predictability exists for the location and time of occurrence insofar as the tornado is almost always associated with an intense convective disturbance (thunderstorm) and the latter is to some extent predictable. A gross physical positioning of the tornado near the region of maximum shear is suggested by partially dynamical considerations [130]. There exists, we may

note, a significant geographical, seasonal, and diurnal predictability of tornado occurrence by synoptic and empirical methods [136].

4.4.10.3.1.2 Time

See Section 4.4.10.3.1.1 (above).

4.4.10.3.1.3 Initial Structure

No dynamical predictability.

4.4.10.3.2 Development

4.4.10.3.2.1 Movement

A small dynamical predictability exists by virtue of the predictability of the motion of the parent convective cloud in the general direction of the tropospheric mean air flow. The tornado's movement is, however, often erratic.

4.4.10.3.2.2 Structural Changes

The dynamics of steady-state vortex motions resembling the tornado have been examined and constitute a certain dynamical predictability [137, 138]. The funnel's dimensions and a seemingly realistic rotational wind field are considered. The prediction or even specification of structural changes in the tornado, however, has not yet been made by dynamical methods.

4.4.10.3.2.3 Associated Phenomena

No dynamical predictability.

4.4.10.3.3 Dissolution

4.4.10.3.3.1 Location

No dynamical predictability.

4.4.10.3.3.2 Time

No dynamical predictability.

4.4.10.3.3.3 Final Structure

No dynamical predictability.

4.4.10.4 Predictability Extension

Continued study of intense tornado-like vortices is in order, but probably

the most significant extension of tornado predictability would result from a more complete measurement and observational program. Without such information, a meaningful dynamical analogue probably cannot be constructed.

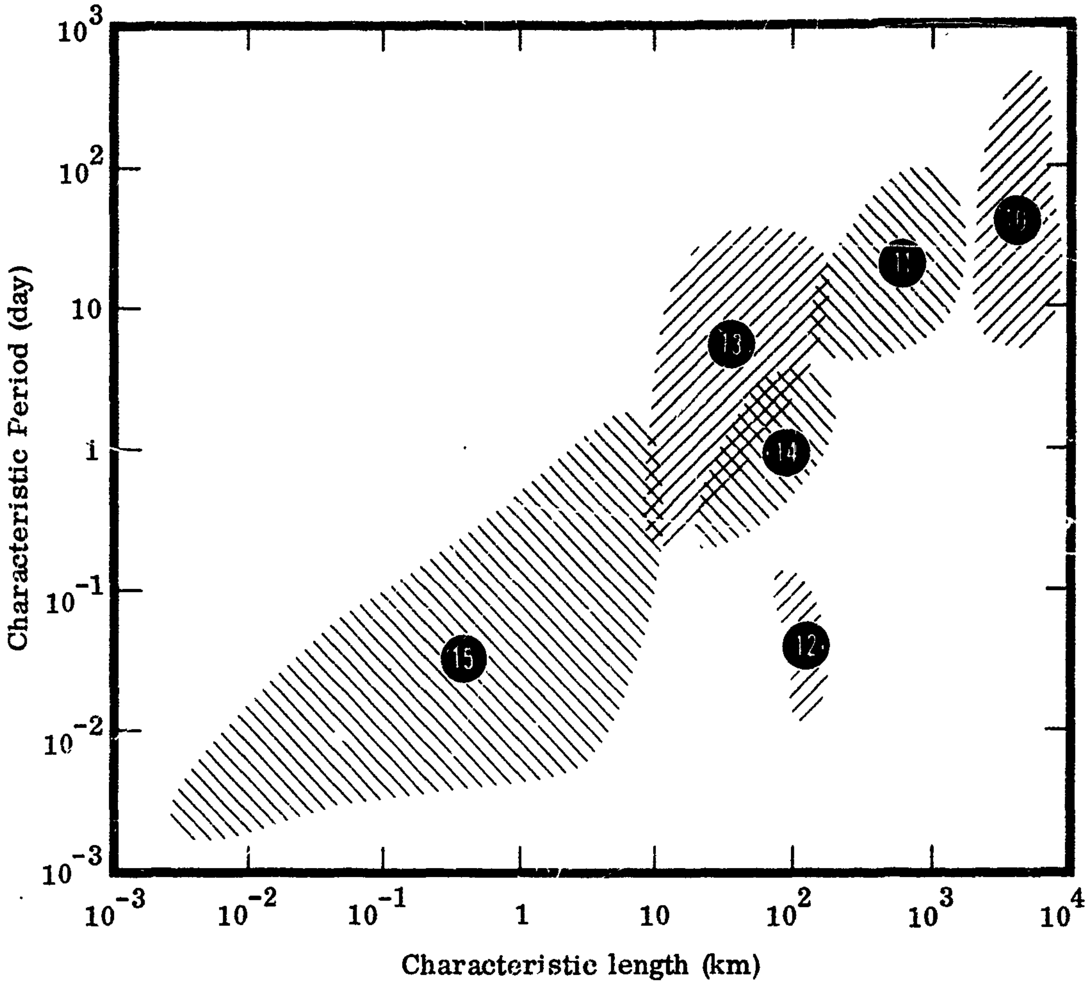

10 Large-scale flow
11 Meanders
12 Tsunami
13 Internal waves
14 Surges
15 Convective cells

Fig. 4-2. Summary of oceanic phenomena.

4.4.11 Large-scale Oceanic Flow

4.4.11.1 Dynamical Predictability Summary

10

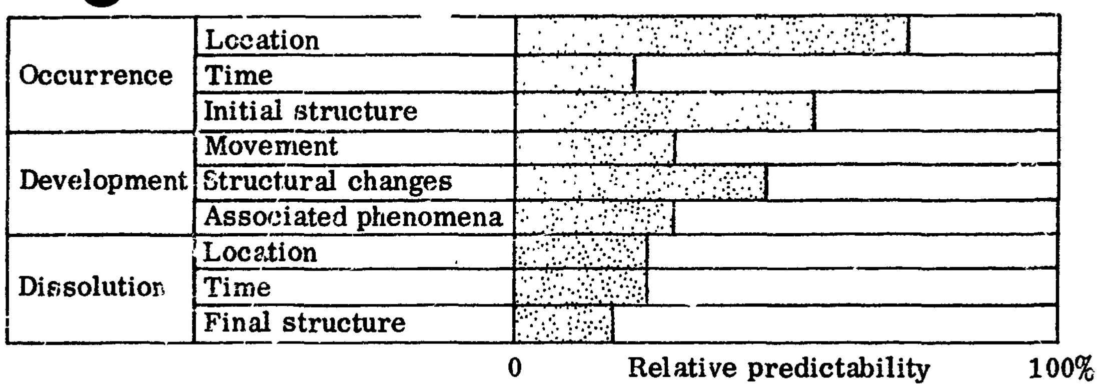

4.4.11.2 Introduction

The circulation of the oceans on a large scale is typified by the generally anticyclonic gyral flow in the major ocean basins, whose component parts at the surface are recognized as the major semi-permanent ocean currents. In the western portions of the North Atlantic and North Pacific Oceans at leaset this flow is locally intensified as the Gulf Stream and Kuroshio current systems. In the lower latitudes a system of tropical and equatorial currents is present. In the central and deep portions of the oceans a somewhat weaker thermo haline circulation is believed to be present, which in some cases flows in a direction opposite to that of the upper level currents. The relative importance of these density-driven currents and the surface wind-driven currents in the transport of water and heat in the oceans is yet to be fully resolved, although significant delineation has taken place with the development of adequate dynamical theory initiated by Sverdrup [139] and Stommel [140]. Concurrent with this research has been the growth of a dynamical predictability to a level surpassing that of many atmospheric phenomena.

4.4.11.3 Predictability Survey

4.4.11.3.1 Occurrence

4.4.11.3.1.1 Location

The location of the large-scale oceanic currents is evidently predictable to a relatively high degree by dynamical methods. This capability was first clearly demonstrated by Munk [141] for an idealized rectangular ocean basin, and has since been extended to actual oceans [143]. In these studies the large-scale current is viewed as a wind-driven process, and the observed variation of the wind stress over the oceans serves to outline the broad features of the current, together with the earth's rotation and the ocean basin shape. The position of the intense current along the western ocean boundary is predicted, as well as the locations of the equatorial currents. Here the accuracy appears to be about $\pm$ 1 deg lat. The current location specification is poorer in the interior of oceans, although partially dynamic arguments may be applied to the specification of a world-wide system of deep and bottom currents [143].

4.4.11.3.1.2 Time

The timing or initial growth rate of the oceanic large-scale flow can only be estimated by dynamical theory. It appears that a period of the order of one year would be required to establish the surface or barotropic circulation mode in the oceans, and about 100 years to set up the internal or baroclinic mode. The accuracy of such estimates could presumably be checked by recourse to an experimental anologue.

4.4.11.3.1.3 Initial Structure

The large-scale currents' initial structure in terms of total current strength, width, and general length are reasonably well predicted by dynamical methods [141]. Some uncertainty centers on the more detailed structure of the western boundary currents [144], and on the magnitude and vertical extent of the current systems in the deeper parts of the oceans [145, 146].

4.4.11.3.2 Development

4.4.11.3.2.1 Movement

Inasmuch as most dynamical studies of the large-scale currents consider the flow to be steady, it is difficult to estimate their predictability of the movement

or displacement of the currents. Preliminary studies of the transient development of large-scale currents indicate some predictability [147], which may be estimated in an overall fashion as about 30 percent.

4.4.11.3.2.2 Structural Changes

As the currents' site or transport change in response to changed wind stress or changed thermalhaline forcing functions, a dynamical predictability is evident from studies of idealized oceans [147, 145, 146], and it seems reasonable to estimate a significant predictability for the actual oceans. The study of laboratory analogues, we may note, offers considerable insight in this connection.

4.4.11.3.2.3 Associated Phenomena

The principal phenomenon associated with the large-scale currents is the formation of eddies or meanders; this phenomenon is considered separately elsewhere.

4.4.11.3.3 Dissolution

4.4.11.3.3.1 Location

The location and timing of the dissolution of the large-scale current systems is probable not highly predictable by present dynamical methods. The role of lateral eddy diffusion and bottom frictional effects are not adequately treated. Studies of idealized currents' variations in time suggest some predictability, but its accuracy has not yet been evaluated.

4.4.11.3.3.2 Time

See Section 4.4.11.3.3.1 (above).

4.4.11.3.3.3 Final Structure

The dissipating currents' structure is largely determined by the energy losses occurring, and the manner in which these are balanced (or not balanced) against whatever residual driving forces may exist. In the central portion of the oceans, currents are characteristically weak and diffuse, and there is little dynamical predictability existing.

4.4.11.4 Predictability Extension

The systematic application of the wind-driven current theory to all the world's oceans would provide an immediate extension of the dynamical predictability; the inclusion of the effects of ocean bottom topography and of internal density variations would also contribute significantly. The predictability of the currents' transient behavior and structure during both the formative and dissipative stages could be improved by further studies of time-dependent non-linear systems, possibly aided by a parallel program of laboratory investigation.

4.4.12 Oceanic Meanders

4.4.12.1 Dynamical Predictability Summary

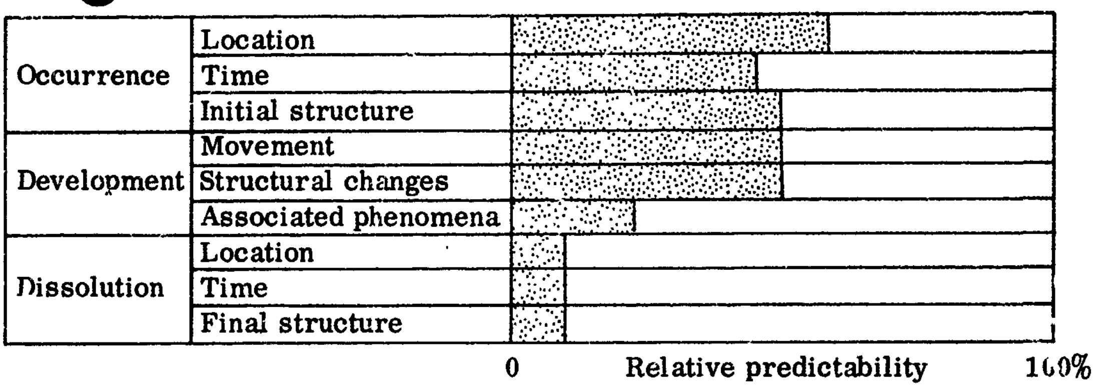

4.4.12.2 Introduction

Meanders or large-scale eddies were first adequately observed in 1950 [148] in the Gulf Stream current, although their existence had long been suspected from the accumulation of seemingly erratic temperature and current observations in the north-western portions of the North Atlantic and North Pacific. These wave-like perturbations of the current may occur on scales of several hundred miles and persist for several weeks. On occasion a wave develops into a loop and completely separates from the main current, in a manner somewhat similar to the formation of a cut-off cyclone in the atmospheric westerlies. From the dynamical viewpoint, meanders have usually been regarded as an instability of the current, and treated by a perturbation technique [144]. More recently the possible role of bottom topography has been emphasized [149], and the meanders' dynamical predictability has thereby been significantly increased.

4.4.12.3 Predictability Survey

4.4.12.3.1 Occurrence

4.4.12.3.1.1 Location

The incipient meander's location may be estimated from analyses of the currents' dynamical stability [144], although such predictions have not proven particularly successful. More significant is the apparently dominant effect of

the water depth variation in the path of the stream, with the conservation of potential vorticity evidently attempted by the current [149]. Subsurface topography thus favors certain locations for meander formation, in relatively good agreement with observation.

4.4.12.3.1.2 Time

A certain predictability for the timing of meander formation follows from the apparent predictability of the eddies' position, although this latter predictability has been so far established for steady or average conditions. Time-dependent numerical integrations of wind-driven currents (in water of constant depth, however) show the quasi-periodic formation of meanders as the basic currents' strength changes [147], but the physical reality of such variations has not yet been established.

4.4.12.3 1.3 Initial Structure

The meanders' initial size is reasonably well predicted by dynamic theory [147, 149], although the details of the current and temperature distributions are not yet adequately treated. The vertical extent of the growing eddy is also not explicitly considered.

4.4.12.3.2 Development

4.4.12.3.2.1 Movement

In numerical solutions for the time-dependent behavior of the western boundary current [147], the movement and development of current meanders is predicted in a seemingly reasonable fashion. The meanders amplify over a period of about 10 days, propagate slowly downstream at approximately 1/2 mph, and generally preserve their identity in much the manner of observed meander [148].

4.4.12.3.2.2 Structural Changes

See Section 4.4.12.3.2.1 (above).

4.4.12.3.2.3 Associated Phenomena

The apparent formation of even smaller-scale eddies by the developing meanders may be an important associated phenomenon, but rather little dynamical predictability exists on this scale at present. Likewise, the sea surface

temperature distribution in a meander is not now directly predicted, although a certain coherence with the surface current or surface geopotential topography is present.

4.4.12.3.3 Dissolution

4.4.12.3.3.1 Location

There is very little demonstrated dynamical predictability for the dissipating stages of current meanders, either in location or time. The present dynamical model integrations are strongly influenced in this respect by artificial boundaries [147].

4.4.12.3.3.2 Time

See Section 4.4.12.3.3.1 (above).

4.4.12.3.3.3 Final Structure

The slow reduction of the current and temperature gradients characterizing an oceanic meander is consistent with dynamical theory, although the predictability of these processes is now small. Interactions with the deeper part of the ocean and with the atmosphere are apparently important processes in meander dissolution.

4.4.12.4 Predictability Extension

The application of available dynamical models to actual ocean basins would probably contribute a significant predictability increase of meander formation and behavior. The dissipating stages' dynamics are probably more complicated, although simplified model integrations may well provide some new predictability or at least description of this stage. The problem of adequate data resolution is quite important for the study of oceanic meanders; insufficient coverage on the scales from 25–250 mi can easily obscure or seriously distort the meanders' apparent structure [150].

4.4.13 Long Oceanic Waves and Tsunami

4.4.13.1 Dynamical Predictability Summary

12

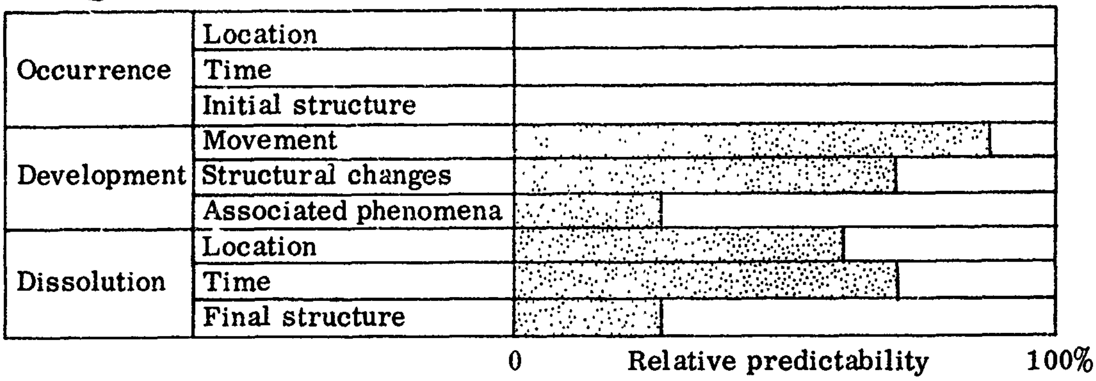

4.4.13.2 Introduction

Long oceanic waves are those large-scale motions of the sea surface caused by an impulsive disturbance in the sea with the wave energy spreading outward across the ocean. Submarine volcanos, landslides, and earthquakes are the principal natural causes of such waves, to which underwater nuclear explosions may now be added as an artificial source. The surface waves, often referred to as seismic sea waves or tsunami, are of very small amplitude in the open sea, but may assume very large size upon moving into shallow (coastal) waters. From the dynamical viewpoint such waves' behavior in the open sea appears predictable with considerable acuracy; it is the occurrence of such waves which is at present almost totally uncertain.

4.4.13.3 Predictability Survey

4.4.13.3.1 Occurrence

4.4.13.3.1.1 Location

No dynamical predictability, although the general region of the North Pacific basin is known to be that of greatest natural tsunami occurrence.

4.4.13.3.1.2 Time

No dynamical predictability of tsunami initiation; see Section 4.4.13.3.2.1 (below).

4.4.13.3.1.3 Initial Structure

No dynamical predictability.

4.4.13.3.2 Development

4.4.13.3.2.1 Movement

Once a tsunami wave train is initiated, its movement across the ocean is governed to a large extent by the shape and depth of the ocean bottom contours [151]. The tsunami moves as a long external gravity wave (or "shallow water" wave), and is refracted in much the same manner as oceanic coastal swell. Travel times to a given coastal point are predictable with an accuracy of about 3% [152], or about $\pm$ 10 min for oceanic dimensions and speeds of about 500 mph.

4.4.13.3.2.2 Structural Changes

During its development and movement, the tsunami wave height remains quite small, but may rapidly amplify to the order of 5—10 m upon entering shallow water. This amplification is to some extent predictable by dynamical methods, from a knowledge of the local water depths. The observed local wave height variability, however, is quite large [153].

4.4.13.3.2.3 Associated Phenomena

The more important phenomena associated with tsunami waves are probably the effects on an exposed shore, such as the coastal sand and sediment transport and the local current systems induced in harbors and bays. Such effects have a relatively small dynamical predictability.

4.4.13.3.3 Dissolution

4.4.13.3.3.1 Location

Most of the tsunami wave energy is dissipated in surf at coasts, and in this sense there exists a dynamical predictability for the location of dissolution. A part of the tsunami wave energy may be reflected from some coasts [154], and there is probably a continuous dissipation as the waves propagate across the ocean.

4.4.13.3.3.2 Time

See Sections 4.4.13.3.2.1 and 4.4.13.3.3.1 (above).

4.4.13.3.3.3 Final Structure

Interpreting the final structure of the dissipating tsunami as that of the coastal "tidal wave" and the induced local flows, only a relatively small dynamical predictability now exists.

See Section 4.4.13.3.2.3 (above).

4.4.13.4 Predictability Extension

Further research on the in-transit dissipation of long wave energy and on the effects of internal oceanic stratification on wave propagation should contribute to an increased predictability of tsunami structure. Research on the effects of local water depth in coastal areas on the tsunami wave height is also very much in order.

4.4.14 Internal Oceanic Waves

4.4.14.1 Dynamical Predictability Summary

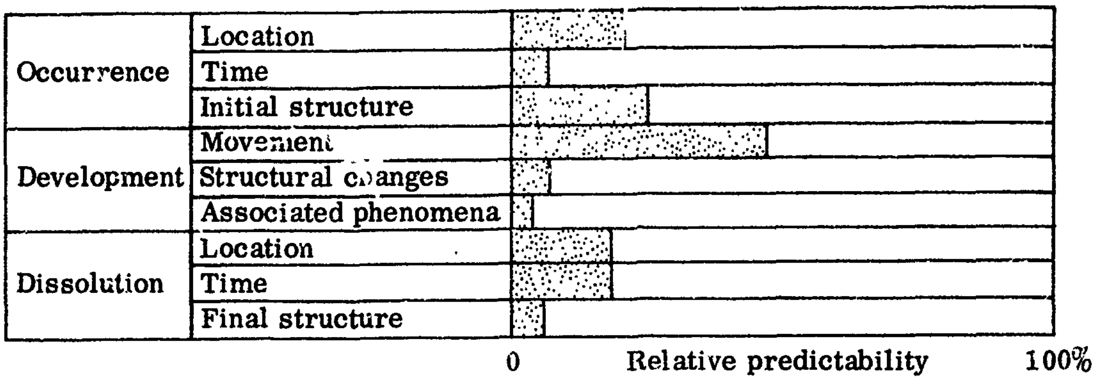

4.4.14.2 Introduction

Internal waves occur in the ocean in regions of strong density gradients, caused either by temperature or salinity differences. Some of the properties and behavior of these waves are predictable by dynamical theory, in much the same manner as the corresponding atmospheric phenomena.

4.4.14.3 Predictability Survey

4.4.14.3.1 Occurrence

4.4.14.3.1.1 Location

Favored regions for internal wave occurrence are; the oceanic thermocline, the lower boundary of relatively fresh surface waters, and the boundary between two water masses of significantly different salinities. The theory of the general circulation of ocean currents and the theory of the upper mixed oceanic layer hence provide a certain predictability for the location of internal wave occurrence. The overall accuracy is low, however, in view of the apparently widespread occurrence of internal waves.

4.4.14.3.1.2 Time

Very little dynamical predictability exists for the timing of the occurrence of oceanic internal waves. The progressive formation of density gradients can be predicted in only a gross fashion, with very little resolution on the scale of

the internal waves.

4.4.14.3.1.3 Initial Structure

Given the occurrence of an internal wave perturbation, the distribution of velocity and density (temperature and/or salinity) with respect to an interface or zone of maximum gradient is predictable by dynamical theory [155], as long as the initial amplitude of the wave is relatively small. The accuracy may be estimated as about 30%, in view of the prominent irregularities in natural oceanic internal waves [156].

4.4.14.3.2 Development

4.4.14.3.2.1 Movement

The internal wave's propagation speed is predictable with an accuracy of about 50% by the perturbation theory [155]. In many instances, however, the waves are distorted or dissipated over relatively short distances of the order of a few wavelengths.

4.4.14.3.2.2 Structural Changes

The waves' structural changes are rather poorly predicted by dynamical methods. The waves' amplitude (as measured, say, by isotherm displacement) often reaches the order of 30 ft, with an attendant amplification of the internal current field. Such effects are not adequately handled by the present linear models of wave motion, although non-linear formulations presumably could improve the situation.

4.4.14.3.2.3 Associated Phenomena

Very little dynamical predictability exists for secondary phenomena associated with internal oceanic waves.

4.4.14.3.3 Dissolution

4.4.14.3.3.1 Location

The prediction of the waves' dissipation by dynamical methods is possible only in general outline, in view of the relatively incomplete knowledge of the diffusive and frictional processes acting [157]. This is true with respect to both the location and time of internal wave dissolution.

4.4.14.3.3.2 Time

See Section 4.4.14.3.3.1 (above).

4.4.14.3.3.3 Final Structure

Very little predictability by dynamical methods.

4.4.14.4 Predictability Extension

The application of numerical integration techniques based upon a non-linear dynamical model of the internal oceanic waves may be expected to significantly increase the predictability of the waves' structural changes and amplification. The role of turbulent dissipation also needs further attention, and the importance of obtaining adequate data resolution in depth continues to require consideration.

4.4.15 Surges

4.4.15.1 Dynamical Predictability Summary

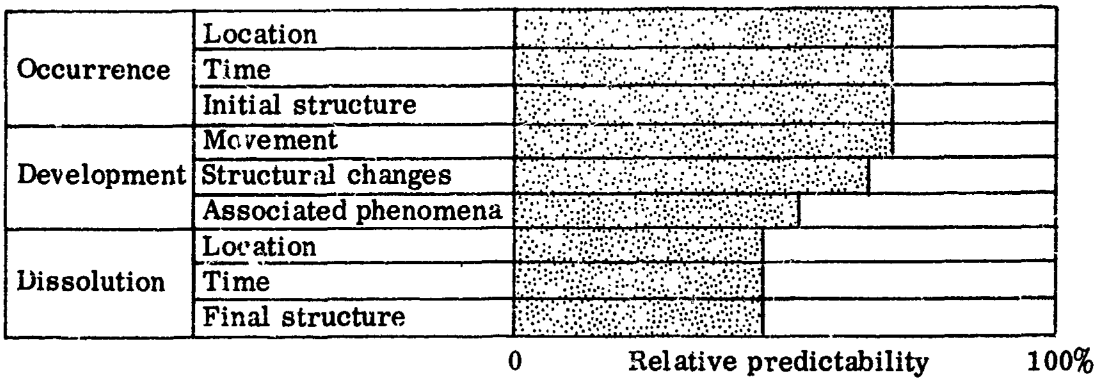

4.4.15.2 Introduction

The surge or oceanic storm tide represents the piling up or driving of water against coastal areas by a strong and usually persisting wind field. Until quite recently the surge and the accompanying serious coastal flooding could only be forecast in a general empirical fashion. In the past few years, a rather significant dynamical predictability has been developed which places the storm surge among those geophysical phenomena of the highest predictability. This success has resulted in an operational surge prediction capability linked to that for the low-level wind.

4.4.15.3 Predictability Survey

4.4.15.3.1 Occurrence

4.4.15.3.1.1 Location

The location and timing of the surge occurrence follows directly from the numerical solution of the governing dynamical model, in which the water height is directly predicted as a function of time over the affected ocean area, bay or lake [158, 159, 160, 161]. The accuracy is relatively high; of the order of 75% on an overall verification basis, with the local timing of the surge accurate to about $\pm$ 1 hr and the water height accurate to about $\pm$ 1 ft. Perhaps more significant is the dynamical ability to delineate the areas of high (and low) water with

this same order of accuracy.

4.4.15.3.1.2 Time

See Section 4.4.15.3.1.1 (above).

4.4.15.3.1.3 Initial Structure

See Section 4.4.15.3.1.1 (above).

4.4.15.3.2 Development

4.4.15.3.2.1 Movement

With a continuously changing wind field, the surge tide may recede or propagate to new coastal areas, or, in the case of lakes, a free oscillation of the total water mass may be set up. A series or succession of surges may then occur long after the cessation of the wind field [160]. These movements and the associated water heights likewise appear predictable with present theory with an accuracy of about 75 percent.

4.4.15.3.2.2 Structural Changes

See Section 4.4.15.3.2.1 (above).

4.4.15.3.2.3 Associated Phenomena

The prediction of water height directly provides a prediction of the transient current. Verification in this case is more difficult, and the purely surge-induced current may be obscured by tidal or other internal flows. A present practical accuracy of about 50% may be estimated.

4.4.15.3.3 Dissolution

4.4.15.3.3.1 Location

As the surge dissipates or recedes into the open ocean, its distinctive character is gradually lost as the effects of turbulent dissipation and friction become dominant. The dynamical models' solutions have been extended into this stage with some success, although the predictability is clearly less than that for the earlier stages.

4.4.15.3.3.2 Time

See Section 4.4.15.3.3.1 (above).

4.4.15.3.3 Final Structure

See Section 4.4.15.3.3.1 (above).

4.4.15.4 Predictability Extension

The improvement of low-level wind predictability would have a direct reflection on the dynamical predictability of surges. A further improvement could be expected as the result of continued research on the dissipative processes of bottom and lateral friction. The effects of an internal density stratification upon surge behavior also need attention.

4.4.16 Oceanic Convective Cells

4.4.16.1 Dynamical Predictability Summary

15

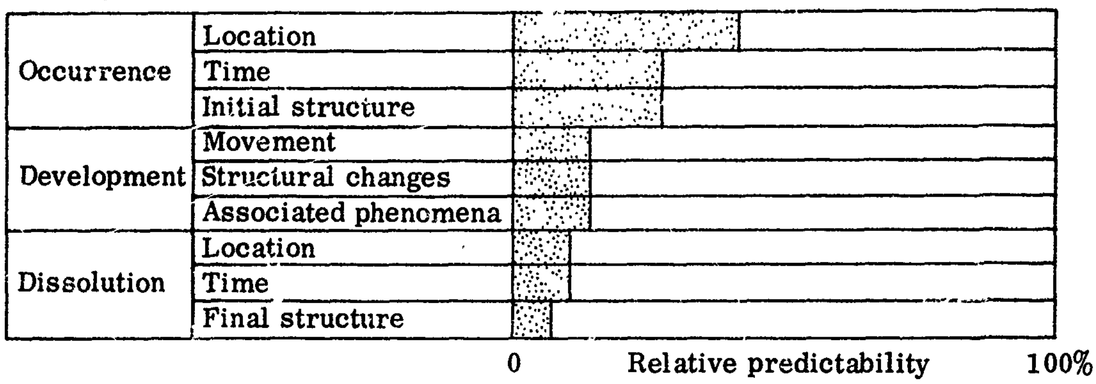

4.4.16.2 Introduction

Convective motion in the ocean appears to occur principally in the upper water layers, under the influence of the surface exchange processes with the atmosphere. The wind stress variations induce a system of convective circulations which penetrate to several hundred meters depth, with an accompanying mixing of the surface waters. This action of the wind was first studied dynamically by Ekman in 1905 [162], and extension and modifications of his basic theory continue to be made. In particular, the effects of the internal density stratification have begun to be considered [163, 164], although significant dynamical predictability is still confined to convective motion in the upper layers.

4.4.16.3 Predictability Survey

4.4.16.3.1 Occurrence

4.4.16.3.1.1 Location

The horizontal and vertical water circulations induced by surface wind and surface temperature variations are predictable by dynamical theory [162, 163, 164] to the extent of a specification of the general size, shape and intensity of the convective cells. The cells' growth rates may also be estimated.

4.4.16.3.1.2 Time

See Section 4.4.16.3.1.1 (above).

4.4.16. 3.1.3 Initial Structure

The wind-induced vertical motions at the base of the oceanic thermocline are reasonably well predicted by dynamical theory [164], but the accompanying thermal structure changes are not.

4.4.16. 3.2 Development

4.4.16. 3.2.1 Movement

There is less dynamical predictability of the transient changes or movement of the oceanic convective cells than of their steady-state features. With continued surface forcing, the convective cells probably propagate dow ward; at present only the outlines of such action have been studied under idealized conditions [165]. There is a growing empirical and statistical predictability of the behavior of the mixed layer, however.

4.4.16. 3.2.2 Structural Changes

See Section 4.4.16. 3.2.1 (above).

4.4.16. 3.2.3 Associated Phenomena

See Section 4.4.16. 3.2.1 (above).

4.4.16. 3.3 Dissolution

4.4.16. 3.3.1 Location

There is little dynamical predictability at this stage; the effects of turbulent mixing and internal friction are probably dominant and are inadequately considered in present theory. The same remarks apply to the timing of the dissipative stage as well as to the cells' final structure.

4.4.16. 3.3.2 Time

See Section 4.4.16. 3.3.1 (above).

4.4.16. 3.3.3 Final Structure

See Section 4.4.16. 3.3.1 (above).

4.4.16.4 Predictability Extension

The further treatment of transient effects in oceanic convective motions and increased consideration of the internal density structure may be expected to extend the dynamical predictability significantly. The total dynamics of these motions involve the entire problem of the ocean-atmosphere interaction; an

extensive research program on this general subject would doubtless advance the predictability not only of the oceanic convective motions, but of many other prominent atmospheric and oceanic phenomena as well. The systematic collection of observational data is probably as important in such an effort as is the development of theory: the greatest predictability advances in geophysical phenomena to date appear to have resulted from an effective union of both efforts. The phenomenon of oceanic convective cells is no exception in this regard.

4.5 Predictability Summary

The current status and foreseeable advances in the prediction of various geophysical phenomena have been reviewed from the statistical point of view in Section 4.3. The results are summarized in Table 4-1, which classifies each phenomenon in terms of the operational readiness of statistical forecasting techniques. No attempt has been made to estimate the accuracy attainable by these techniques but it is implied a "successful" technique is under discussion, i.e., one with sufficient accuracy to be considered operationally acceptable. An attempt has been made to be comprehensive in the survey of statistical methods since in the present and foreseeable state of the art these are more widely applicable to the many geophysical phenomena of potential interest than other available methods.

While the detailed reviews of statistical prediction have been referred to specific, individual phenomena, there are also sets of conditions relatable to operational interests as given by the items in Table 2-2, for which it is desirable to estimate predictability. An attempt has been made to do this, largely on a judgmental basis, by identifying the individual phenomena in the set and referring back to the detailed review of the individual phenomena. The results are shown in Table 4-1 under the heading "Combinations of Phenomena."

A parallel survey of prediction by dynamical methods has been made in Section 4.4. The results are summarized in Table 4-2, which presents an overall estimate of predictability for each geophysical item. These estimates are weighted heavily in terms of the present state of developments and hence are to be read as reflecting presently feasible systems with prediction accuracies as shown in the table. It is noted that relatively fewer phenomena have been surveyed in the dynamical case, reflecting the lower number of phenomena for which dynamical techniques exist. This latter is, of course, a direct consequence of the essential requirement for understanding the process involved if dynamical techniques are to be developed. It is readily understandable that extensive observation should precede comprehension and therefore that statistical prediction should find wider application. For those cases shown in Table 4-2, where dynamical techniques are feasible, the results can be taken together with those for the

corresponding statistical methods to obtain an estimate of the best attainable predictability of the phenomenon without regard to method. Such a comparison cannot be made between Tables 4-1 and 4-2, since the results are in somewhat different form. This matter will be taken up in conjunction with overall estimates of prediction feasibility in Section 6.0.

TABLE 4-1
PREDICTABILITY OF GEOPHYSICAL PHENOMENA BY STATISTICAL METHODS

Geophysical phenomena	Currently operational	Techniques demonstrated or in development	May be possible but not yet done	May be possible when data bank obtained	Highly improbable
Geological phenomena					
Earthquakes			X		
Volcanoes			X		
Landslides			X		
Atmospheric phenomena					
Turbulence (high level)					
Turbulence (low level)			X		
Turbulence (boundary level)			X		
Tornadoes			X		
Thunderstorms			X		
Hurricanes	X				
Blizzards			X		
Cyclogenesis	X				
Lightning			X		
Clouds	X				
Precipitation	X				
Fog		X			
Planetary boundary layer shear		X			
Upper level winds		X			
Ionospheric structure			X		
Ozone layer			X		
Oceanographic phenomena					
Surface waves		X			
Internal waves				X	
Ocean currents				X	
Tsunamis					X
Storm surges (seiches)	X				
Oceanic turbulence				X	
Submarine eruptions					X
Combinations of phenomena					
Nightglow			X		
Magnetic storms			X		
Underwater sound transmission		X			
Submarine-surface-air communications			X		
Surface and missile vehicle stability		X			
Ambient noise in sea			X		
Electromagnetic propagation		X			
Submarine vehicle stability				X	
Magnetic anomaly		X			
Soil trafficability		X			
Properties of ocean bottom			X		

TABLE 4-2
PREDICTABILITY OF GEOPHYSICAL PHENOMENA BY DYNAMICAL METHODS

Phenomena	Present relative accuracy, %
Atmospheric	
1. Large-scale atmospheric disturbances	60
2. Synoptic-scale atmospheric disturbances	35
3. Hurricanes	25
4. Internal and orographic waves	20
5. Squall line	30
6. Sea breeze	45
7. Thunderstorm	25
8. Convective cloud	40
9. Tornado	10
Oceanic	
1. Large-scale oceanic flow	50
2. Oceanic meanders	25
3. Long oceanic waves and tsunami	50
4. Internal oceanic waves	25
5. Surges	60
6. Oceanic convective cells	20
7. Sea surface waves and swell	20

4.6 Future Developments in Prediction

Wheras the outlook for improved prediction of individual geophysical factors has been indicated in Sections 4.3 and 4.4, it is desirable to consider future developments from a somewhat different and perhaps broader point of view. This point of view is provided by examining the directions and levels of effort which characterize current research devoted to fields capable of enlarging the foundations upon which improved prediction techniques must rest.

Although there has been recurrent interest in modelling techniques, it has generally been at a very low level and spasmodic in nature. Since this situation still persists at present with no well developed program in view, it appears highly unlikely that this approach will exercise a pervasive influence in the prediction of varied geophysical factors, although individual developments of some significance are not improbable.

The development of dynamical methods, on the other hand, continues to receive rather widespread attention, and some important successes have been achieved. Nevertheless, the attention and the successes both have been generally restricted to the large scale phenomena characteristic of planetary circulations. This need not be the case, however, and increasing attention to smaller scale geophysical phenomena of more immediate and direct interest to naval operations can be expected.

In the case of statistical prediction it is important to differentiate between studies of geophysical prediction and statistical developments generally which are applicable to geophysical prediction. In the former case there is a modest but growing activity in which The Travelers Research Center, Inc., is a principal force, and the outlook is for extensively increased efforts in this direction as the military meteorological services and the U.S. Weather Bureau turn ever more to automation, computer-based systems, and objective forecasting techniques. An important consideration in addition, however, is the latter case represented by widespread research programs now going on in the field of mathematical statistics which are concerned with problems having a direct bearing on the prediction problem.

The framework within which the application of statistics is likely to be viewed in the future is that of data analysis, a term which has been given special significance by Professor John W. Tukey. Professor Tukey has discussed his views on

data analysis in a sixty-seven page article entitled "The Future of Data Analysis" in the March 1962 issue of the Annals of Mathematical Statistics. He takes data analysis to include, among other things, "... procedures for analyzing data, techniques for interpreting the results of such procedures, ways of planning the gathering of data to make its analysis easier, more precise or more accurate, and all the machinery and results of (mathematical) statistics which apply to analyzing data."

With the general availability of high speed computers it is reasonable to extend the present concepts of data analysis to include the objective classification of prediction problems. The objectives would be to establish automated means for identifying and applying the most appropriate statistical prediction technique or techniques to the particular set of data, geophysical or otherwise, under consideration. To avoid the unnecessary, processing is assumed to be confined to admissible and preferably complete classes of statistical procedures.

The concept of objective problem classification in the framework of data analysis, perhaps in conjunction with an extensive network of interconnected computer installations throughout the country, has been considered and an outline of the components of such a data analyzer system is given in Appendix 4-B. Whether such a system ever becomes fully automated or not, the outline suggests the range of consideration which enter into the design of prediction techniques, and the great diversity of statistical techniques now available or being further developed which have application to the prediction problem.

The significance of the current emphasis on new and improved statistical techniques, aided and made practicable by modern computers, is important to recognize: it is in the nature of statistical techniques, generally speaking, to be concerned with probability distributions and it can be fairly reliably anticipated that the increasing application of statistical methods to the prediction of geophysical factors will result in the availability and eventual popularization of probability forecasts and the decline of the more familiar categorical forecasts.

The much higher information content of the probability forecast, its fundamentally more adequate recognition of the true relationship between the forecaster and nature, and its more appealing form as a representation of nature from a mathematical and formal point of view, all suggest that the operational decision framework will more and more be adapted to probability forecasts. The potential gains from this development seem particularly great for military operational decision making.

8.0 REFERENCES

1. Brooks, D. L. and G. R. Hilst, Geophysical Factors in Naval Warfare 7662–102, The Travelers Research Center, Inc., Dec. 1963.

2. Linstone, H. A., The Weapon Planning Problem for General Purpose Forces: A Functional Approach. Rpt. RM-3202-ISA, Contract SD-79, RAND Corp., Jul. 1962.

3. Braham, R. R. "The Water and Energy Budgets of the Thunderstorm and their Relation to Thunderstorm Development," J. Meteorol. 9, 227–242, 1952.

4. Kofsky, I. L., "Effects on the Ozonosphere of the Thermal Flux from Nuclear Detonations," J. Geophys. Res. 67:2, 739–744, 1962.

5. Miller, R. G., "Statistical Prediction by Discriminant Analysis," Meteorol. Monogr. 54 pp. Boston: Am. Meteorol. Soc., 1962.

6. Wiener, N., "Non-linear Predictions and Dynamics," Proc. 3rd Berkeley Sympos. Math. Stat. and Prob. 3, 247–252, 1956.

7. Pierson, W. J., G. Neuman and R. W. James, Practical Methods for Observing and Forecasting Ocean Waves, U.S.N. Hydrographic Office, 1955.

8. Hamon, B. V., and E. J. Hamon, "Estimating Relations Between Time Series," J. Geophys. Res., 68:21, 6033-6042, Nov. 1963.

9. Harris, R. G., J. G. Bryan, and J. E. MacMonegle, Terminal Weather Prediction Studies, Tech. Note 3 (Unpubl.). The Travelers Research Center, Inc., 1963.

10. Adams, L. H., (Ed.), "Seismology and Physics of the Earth's Interior," Trans. Am. Geophys. Un. 44:2, 327–364, 1963.

11. Press, F., G. Dewart, and R. Gilman, "A Study of the Diagnostic Techniques for Identifying Earthquakes," J. Geophys. Res. 68:10, 2909–2928, 1963.

12. "Quake Prediction Seen," Science News Letter, p. 404, Dec. 28, 1963.

13. Stacy, F. D., "Seismo-magnetic Effect and the Possibility of Forecasting Earthquakes," Nature, 1083–1085, Dec. 14, 1963.

14. Eaton, J. P., and K. J. Murata, "How Volcanoes Grow," Science 132: 3432, 925–938, 1960.

15. —, "Volcano Geophysics," Trans. Am. Geophys. Un. 44:2, 507–508, 1963.

16. Lorenz, E. N., "Meteorological Statistics and Data Handling," Trans. Am. Geophys. Un. 44:2, 394–395, June 1963.

17. Klein, Wm. H., Doctoral Dissertation, New York Univ.

18. U.S. Weather Bureau, Climatological Service Memoranda 99. Washington, D.C., 1962.

19. Miller, R. G., "Statistical Prediction by Discriminant Analysis," Meteorol. Monogr. 4:25, Am. Meteorol. Soc., 1962.

20. Enger, I., L. G. Reed, and J. E. MacMonegle, An Evaluation of Short Period Aviation Terminal-Forecasting Techniques, 7044-40, The Travelers Research Center, Inc., Nov. 1962.

21. Ball, J. T., A Multiple-discriminant Analysis of Clear-air Turbulence 7044-42, 2-5, The Travelers Research Center, Inc., 1962.

22. Clodman, J., G. M. Morgan, Jr., and J. T. Ball, High Level Turbulence, New York Univ. College of Eng., Res. Div., 1960.

23. Lappe, V. O., A Direct Method of Utilizing Flight Data to Determine Space and Spectrum Gust Velocity Distributions and Airplane Gust Performance Function, Rpt. GM 776-T-45, Cornell Aeronaut. Lab., 1955.

24. Thuillier, R. H., and U. O. Lappe, "Wind and Temperature Profile Characteristics from Observations on a 1400-ft Tower," Talk before 225th Meeting of Am. Meteorol. Soc., Jan. 29–31, 1964. Abstract in Bull. Am. Meteorol. Soc. 44:11, 712, 1963.

25. Enger, I., and F. Rodante, Description of IBM-7090 Programs "Covariance Matrix Generation" and "Screening Regression II". The Travelers Research Center, Inc., Mar. 1963.

26. Russo, J. A., Jr., I. Enger, and E. L. Sorenson, "A Statistical Approach to the Short-period Prediction of Surface Winds," (to be published in) J. Appl. Meteorol., 1964.

27. Solomon, H., (Ed.), Studies in Item Analysis and Prediction, Stanford Univ. Press 27, 1961.

28. Miller, R. G., and R. G. Harris, Prediction of Surface Winds Speeds Over the Ocean by Statistical Methods. 7022-27, The Travelers Research Center, 1962.

29. Bryan, J. G., and K. W. Veigas, Statistical Methods in Forecasting, 7065-31, p. 101, The Travelers Research Center, Inc., 1962.

30. House, D. C., "Forecasting Tornadoes and Severe Thunderstorms," Severe Local Storms Meteorol. Monogr. 5:27, 141–154. Boston: Am. Meteorol. Soc., 1963.

31. Dellert, G. T., Jr., "Data Processing Procedures in Numerical Meso-analysis," Mo. Weath. Rev. 90:4, 133–146, 1962.

32. Veigas, K. W., Prediction of Twelve, Twenty-four and Thirty-six Hour Displacement of Hurricanes by Statistical Methods, TRC 61-3, The Travelers Research Center, Inc.. 1961.

33. —, and F. P. Ostby, Jr., "Application of a Moving-coordinate Prediction Model to East Coast Cyclones," J Appl. Meteorol. 2:1, 24-38, 1963.

34. Arakawa, H., "Supplementary Note on the Statistical Technique of Typhoon Movement," Proceedings of the Inter-Regional Seminar on Tropical Cyclones in Tokyo, Tech. Rpt. J.M.A. 21, 207–213, Japan Meteorol. Agency, Tokyo, 1962.

35. —, "Regression Equations to Forecast the Movements and Surface Pressures of Typhoons in the Western North Pacific," Proceedings of the Inter-Regional Seminar on Tropical Cyclones in Tokyo, Tech. Rpt. J.M.A. 21, 201–206, Japan Meteorol. Agency, Tokyo, 1963.

36. Dunn, Gordon E., and B. I. Miller, Atlantic Hurricanes, Louisiana State Univ. Press, 1960.

37. Tracey, J. D. "Verification of Forecasts of Hurricanes Motion Using Various Techniques," Proc. Second Tech. Conf. on Hurricanes, 391–394, U.S. Weath. Bureau, 1961.

38. Riehl, H., W. H. Haggard, and R. W. Sanborn, "On the Prediction of 24-hr Hurricane Movement," J. Meteorol. 13, 415–420, 1956.

39. Vanderman, L. W., "An Improved NWP Model for Forecasting the Paths of Tropical Cyclones," Proc. Second Tech. Conf. on Hurricanes 391–394. U.S. Weath. Bureau, 1961.

40. Ostby, F. P., Jr., and K. W. Veigas, Forecasting the Movement and Intensification of Cyclones and Anticyclones Over Europe and Asia, 7045-58. The Travelers Research Center, Inc., 1963.

41. Harris, R. G., and J. E. MacMonegle, Evaluation of Existing Statistical and Analog Techniques for Short Period (2-7 hr) Terminal Prediction 7045-52, The Travelers Research Center, Inc., 1963.

42. Ostby, F. P., D. A. Chisholm, and R. J. Ball, Relations Derived Between Circulation and Total Cloud Amount by Statistical Methods, 7045-95, The Travelers Research Center, Inc., 1963.

43. Chisholm, D. A., and F. P. Ostby, Jr., Relations Derived Between Circulation Variables and Total Cloud Amount for the Winter Season by Statistical Methods. 7459-100, The Travelers Research Center, Inc., 1963.

44. Meteorological Abstracts and Bibliography, 3:5, 471–517, Am. Meteorol. Soc., 1952.

45. Brier, Glenn W., Notes on Interdiurnal Pressure and Temperature Changes in the Upper Air. Res. Paper 12, U.S. Weath. Bureau, May 1946.

46. —, A Study of Quantitative Precipitation Forecasting in the T.V.A. Basin, Res. Paper 26, p. 40, U.S. Weath. Bureau, Nov. 1946.

47. Maeda, I., and H. Kato, "An Objective Method of Forecasting Precipitation," J. Meteorol. Res. 11:3, 195–205, Tokyo, Mar. 1959.

48. Glahn, H. R., "An Experiment in Forecasting Rainfall Probabilities by Objective Methods," Mo. Weath. Rev. 90:2, 59–67, Feb. 1962.

49. St. John, G. M., "Numerical Computation of Winds for a Computer Flight Planning Program," Talk presented before the Fifth Conference on Applied Meteorology. Am. Meteorol. Soc., Atlantic City, N.J. Mar. 2–6, 1964. Abstract in Bull. Am. Meteorol. Soc. 45:1, 36, 1964.

50. Spiegler, D. B., J. J. Rahn, and K. W. Veigas, A Stratospheric Prediction Technique based on Mid- and Upper-tropospheric Numerical Diagnosis 7045-81, The Travelers Research Center, Inc., 1963.

51. Meteorological and Geoastrophysical Abstracts, 13:6, Am. Meteorol. Soc., 1962.

52. Meteorological and Geoastrophysical Abstracts, 13:10, Am. Meteorol. Soc., 1962.

53. Jones, W. B., and R. M. Gallet, "Representation of Diurnal and Geographic Variations of Ionospheric Data by Numerical Methods," J. Res. Nat. Bur. Standards-D. Radio Propagation, 66D:4, 419–438, 1962.

54. Ohring, G., and H. S. Muench, "Relationships between Ozone and Meteorological Parameters in the Lower Stratosphere." J. Meteorol. 17:2, 195–206, 1960.

55. Martin, D. W., and A W. Brewer, "A Synoptic Study of Day-to-day Changes of Ozone over the British Isles," Roy. Meteorol. Soc. Quart. J. 85:366, 393–403, 1959.

56. Ishoda, K., and T. Okabayashi, "On the Relationships between Atmospheric Ozone and Meteorological Factors." J. Meteorol. Res., Tokyo, 14:16, 402–407, 1962.

57. Nat. Acad. Sci., Ocean Wave Spectra Proceedings of a Conference, New Jersey: Prentice-Hall, Inc., 1963.

58. Barber, N. F., and M. J. Tucker, "Wind Waves," The Sea,-I: Physical Oceanography, 664–699, New York: John Wiley and Sons, 1962.

59. Pierson, W. J., Jr., "Gravity Waves." Trans. Am. Geophys. Un. 44:2, 485–489, June 1963.

60. Ursell, F., Surveys in Mechanics, G. K. Batchelor, and R. M. Davies, (Eds.), p. 216, London: Cambridge Univ. Press, 1956.

61. Walden, H., "Comparison of One-dimensional Wave Spectra Recorded in the German Bight with Various 'Theoretical Spectra,'" Ocean Wave Spectra Proceedings of a Conference, New Jersey: Prentice-Hall, Inc., 1963.

62. Bretschneider, C. L., Wind Variability and Wave Spectra for Wind-generated Gravity Waves, Tech. Memo. 118, Beach Erosion Board, 1959.

63. Fleet Numerical Weather Facility, Progress Reports dated Apr. 1962, July–Dec. 1962, Aug. 1963. U.S. Naval Post Graduate School, Monterey, Calif., 1962–63.

64. Moskowitz, L., Estimates of the Power Spectra for Fully Developed Seas for Wind Speeds of 20 to 40 knots. U.S.N.O.O. Contract No. 62306-1042, New York Univ., Sch. Eng. Sci., 1963.

65. Dodson, A. T., "Oceanic Tides," Advances in Geophys. 5, 118–153. New York: Academic Press, 1958.

66. Harris, D. L., N. A. Pore, and R. Cummings, "The Application of High Speed Computers to Practical Tide Problems," Unpublished Rpt., U.S. Weath. Bureau, 1963.

67. Van Dorn, W. G., "Some Characteristics of Surface Gravity Waves in the Sea by Nuclear Explosions," J. Geophys. Res. 66, 3845–3862, 1961.

68. Zetler, B. D., "Travel Times of Seismic Sea Waves to Honolulu," Pacific Science 1:3, 185–188, 1947.

69. Munk, W. H., "Long Ocean Waves," The Sea, Vol. I, Physical Oceanography, M. N. Hill, (Ed.) 647–663, New York: John Wiley & Sons, 1962.

70. Zetler, B. D., M. D. Schuldt and L. F. Bailey, "Criteria for Tsunami Evaluation," Internatl. Un. Geography and Geodosy Monogr. 24, 1961.

71. Van Dorn, W. G., "Tsunamis" Trans. Am. Geophys. Un. 44:2, 489–490, 1963.

72. Harris, D. L., Characteristics of the Hurricane Storm Surge, Tech. Paper 48, U.S. Weather Bureau, 1963.

73. Groen, P., and G. W. Groves, "Surges" in The Sea, Vol. I, Physical Oceanography, M. N. Hill, (Ed.) 611–643. New York: John Wiley & Sons, 1962.

74. Welander, P., "Numerical Prediction of Storm Surges," Advances in Geophys. 8. H. E. Landsberg and J. Van Mieghem (Eds.) 315–379, New York: Academic Press.

75. Bretschneider, C. L., "Storm Surges," Trans. Am. Geophys. Un. 44:2, 491–492, 1962.

76. Rossiter, J. R., "Interaction Between Tide and Surge in The Thames," Geophys. J. 6:1, 29–53, 1961.

77. Fortak, H. G., "Concerning the General Vertically Averaged Hydrodynamic Equations with Respect to Basic Storm Surge Equations," NHRP Rpt. 51, U.S. Weather Bureau, 1962.

78. Harris, D. L., "An Interim Hurricane Storm Surge Forecasting Guide," NHRP Rpt. 32, U.S. Weather Bureau, 1959.

79. Terada, K., H. Futi, and M. Miyazaki, "Storm Surge Forecasting Method and Telemetering, Recording, Printing, and Indicating System of Tide and Other Elements–so-called 'Call System' in Japan." Oceanographical Magazine 14:1, 43–62, Japan, 1962.

80. Pore, N. A., "The Relation of Wind and Pressure to Extratropical Storm Surges at ACY." Unpublished manuscript. U.S. Weather Bureau, 1963.

81. Huschke, Ralph E., (Ed.), Glossary of Meteorology, 638 pp. Boston: Am. Meteorol. Soc., 1959.

82. Charney, J. G., R. Fjörtoft, and J. von Neuman, "Numerical Integration of the Barotropic Vorticity Equation," Tellus 2, 237–254, 1950.

83. —, and A. Eliassen, "A Numerical Method for Predicting the Perturbations of the Middle-latitude Westerlies," Tellus 1:2, 38–54, 1949.

84. JNWPU, Staff Member, "One Year of Operational Numerical Weather Prediction," Bull. Am. Meteorol. Soc. 38, 263–268 and 315–328, 1957.

85. Edelmann, W., and H. Reiser, "Baroclinic Forecasts with the Unfiltered 5-layer Model," Tech. Note 5, 33 pp., Offenbach/M: German Weather Serv. (Res. Div.), 1962.

86. Bolin, B., E. N. Dobrishman, K. Hinkelmann, E. Knighting, and P. D. Thompson, "Numerical Methods of Weather Analysis and Forecasting," Tech. Note 44, Geneva: World Meteorol. Organiz., 31 pp., 1962.

87. Eady, E. T., "Long Waves and Cyclone Waves," Tellus 1:3, 33–52, 1949.

88. Kuo, H. L., "The Stability Properties and Structure of Disturbances in a Baroclinic Atmosphere," J. Meteorol. 10, 235–243, 1953.

89. Knighting, E., G. A. Corby, F. H. Bushby, and C. E. Wallington, "An Experiment in Numerical Forecasting," Meteorol. Off. Sci. Paper 5, London: H.M.S.O., 1961.

90. Thompson, P. D., and W. L. Gates. "A Test of Numerical Prediction Methods Based on the Barotropic and Two-parameter Baroclinic Models," J. Meteorol. 13, 127–141, 1956.

91. Smagorinsky, J., and G. Collins, "On the Numerical Prediction of Precipitation," Mo. Weath. Rev. 83, 53–68, 1955.

92. Bushby, F. H., and M. K. Hinds, "Further Computations of 24-hr Pressure Changes Based on a Two-parameter Model," Quart. J. Roy. Meteorol. Soc. 81, 396–402, 1955.

93. Cressman, G. P., "Improved Terrain Effects in Barotropic Forecasts," Mo. Weath. Rev. 88, 327--342, 1960.

94. Thompson, P. D., Numerical Weather Analysis and Prediction, 170 pp., MacMillan, 1961.

95. Bristor, C. L., "Effect of Data Coverage on the Accuracy of 500-mb Forecasts," Mo. Weath. Rev. 86, 299–308, 1958.

96. Alaka, M. A., "Instability Aspects of Hurricane Genesis," Natl. Hurr. Res. Proj. 64, 23 pp., Miami, 1963.

97. Yanai, N., "Dynamical Aspects of Typhoon Formation," J. Meteorol. Soc. Japan 39, 282–309, 1961.

98. Kasahara, A., "A Numerical Experiment on the Development of a Tropical Cyclone," J. Meteorol. 18, 259—282, 1961.

99. Kuo, H. L., "On the Initiation of Tropical Depressions and Convection in a Conditionally Unstable Atmosphere," Natl. Hurr. Res. Proj. Rpt. 40, 46 pp., 1960.

100. —, "Mechanism Leading to Hurricane Formation," Natl. Hurr. Res. Proj. Rpt. 50, 277–283, 1962.

101. Hubert, L. F., "Numerical Weather Prediction of Hurricane Motion," Natl. Hurr. Res. Proj. Rpt. 2, U.S.W.B., Washington, D.C., 1956.

102. —, "An Operational Test of a Numerical Prediction Method for Hurricanes," Mo. Weath. Rev. 87, 222-230, 1959.

103. Vanderman, L. W., "An Improved NWP Model for Forecasting the Paths of Tropical Cyclones," Mo. Weath. Rev. 90, 19–22, 1962.

104. —, "Summary of Verification of Numerical Operational Tropical Cyclone Forecast Tracks for 1962," Tech. Memo. 27, 16 pp., Natl. Meteorol. Center, U.S.W.B., 1963.

105. Kasahara, A., "The Numerical Prediction of Hurricane Movement with the Barotropic Model," J. Meteorol. 14, 386–402, 1957.

106. Birchfield, G. E., "Numerican Prediction of Hurricane Movement with the Use of a Fine Grid," J. Meteorol. 17, 406–414, 1960.

107. Kasahara, A., "The Numerical Prediction of Hurricane Movement with a Two-level Baroclinic Model," J. Meteorol. 17, 357—370, 1960.

108. Estoque, M. A., "Some Numerical Studies of Tropical Cyclone," Sci. Rpt. 2, 26 pp., Hawaii Inst. Geophys., Univ. Hawaii, 1963.

109. Rosenthal, S. L., "Some Attempts to Simulate the Development of Tropical Cyclones by Numerical Methods," Mo. Weath. Rev. 92, 1–21, 1964.

110. Charney, J. G., "On the Growth of the Hurricane Depression," J. Atmos. Sci. 21, 68–75, 1964.

111. Corby, G. A., and C. E. Wallington, "Airflow over Mountains: the Lee Wave Amplitude," Quart. J. Roy. Meteorol. Soc. 82, 266–274, 1956.

112. Scorer, R. S., "Theory of Airflow over Mountains," Quart. J. Roy. Meteorol. Soc. 75, 41–56, 1949.

113. —, "Theory of Airflow over Mountains: II-The Flow Over a Ridge," Quart. J. Roy. Meteorol. Soc. 79, 70–83, 1953.

114. Charney, J. G., "On the Scale of Atmospheric Motion," Geofys. Publ. 17, 3–17, 1948.

115. Tepper, M., "A Proposed Mechanism of Squall Lines: The Pressure Jump Line," J. Meteorol. 7, 21–29, 1950.

116. —, "An Application of the Hydraulic A[illegible] Certain Atmospheric Flow Problems," Res. Paper 35, 50 pp., Washington, [illegible], U.S.W.B., 1952.

117. Sasaki, Y., "A Numerical Experiment of Squall-line Formation," J. Meteorol. 16, 347–353, 1959.

118. Estoque, M. A., "A Preliminary Report on a Boundary Layer Numerical Experiment," GRD Res. Note 20, 29 pp., Bedford, Mass., 1959.

119. —, "A Numerical Model of the Atmospheric Boundary Layer," J. Geophys. Res. 68, 1103–1113, 1963.

120. —, "The Sea Breeze as a Function of The Prevailing Synoptic Situation," J. Atmos. Sci. 19, 244–250, 1962.

121. —, "A Theoretical Investigation of the Sea Breeze," Quart. J. Roy. Meteorol. Soc. 87, 136–146, 1961.

122. Fisher, F. L., and P. Caplan, "An Experiment in Numerical Prediction of Fog and Stratus," J. Atmos. Sci. 20, 425–437, 1963.

123. Fisher, E. L., "A Theoretical Study of the Sea Breeze," J. Meteorol. 18, 216–233, 1961.

124. Byers, H. R., and R. R. Braham, Jr., The Thunderstorm, 287 pp., Washington, D.C.: U.S. Govt. Print Off., 1949.

125. Ogura, Y., "A Review of Numerical Modeling Research on Small Scale Convection in the Atmosphere," Meteorol. Monogr. 5:27, 65–76, 1963.

126. House, D. C., "The Divergence Equation as Related to Severe Thunderstorm Forecasting," Bull. Am. Meteorol. Soc. 42, 803–816, 1961.

127. Ogura, Y., "Convection of Isolated Masses of a Buoyant Fluid: A Numerical Calculation," J. Atmos. Sci. 19, 492–502, 1962.

128. —, "The Evolution of a Moist Convective Element in a Shallow, Conditionally Unstable Atmosphere: A Numerical Calculation," J. Atmos. Sci. 20, 407–424, 1963.

129. Ludlam, F. H., "Severe Local Storms: A Review," Meteorol. Monogr. 5:27, 1–30, 1963.

130. Newton, C. W., "Dynamics of Severe Convective Storms," Meteorol. Monogr. 5:27, 33–58, 1963.

131. —, and H. R. Newton, "Dynamical Interactions Between Large Convective Clouds and Environment with Vertical Shear," J. Meteorol. 16, 483–496, 1959.

132. Petterssen, S., E. Knighting, R. W. James, and N. Herlofson, "Convection in Theory and Practice," Geofys. Publ. 16:10, 1945.

133. Lilly, D. K., "On the Numerical Simulation of Buoyant Convection," Tellus 14, 148–172, 1962.

134. Malkus, J. S., and G. Witt, "The Evolution of a Convective Element: A Numerical Experiment," in The Atmosphere and the Sea in Motion, 425–439, New York: Rockefeller Inst. Press, 1959.

135. Fawbush, E. J., R. C. Miller, and L. G. Starrett, "An Empirical Method of Forecasting Tornado Development," Bull. Am. Meteorol. Soc. 32, 1–9, 1951.

136. House, D. C., "Forecasting Tornadoes and Severe Thunderstorms," Meteorol. Monogr. 5:27, 141–155, 1963.

137. Fulks, J. R., "On the Mechanics of the Tornado," Nat. Severe Storms Proj. Rpt. 4, 33 pp., Washington, D.C.: U.S.W.B., 1962.

138. Gutman, L. N., "Theoretical Model of a Waterspout," Izv. Akad. Nauk S.S.S.R. ser. Geofiz. 1, 79–93, 1957.

139. Sverdrup, H. V., "Wind-driven Currents in a Baroclinic Ocean; with Application to the Equatorial Currents of the Eastern Pacific," Proc. Natl. Acad. Sci. 33, 318–326, 1947.

140. Stommel, H., "The Westward Intensification of Wind-driven Ocean Currents," Trans. Am. Geophys. Un. 29, 202–206, 1948.

141. Munk, W. H., "On the Wind-driven Ocean Circulation," J. Meteorol. 7, 79–93, 1950.

142. Gurikova, Z. F., "On the Calculation of the Currents in the Surface Layer in the Northern Sector of the Pacific," Izv. Akad. Nauk. S.S.S.R. ser. Geofiz. 9, 1962.

143. Stommel, H., "A Survey of Ocean Current Theory," Deep-Sea Res. 4, 149–184, 1957.

144. Carrier, G. F., and A. R. Robinson, "On the Theory of the Wind-driven Ocean Circulation," J. Fluid Mech. 12:1, 49–80, 1962.

145. Stommel, H., and A. B. Arons, "On the Abyssal Circulation of the World Ocean—I. Stationary Planetary Flow Patterns on a Sphere," Deep-Sea Res. 6, 140–154, 1960.

146. —, —, "On the Abyssal Circulation of the World Ocean—II. An Idealized Model of the Circulation Pattern and Amplitude in Oceanic Basins," Deep-Sea Res. 6, 217–233, 1960.

147. Bryan, K., "A Numerical Investigation of a Non-linear Model of a Wind-driven Ocean," J. Atmos. Sci. 20, 594–606, 1963.

148. Fuglister, F. C., and L. V. Worthington, "Some Results of a Multiple Ship Survey of the Gulf Stream," Tellus 3, 1–14, 1951.

149. Warren, B. A., "Topographic Influences on the Path of the Gulf Stream," Tellus 15, 167–183, 1963.

150. Fuglister, F. C., "Alternative Analyses of Current Surveys," Deep-Sea Res. 2, 213–229, 1955.

151. Cochrane, J. D., and R. S. Arthur, "Reflection of Tsunamis," J. Mar. Res. 8, 239–251, 1948.

152. Zetler, B. D., "Travel Times of Seismic Sea Waves to Honolulu," Pacific Sci. 1, 185–188, 1947.

153. Shepard, F. P., Submarine Geology, 2nd Ed., 557 pp., New York: Harper and Row, 1963.

154. Munk, W. H., "Some Comments Regarding Diffusion and Absorption of Tsunamis," Bull. I.U.G.G., 1961.

155. Fjeldstad, J. E., "Interne Wellen," Geofys. Publ. 10:6, 53 pp., 1933.

156. Cox, C. S., "Internal Waves," in The Sea, 752–763. New York: Interscience, 1962.

157. Rattray, M., Jr., "Propagation and Dissipation of Long Internal Waves," Trans. Am. Geophys. Un. 38, 495–500, 1957.

158. Groen, P., and G. W. Groves, "Surges," in The Sea, 611–646. New York: Interscience, 1962.

159. Hansen, W., "Theorie Zur Errechnung des Wasserstandes und der Strömungen in Randmeeren nebst Anwendungen," Tellus 8, 287–300, 1956.

160. Platzman, G. W., "The Dynamic Prediction of Wind Tides on Lake Erie," Meteorol. Monogr. 4:26, 44 pp., 1963.

161. Welander, P., "Numerical Prediction of Storm Surges," in Advances in Geophysics 9, 316–379, 1961.

162. Ekman, V. W., "On the Influence of the Earth's Rotation on Ocean Currents," Arch. Math. Astr. Fys. 2:11, 52 pp., 1905.

163. Lineikin, P. S., "On the Determination of the Thickness of the Baroclinic Layer in the Sea," Doklady Akad. Nauk S.S.S.R. 101, 461–464, 1955.

164. Stommel, H., and G. Veronis, "Steady Convective Motion in a Horizontal Layer of Fluid Heated Uniformly from Above and Cooled Non-Uniformly from Below," Tellus 9, 401–407, 1957.

165. Veronis, G., and H. Stommel, "The Action of Variable Wind Stress on a Stratified Ocean," J. Marine Res. 15, 43–75, 1956.

APPENDIX E. CYCLOGENESIS*

E.1.0 GENERAL DESCRIPTION

E.1.1 Phenomena Types

Our principal concern is with the major synoptic scale weather systems: extratropical cyclones and anticyclones, and the related subject of air masses.

E.1.2 Associated Weather Phenomena

We shall consider as well the particular phenomena of large areas of strong surface winds, cold waves, synoptic scale precipitation areas and blizzards.

E.1.3 Characteristic Geographic Extent

The major areas of stormy and fair weather in the temperate zones of the earth are associated with cyclones and anticyclones, respectively. Variations in the weather conditions from one cyclone or anticyclone to another are due in part to variations in the air masses associated with them. A cyclone is a region of winds having an approximately rotational flow which is counterclockwise (clockwise) in the Northern (Southern) Hemisphere. The horizontal extent of the cyclone may be of the order of 1000 to 3000 km. The vertical extent of either the cyclone or anticyclone may be defined in terms of the vertical extent of the cyclonic or anticyclonic vorticity, respectively. The vertical extent of the cyclone is sometimes definable to an altitude of 5 to 10 km above the earth's surface. The anticyclone is usually characterized by a region of calm air near the center surrounded by winds blowing clockwise (counterclockwise) near the periphery in the Northern (Southern) Hemisphere. The horizontal extent of the anticyclone may be as great as 2000 to 4000 km. The vertical extent depends on the nature of the air masses involved, the cold anticyclone being shallow (usually less than 5 km) and the warm anticyclone being deep (perhaps 10 km or more). The nearly calm area of the anticyclone is often thought of as the region of formation of air masses while the cyclone is the region of their interaction.

*by Frederick Sanders, Massachusetts Institute of Technology, and Duane S. Cooley, The Travelers Research Center, Inc

The specific weather phenomena mentioned generally occupy only portions of the cyclonic or anticyclonic wind regions. However, their scale is comparable to that of the major systems—that is, of the order of 1000 km. We shall regard these specific phenomena as by-products of the cyclone-anticyclone system.

E.1.4 Characteristic Process and Property Involvement

E.1.4.1 Basic Forces

Pressure gradient
coriolis
centrifugal
gravity
buoyancy

E.1.4.2 Modifying Factors

Surface friction
eddy viscosity of air
obstacles (mountains)
radiation

E.1.4.3 Property Transports

Mass of air
energy (kinetic, potential, internal including latent)
momentum
vorticity
humidity
liquid and solid water
aerosols and particulates
other gaseous components

E.1.5 Characteristic Variations (Life Cycle)

The migratory cyclone may develop in from 10 to 20 hr and its lifetime as a recognizable wind system may range from about 1 day to 1 week. The migratory anticyclone may develop more slowly but have a similar lifetime as a moving wind system. The "decay" phase of these vortices may consist of a merging of them with the semi-permanent surface cyclonic and anticyclonic wind

wind systems, respectively, or with other migratory systems. The semi-permanent wind systems are a somewhat larger scale of entities, such as the Icelandic or Aleutian low-pressure regions in the case of cyclones and the subtropical belts of high-pressure in the case of anticyclones. In this merger of wind systems we see the first inkling of a major difficulty that arises in dealing with the migratory synoptic circulations. More generally it is one aspect of interaction with the environment which calls into serious question the validity of trying to deal with these circulations as separate entities. We shall look at the question in further detail when we consider the energy budgets of these systems.

Since the weather in either cyclones or anticyclones depends to a large extent on the static stability and the moisture content of the air, among other factors, the natural rate of modification of these characteristics in a mass of air is of interest. This rate of modification depends on the rate of flow of the air across parallels of latitude, over masses of land and mountain barriers, and over bodies of water, all of which tend to change the temperature and moisture distribution of the air. The time required for appreciable natural modification may range from 1 to 15 days.

E.2.0 ASSESSMENT OF GEOPHYSICAL FORCES AND MASS OR PROPERTY TRANSFERS

E.2.1 Basic Physical Equations

Equation of horizontal motion:

$$\frac{d\vec{V}}{dt} = - f\vec{k} \times \vec{V} - \frac{1}{\rho}\nabla p + \frac{1}{\rho}\vec{F} \tag{E-1}$$

Continuity equation:

$$\frac{d\rho}{dt} = - \nabla\cdot\rho\vec{V} - \frac{\partial \rho w}{\partial z} \tag{E-2}$$

Hydrostatic equation:

$$\frac{\partial p}{\partial z} = - \rho g \tag{E-3}$$

Thermodynamic equation:

$$\frac{\partial \theta}{\partial t} = - \vec{V}\cdot\nabla\theta - w\frac{\partial \theta}{\partial z} + \frac{d\theta}{dt} \tag{E-4}$$

Water vapor transfer equation:

$$\frac{\partial q}{\partial t} = - \vec{V}\cdot\nabla q - w\frac{\partial q}{\partial z} + \frac{dq}{dt}$$

The symbols are defined as follows:

$\vec{V}$ = horizontal wind vector

w = vertical wind component

f = $2\Omega \sin \varphi$, coriolis parameter

$\vec{k}$ = vertical unit vector

ρ = air density

$\vec{F}$ = frictional force per unit mass

z = vertical coordinate (positive upward)

g = acceleration of gravity

θ = potential temperature

q = specific humidity

Ω = rate of angular rotation of the earth

ϕ = latitude

E.2.2 Scale Analysis

Forces act on a horizontal scale of 1000 km and a vertical scale of 1 to 10 km. Forces are given per unit of mass.

TABLE E-1
FORCE AND TERM ANALYSIS

Description	Quantity	Order of magnitude
Coriolis force	$(-f\vec{k} \times \vec{V})$	10^{-1} cm sec^{-2}
Horizontal pressure force	$(-\rho^{-1} \nabla p)$	10^{-1} cm sec^{-2}
Horizontal surface frictional force	$(\vec{F})$	5×10^{-2} cm sec^{-2}
Horizontal mass divergence	$(\nabla . \rho\vec{V})$	10^{-8} gm cm^{-3} sec^{-1}
Vertical mass divergence	$(\partial \rho w/ \partial z)$	10^{-8} gm cm^{-3} sec^{-1}
Vertical pressure gradient	$(\partial p/ \partial z)$	1 gm cm^{-2} sec^{-2}
Thermal advection	$(\vec{V} \cdot \nabla \theta)$	10^{-4} °K sec^{-1}
Vertical heat transport	$(w \frac{\partial \theta}{\partial z})$	5×10^{-6} to 5×10^{-5} °K sec^{-1}
Individual temperature change	$(\frac{d\theta}{dt})$	10^{-5} to 10^{-4} °K sec^{-1}
Advection of specific humidity	$(\vec{V} \cdot \nabla q)$	10^{-8} to 10^{-7} sec^{-1}
Vertical transport of specific humidity	$(w \frac{\partial q}{\partial z})$	10^{-8} to 10^{-7} sec^{-1}
Individual humidity change	$(\frac{dq}{dt})$	10^{-8} to 10^{-7} sec^{-1}

The individual temperature-change term includes diabatic effects such as radiation, latent heat transformations, eddy conduction of sensible and latent heat. The individual humidity change term includes evaporation and condensation and the magnitude is expressed in terms of the average through the whole mass depth of the atmosphere. Part of the individual humidity change term may be due to the eddy flux of humidity.

E.2.3 Characteristic Structure

Wind speeds near the earth's surface in migratory cyclones or in the periphery of migratory anticyclones are typically from 10 to 30 m sec^{-1}. The westerly wind speeds generally increase with height in the temperate latitudes while the easterly components generally decrease with height. In moderate winds the isobaric slope may be of the order of 10^{-4}, corresponding to a horizontal pressure gradient of 1 mb per 100 km.

There are preferred regions of formation and to some extent preferred paths of cyclones and anticyclones.

E.3.0 ASSESSMENT OF GEOPHYSICAL ENERGY

E.3.1 Energy Budget

What is surface cyclogenesis? Early views (Margules [1]) held that the growing strength of the winds of the developing storm was to be regarded as a transformation from gravitational potential energy of mass stratification into kinetic energy of the winds. The loss of potential energy was brought about by a systematic tendency of the more dense air to sink and for the less dense air to rise. An inference, often drawn though perhaps not intended, was that the potential energy was supplied in situ, and that the cyclone could be considered to some extent as an energetically closed system.

It became apparent, however, that this view was not realistic. Spar 17 [2], for example, showed that there was little correlation between cyclone intensification and contemporary local changes in potential energy. More recent theoretical and observational studies of the steady-state general circulation have shown that energy transformations of the type visualized by Margules [1] are indeed occurring in a statistical sense. The role of the cyclone, however, is rather one of an agent, receiving its kinetic energy from potential energy, and passing this kinetic energy on in part to the larger scale motions (and losing some through friction). Radiational and other diabatic heating and cooling processes, such as transformations involving latent heat, together with motions on a variety of scales, act to restore the potential energy distribution. Cyclones and anticyclones play a similar role in the transfer of momentum in the general circulation. The overwhelming importance of interaction is clearly evident.

The cyclones and anticyclones are large-scale eddies in the general circulation of the atmosphere. Lorenz [3] has described the relations between the energy of the large scale eddies and the energy of the zonal flow. In this diagram A and K are the average over the earth of the available potential and the kinetic energies, respectively. The quantities G_z and G_e are the zonal generation and eddy generation (or destruction) of available potential energy by non-adiabatic processes. The quantities D_z and D_e are the zonal dissipation and the eddy dissipation of kinetic energy by friction. The functions C_a, C_k,

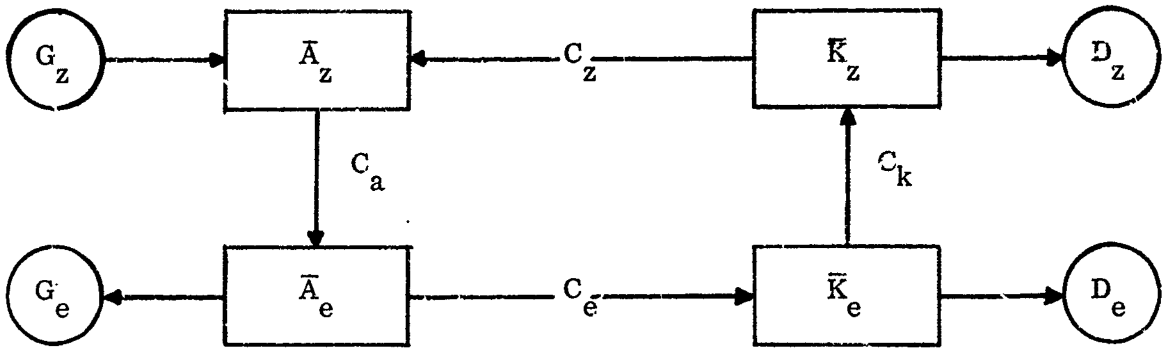

Fig. E-1. Schematic energy transformation diagram.

C_z, and C_e represent transforations of available potential and kinetic energy between zonal forms (whose magnitude may vary with latitude) and eddy forms (forms whose magnitude may vary with longitude).

The nature of the general circulation as postulated by Lorenz [3] is well-described by Oort [4]:

"The earth's surface (per unit area) receives more short wave radiation from the sun ... at low latitudes than at high latitudes, while the amount of long wave radiation leaving the atmosphere per unit area is, as a first approximation, independent of latitude. The net effect is an excess of incoming over outgoing radiation at low latitudes and a deficit at high latitudes. This process brings a north-south temperature gradient into existence, which is unstable for certain baroclinic wave disturbances. Maximum instability is found at about the wavelength of typical cyclones and anticyclones. These eddy circulations ("eddies") cause an east-west temperature gradient and thus convert zonal into eddy available potential energy. Through the action of vertical motions the eddy potential energy is partly converted into eddy kinetic energy. The eddies appear to lose further energy through the combined action of radiation, condensation, evaporation and heat fluxes near the ground. The kinetic energy of these large-scale eddies is subject to the probable destructive influence of smaller-scale eddies which transfer the kinetic energy to still smaller eddies. This cascade of the kinetic energy to smaller and smaller scales, results finally at the molecular scale in the transformation of the

kinetic energy into heat. A significant percentage of the large-scale eddy kinetic energy is in this way destroyed. The remaining part of this energy is converted up the scale into kinetic energy for the zonal current (the conversion being expressed by C_k), and thus maintains the zonal current against the frictional dissipation of the smaller eddies. Finally, the conversion of zonal potential into kinetic energy, C_z, brings us back to the beginning of the cycle, i.e., the zonal available potential energy. This conversion has proved to be small and may even have a negative value, i.e., K_z is converted into $\bar{A}_z$.

Thus, the cyclones and anticyclones are so much a part of the whole circulation of the atmosphere, that an evaluation of the energy balance of an individual eddy is very difficult if not impossible to make. Instead we shall present estimates of the average values of the terms in the energy cycle shown in the figure for a major part of the atmosphere, usually the Northern Hemisphere. While we are concerned with the problem of instigating energy transformations with respect to, say, one cyclone or anticyclone, the magnitude of the average dependence of the eddies on the zonal flow would seem to be of importance.

The presence of net heating in low latitudes and net cooling in high latitudes is the primary source of the energy of the general circulation and this is represented by the zonal generation, G_z, of zonal available potential energy, $\bar{A}_z$. Most of this energy is converted into eddy available potential energy, $\bar{A}_e$. According to Lorenz [3] the eddies probably destroy potential energy so that G_e is usually negative. The destruction process occurs through the non-adiabatic heating of southward moving air and the non-adiabatic cooling of northward moving air. This would imply that "local" generation of eddy available potential energy would have to overcome this natural dissipation except near longitudes preferred for energy release. The kinetic energy large-scale eddies and zonal flow is dissipated by friction including small scale turbulence. The estimates of the energy budget of the aggregate of cyclones and anticyclones will now be considered.

E.3.1.1 Storage Estimates

From Saltzman and Fleisher [5] it is estimated that for the Northern Hemisphere in winter:

$$A_z = \text{Zonal available potential energy} \approx 5.5 \times 10^{28} \text{ ergs},$$

$$A_e = \text{Eddy available potential energy} \approx 1.4 \times 10^{28} \text{ ergs}$$

It can be shown that for a large cyclone, assuming a radius of 2000 km and a depth of 12 km with the mean temperature 250 deg K and $\rho = 7 \times 10^{-4}$ gcm^{-3}:

$A_e = 200^{-1}$ (P+I) (according to Lorenz [3], where P and I are the potential and internal energies)

$$A_e = 200^{-1} (g\bar{\rho}\,\bar{Z} + c_c\bar{\rho}\bar{T}) \times \text{volume of the cyclone}$$

$$= 110 \times 10^{25} \text{ ergs.}$$

From another paper of Saltzman and Fleisher [6] it is estimated that for the Northern Hemisphere in winter:

$$K_z = \text{zonal kinetic energy}$$

$$= 370 \times 10^{25} \text{ ergs}$$

$$K_e = \text{eddy kinetic energy}$$

$$= 480 \times 10^{25} \text{ ergs}$$

For a large cyclone, assuming a depth of 0.8 ρ_0, and V=20 m sec^{-1},

$$K_e = 10^{26} \text{ ergs.}$$

For a small cyclone, assuming a depth of 0.1 ρ_0 and V=20 m sec^{-1}, with a radius of 750 km,

$$K_e = 4 \times 10^{24} \text{ ergs.}$$

E.3.1.3 Transformation-rate Estimates

We have adapted the values stated below from Ooort's summary [4] of the estimates for the Northern Hemisphere winter made by several authors.

G_z = Zonal generation of zonal available potential energy $\approx 70 \times 10^{25}$ erg day^{-1}.

C_a = Transformation rate of zonal available potential energy to eddy available potential energy, $C_a \approx 70 \times 10^{25}$ erg day^{-1}. The evaluation of C_a depends on the correlation of temperature deviations with horizontal eddy components of the wind.

C_e = rate of eddy generation (or destruction) of available potential energy by non-adiabatic processes, $G_e \approx 10 \times 10^{25}$ erg day^{-1}.

C_e = transformation rate of eddy available potential energy to eddy kinetic energy, $C_e \approx 60 \times 10^{25}$ erg day^{-1}. It is doubtful that this quantity has been evaluated for individual cyclones and anticyclones.

C_k = rate of transformation of eddy kinetic energy to zonal kinetic energy, $C_k \approx 10 \quad 10^{25}$ erg day^{-1}.

C_z = rate of transformation of zonal kinetic energy to available zonal potential energy ≈ 0.

Evaluation of these transformation-rate terms for individual cyclones or anticyclones may be extremely difficult. It should be noted that the formulations of C_a, C_e, and C_k given by Lorenz [3] are applicable only to a closed system such as the whole atmosphere. Due to limited data many of the above estimates were made for most of the Northern Hemisphere, assuming that transfer across the equator is negligible.

This leaves us with the question of the natural rate of air mass modification. Consider nature's best moderator, the Gulf Stream. Estimates of the energy provided by the ocean in the modification of winter continental air masses can be as large as 1 ly min^{-1} or 7.1×10^{5} erg cm^{-2} sec^{-1}.

E.3.1.3 Dissipation-rate Estimates

D_e = rate of frictional dissipation of eddy kinetic energy. From the transformation-rate estimates of C_e and C_k for the Northern Hemisphere: $D_e \approx 50 \times 10^{25}$ erg day^{-1}.

D_z = rate of frictional dissipation of zonal kinetic energy $\approx 10 \times 10^{25}$ erg day^{-1}.

E.3.2 Instabilities

Theoretical studies of hydrodynamical instability applied to meteorology have expressed the limitations on the growth of wave perturbations in a zonal current with or without vertical wind shear [7, 8, 9, 10, 11]. The growth of disturbances in the lower and middle atmosphere has been observed for several decades. Petterssen [12] sees the development (cyclogenesis) processes as immensely complex and greatly dependent on the height and configuration of the level of non-divergence and on the structure of the atmosphere below this level. However, it is well-known that there are preferred regions of instability of lower atmospheric flow and that these are over strong surface warming or in the lee of mountain ranges, or both. The extent to which it is possible to implement or dampen cyclogenesis by augmenting or depleting these effects is not well understood.

E.4.0 PREDICTABILITY AND SIMULATION

E.4.1 Theoretical

At present the general theory of the predictability of hydrodynamic flow is incomplete. Lorenz [13] comments: "It may be that within a few years, when even bigger (sic) and faster computers are available, and we have included the physical processes which we know about now, we shall obtain highly accurate short-range forecasts. Perhaps, on the other hand, we have nearly reached the limit which current errors in measurement place on predictability by dynamical methods."

Further, on statistical forecasting [13]: "The main stumbling block in statistical forecasting is the necessity for any sample of observations of the past behavior of a system to be finite in size. As a result, we can always find an infinity of formulas which the sample of data fits exactly, provided that we allow the formulas to become complicated enough. The sample itself provides no basis for selection among these formulas, which ordinarily give widely varying results when applied to new data, and which probably do not include the most appropriate formula, anyway.

"There is therefore no such thing as a "best" formula, from the point of view of a single sample, and we must seek instead the best formula of a specified restricted type. In all probability the arbitrary restrictions will exclude the formula which is really most appropriate."

E.4.2 Experimental

Some useful studies of the effects of weather modification by heating or cooling certain regions may be made in the laboratory by examining the effects of heating and cooling on rotating fluids. More general quantitative results can probably be obtained by simulating the atmosphere in the form of mathematical models for solution on electronic computers. The behavior of these models can then be observed under varying conditions to improve predictions and explore methods of modification [14]. Several years of such research will probably be necessary before any reasonable attempt can be made to modify the synoptic scale systems in the real atmosphere.

E.4.3 Empirical

An example of the predictability of surface cyclones is given by Veigas and Ostby [15] in their application of a statistical model to the motion and intensification of cyclones near the east coast of the United States. Their verification results on 106 independent cases show a 24-hr forecast rms vector error of four degrees latitude and a 24-hr forecast deepening rms error of 8.6 mb. A comparison was also made of 31 statistical forecasts with forecasts made by the National Meteorological Center (NMC). The NMC forecasts of cyclone motion and intensification are made subjectively with the aid of dynamical computer forecasts of upper air conditions. The rms vector error for cyclone location was 2.25 deg of latitude for the 24-hr statistical forecasts and 3.87 deg of latitude for the 18-hr NMC forecasts. Rms errors of central pressure forecasts were 8.14 mb for the statistical forecasts and 7.25 mb for the NMC forecasts. The NMC forecasts were made during January and February 1960, and it is believed that improvements have been made in the NMC forecasts since that time.

E.5.0 MODIFICATION OR CONTROL FEASIBILITY

It is highly probable that attempts to suppress cyclone development in one region would simply make cyclogenesis more likely elsewhere (not in itself a hopeless conclusion). In any case, consider the problem of cyclone inhibition. This is often regarded (subject to objections we shall raise later) as the same problem as inhibiting instability of waves in a baroclinic flow. Numerous theoretical analyses of the stability of small perturbations agree that instability is possible for waves of cyclone scale, provided that normal values of static stability are present along with only rather modest values of vertical wind shear. Since the former quantity depends upon the vertical gradient of temperature while the latter depends on horizontal gradient, the possibility exists that instability might be inhibited "locally" (e.g. over a 60-degree longitude span) by modifying the temperature structure of the atmosphere. Difficulties arise, however. In the case of vertical temperature gradient, the stability which is important is through a deep layer of the middle troposphere (where synoptic scale vertical motions are large). Yet the layer most easily modified by fires or ice, for example, is near the ground, quite unimportant* so far as the large-scale dynamics are concerned. In the case of horizontal temperature gradient, the effect must again extend through reasonably deep layers of the troposphere. But suppose we could eliminate the temperature gradient between, say, 40°N and 50°N by large-scale heating. Then the temperature gradient poleward of 50°N would be enhanced and so, presumably, would cyclonic activity.

But the argument based on instability of baroclinic waves throughout the depth of the troposphere may not be valid, aside from the obvious limitations of perturbation theory. In particular, intensification of a wave throughout the bulk of the troposphere often occurs without significant cyclonic development at the ground. Conversely, vigorous surface cyclogenesis often (nay, almost typically) occurs when a pre-existing upper trough of finite amplitude overtakes a quasi-stationary baroclinic zone at low levels. (Interaction again!) Instability in such a physical situation was found in a perturbation study by Mihaljan [16]

*Unimportant, if the lapse rate in only the lower one or two km is changed for just a short period of time.

and has been repeatedly shown by numerical calculation from observed initial data at NMC. Indeed, in synoptic practice this physical situation is one of the better understood circulation evolutions.

However, surface cyclogenesis does not occur in the forward quadrant of every mobile upper-level trough. These favorable conditions at upper levels have little geographical preference. Yet surface cyclogenesis (e.g. Petterssen, [17] shows strong geographical preference. So by modifying the geography perhaps we can modify the favored geographical regions for cyclone development. Petterssen's results show that surface cyclogenesis is favored: 1) in the lee of major mountain barriers, and 2) over relatively warm water surfaces. The mechanical type of surface cyclogenesis can be mitigated by eliminating the mountain barriers, while the thermodynamic type can be inhibited by preventing the transfer of latent and sensible heat from the water to the atmosphere. Interestingly, some regions (e.g. the Gulf Stream east of the Carolinas) are favored even in the summer when the adjacent land surface is at least as warm as the water. The explanation may lie in the supply of latent heat but perhaps also in the relative smoothness of the water surface. We could fix this by ruffling up the water but this would probably require strong winds, which would largely defeat our purposes.

It would also appear that the problem of alleviating the severe conditions of strong winds, cold blasts, and blizzards would be extremely difficult, even with the expenditure of large quantities of energy. Local modification of precipitation amounts by either increases or decreases of 10 to 20 percent may be possible within the next few years. Attempts at local modification of cold waves and blizzards may result in some increase in low level temperatures with the possible danger of creation of tornadic winds if the heating is not carefully controlled.

Obviously, there are reservations implicit in the above about our ability to produce non-trivial effects on a large scale.

E.6.0 REFERENCES

1. Margules, M., "Über die Energie der Stürme," Jahrb. Kais.-Kön. Zent. für Met. Vienna 1903. Translation by C. Abbe in Smithson. Misc. Coll., 51, 1910.

2. Spar, J., "Synoptic Studies of the Potential Energy in Cyclones," J. Meteorol. 7:1, 48–53, 1950.

3. Lorenz, E. N., "Available Potential Energy and the Maintenance of the General Circulation," Tellus, 7:2, 157–167, 1955.

4. Oort, A. H., On the Energy Cycle in the Lower Stratosphere, Contract No. AT (30-1) 2241, Rpt. No. 9, M.I.T. 15, Dec. 1963.

5. Saltzman, B., and A. Fleisher, "Further Statistics on the Modes of Release of Available Potential Energy," J. Geophys. Res. 66:7, 2271–3, 1961.

6. —, and —, "Spectral Statistics of the Wind at 500 mb." J. Atmos. Sci. 19:2, 195–204, 1962.

7. Charney, J. G., "The Dynamics of Long Waves in a Baroclinic Westerly Current," J. Meteorol. 4, 135–162, 1947.

8. Eady, E. T., "Long Waves and Cyclone Waves," Tellus, 1:1, 33–52, 1949.

9. Kuo. H. L., "Dynamic Instability of Two-dimensional Non-divergent Flow in a Barotropic Atmosphere," J. Meteorol. 6, 1005–122, 1949.

10. —, Kuo, H. L., "Three-dimensional Disturbances in a Baroclinic Zonal Current," J. Meteorol. 9, 260–278, 1952.

11. Pocinki, L. S., "The Stability of a Simple Baroclinic Flow with Horizontal Shear," Geophys. Res. Pap. 38, 78 pp. Cambridge, Mass. 1955.

12. Petterssen, S., "Some Aspects of the General Circulation of the Atmosphere," Cent. Proc. Roy. Meteorol. Soc. London, 120–155, 1950.

13. Lorenz, E. N., "The Predictability of Hydrodynamic Flow," Trans. N.Y. Acad. Sci. II, 25:4, 409–432, 1963.

14. —, "Simplified Dynamic Equations Applied to the Rotating-basin Experiments," J. Atmos. Sci. 19:1, 39–51, 1962.

15. Veigas, K. W., and F. P. Ostby, "Application of a Moving-coordinate Prediction Model to East Coast Cyclones," J. Appl. Meteorol. 2:1, 24–38, 1963.

16. Mihaljan, J. M., "The Baroclinic Instability of a '2-1/2 Dimensional Model Atmosphere' in Which the Upper Level is Non-divergent," Tellus 14:1, 116–122, 1962.

17. Petterssen, S., "A General Survey of Factors Influencing Development at Sea Level," J. Meteorol. 12:1, 36–42, 1955.

APPENDIX F. CONVECTIVE STORMS (THUNDERSTORMS)*

F.1.0 ENERGY BUDGET OF A CONVECTIVE STORM

The energy budget of a large single-cell convective cloud that develops in a conditionally stable atmosphere (i.e., unstable for rising motions but stable for descending motions) can be described in terms of sources and sinks. The energy sources in the convective cloud are:

(a) the released heats of condensation and fusion

(b) the force of gravity acting on cold air in the downdraft during the precipitating stage of the cloud.

The energy sinks are:

(a) increases in internal and potential energy of the environment

(b) energy expended in lifting water particles

(c) work done in separating electrical charges which discharge to ground

(d) friction.

On the basis of the data provided by the Thunderstorm Project, Braham [1] computed the energy budget for an average thunderstorm. In his computations, the thunderstorm cloud plus its environment, which may be arbitrarily extensive, are considered a closed system. The energy budget pertains to both the development and mature stage of the thunderstorm, which means that the downdraft portion of the storm is included. At the end of the mature stage, a certain amount of air has moved out of the upper portion of the cloud and subsided upon the environment air, and, below the level of nondivergence, air has moved into the cloud, except near the surface, where an outward flow is caused by a cold dome of sinking air.

*By Pieter J. Feteris.

F.2.0 SAMPLE COMPUTATION OF THE INCREASE IN INTERNAL AND POTENTIAL ENERGY OF A STORM'S ENVIRONMENT

The amount of heat added to the air by virtue of the air's subsidence will depend on the size of the area over which the subsidence takes place. Instead of computing the heating on the basis of some assumed ratio of the area of the cloud to the area of the clear air, Braham developed the relationship as follows.

The internal energy of a column of air of unit cross section between pressure p_0 and p is

$$\frac{E_i}{A} = \int_0^H \int_0^T \rho C_v \, dT \, dz = \int_0^H \rho C_v T \, dz = - \int_{p_0}^{p_H} \rho \cdot \frac{C_v T}{\rho g} \, dp$$

$$= \frac{C_v}{g} \int_{p_H}^{p_0} T \, dp. \tag{F-1}$$

A small change in the internal energy over an arbitrary area A can be written

$$dE_i = A \times \frac{C_v}{g} \int_{p_2}^{p_1} dT \, dp = A \, \frac{C_v}{g} \, dT \, (p_1 - p_2)$$

$$= A \, \frac{C_v}{g} \, \Delta p \, dT. \tag{F-2}$$

This expression relates the total change in internal energy of a layer Δp over an area A to the temperature change dT. ρ is the density, C_v is the specific heat for constant volume, and g is the acceleration of gravity.

Assuming that the temperature rise dT during the subsidence has been the same for each layer, so that the lapse rate remains unchanged during the process, we can write

$$\Delta T = \frac{V(\Gamma - \gamma)}{A}, \tag{F-3}$$

in which V is the volume of air passing through Δp, Γ is the dry-adiabatic lapse rate, and γ is the actual lapse rate.

Substituting Eq. (F-3) in Eq. (F-2), we have

$$\Delta E_i = \frac{C_v}{g} \cdot V(\Gamma - \gamma) \Delta p, \tag{F-4}$$

which enables us to compute the change in internal energy for the pressure interval Δp.

The relation between internal and potential energy can be found as follows. The potential energy of a column of air of unit cross section and height H is

$$E_p = \int_0^H \rho g z\, dz = \int_0^H - z\, dp = - p_H H + \int_0^H p\, dz$$

$$= - p_H H = R \int_0^H \rho T\, dz. \tag{F-5}$$

For the internal energy, we have Eq. (F-2), which must be multiplied by J to express it in mechanical units:

$$I = E_i = J \frac{C_v}{g} \int_{p_H}^{p_0} T\, dp. \tag{F-6}$$

Then the potential energy will be

$$E_p = - p_H H + (R/JC_v) E_i. \tag{F-7}$$

For a finite H, $p_H \rightarrow 0$, so that

$$E_p = \frac{R}{JC_v} E_i = \frac{C_p - C_v}{C_v} \frac{E_i}{J}$$

and

$$\Delta E_p = \frac{C_p - C_v}{C_v} \frac{\Delta E_i}{J} = 0.405\, \Delta E_i \tag{F-8}$$

if expressed in calories. The total increase in internal energy ΔE of the layer is then given by

$$\Delta E = \Delta E_p + \Delta E_i = 1.4 \frac{C_v}{g} \Delta p\ V (\Gamma - \gamma). \tag{F-9}$$

If the amount of air passing through the layer is given in kilograms, $V = m/\bar{\rho}$, where $\bar{\rho}$ is the average density of the layer Δp, and

$$\Delta E = 1.4 \frac{C_v}{g} \Delta p (\Gamma - \gamma) \frac{m}{\rho}. \tag{F-10}$$

This equation can be used to determine the work done against the environment by a convective cell.

By specifying Δp, and $v = \frac{m}{\rho}$ in Eq. (F-10), we can estimate the effect of slow vertical motions on the work which the convective cell has to perform against the environment. Suppose a rising motion of 1 cm sec^{-1} over an area of 10^5 km^2, $(\Gamma - \gamma) = 0.2°C$ per 100 m and $\Delta p = 500$ mb. $\frac{\Delta E}{\Delta t}$ will then be approximately 3×10^{10} cal sec^{-1}. The lifetime of a convective cell is of the order of an hour, which means that about 10^{13} calories will be applied to the environment of the convective cell over an area of 10^5 km^2 by forces operative on the synoptic scale. This amount of energy is feasible for a convective storm as will be seen in Section F.3.0. Although it is difficult to specify the area influenced by a single convective cell, experience in synoptic and meso-scale analysis suggests that slow large-scale vertical motions may alter profoundly the net amount of work done against the environment by a single cell thunderstorm.

F.3.0 SUMMARY OF THE COMPUTATIONS OF THE ENERGY BUDGET

For an average thunderstorm-cell height (10 km) and diameter (6.5 km), Braham [1] found ΔE_1 to be 2.6×10^{14} cal. The other, less important energy sinks will be mentioned briefly.

The magnitude of the energy involved in lightning, ΔE_2, was found to be between 10^{10} and 10^{11} cal. Assuming that the total amount of condensed water in a storm is lifted to a height of 10 km, Braham found that the work done by the storm, E_3, is 2.3×10^{12} cal. These two energies are a few orders of magnitude smaller than ΔE_1.

Braham did not consider friction, but later work on energy transformations (e.g., [2]) suggests that ground friction dissipates an amount of energy that is at least two orders of magnitude smaller than that produced by the latent heat of condensation.

The latent heat, E_L, released by condensation of 1 gm of water vapor is

$$E_L = A \cdot \int_{z_1}^{z_2} \int_{t_1}^{t_2} L_v \, wG \, dz \, dt, \tag{F-11}$$

where w is the vertical velocity, and $G = - \partial\rho_w/\partial z$, the decrease in saturation vapor density with height. The latent heat, L_F, released by fusion is given by

$$E_F = A \cdot L_F \cdot \alpha \int_{z_1}^{z_2} \int_{t_1}^{t_2} wG \, dz \, dt, \tag{F-12}$$

where α is the fraction of condensed water which freezes. Changing the order of integration, we may write the equations as

$$E_L = AL_v \int_{t_1}^{t_2} \int_{z_1}^{z_2} wG \frac{dz}{dt} = AL_v \int_{z_1}^{z_2} \int_{z_1}^{z_2} wG \, dz \, dz \tag{F-13}$$

and

$$E_F = AL_F \, \alpha \int_{z_1}^{z_2} \int_{z_1}^{z_2} wG \, dz \, dz. \tag{F-14}$$

Since part of the condensed water evaporates at the boundaries of the cloud in the anvil and in the downdraft portion, these expressions overestimate the

release of latent heat. Neither can the release of latent heat be estimated from the amount of rainfall that reaches the surface. Braham estimated the total inflow of water to be 8.9×10^8 kgm, the reevaporation in the downdraft above the cloud base to be 2.4×10^8 kgm, and the evaporation in the anvil (outflow) plus the loss at the edges to be 1.2×10^8 kgm, so that a total of 5.3×10^8 kgm of water was condensed. The latent heat produced was 3.2×10^{14} cal, which is of the same order of magnitude as the work done by the storm. The small difference between the two numbers suggests that under some circumstances (dry atmosphere, great losses by reevaporation) energy must be added to maintain the growth of a large convective cloud. In unstable moist atmospheres, an excess of energy may be converted to kinetic energy to trigger the development of larger, more vigorous storms.

F.4.0 ENERGY NEEDED TO RELEASE CONVECTION IN A CONDITIONALLY UNSTABLE ATMOSPHERE

The energy needed to trigger a convective cloud in a conditionally unstable cloudless atmosphere is likely to be smaller than that released by the convective system itself. In some cases, it may be enough to lift by 1 km (for instance, from the surface to past the lifting-condensation level) the lowest 2 km of the atmosphere contained within a 1-km radius.

Because the lapse rate of the environment may be between Γ and γ_w, the lifted air will be colder than its environment. To raise it to the temperature of the environment, heat must be added, the amount of which can be calculated as follows. The temperature rise necessary to lift a parcel of air to a height z, is given by

$$\Delta T = \int_{z_0}^{z_1} (\Gamma - \gamma)\, dz. \tag{F-15}$$

The work done to raise this parcel against gravity to the height z_1 is

$$E_w = \int_{z_0}^{z_1} dE_w. \tag{F-16}$$

For an infinitely small height interval dz, $dE_w = (\rho - \rho') \, gdz$, where $\rho - \rho'$ is a function of z. Substituting $\rho = \frac{P}{RT}$ yields

$$dE_w = \left(\frac{P_1}{RT_1} - \frac{P_2}{RT_2}\right) gdz. \tag{F-17}$$

Assuming that $P_1 = P_2$, and since in most cases $T_1 \approx T_2$ within 3%, one may write

$$dE_w = \frac{P}{R}\left(\frac{1}{T_1} - \frac{1}{T_2}\right) gdz = \frac{P}{RT}\,\frac{\Delta T}{T}\, gdz = \rho\,\frac{\Delta T}{T}\, gdz \approx \bar{\rho} g\,\frac{\Delta T}{T}\,\Delta z \tag{F-18}$$

for finite height intervals. The work done on the parcel will be found by substituting Eq. (F-15) into Eq. (F-18):

$$\Delta E_w = \rho g \int_{z_0}^{z_1}\int_{z_0}^{z_1} \frac{\Gamma - \gamma}{\bar{T}}\, dz\, dz = \frac{1}{2}\,\rho g\,\frac{\Gamma - \gamma}{\bar{T}}\,(z_1^2 - z_0^2), \tag{F-19}$$

in which $\bar{T}$ is the average temperature (°K) over the distance z. To find the total energy E, $\bar{T}$ must be multiplied by the volume of air that is forced to rise. For $z_1 - z_0 = 1$ km, $\gamma = 7°C\ km^{-1}$, $g = 10\ m\ sec^{-2}$, $\rho = 1\ kgm\ m^{-3}$, and $\bar{T} = 300°K$, E_w will be $5 \times 10^4\ kgm\ m^{-2}$ or $1.15 \times 10^5\ cal\ m^{-2}$.

There are very few reports of experimental work on the production of convective clouds in a conditionally unstable atmosphere. Dessens [3] produced (by fire) 9×10^{11} cal over an area of $25 \times 10^4\ m^2$ in 30 min; this is 4×10^3 cal $m^{-2}\ sec^{-1}$. He observed the formation of a cumulus cloud above the fire. Its top soon rose at a rate of 22 m sec^{-1}. The cloud continued to exist and rained several hours after the fire was burned out. Comparing the number of calories per square meter per second applied by Dessens with the energy necessary for the triggering of a single-cell cloud, we find that Dessens produced about 10 times more heat than that required to lift a kilometer-high column of air 1 km. It must be remembered, however, that to trigger the release of heat by condensation, we must lift the entire column of air, not apply heat slowly from below (which is then used only to change its temperature and not to condense its water vapor). This can be illustrated as follows.

With reference to Fig. F-1, suppose that the temperature of the air decreases with height following the curve $T_0 = T_6$ and that the humidity-mixing ratio diminishes following the line x_0x_6. The lapse rate is dry-adiabatic from T_0 to B and conditionally unstable between CCL and T_6 (vertical lines are saturated adiabats, dotted lines are dry adiabats). A gentle warming of the air over an area of several kilometers' diameter during a period in which there is time for upward transfer of heat would raise the temperature in the whole air column, but the lapse rate would remain dry adiabatic. Eventually, with a surface temperature T_x, convection could start at level H_2 (CCL), but any shower or thunderstorm thus produced would have a high base and its rain would almost entirely evaporate into the dry air before it could reach the surface. Very little precipitation would be obtained at the expense of a supply of the order of 10^{14} cal (T_0T_xCCL-T_0) if, for example, the air had to be warmed by about 10°C over a volume of about 10 km^3. The energy applied to lift an air column of the same diameter and depth H_0H_1 to H_1H_3 would be the pressure-volume work done to

subside its surroundings [Eq. (F-10)], which is of the same order of magnitude as that corresponding to the area $T_0T_xCCLT_0$.

If the energy is applied to the column within a short time, so that upward transfer of heat and mixing with the surroundings is kept to a minimum, a region will be created in which the temperature lapse rate follows the line $T_0LCL_0CT_6$. Because condensation starts at LCL_0 (the lifting-condensation level), the lapse rate will now be unstable for rising motions and the cloud that develops will have a low base and may have a greater chance to produce precipitation at the surface. With the lapse rates given in Fig. F-1, convection can be triggered in air that is forced to rise over a steep mountain ridge. Artificial means for triggering convection would have to be either a large explosion or a fire with a high yield of calories per unit of time.

F.5.0 ENERGY NEEDED TO TRIGGER CONVECTION IN A POTENTIALLY UNSTABLE ATMOSPHERE

Instead of applying heat to air with a vertical distribution of temperature and humidity as displayed in Fig. F-1, a much more harmless method would be to cool the layer between B and C by evaporating water into it. Because the wet-bulb potential temperature decreases with height, saturation of the layer would render the lapse rate between B and C unstable and would permit the moist air in the layer H_1H_0 to escape through a column wide enough for the formation of a tall convective cloud. The water must be distributed in the form of tiny drops (less than 0.1 mm in diameter) which evaporate quickly and which exert little drag on the air to prevent the initiation of rapid sinking motions. Because the saturated air becomes colder than its environment, sinking motions are unavoidable. Unless the whole column of air is saturated quickly (more quickly than the air can subside over a height interval of, say, a few hundred meters at a rate of, say, 1 m sec^{-1}), adiabatic warming associated with the descending motions may create a new inversion and may also cause drying of the initially moist surface layer.

Computations of the amount of water vapor required to saturate a 2.5-km-deep air column in a maritime tropical air mass having temperature and moisture distributions as given in Fig. F-2 showed that about 2 gm of water per cubic meter would have to be distributed over a volume of about 8×10^9 m^3; the total amount of water needed would be about 17 m^3. Although this amount is within reasonable limits, its distribution into very tiny drops within a few minutes may be difficult. Also, the dynamical interactions between the sprinkled area and its environment require further study before an experiment can be attempted.

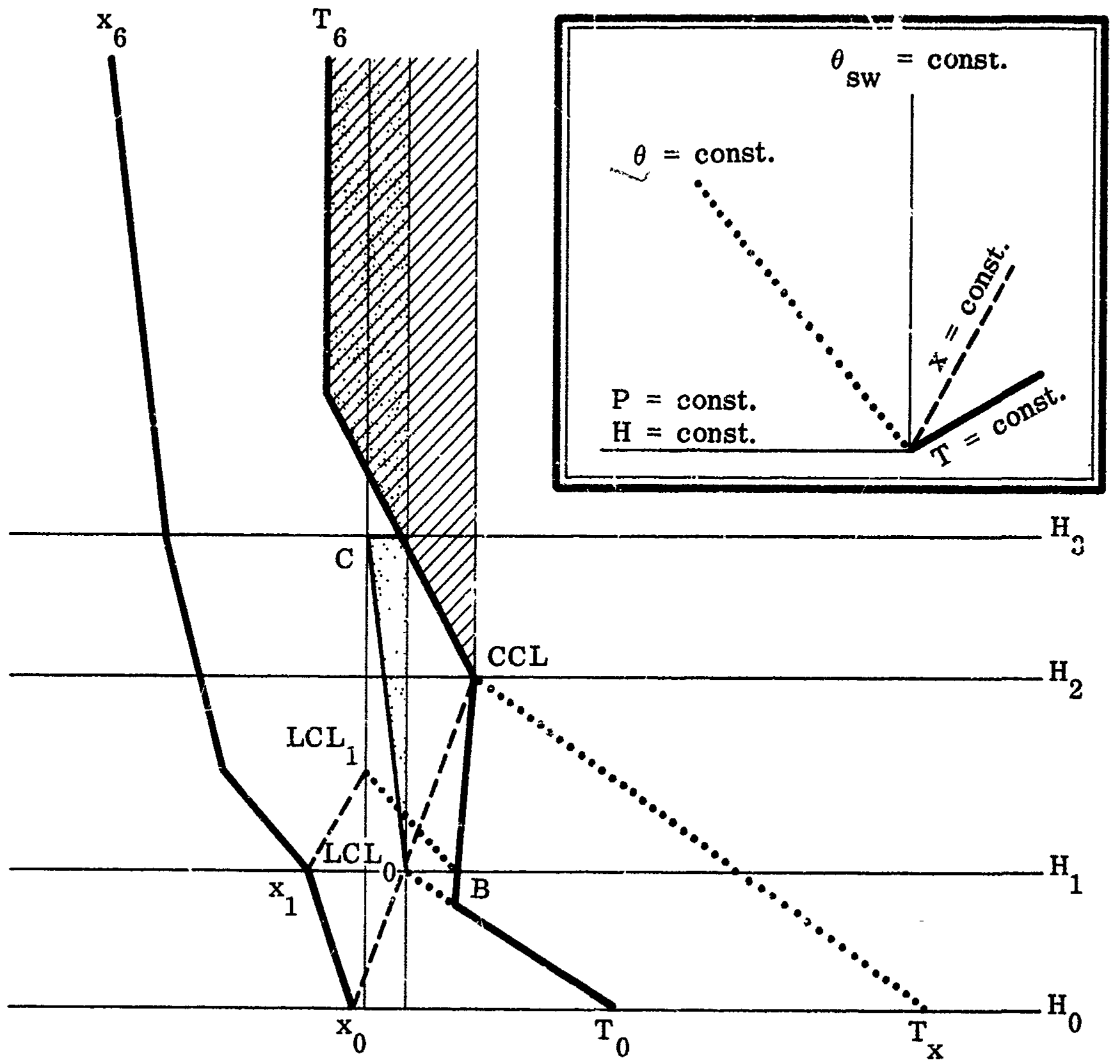

Fig. F-1. Sounding representing a potentially unstable atmosphere. The slopes of the isobars, isotherms, adiabats, and lines of constant mixing ratio are shown in the upper right-hand corner. Slow heating of the layer H_0H_2 results eventually in an increase of the surface temperature from T_0 to T_x and vigorous convection at the level CCL. Clouds forming in such an unstable dry atmosphere produce very little rain. Rapid (explosive) heating of the layer H_0H_1 causes it to rise to become layer H_1H_3. The temperature lapse rate is changed locally to $T_0LCL_0CT_6$, which is less unstable, but the air has now become saturated. Note that the lifting-condensation level LCL_0 is much lower than CCL so that any rain falling from a convective cloud in this atmosphere will have less chance to evaporate.

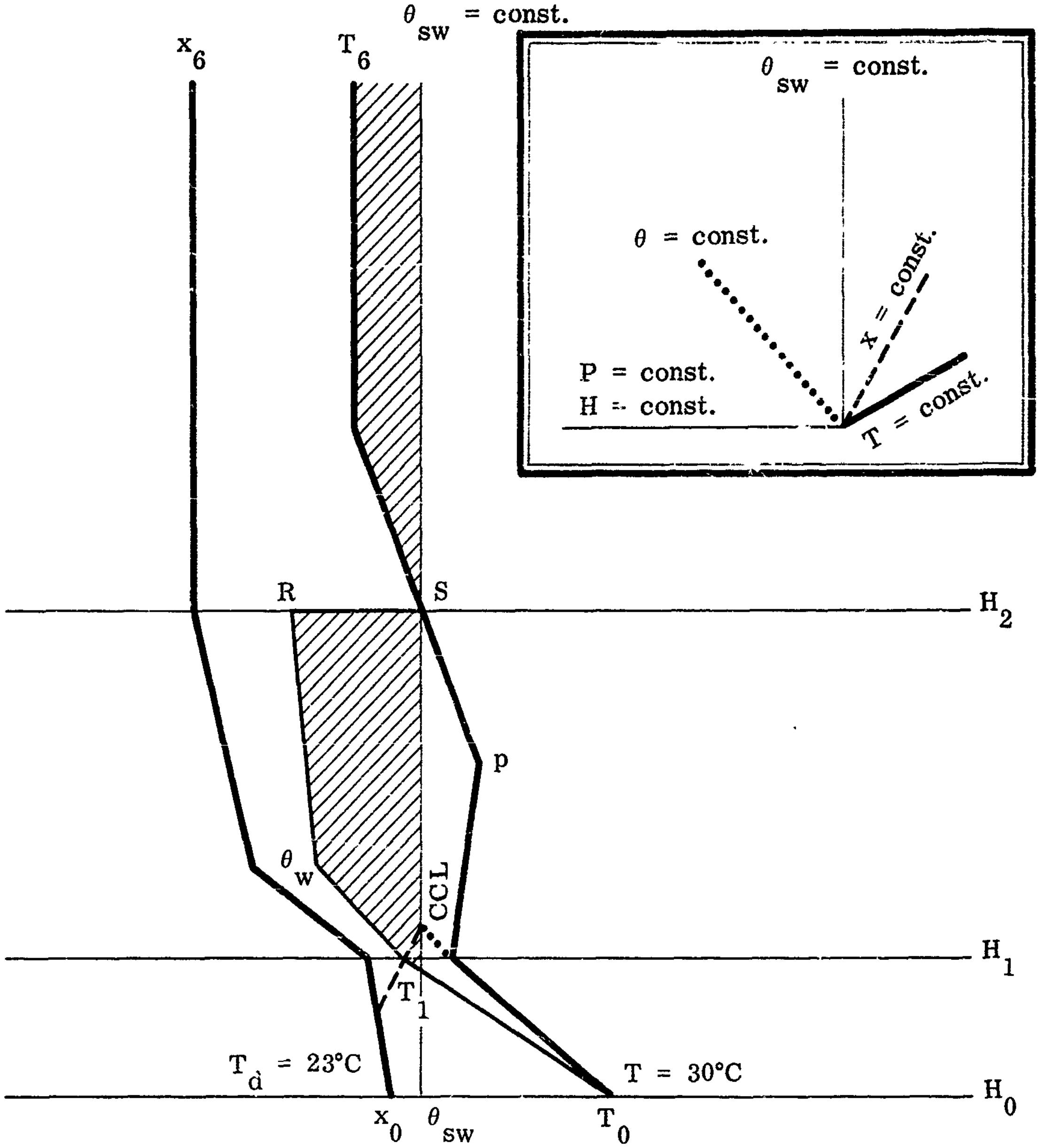

Fig. F-2. T_0PST_6 and x_0x_6 represent a sounding in a potentially unstable maritime-tropical air mass. The wet-bulb temperature decreases with height according to $\theta_{sw}T_1\theta_wR$. Saturation of the layer H_1H_2 can change the temperature lapse rate to $T_0T_1\theta_wRST_6$, which just permits deep convection.

F.6.0 REFERENCES

1. Braham, R. R., "The Water and Energy Budgets of the Thunderstorm and their Relation to Thunderstorm Development," J. Meteorol. 9, 227–242, 1952.

2. Malkus, J. S., and H. Riehl, "On the Dynamics and Energy Transformations in Steady-state Hurricanes," Tellus 12, 1–20, 1960.

3. Dessens, "Étude preliminaire des cumulus et des pluies obtenus par convection provoquée," Bull. obs. Puy de Dome 2, 1957.

APPENDIX G. HURRICANES*

G.1.0 INTRODUCTION

Scientific endeavor is frequently divided into four phases; description, understanding, prediction and control. As related to hurricanes or typhoons, work is currently underway in all four phases. Thus, in considering the possibility of improving prediction of, and effecting some measure of control over, the formation and behavior of hurricanes, it is convenient to divide the discussion into four main sections with the above mentioned phases as section titles.

*By Keith W. Veigas

G.2.0 DESCRIPTION

Development of an adequate description of the structure of tropical cyclones through their life cycle has been a rather difficult task since they are primarily a maritime phenomenon. The advent of radar and aircraft weather reconnaisance provided important new data sources to augment conventional observational networks and as a result we now have a reasonably complete description of the typical three dimensional structure of hurricanes through most of their life cycle.

G.2.1 Geographical Extent

Hurricanes form over all tropical oceans with the exception of the South Atlantic and Eastern South Pacific. Before their life cycle, averaging about a week in duration, is complete many migrate through the mid-latitude zone.

G.2.2 Life Cycle

Dunn [1] and McDonald [2] have divided the life cycle into four stages:

(a) Formative Stage. This begins when a cyclonic circulation develops in an easterly wave or in the intertropical convergence zone. At this stage the cloud and rain patterns are quite variable from storm to storm. Highest winds are usually associated with squalls, and are frequently located as far as 150 km from the developing center. The central surface pressure generally drops to 1000 mb during the formative stage.

(b) Immature Stage. Those disturbances that intensify beyond the formative stage are marked by a rapid drop in central pressure. Winds increase to hurricane force and the area of maximum winds forms a narrow circular band close (30-45 km) to the center. The rain squalls become organized into narrow bands spiraling inward and merge forming the "eye" wall clouds. During this stage the cyclonic circulation covers only a relatively small area (radius 100-200 km).

(c) Mature Stage. This is marked by an expansion of the circulation with little or no further decrease in central pressure and, although the area covered by hurricane and gale force winds expands, the maximum wind remains

constant or decreases slightly. The mature storm varies widely in size. The circulation may be confined to a radius of 200 km or less or may expand to a radius of 1,000 km.

(d) Decaying Stage. This is marked by either movement over land (where it dissipates) or movement northward where the hurricane takes on the characteristics of an extratropical cyclone.

G.2.3 Surface Pressure Distribution

Central pressures of 950 to 960 mb are not uncommon during the life cycle of a hurricane. Central pressures below 900 mb have been reported on occasion [3]. Pressure gradients are a maximum near the core with reliable estimates ranging as high as 3.7 mb per mile.

G.2.4 Surface Temperatures

The temperatures outside the eye of a hurricane remain essentially constant or decrease slightly toward the center [4]. Since inflowing air experiences expansion and cooling this must be counteracted by a transfer of heat from the ocean surface. The rate of transfer of both sensible and latent heat is increased as the area of maximum winds is approached.

G.2.5 Low Level Wind Structure

The general features of the wind distribution about a hurricane are rather well known. The winds blowing counterclockwise (northern hemisphere) about the center gradually increase toward the center in the outer portion of the storm and the rate of increase steadily grows until the maximum wind is reached in the vicinity of the outer edge of the eye. The speed rapidly decreases from the maximum to near calm in the eye. The distribution of speed is asymmetric with higher winds to the right of the direction of motion. If one subtracts the motion of the storm center from the wind observations the tangential component of the residual wind field is approximately symmetrical about the center. The radial component of the wind relative to the storm center is almost everywhere directed inward with the largest components in the right front quadrant. The maximum inflow is within 1 degree of latitude of the storm center.

Maximum winds in a hurricane generally exceed 45 m sec^{-1} and in extreme

storms much higher maximum values are experienced. Anemometers generally fail between 54-70 m sec^{-1} but estimates from damage place the maximum in extreme storms in excess of 90 m sec^{-1}.

G.2.6 Eye

Just within the ring of maximum winds and torrential rains at the storm center is found one of the most striking phenomena in meteorology, the "eye" of the storm. The eye is approximately circular and relatively cloud free. There is generally a scattered-to-broken layer of low clouds and occasionally some high cirrus clouds. The eye diameter of mature hurricanes averages about 15 miles near the ocean surface. The wind abruptly decreases from hurricane force just at the edge of the eye to 0–7 m sec^{-1} within the eye. Marked subsidence takes place within the eye through a layer extending from the upper troposphere to within about 1 km of the ocean surface. Simpson [5] measured a temperature of +16°C at 500 mb in the eye of a 1951 Pacific typhoon. Aircraft observations indicate that the diameter of this warm air column increases significantly above 300 mb giving rise to excessive surface pressure gradients just outside the perimeter of the low-level eye. A detailed description of the circulation within the eye has not yet been established. However there is considerable evidence of some mixing between the subsiding air in the eye and the adjacent convective zone.

G.2.7 Clouds and Precipitation

The principle cloud-generating zones in a hurricane are narrow zones of low-level convergence originating on the fringe of the storm and forming a cyclonic spiral pattern. These bands spiral inward and merge to form the wall cloud about the eye of the storm. The radial component of the wind is directed outward in the upper levels giving rise to layers of cirrus, altostratus and altocumulus clouds throughout much of the storm area. Heaviest precipitation is concentrated along the convective bands and reaches a maximum in the inner core where the several convective bands merge.

Rainfall amounts of 50 cm are not uncommon. Orographic effects, size of the storm rate of movement of the center, rain intensity and location of a

station relative to the hurricane are all factors in total rainfall accumulated. As much as 245 cm have been reported with the passage of a single storm [1].

G.2.8 Upper Wind Structure of Hurricanes

The intensity and areal extent of the cyclonic circulation gradually diminish with height. In the upper troposphere cyclonic flow is replaced by anticyclonic flow except within a small area near the center. The inflow in the lowest layers also decreases with height. The radial component is generally very small from 700 to 300 mb. Above 300 mb there is marked outflow.

G.2.9 Engery Considerations

By far the principal source of energy in a hurricane is the latent heat of condensation. Estimates [6, 7] place the rate of release of latent heat at about $.5 - 1.0 \times 10^{19}$ cal day^{-1}. The hurricane functions as a simple heat engine operating at 2–3% efficiency. The same sources cited above place the rate of generation of kinetic energy at about 3×10^{17} cal day^{-1}. The rate of dissipation of kinetic energy by friction and internal eddies is of the same order of magnitude as the generation rate. An analysis of hurricane Daisy by Riehl and Malkus [8] indicates that dissipation by friction and internal eddies are approximately equal. The ocean is an important heat source in maintaining the warm core thermal structure of the hurricane. Temperature observations in lower 1000 ft of the hurricane indicate that the inflowing air in this layer goes isothermal expansion, implying that the air gains sensible heat as well as latent heat from the underlying surface. As the air approaches the storm center and the area of extreme winds, the ocean is greatly agitated and large quantities of spray accelerate the transfer process.

Estimates of radiation flux are uncertain [8]. There is, however, general agreement that it is only a small fraction of the vertical transport of heat in a hurricane and there must be sizable energy transfers of energy to the environment in the upper troposphere or outflow region. Mixing of the warm ascended air with the cooler air in the environment serves to maintain the energy-producing thermal structure.

G.2.10 Future Work in the Descriptive Phase

It has been exceedingly difficult to obtain adequate observational surveillance over areas where there exists a potential for hurricane formation. Thus, our description of the hurricane in the early formation stage is at best sketchy; this is also true of "suspicious" disturbances that fail to develop into hurricanes. The recent observational tool, the weather satellite, offers hope of at least partially filling this observational gap.

At the same time the introduction of satellite observations reemphasises a problem of the descriptive phase that requires further attention. For both research and operational use it would appear that many types and in some cases vast quantitites of data will soon be available from which both research and operational units will wish to construct the best three dimensional description of the atmosphere possible. The volume of data, from satellites, for example, dictates machine methods should be used and the variability in reliability of the many data sources indicates that techniques to assess the optimum weighting of the various types of observations in objective analysis procedures must be developed. Statistical methods such as those described in Miller [9] and Spiegler et al. [10] could form a suitable framework for the development of new analysis procedures.

Detailed case studies utilizing special observations from research aircraft are essential to complete our description of the phenomena and to provide insight to aid in developing theoretical models which closely resemble the real world.

G.3.0 UNDERSTANDING

While our understanding of the formation and subsequent behavior of hurricanes is far from complete, recent theoretical and observational studies have pointed up the relative importance of the physical processes. There is little doubt for example, that the mature storm is maintained largely by the release of the latent heat of condensation. Inward flowing air in the lowest layers of the atmosphere acquires by turbulent exchange both sensible heat and water vapor. Ascent of this air is concentrated in spiral convection bands and increases to a maximum near the hurricane center where the bands merge to form the eye wall. The observed temperature distributions indicate a minimum of entrainment of mid-tropospheric air of low heat content in the primary convection zones. This coupled with outflow and cooling by lateral mixing of the relatively warm ascended air in the high troposphere maintains an energy producing circulation; that is, the ascending air is warmer than the air in the periphery of the storm.

The initial establishment of the above warm core circulation is not clearly understood. Theoretical studies, such as that of Kuo [11], indicate that in a conditionally unstable atmosphere the preferred scale of the disturbance resulting from small random perturbations is that of a cumulus cloud. Even if pre-existing disturbances in the tropical circulation bring about some degree of non-randomness to the organization of individual convective cells, mid-tropospheric entrainment inhibits the formation of a warmer-than-normal atmosphere over a limited area. It has been pointed out by Riehl [12] that many pre-hurricane tropical disturbances in fact exhibit a cold core thermal structure. There is evidence that several processes may be active in generating the initial warm core structure of the hurricane in the formative stages. If a cirrus layer develops in the high troposphere over a tropical disturbance there is a decrease in the outward flux of long wave radiation compared to adjacent cirrus-free areas. It is expected that satellite radiation measurements in the vicinity of tropical disturbances will yield quantitative measures of the importance of this process. Cooling by advection in the outer reaches of the storm is a factor of importance in at least some cases of hurricane development [13].

G.4.0 PREDICTION

G.4.1 Present Status

That skill in prediction hinges on advances of the two previous phases of research is clearly illustrated in the case of hurricanes. About the best we can do today in the problem of predicting the formation of a hurricane is to delineate large areas where it can be said with a good deal of certainty that there will be no formation. However, there remains rather large suspicious areas where hurricane formation is still a rare event. It is no coincidence that our description and understanding of hurricane formation is inadequate.

This is not to say that prediction of the behavior of the hurricane once it has formed is flawless. There has, however, been some progress in this area. Prediction techniques have evolved from two general approaches. One approach has been the application of numerical weather prediction techniques [14, 15]. A second approach has been the application of statistical techniques to relate initial and near past measures of the circulation patterns to subsequent motion and change in intensity of hurricanes. Examples of application of this approach are contained in [16, 17, 18]. An operational test of several of these techniques for 24- and 36-hr displacements is reported by Tracy [19]. The tests results indicated the statistical methods yielded smaller errors than the NWP technique tested.

G.4.2 Future Work

Success in the development of techniques for the prediction of hurricane formation will hinge on progress in the descriptive and understanding phases. However, even with adequate description and understanding of the phenomena the problem of application would likely be seriously hampered by inadequacies of the present day or near future observational capabilities. For this reason it seems appropriate, in addition to an approach employing a dynamic prediction model, to initiate a parallel effort to develop a statistical-physical model. It is conceivable that conditions crucial in the determination of whether or not a disturbance will develop into a hurricane may not be explicitly depicted by the available observations. The suggested alternate approach allows the freedom of

inferring such crucial conditions from data which is available in our present observations. An additional advantage of such an approach is the fact that a quantitative measure of the uncertainty associated with a given prediction may be derived. An example of some preliminary work employing such an approach is reported by Riehl et al. [20].

The improvements in predicting the behavior of hurricanes that can be brought about by increasing the observational coverage and by developing techniques to more accurately sythesize data from a variety of sources cannot be overemphasized. The verification results of Tracy [19] (where forecast errors in data-dense areas are compared with forecast errors in data-sparse areas) clearly illustrate this point.

There is clear evidence in other prediction problems that information contained in numerical and statistical prediction models is not redundant. For example, Klein [21] has demonstrated that in the prediction of surface pressure the addition of dynamic prognosis to a statistical prediction model resulted in a significant increase in skill. A scrutiny of prediction errors associated with a statistical prediction model and mid-tropospheric dynamical predictions over the past several years leads the author to the judgement that such an approach to the hurricane prediction problem would be fruitful.

G.5.0 CONTROL

Research in the descriptive, understanding and prediction phases has reached a point where some speculations can be made concerning the possibility of controlling the development or behavior of hurricanes. The speculative nature of the statements should be emphasized. Until our knowledge has progressed to the point where we can accurately simulate the atmosphere's behavior with a prediction model, the problem of designing definitive control experiments is formidable if not impossible. The rate of kinetic energy generation of a hurricane is two orders of magnitude greater than the rate of generation of electric power in the United States. Thus it seems reasonable to look for means other than direct energy confrontation as possible methods of control.

The condensation-precipitation process is of major importance in hurricanes, and Schaefer and Langmuir [22] have demonstrated that man can effect changes in this process. LaSeur [23], in analysing observations compiled on research flights of the National Hurricane Research Project of the U. S. Weather Bureau, points out several clues that indicate that the organization of convection in tropical disturbances may play in important role in their intensification. If these ideas are substantiated as we increase our ability to discriminate between those disturbances that subsequently develop into hurricanes and those that do not, it is possible that the natural organization of convective bands could be altered by selective seeding.

The fact that hurricane formation in a pre-existing disturbance is such a rare event implies that it takes a finely balanced sequence of events to bring about the generation of a hurricane. Altering any process such that it inhibits the formation of a warm core disturbance may prevent the evolution of a hurricane. A reduction of the rate of transfer of sensible and latent heat from ocean to atmosphere near the developing storm center would slow down the generation of a warm core. Likewise, development of high tropospheric cirrus on the periphery of the storm (say by aircraft condensation trails) would reduce the outward flux of long wave radiation and lower the temperature contrast between

the storm center and the outlying regions.

An analysis of cloud and radar photographs of hurricane Daisy of 1958 by Malkus [24] revealed that intense convection covered only 6% of the area within 80 km of the wall cloud of the eye. Thus, artificial modification of the important convective bands may require focusing attention on only a small portion of the total storm area. Since great emphasis has been placed on the role of intense "hot tower" convection in maintaining the thermal structure necessary for kinetic energy generation, it seems possible that modification of the spatial distribution of intense convective areas might well modify the structure of the hurricane.

In summary, control of hurricanes may well be within our grasp in the future. Today the main task at hand is to advance description, understanding and prediction of the phenomena to the point where meaningful control experiments may be intelligently designed.

G.6.0 REFERENCES

1. Dunn, C., "Tropical Cyclones," Compendium of Meteorology, pp. 887–901, Boston, Mass.; Am. Meteorol. Soc., 1951.

2. McDonald, W., "On a Hypothesis Concerning Normal Development and Disintegration of Tropical Hurricanes," Bull. Am. Meteorol. Soc. 23, pp. 73–78, 1942.

3. Dunn, C., and B. Miller, Atlantic Hurricanes, p. 326, Louisiana State University Press, 1960.

4. Depperman, C., "Is There a Ring of Violent Upward Convection in Hurricanes?" Bull. Am. Meteorol. Soc. 27, pp. 6–8, 1946.

5. Simson, R., "Exploring the Eye of Typhoon Marge, 1951", Bull. Am. Meteorol. Soc. 33, pp. 286–298, 1952.

6. Palmén, E., and H. Riehl, "Budget of Angular Momentum and Energy in Tropical Cyclones," J. Meteorol. 14, pp. 150–159, 1957.

7. Hughes, L., "On the Low-Level Wind Structure of Tropical Storms," J. Meteorol. 9, pp. 422–428, 1952.

8. Riehl, H., and J. Malkus, "Some Aspects of Hurricane Daisy," Tellus 13, pp. 181–213, 1961.

9. Miller, R., "Statistical Prediction by Discriminant Analysis," Meteorol. Monogr., Am. Meteorol. Soc., 1962.

10. Spiegler, D., K. Veigas, and J. Rahn, Objective Analysis of the Stratosphere Based on Mid- and Upper-Tropospheric Data p. 125, 7045-44, The Travelers Research Center, Inc., Hartford, Conn. 1962.

11. Kuo, H., "Convection in Conditionally Unstable Atmosphere," Tellus 13, pp. 441–459, 1961.

12. Riehl, H., Tropical Meteorology, p. 394, New York: McGraw Hill, 1954.

13. —, "On the Origin and Possible Modification of Hurricanes," Science 141, pp. 1001–1010, 1963.

14. Kasahara, A., and C. Platzman, "Interaction of a Hurricane with the Steering Flow and its Effect Upon the Hurricane Trajectory," NHRP Proc. of Second Tech. Conf. on Hurricanes, Rpt. No. 50, p. 390, June 27–30, 1961.

15. Vanderman, L., "An Improved NWP Model for Forecasting the Paths of Tropical Cyclones," NHRP Proc. of Second Tech. Conf. on Hurricanes, Rpt. No. 50, pp. 391-392, June 27–30, 1961.

16. Riehl, H., W. Haggard, and R. Sanborn, "On the Prediction of 24-hr Hurricane Movement," J. Meteorol. 13, pp. 415–420, 1956.

17. Veigas, K., Prediction of Twelve, Twenty-four and Thirty-six Hour Displacements of Hurricanes by Statistical Methods, TRC 61-3, p. 36, The Travelers Research Center, Inc., Hartford, Conn. 1961.

18. Arakawa, H., "Prediction of Movements and Surface Pressure of Typhoon Centers in the Far East by Statistical Methods," Meteorol. Soc. of Japan, pp. 363–374, 1962.

19. Tracy, J., "Verification of Forecasts of Hurricane Motion Using Various Techniques," NHRP Proc. of Second Tech. Conf. on Hurricanes, Rpt. No. 50, pp. 373 -382, June 27–30, 1961.

20. Riehl, H., F. Baer, and K. Veigas, Hurricane Formation in the Gulf of Mexico, Third Tech. Rpt. for American Petroleum Institute (Panel on Hurricanes), 1962.

21. Klien, W. H., and B. M. Lewis, "Hemispheric Specification of Daily Sea Level Pressure from Numerical Height Forecasts," Abstract in Bull. Am. Meteorol. Soc. 45, pp. 173, 1964.

22. Schaefer, "Snow and its Relationship to Experimental Meteorology," pendium of Meteorology, pp. 221-235, Am. Meteorol. Soc., 1951.

23. LaSeur, N., "On the Role of Convection in Hurricanes," NHRP Proc. of Second Tech. Conf. on Hurricanes, Rpt. No. 50, pp. 323–335, June 27–30, 1961.

24. Malkus, J., C. Ronne, and M. Chaffee, "Cloud Patterns in Hurricane Daisy, 1958", Tellus 13, pp. 8–30, 1961.

APPENDIX H. PRECIPITATION MODIFICATION

A. Microphysical Parameters*

H.1.0 INTRODUCTION

Considerations of problems of weather modification, of the hydrologic cycle, and of the interpretation of cloud and precipitation observations by radar, artificial satellite, and other means should be assisted by knowledge of relations between water-substance distributions and wind fields. This study develops the implications of continuity in specified wind fields, and extends earlier kinematic models (e.g., [1,2] to incorporate simplified microphysical processes and the development with time of vapor, cloud, and precipitation phases. From the calculated roles of microphysical processes in a model wind system, speculations are offered regarding effects of artificial modification of the microphysical parameters in the real world. The dynamical interactions between microphysical parameters and developing distributions of water substance, and the shape and intensity of the associated wind field, are not considered in this paper.

---

*By Pieter J. Feteris

H.2.0 CONTINUITY EQUATIONS

The continuity equations treated here are

$$\frac{\partial M}{\partial t} = - u \frac{\partial M}{\partial x} - v \frac{\partial M}{\partial y} - w \frac{\partial M}{\partial z} - \frac{\partial}{\partial z} MV + Mw \frac{\partial \ln \rho}{\partial z}$$

+ cloud conversion + cloud collection - evaporation of precipitation and (H-1)

$$\frac{\partial m}{\partial t} = - u \frac{\partial m}{\partial x} - v \frac{\partial m}{\partial y} - w \frac{\partial m}{\partial z} + wG + mw \frac{\partial \ln \rho}{\partial z}$$

- cloud conversion - cloud collection + evaporation of precipitation. (H-2)

Implicit in these is the following equation of continuity for air:

$$\frac{\partial u}{\partial x} + \frac{\partial v}{\partial y} + \frac{\partial w}{\partial z} + w \frac{\partial \ln \rho}{\partial z} = 0. \qquad \text{(H-3)}$$

The derivation of Eqs. (H-1) and (H-2) is detailed by Kessler et al. [3, (7048-65)]. In Eq. (H-1), M is the density of precipitation and refers to condensate that has an appreciable fall speed relative to the air. V, a negative quantity, can be the terminal fall velocity of the precipitation particle whose diameter divides an assumed inverse exponential size distribution [4] into portions of equal water content. The terms in the density ρ of the air account for the compressibility of the atmosphere.

In Eq. (H-2), m is the cloud density plus the vapor density minus the saturation vapor density. When m is positive, it represents the density of cloud, i.e., condensate with zero terminal fall speed. When m is negative, it represents the saturation deficit. G, a function of height, defines the rate of cloud creation in saturated updrafts; $G = -\rho \, (dQ_s/dz)$, where Q_s is the saturation mixing ratio of water vapor in air.

The remaining terms in Eqs. (H-1) and (H-2), when written in mathematical form, define rates of spontaneous conversion of cloud to precipitation, the collection of cloud particles by precipitation. and the evaporation of precipitation. Because the model requires immediate evaporation of cloud in subsaturated air, evaporation of precipitation does not occur at the same time and place as cloud conversion and accretion, or any place where cloud exists.

H.3.0 MICROPHYSICAL PARAMETERS

In the present study, complicated processes that convert cloud to precipitation are represented by the simple expressions

$$\text{cloud conversion} = K_1\,(m - a)\ \text{gm m}^{-3}\ \text{sec}^{-1} \qquad (m > a)$$

and

$$\text{cloud conversion} = 0 \qquad (m < a). \tag{H-4}$$

The use of such a simplification is not clearly supported or refuted by the literature, but seems reasonable in a first experiment and obviates the need for a greater number of basic equations. Further discussion is given by Kessler et al. [3, (7048-65)].

The cloud-collection term is derived as follows. Note that the rate at which volume is swept out by one drop of diameter D_i falling at a speed V_i is $-\pi D_i^2 V_i/4$ (where $V_i < 0$) and that the rate of accumulation of cloud water by a single precipitation particle of mass M_i is

$$\frac{\delta M_i}{\delta t} = -\frac{\pi D_i^2}{4} E_i V_i m \qquad (m > 0), \tag{H-5}$$

where E_i is the efficiency of catch.

The rate of growth of the liquid-water content in an entire distribution of precipitation particles is given by multiplying Eq. (H-4) by the number of particles n and integrating over all particle diameters, i.e.,

$$\frac{dM}{dt} = \int_0^\infty \frac{\delta M}{\delta t}\, n\, dD. \tag{H-6}$$

A formal integration is accomplished by substituting for V_i in Eq. (H-5) according to the relation $V = -130\, D^{0.5}$ m sec^{-1}, based on Spilhaus [5], and for n according to $n = n_0 e^{\lambda D}$ m^{-4} [6]. Then with E independent of D,

$$\frac{dM}{dt} = \frac{130}{4} \pi E n_0 m \int_0^\infty D^{5/2} e^{-\lambda D}\, dD; \tag{H-7}$$

$$\frac{dM}{dt} = \frac{130}{4} \pi E n_0 m \frac{\Gamma(3.5)}{\lambda^{3.5}}. \tag{H-8}$$

It can be shown that $\lambda = 42\, n_0^{0.25}\, M^{-0.25}$ m^{-1}. Equation (H-9) defines the rate of collection of cloud by precipitation and is obtained by substituting for λ in Eq. (H-8):

$$\frac{dM}{dt}\text{ (collection)} = 6.96 \times 10^{-4}\ En_0^{0.125}\ mM^{0.875}\ \text{gm m}^{-3}\ \text{sec}^{-1}$$

$$(m > 0). \qquad \text{(H-9)}$$

An approximate modeling of the tabulated evaporation functions of Kinzer and Gunn [6] leads to the following equation for the evaporation rate.

$$\frac{dM}{dt}\text{ (evaporation)} = 1.35 \times 10^{-6}\ n_0^{0.35}\ mM^{0.65}\ \text{gm m}^{-3}\ \text{sec}^{-1}$$

$$(m < 0), \qquad \text{(H-10)}$$

and the fall speed V of the median volume diameter precipitation particle in the assumed size distribution is

$$V = -\ 38.6\ n_0^{-0.125}\ M^{0.125}\ \text{m sec}^{-1}. \qquad \text{(H-11)}$$

H.4.0 ROLE OF MICROPHYSICAL PARAMETERS IN CLOUD AND PRECIPITATION DEVELOPMENT

Exact solutions of a model of the onset of precipitation have been presented elsewhere [3, 7]; these show that the existence of alternative processes for precipitation production, e.g., cloud conversion and accretion, implies that precipitation onset is principally sensitive to the stronger of the precipitation-forming processes. In other words, if coalescence and aggregation processes among many tiny cloud drops are relatively rapid, the efficiency with which raindrops collect cloud is of little consequence to the rate of depletion of cloud; and if the collection of cloud by raindrops is relatively rapid, then the magnitude of the rate of cloud conversion is not critical, so long as it is more than zero.

The role of microphysical parameters has been further examined by numerically integrating for a fixed updraft profile in an initially saturated atmosphere, the equations obtained by omitting the horizontal advection and compressibility terms in Eqs. (H-1) and (H-2). This model best applies to a shower core or to widespread precipitation in which the horizontal advection is small. The results are summarized here and illustrated by Figs. H-1 and H-2; a more comprehensive treatment is available elsewhere [7]. These illustrations are based on the following parameter values, except for one parameter that varies over the set of curves in each figure.

Parameters Used in Finite-difference Computations

Updraft speed $w = (4w_{max}/H)(z - z^2/H)$ m sec^{-1}

Maximum updraft speed $w_{max} = 0.5$ m sec^{-1}

Tropical generating function $G = (3 \times 10^{-3} - 3 \times 10^{-7} z)$ gm m^{-4}

Height of updraft column $H = 6000$ m

Precipitation-onset parameter $a = 0.5$ gm m^{-3}

Cloud-conversion rate $k_1 = 10^{-3}$ sec^{-1}

Precipitation-size-distribution parameter $n_0 = 10^7$ m^{-4}

Collection efficiency $E = 1$

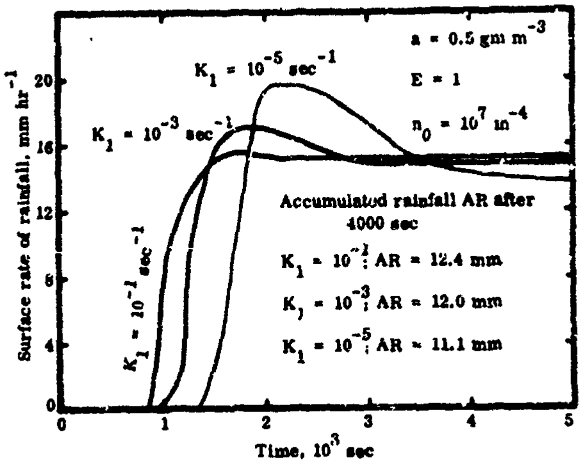

Fig. H-1(a). Precipitation rate vs time at the ground for three magnitudes of the conversion parameter k_1.

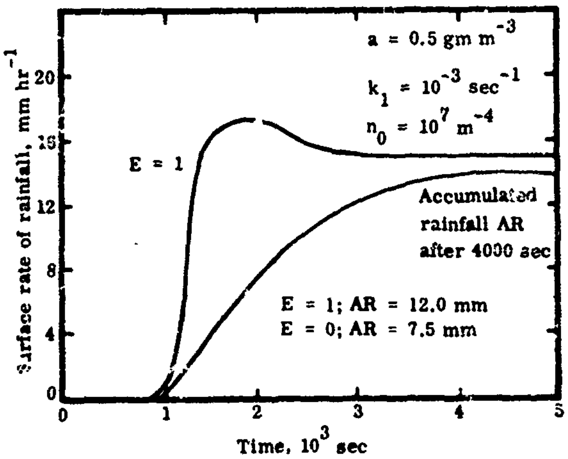

Fig. H-1(b). Precipitate at the ground for extrema of the collection efficiency E. When E = 0, cloud conversion acting alone changes cloud to precipitation.

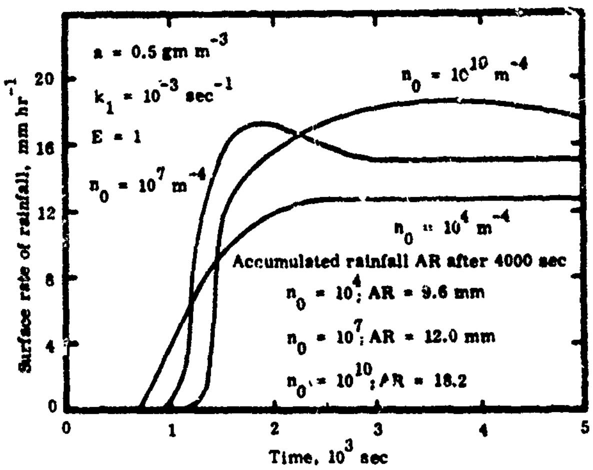

Fig. H-1(c). Development of precipitation for three values of n_0. When $n_0 = 10^{10}$, most of the precipitation water content is contained in drizzle-size and smaller drops.

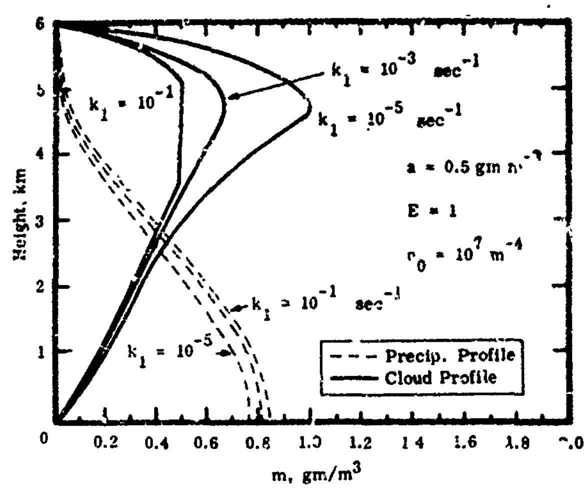

Fig. H-2(a). Steady cloud and precipitation-content profiles for three values of the conversion parameter.

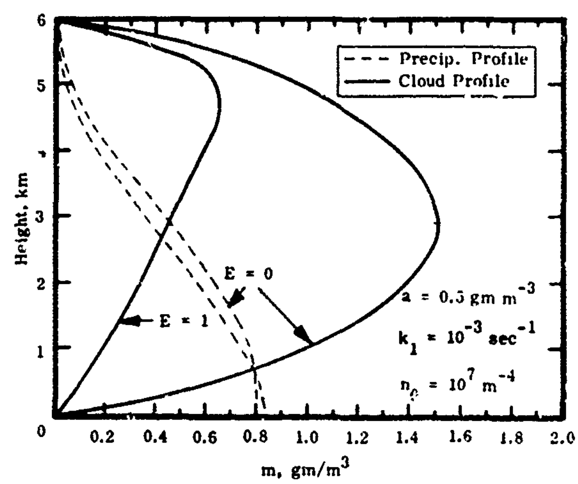

Fig. H-2(b). Steady-state profiles of cloud and precipitation content for extrema of the collection efficiency.

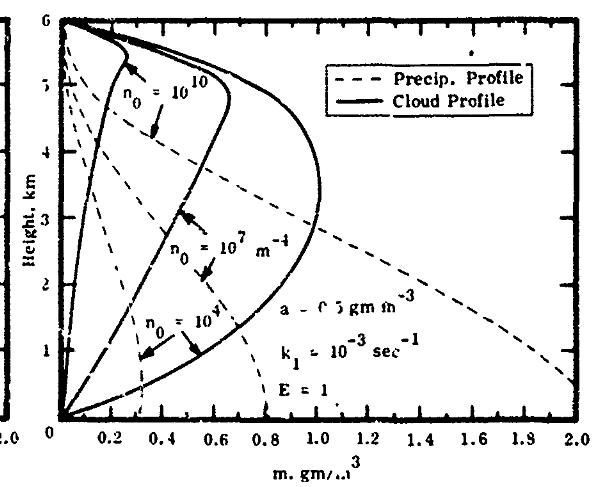

Fig. H-2(c). Steady-state profiles of cloud and precipitation content for three magnitudes of n_0. $n_0 = 10^7$ is typical of natural rains.

The figures illustrate that with fixed updrafts, alteration of a microphysical process or parameter produces a water-distribution change that tends to offset the effects of the microphysical change on the surface precipitation rate. For example, in Figs. H-1(b) and H-2(b), large cloud collection is more prominently associated with decreased cloud than with increased precipitation.

In all cases, the illustrated updrafts are smaller than precipitation fall speeds, and steady-state conditions are eventually attained. These steady states are independent of the initial moisture stratification,* weakly dependent on the microphysical parameters, and strongly dependent on the updrafts.

Where cloud conversion and accretion transfer water from cloud to the precipitation phase in a short time compared with the time taken for an air parcel to rise from low to high levels in an updraft column, the steady surface precipitation rate beneath the updraft column is approximately the same as the condensation rate integrated through the depth of the column. This approximate equality characterizes all the cases illustrated here. However, the precipitation is concentrated at the updraft center (at the expense of that away from the center; see Kessler et al. [1, 3] for details) as the average fall speed of the precipitation particles decreases, i.e., as n_0 increases.

On the other hand, when the time required for transfer from cloud to precipitation is long compared with the time of ascent of air parcels, the precipitation rate beneath the updraft column is small compared with the integrated condensation rate; much of the condensate in such cases is spread laterally at high levels by the horizontal divergence that necessarily accompanies all updrafts. The cloud so spread aloft may fall as precipitation at places removed from the updraft center or may evaporate in downdrafts, depending on the shape of the 3-dimensional wind field. For the 0.5-m sec^{-1} maximum updraft of the illustrated examples, steady precipitation rates considerably less than condensation rates occur only when cloud-conversion rates and collection efficiencies are simultaneously small.

*Except when the air is initially so dry that ascent of air does not produce precipitation.

H.5.0 IMPLICATIONS FOR WEATHER MODIFICATION

Consider some changes of water-substance distributions implied by changes of the microphysical parameters. When the cloud-conversion rate and collection rate are smaller, the onset of precipitation from transient showers is delayed; in an advective situation, such delay would be associated with a downwind displacement of precipitation at the ground. Figure H-2 shows how reduced cloud-conversion and collection rates are probably associated with larger amounts of cloud aloft; in an orographically influenced situation, some of the increased cloud might be carried over mountains to contribute to precipitation on the ordinarily dry lee side, with loss of relatively unneeded precipitation at windward. If raindrops could be made smaller than natural size, they would fall more slowly, and the probability of significant precipitation downwind and over a ridge would rise. Cloud amounts associated with more numerous smaller drops would probably decrease, however, as suggested by Fig. H-2(c).

If cloud-conversion and accretion rates were made smaller in a particular case, rainfall would decrease and the amount of cloud evaporating in the descending branches of the circulation would increase. Moisture not precipitated would be retained in the atmosphere and possibly contribute to future precipitation from the air mass. Squires and Twomey, in their study of differences between continental and maritime cumuli [8], have cited the absence of giant salt nuclei in the continental air and the presence there of many small nuclei and cloud drops, as explanations for a noticeable inefficiency of the continental clouds with respect to the release of warm rain.

If cloud-conversion and accretion rates were made larger in a particular case, rainfall would start sooner and its steady rate would increase, provided that the rainfall rate is not already as great as the rate of condensation. Although the examples illustrated by Figs. H-1 and H-2 are characterized by a near balance between steady precipitation and condensation rates, the equations are equally appropriate for analyses of important cases where such a balance does not prevail.

Attempts to modify the distribution of tropical precipitation might start by selecting a region where the precipitation regime is nearly steady and air

trajectories are known or measureable. Such places exist at times in the Hawaiian Islands, and probably around the central plateau of Mexico and elsewhere. Analyses of the weather situations, including measurements of cloud-water contents and of the distributions of surface rainfall, should indicate approximate values of microphysical parameters and updrafts which could be incorporated into a quantitative analysis to show whether appreciable benefits would accrue from their artificial modification. Cloud conversion might be assisted by introduction of relatively small numbers of giant salt nuclei and water drops. Conversion might be decreased by introducing very large numbers of very small nuclei; Weickmann has presented a preliminary quantitative analysis of this idea and a discussion of related field experiments [9]. Raindrops might be made smaller by introducing a surface-active agent to reduce the drops' surface tension and promote breakup. Where important, a freezing process might be suppressed by introduction of organic substances that become absorbed on the surfaces of freezing nuclei with a lowering of their activation temperature [10].

In weather-modification studies, the kinematic theory discussed here should be a useful tool. More valuable results are expected from analyses of water budgets in 2-dimensional rectilinear and radially symmetric model wind fields [1], and from a model which combines thermohydrodynamic equations with continuity equations for water substance.

H.6.0 MICROPHYSICAL PARAMETERS AND GLOBAL CLIMATE

The cloudiness of the earth's atmosphere depends largely on the colloidal stability of clouds. When cloud conversion and accretion are small, little precipitation is formed and deposited at the ground, and a great portion of condensate evaporates at high levels, either in relatively dry air diffusively entrained or in the downdrafts that accompany updrafts. If these microphysical parameters were reduced on a global scale, a new state of statistical equilibrium might be attained by the atmosphere where a greater plenty of clouds would tend to offset their reduced effectiveness as precipitation producers. Significantly increased cloudiness would be associated with a significant increase of the albedo, with accompanying changes that cannot be rationally treated without reference to a consistent theory or model. It does not seem amiss, however, to speculate that the new equilibrium would be associated with a lower average temperature at the earth's surface. If changes of the microphysical parameters were confired to either of the warm (coalescence) or cold (ice-crystal) regimes, or if changes were substantially different for these two regimes, the shape of the mean latitudinal profile of temperature might be altered, with further consequences for the shape and intensity of the general circulation. Might variations of the microphysical processes be a key to appreciable alterations of the atmosphere's cloudiness and world climates in prehistoric and historic time?

H.7.0 REFERENCES

1. Kessler, E. III, "Elementary Theory of Relationships Between Atmospheric Motions and Distributions of Water Content," Mo. Weath. Rev. 91:1, 1963.

2. Wexler, R., and D. Atlas, "Moisture Supply and Growth of Stratiform Precipitation," J. Meteorol. 15:6, 1957.

3. Kessler, E. III, P. J. Feteris, and E. A. Newburg, Relationships Between Tropical Precipitation and Kinematic Cloud Models 7048-38, 7048-49, 7048-65. The Travelers Research Center, Inc., Hartford, 1962 and 1963.

4. Marshall, J. S., and W. McK. Palmer, "The Distribution of Raindrops with Size," J. Meteorol. 5:4, 1948.

5. Spilhaus, A. F., "Raindrop Size, Shape, and Falling Speed," J. Meteorol. 5:4, 1948.

6. Kinzer, G. D., and R. Gunn, "The Evaporation, Temperature, and Thermal Relaxation Time of Freely Falling Water Drops," J. Meteorol. 8:2, 1951.

7. Kessler, E. III, P. J. Feteris, and E. A. Newburg, "Role of Microphysical Processes in Shaping Vertical Profiles of Precipitation and Cloud," Proc. 10th Weath. Radar Conf., Am. Meteorol. Soc., Boston, 1963.

8. Squires, P., and S. Twomey, "The Relation Between Cloud Drop Spectra and the Spectrum of Cloud Nuclei," Geophys. Monogr. 5, Am. Geophys. Un., Washington, D.C., 1960.

9. Weickmann, H., "Condensation Nuclei Seeding, a New Technique, and its Objective for Cloud Modification," paper presented at the Paris Symp. on Condensation Nuclei, May 1963.

0. Birstein, S. J., Adsorption Studies of Heterogeneous Phase Transitions Geophys. Res. Paper 31, AF Cambridge Res. Center, Bedford, Mass., 1954.

B. Literature Review*

H.8.0 INTRODUCTION

Increasing understanding of the microphysical processes governing the conversion of cloud to precipitation during the past 20 years has suggested numerous techniques for modifying precipitation. Although many precipitation modification experiments have been tried and many millions of dollars spent (primarily in commercial cloud seeding with AgI), very few proven techniques have been developed. This is partially the fault of poorly-designed experiments and commercial companies out to make rain, rather than to prove whether it is economically and physically feasible. The primary difficulty lies in the need for a more complete understanding of the precipitation mechanisms operating on all scales. There has been a reluctance (very rightly so) among meteorologists to attempt weather modification experiments in the atmosphere without a complete understanding of the effect they will produce.

*By James W. Wilson

H.9.0 PRECIPITATION STIMULATION

H.9.1 Chemical Seeding

H.9.1.1 Salt and Water

The growth of water droplets in warm clouds is very dependent on the drop-size distribution. Raindrops develop through the presence of a small number of large droplets growing at the expense of the small droplets. Langmuir [1] suggested that the growth of precipitation in warm clouds could then be influenced by seeding clouds with water droplets or large hygroscopic nuclei. Davies [2] seeded clouds in East Africa with finely-ground salt. A large portion of the treated clouds rained 7–35 min after seeding. A carefully controlled randomized program, conducted by the University of Chicago (Braham, Battan, Byers, [3]), showed that a water spray initiated precipitation in tropical cumuli. The results of this experiment were significant at the 2% level. Although experimental and theoretical work indicates precipitation can be stimulated by seeding cumulus with water or large hygroscopic nuclei, it is not possible at present to estimate what rainfall increase might be expected.

H.9.1.2 Solid CO_2 and AgI

In subfreezing clouds, another means of precipitation growth is available. Ice crystals surrounded by supercooled water droplets grow very rapidly to a size sufficient to fall to the ground. However, since natural-occurring nuclei vary widely in concentration and effectiveness, another means of precipitation stimulation is suggested; i.e., artificial production of ice crystals.

Schaefer [4] observed that ice crystals could be produced in supercooled clouds by seeding them with dry ice. Vonnegut [5] showed that silver iodide crystals are effective in producing ice crystals in water clouds with temperatures below -5°C. These two discoveries, which have been substantiated by extensive field experiments by aufm Kampe, Kelly, and Weickmann [6], have provided the impetus for rain-making experiments conducted the world over.

Although it has been convincingly demonstrated that individual clouds seeded with dry ice or AgI have been modified sufficiently to produce light rain or snow, the outcome or seeding operations aimed at producing significant increases of

precipitation over large areas is much less conclusive. The major difficulty in evaluating these experiments is that there is no means for determining how much precipitation would have fallen if the cloud had not been seeded. Therefore, it has been necessary to rely on statistical techniques for determining if the seeding produced any significant effect. The great variability in natural rain, inadequate means of measuring precipitation, and the fact that most projects did not have proper statistical design have made evaluation particularly difficult.

The President's Advisory Committee on Weather Control [7], using its own statistical procedures and scientists, evaluated the cloud seeding operations of 12 commercial companies. The committee concluded that "the seeding of winter-type storm clouds in mountainous areas in western United States produced an average increase of precipitation of 10-15% from seeded storms with heavy odds that this increase was not the result of natural variations in the amount of rainfall." The committee used the same statistical procedures to evaluate cloud seeding operations in non-mountainous regions and did not detect an increase in precipitation. A committee of the American Meteorological Society [8] and one from the World Meteorological Organization [9] were in agreement that orographic clouds were the most likely clouds to yield additional rainfall, but neither organization regarded this point as having been definitely established. The contention that orographic clouds are favorable for rain-making is supported on theoretical grounds by Ludlam [10].

The report of the Advisory Committee on Weather Control has been criticized by Brownlee [11], and Neyman and Scott [12]. They maintain that the conclusions of the committee are invalid since the report was based on non-randomized seeding operations of commercial seeders. Recent experiments using randomizing techniques for cloud seeding have been conducted in California (Neyman, Scott, and Vasilevskis, [13]), Arizona (Battan and Kassander, [14]), and Australia (Smith, Adderley, and Walsh [15]). The results of these experiments, while in some ways being suggestive of positive effects of cloud seeding, are essentially inconclusive.

Laboratory tests in search of other agents for seeding supercooled clouds has revealed nothing nearly as efficient as dry ice and silver iodide (Mason, [16]).

H.9.1.3 Wetting Agents

Kessler [17] has suggested that if raindrops could be made smaller than natural size, they would fall slower, and the probability of precipitation downwind of a ridge would rise. Laboratory experiments by Blanchard [18] showed that drops whose surface tension had been reduced by adding a wetting agent (detergent) nearly always broke up in colliding with other drops. Before field tests are conducted, more laboratory experiments are required to determine the change of coalescence efficiency and drop breakup with change of surface tension at various drop sizes (Battan, [19]).

H.9.2 Cloud Electrification

Laboratory experiments by Sartor [20] and Frier [21] have shown that the coalescence efficiency of water droplets increases as the electric field increases. Moore and Vonnegut [22] have suggested, after observing the rapid appearance of rain from thunderstorms in New Mexico, that electrical effects appreciably accelerate the coalescence process. If such electrical forces do operate in clouds, they offer a mechanism for possible stimulation of precipitation. Vonnegut and Moore (Rand Corp., [23]) are presently conducting experiments to test whether they can artificially change the electric properties of cumulus clouds. They have strung wires between mountain peaks in New Mexico. These wires can emit either positive or negative ions to the clouds. The results of this work should be watched carefully.

H.9.3 Convection Stimulation

H.9.3.1 Fires

It has long been suggested that rising convection currents initiated by surface heating can produce significant amounts of rainfall. As early as 1843, Espy [24] suggested that prairies or timber destined to be burned be preserved until periods of drought. Dessens [25] produced weak precipitation in the Congo under clear sky conditions by igniting brush fires. Recently, Dessens [26] has been experimenting with oil burners in the Congo and Pyrenees Mountains in attempts to stimulate convection. Although several small tornadoes were reported to have been produced in this manner (Dessens, [27]), it has not been determined whether

this scheme is capable of producing sufficient rain to be economically feasible.

H.9.3.2 Asphalt

Black and Tarmy [28] have suggested that rainfall might be artificially increased by coating large sections of ground with asphalt. A quantitative estimate of the rainfall amount and cost in a subtropical region suggests that rainfall could be produced at the low cost of 3¢ per 1000 gal. The calculations made by Black and Tarmy are based on studies by Malkus [29] of airflow over small heated islands. Malkus has reported on the formation of clouds and precipitation produced by convection currents rising off the small flat island of Anegada and concludes "that Anegada sized asphalt coatings are quite likely to produce precipitation in some amount, somewhere, on some occasions, and are thus as promising a technique of rain-making as has been advocated."

H.9.3.3 Nuclear Energy

If further work with artificial heat sources indicates that moderate quantities of heat can produce convective clouds capable of producing significant rain, it might be well to consider the use of nuclear reactors as a means for generating the required heat.

H.9.3.4 Carbon Black

Van Straten and others [30] suggested that carbon black particles dispersed into clear air under unstable conditions could lead to the formation of convective clouds since the carbon particle would absorb solar radiation and heat the air.

H.10.0 PRECIPITATION SUPPRESSION

H.10.1 Chemical Seeding

H.10.1.1 Methylamine

Laboratory experiments by Birstein [31] have shown that it is possible to inhibit ice crystal formation by natural nuclei by treating the air with methylamine. The methylamine reduces the temperature of nucleation. If this effect can be reproduced in clouds, it suggests a means for suppressing rain.

H.10.1.2 "Overseeding" with AgI and solid CO_2

If sufficient quantities of AgI or dry ice can be introduced into a building cumulus cloud, it may be possible to convert a large portion of the supercooled water content to ice crystals. This might reduce the coalescence efficiency to a point where very few particles could grow to a size sufficient to fall through the updrafts. Results of experiments in Project Skyfire (Barrows and others, [32]) show that small cumulus clouds are dissipated by seeding with large quantities of AgI. Field experiments in "overseeding" with AgI have been hampered by the lack of generators capable of producing the required number of nuclei.

H.10.1.3 Carbon Seeding

In order to dissipate warm cumulus clouds, van Straten and others [30] have reported on experiments in which the tops of cumulus were dusted with carbon black. It was reported that cumulus clouds dusted with 1-1/2 to 6 pounds of carbon black dissipated about 10 min after dusting. It is reasoned that the minute carbon particles are captured by the cloud and absorb solar radiation, which leads to warming of the cloud top and dissipation. Although it is not possible to draw positive conclusions from these preliminary experiments, the results are encouraging and warrant further study.

H.10.1.4 Evaporation Control

Since the majority of the water vapor present in the atmosphere originates in evaporation from large bodies of water, control of evaporation from these sources suggests a means of precipitation control.

Hydrologists (Roberts, [33]; Cruse, [34]) have found that monomolecular films such as hexdecanol, dodecanol, and cetyl alcohol spread over water sources

can substantially reduce evaporation. If such films were spread over vast stretches of water, this might substantially reduce the amount of water vapor available for rain, as well as increase the temperature of the water surface. However, as indicated by Houghton [35], "It would be unthinkable to embark on such a vast experiment before we are able to predict with some certainty what the effect would be. Without such knowledge, the effects might be catastrophic or, a lesser evil, there might be no noticeable effect after the expenditure of large sums. A much more reasonable approach lies in continuation of basic research."

H.11.0 HAIL SUPPRESSION

H.11.1 AgI and solid CO_2 "Overseeding"

As indicated in the previous section, the introduction of large quantities of AgI or dry ice into a building cumulus may convert a large portion of the available water vapor to ice crystals. Hail develops when the rate at which an ice particle grows by collision when falling through a supercooled cloud becomes so great that some of the water is accreted in liquid form. Hail is therefore associated with supercooled clouds of high water content. Therefore, if a large portion of the supercooled water vapor in a cloud can be converted to ice crystals by "overseeding" with AgI or dry ice, the growth of hail may be greatly inhibited.

Many experiments have been made in Europe and America in seeding cumulus with AgI and dry ice in attempts to suppress hail. Evaluation of cloud seeding experiments in hail suppression is even more difficult than those in precipitation stimulation since hail is even more variable than rain. The Advisory Committee on Weather Control reported that the available data led to inconclusive results. Battan [19] indicates that, when consideration of the quantity of AgI dispersed in almost all hail-suppression tests is made, it is evident that the quantities were too small to "overseed" building cumulus clouds. Before the effect of "overseeding" can be evaluated, it will be necessary to conduct carefully-controlled randomized cloud seeding experiments with generators capable of producing a quantity of nuclei several orders of magnitude greater than those previously used.

H.11.2 Explosion

In Switzerland and Italy, many farmers have been shooting inexpensive rockets into hailstorms in an attempt to reduce hail damage. The rockets containing gunpowder are exploded at a height of 1–1.5 km. The farmers claim the hailstones become "mush" within a few minutes after the rockets are fired. This led Vittori [36] to investigate the effects of blast waves on ice particles. His experiments, based on theory, led him to the conclusion that blast waves are capable of breaking up watery hailstones up to a distance of 150 m from the explosion. After Roncali [37], challenged the results of Vittori's experiments, List [38] repeated the tests. List concluded from his tests that "no effect is produced by

blast waves from charges up to 1 kg TNT on the mechanical cohesion of ice objects at a distance of 5 m." According to List, Vittori wrongly attributed the phenomena he observed to explosions instead of to the force of freezing water. On the basis of List's experiments, there is no justification for attempting to modify hail with explosions.

H.12.0 REFERENCES

1. Langmuir, I. "Production of Rain by a Chain Reaction in Cumulus Clouds at Temperatures Above Freezing." J. Meteorol. 5, 175–192, 1948.

2. Davies, D. A., "Experiments on Artificial Stimulation of Rain in East Africa." Nature, 174, 256–258, 1954.

3. Braham, R. R., L. J. Battan, and H. R. Byers, "Artificial Nucleation of Cumulus Clouds." Meteorol. Monogr. 2, 47–85, 1957.

4. Schaefer, V. J., "The Production of Ice-crystals in a Cloud of Super-cooled Water Droplets." Science 104, 457–459. 1946.

5. Vonnegut, B., "The Nucleation of Ice Formation by Silver Iodied." J. Appl. Phys. 18, 593–595, 1947.

6. aufm Kampe, H. J., J. J. Kelly, and H. R. Weickmann; "Seeding Experiments in Supercooled Stratus Clouds." Meteorol. Monogr. 2, 86–111, 1957.

7. Advisory Committee, 1957: Final Report Advisory Committee on Weather Control, 1, U.S. Government Printing Office.

8. American Meteorological Soc., 1957: "Statement of Weather Modification." Bull. Am. Meteorol. Soc. 38, pg. 366.

9. World Meteorol. Org., "Artific[illegible]ol of Clouds and Hydrometeors," World Meteorol. Org. Tech. Note No. 13, 1955.

10. Ludlam, F. H., "Artificial Snowfall from Mountain Clouds," Tellus 7, 277, 1955.

11. Brownlee, K. A., "Statistical Evaluation of Cloud Seeding Operations," J. Am. Stat. Assoc. 55, 446–453, 1960.

12. Neyman, J., and E. L. Scott, "Further Comments on the 'Final Report of the Advisory Committee on Weather Control'," J. Am. Stat. Assoc. 56, 580–600, 1961.

13. —, —, and M. Vasilevskis, "Statistical Evaluation of the Santa Barbara Randomized Cloud-seeding Experiment." Bull. Am. Meteorol. Soc. 41, 531–547, 1960.

14. Battan, L. J. and A. R. Kassander, "Evaluation of Effects of Airborne Silver Iodide Seeding of Convective Clouds." Arizona Univ. Institute of Atmos. Phys. Sci. Rpt. No. 18, (final report to National Science Foundation) 1962.

15. Smith, E. J., E. E. Adderley, and D. T. Walsh, "A Cloud-seeding Experiment in the Snowy Mountains, Australia." J. Appl. Meteorol. 2, 324–332, 1963.

16. Mason, B. J., "The Growth of Snow Crystals." Sci. Am. 204, 120–131, 1961.

17. Kessler, E. III, "Microphysical Parameters in Relation to Tropical Cloud and Precipitation Distributions and their Modification." Geophys. Factors in Naval Warfare, 7662-102. The Travelers Research Center, Inc., Hartford, 1963.

18. Blanchard, D. C., "Experiments with Water Drops and the Interaction Between them at Terminal Velocities in Air." Occasional Rep. No. 17, Proj. Cirrus, G. E. Res. Labs., Schenectady, N.Y. 1949.

19. Battan, L. J., "Assessment of the State-of-the-Art of Cloud Modification," Geophys. Warfare Study, ARDC SR-19770 (prepared by Northrop Corp.) 1961.

20. Sartor, J. D., "A Laboratory Investigation of Collision Efficiencies, Coalescence and Electrical Charging of Simulated Cloud Droplets," J. Meteorol. 11, 91–103, 1954.

21. Frier, G., "The coalescence of Water Drops in an Electric Field." J. Geophys. Res. 65, 3979–3985, 1960.

22. Moore, C. B. and B. Vonnegut, "Estimates of Raindrop Collection Efficiencies in Electrified Clouds," Physics of Precipitation, 291–304, Baltimore: Waverly Press, Inc., 1959.

23. Rand Corp., Weather Modification Fourth Annual Report. (Prepared for the National Science Foundation.) U.S. Govt. Printing Office, 1962.

24. Espy, J. P., Reports 1-4 on Meteorology, 309 pp. (3 Vols.), Washington, D.C., 1843-1857.

25. Dessens, H., and J. Dessens, "La Formation Artificialle de Grands Cumulus Producteurs de Pluie." Academie des Sciences, Paris, Comptes Rendus, 1956.

26. —, "A Project for a Formation of Cumulonimbus by Artificial Convection." Phys. of Precip. Geophys. Monogr. No. 5, Am. Geophys. Un., 396–401, 1960.

27. —, "Man-made Tornadoes." Nature 193, 13–14, 1962.

28. Black, J. F., and B. J. Tarmy, "The Use of Asphalt Coating to Increase Rainfall," J. Appl. Meteorol. 2, 557–564, 1963.

29. Malkus, J. S., "Tropical Rain Induced by a Small Natural Heat Source." J. Appl. Meteorol. 2, 547–556, 1963.

30. van Straten, F. W., R. E. Ruskin, and J. E. Dinger, "Preliminary Experiments Using Carbon Black for Cloud Modification and Formation." Rpt. No. 5235, U.S. Naval Res. Lab., Washington, D.C. 1958.

31. Birstein, S. J., "Studies on the Effect of Chemisorbed Impurities on Heterogeneous Nucleation." Physics of Precipitation, Geophys. Monogr. No. 5, Am. Geophys. Un., 247–251, 1960.

32. Barrows, J. S., and others, Project Skyfire. Final Report of the Advisory Committee on Weather Control, Vol. II, 105–124, 1957.

33. Roberts, W. J., "Evaporation Suppression from Water Surfaces." Trans. Am. Geophys. Un. 38, 740–744, 1957.

34. Cruse, R. R., Final Report on the Southwest Cooperative Project on Reservoir Evaporation Control, Southwest Research Institute, 1958.

35. Houghton, H. G., "Other Aspects of Weather Modification." Final Report of the Advisory Committee on Weather Control Vol. II, 286–288, 1957.

36. Vittori, O., "Preliminary Note on the Effects of Pressure Waves upon Hailstones." Nubila 3, 34–52, 1960.

37. Roncali, G., "Sull Influences dell Esplosion: Sui Ehicchi di Grandine." Geofisica e Meterologia 8, 80–82, 1960

38. List, R., "On the Effect of Explosions on Hailstone Models." J. Appl. Meteorol. 2, 494–497, 1963.

APPENDIX I. VISIBILITY AND FOG*

A. Visual Range and Acuity

I.1.0 INTRODUCTION

The greatest distance over which a given object can be seen at a given time when viewed through the atmosphere by a human observer is called the visual range. The degree of sharpness with which the object can be seen at this and lesser distances is called the visual acuity. Acuity is part of a more general quantity called recognition. In general, recognition includes the identification of one or more object parameters (shape, size, structure, color, movement, reality, etc.).

By definition, both visual range and acuity depend on physiological and psychological factors that affect the human observer and on the properties of the object as well as on geophysical factors that influence path-light transmission and object illumination. In the important circumstances in which the position of the object is unknown or uncertain and the determination of visual range and acuity is not the only activity of the observer, the factors of attention and search also have an important influence on the numerical values.

*By Keith D. Hage.

I.2.0 CHARACTERISTIC GEOPHYSICAL PROCESS AND PROPERTY INVOLVEMENT

If we assume no specular reflection from medium or object, a horizontal and homogeneous path, and uniform illumination of object and background sky, the relation between distance x and the apparent contrast c of the object to the background can be written

$$x = \sigma_0^{-1} \ln (c^* c^{-1}), \tag{I-1}$$

where σ_0 is the extinction coefficient and c^* is the intrinsic contrast of the object to the background. An analysis of the assumptions that lead to Eq. (I-1) and of the variables that appear in the equation indicates that the principal geophysical factors that modify visual range are

(a) illumination level of object and background

(b) wavelength dependence of light transmission through the atmosphere

and

(c) space and time variations in the extinction coefficient, namely,

(1) specular reflection from natural interfaces,

(2) scattering,

(3) diffuse reflection, and

(4) absorption.

I.3.0 VISUAL RANGE IN FOG

If attention is restricted to visual ranges of less than 1 or 2 km, water droplets in the form of precipitation, cloud, and fog represent the principal obscurations in the low levels of the atmosphere over much of the earth. The single most frequent obscuration in the lowest few hundred feet of the atmosphere is fog. For this single phenomenon, the principal geophysical factors that govern visual range are:

(a) illumination level of object and background and

(b) space and time variations in the extinction coefficient due to scattering and diffuse reflection.

In special instances, specular reflection from fog boundaries may be of considerable importance. In natural fogs, Eq. (I-1) may be simplified to

$$V_R = k_s^{-1} \ln \epsilon^{-1}, \tag{I-2}$$

where V_R is visual range, k_s is the scattering coefficient, and ϵ is the threshold of brightness contrast. For spherical drops,

$$k_s = \frac{\pi K_s}{4} \sum_i n_i a_i^2, \tag{I-3}$$

where K_s is the scattering cross section, and n_i denotes the number of water drops of diameter a_i. Equations (I-2) and (I-3) reveal the fundamental importance of drop-size distribution as a geophysical factor in relation to visual range.

I.4.0 MODIFICATION FEASIBILITY

A critical review of almost all known fog-dispersal methods and suggested methods has been presented by Junge[1]. His review includes the use of thermal, chemical, potential, and electrical energies for direct and indirect modification of the drop-size distribution. He concludes that, at the time of writing, the mobile heating methods (involving the burning of fuels) appeared to be entirely feasible and superior to all other methods. Several other methods (dessication by hygroscopic chemicals, seeding with dry ice or silver iodide, mechanical collection by falling particles, collection by electrostatic attraction, drainage of foggy air, vertical mixing forced by large fans, collection by forest, etc.) were found to be theoretically sound but not practical because of limited applicability, cost, or installation size.

It is interesting to note that all these methods are concerned with existing fog droplets and that little mention is made of the natural physical processes that lead to the formation of droplets or to processes that determine the natural drop-size distribution. Undoubtedly, this is the result of large gaps in our understanding of the relative importance of the natural processes. If it were known, for example, that under certain circumstances radiative cooling of the air is responsible for fog formation or that exchange processes between the earth's surface and the overlying air are predominant, or if relations could be established between drop-size distribution and the statistics of the condensation-nuclei population, the possibility of investigating the feasibility of modifying basic parameters involved in the predominant natural processes would be opened. Theoretical and experimental studies of fog formation have been intensified recently, but much more effort is required if we are to derive realistic estimates of the magnitudes of the forces and of the rates of transformation and dissipation of energy.

For special applications, the mobile heating methods may not be practical because of the generation of light, because of fire hazards, or because of the need for operation of rather cumbersome burners at ground level over the area of interest. For such applications, it may be useful to investigate other known methods with disadvantages that are less critical to the particular application.

I.5.0 REFERENCE

1. Junge, C. E., Methods of Artificial Fog Dispersal and their Evaluation. AF Surv. in Geophys. 105, Geophys. Res. Dir., AF Cambridge Res. Center, Bedford, Mass., 1958.

B. The Accretion Process in Relation to Visual Range in Fog

I.6.0 INTRODUCTION

The mechanical process of modification of visual range in fog by sweep-out or accretion of small droplets on large falling water drops has been proposed in the past and dismissed with good reason as an impractical method for general use [1, 2]. Nevertheless, the method is believed to be sound in principle and has advantages for certain purposes because of its use of inexpensive, abundant raw material that is nontoxic and noncorrosive and that does not require the production of light, vibration, or open flames. For these reasons, the method is reexamined with a view to its possible use under limited conditions or in limited areas. Empirical evidence of natural occurrences of the accretion process is presented together with rough theoretical estimates of the magnitude of the effect on visual range for selected combinations of falling water drop- and fog drop-size distributions.

I.7.0 STATISTICAL STUDIES OF THE EFFECTS OF ACCRETION BY NATURAL RAIN IN FOG

Recent studies carried out for the United States Weather Bureau [3] indicated the existence of statistical relations between visibility or ceiling and liquid-precipitation intensity. For visibilities below about 0.5 to 1 mi, these relations were attributed tentatively to the process of accretion, i.e., to the effects of the collection of fog droplets by falling drizzle or raindrops. The findings are shown in Figs. I-1 through I-3, taken from the above report. Because the absolute frequencies of each visibility category in Figs. I-1 and I-2 increase rapidly from low to high ranges, and because the absolute frequencies of the various types of obstruction vary widely, the following procedures were used as aids in illustrating the changes in relative importance of each of the indicated obstructions to vision in relation to visibility. To suppress the trend, the individual frequencies associated with each type of obstruction were divided by the average value for all types within the same visibility range. Second, the individual frequency ratios were multiplied by factors that satisfy the requirement that the total contribution due to each type of obstruction in the visibility range from 0 to 3 mi be the same. Thus, if the relative contribution of each obstruction did not vary with visibility, all curves would have appeared in the figures as horizontal straight lines at ordinate value 1.

The significant features of Figs. I-1 and I-2 are the decrease in importance of fog as a contributor to low visibility as the intensity of simultaneous rainfall increases, and the increase in importance of rain itself as a restriction to visibility at higher ranges as the intensity of rain increases. The effect at low visibilities is tentatively attributed to the accretion process, although it is possible that it reflects the action of other, less direct physical processes. A similar effect on ceilings is shown in Fig. I-3.

Additional data summaries not previously reported are shown in Figs. I-4 and I-5. For each visibility value, one observation per station per month of rainfall amount in the previous hour during rainstorms of 3 or more hours' duration was extracted from the data. For the lowest visibilities, it was necessary in a few instances to use two or more observations in one month due to

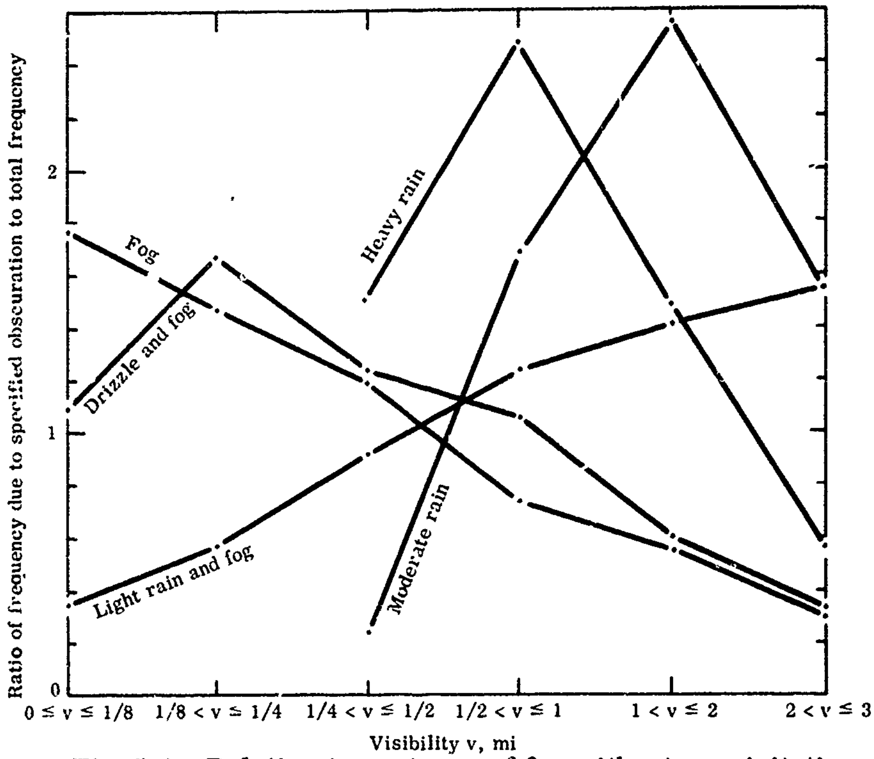

Fig. I-1. Relative importance of fog without precipitation and fog with precipitation of various intensities as obscurations to vision at Idlewild International Airport, from hourly data for the years 1949 through 1958.

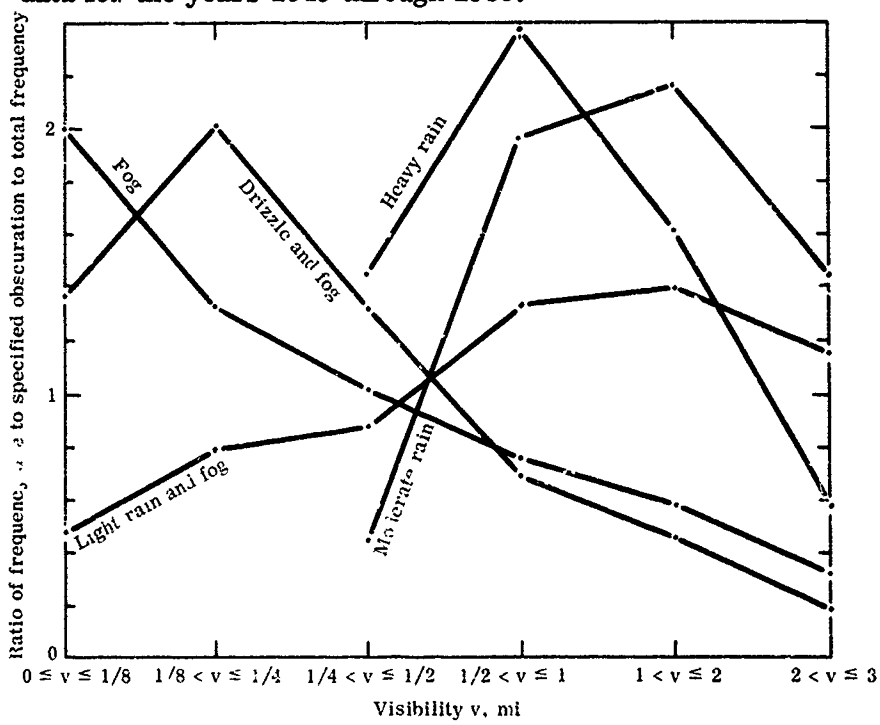

Fig. I-2. Relative importance of fog without precipitation and fog with precipitation of various intensities as obscurations to vision at Newark Airport, from hourly data for the years 1949 through 1958.

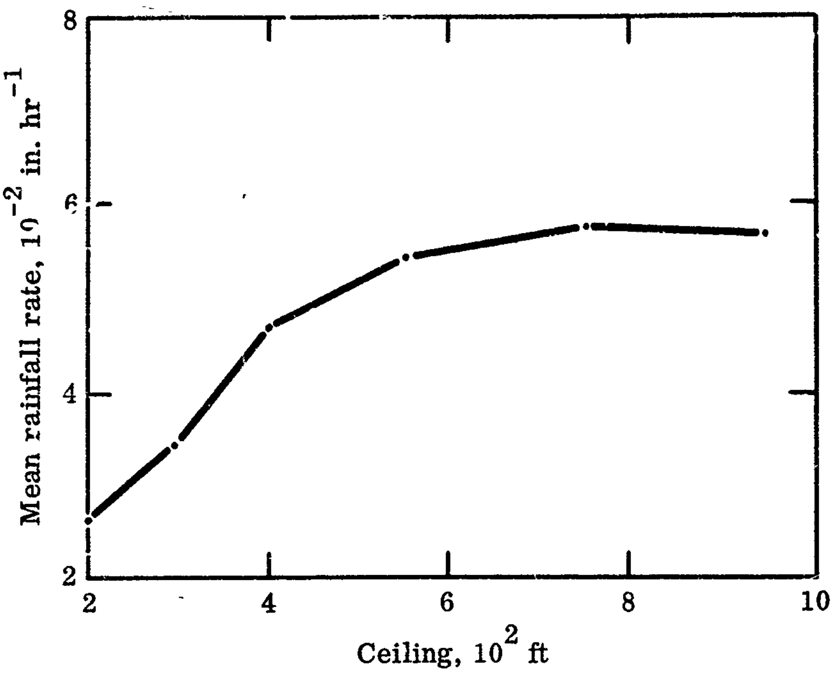

Fig. I-3. Mean rainfall rates based on 3-hr total amounts at Battery Place, New York City, for low ceilings in rain observed at the midpoint of the 3-hr period at Idlewild International Airport (1956 through 1960).

lack of data in other months. The restriction on rainfall duration was imposed to minimize the effect of unrepresentative values caused by inadequate resolution of the data in showery precipitation. The jagged curves in the figures represent the 50-, 80-, and 90-percentile limits of the equal-group-size rainfall-rate frequency distributions for each visibility. The straight line represents the relation $V_m = 11.6R^{-0.63}$ for visual range V_m in rainfall of rate R only, according to Atlas [4]. Within the limits of the approximations used in its derivation, this equation represents a theoretical upper limit for the data under study. The behavior of the distribution curves for visibilities below 1 mi is of particular interest. The trend to low rainfall rates as visibility decreases supports the results in Figs. I-1 and I-2 and is once again tentatively attributed to the accretion process. According to Fig. I-4, 90% of all visibilities of 2000 ft or less in rain, with or without other obstructions, occur with rainfall rates of 0.08 in. hr^{-1} or less. This result is reproduced by the data in Fig. I-5.

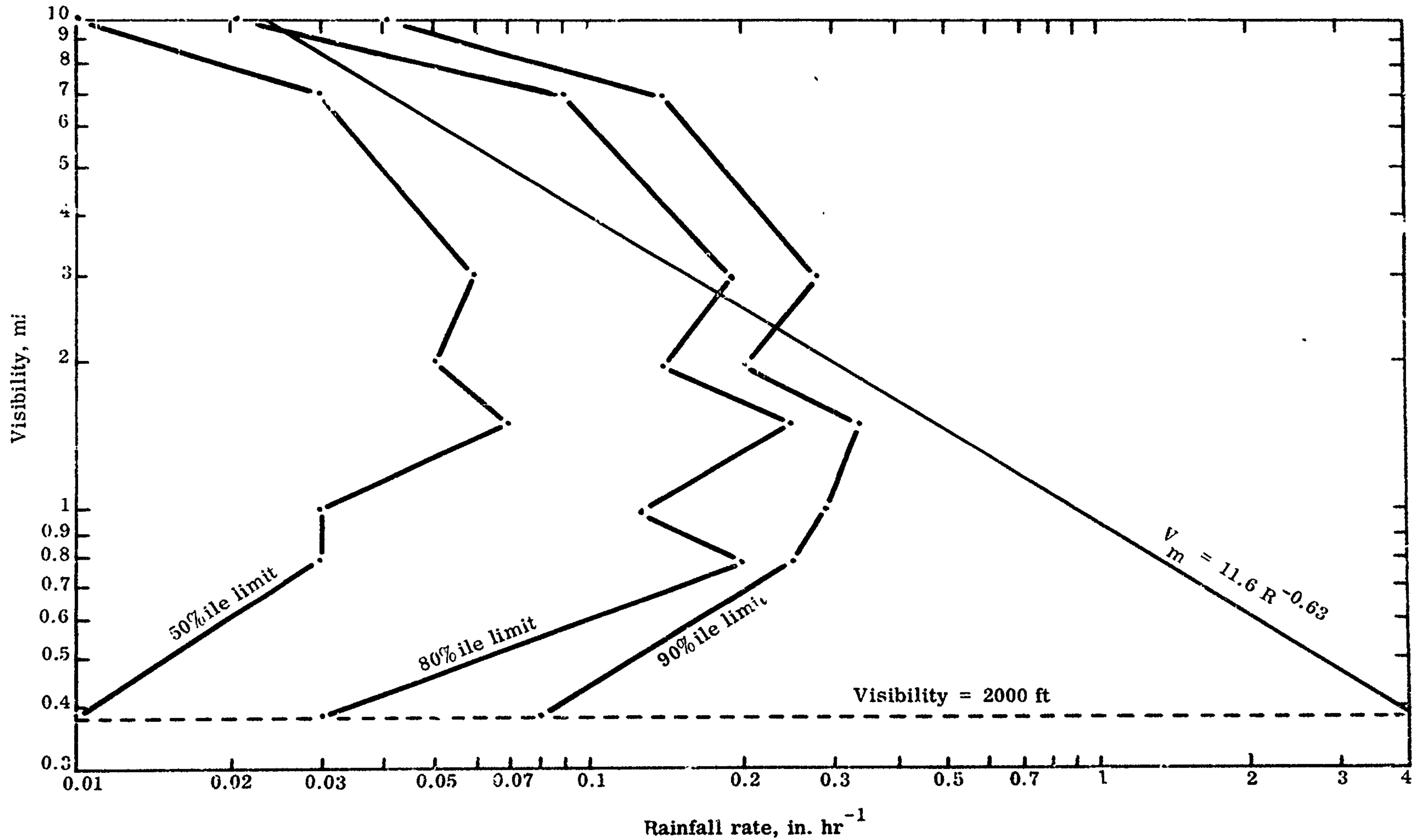

Fig. I-4. Characteristics of the frequency distributions of hourly rainfall rates for selected visibilities at Logan International Airport (Boston), Newark Airport, Washington International Airport, and Atlantic City Airport, Jan. 1 through Dec. 31, 1961 (hourly observations).

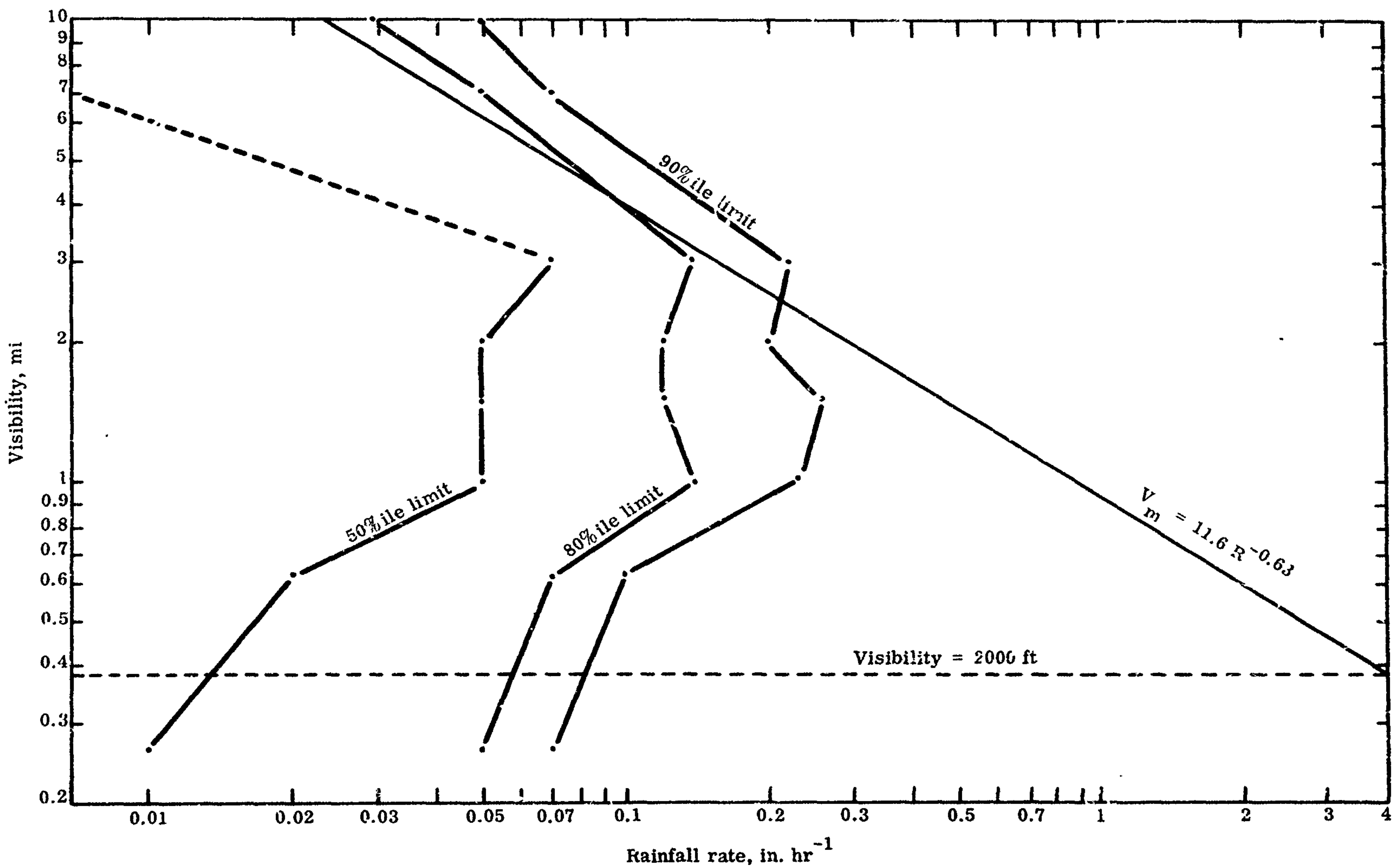

Fig. I-5. Characteristics of the frequency distributions of hourly rainfall rates for selected visibilities at Logan International Airport (Boston), Jan. 1, 1955, through Dec. 31, 1958.

I.8.0 THEORETICAL CONSIDERATIONS OF THE EFFECTS OF ACCRETION ON VISUAL RANGE

The meteorological visual range (V_m) of a blackbody viewed horizontally under uniform monochromatic illumination scattered by particles distributed homogeneously along the path is given by

$$V_m = \sigma_s^{-1} \ln \epsilon^{-1}, \tag{I-1}$$

where σ_s is the extinction coefficient due to scattering and ϵ is the brightness-contrast threshold of the human eye [5]. By definition, for spherical particles,

$$\sigma_s = \frac{n\pi}{4} C_s d^2, \tag{I-2}$$

where the scattering is accomplished by n particles of diameter d per unit volume, and C_s is the scattering cross section. Thus, when attenuation is due to scattering only by heterogeneous droplets,

$$V_m = \frac{4 \ln \epsilon^{-1}}{\sum_i C_{si} n_i d_i^2}. \tag{I-3}$$

If we assume further that C_s and ϵ are independent of d, we may write

$$\frac{V_t}{V_0} = \frac{\sum_i n_{0i} d_i^2}{\sum_i n_{ti} d_i^2}, \tag{I-4}$$

where V_t is the visual range at time t, V_0 is the initial visual range, and n_{0i} and n_{ti} are the numbers of drop-size i at times 0 and t respectively.

Consider the local time changes in the number of fog droplets n_i of diameter d_i. If we neglect the vertical advection of droplets and assume as a first approximation that accretion effects can be represented as an additive term to other source-sink processes, then

$$\frac{\partial n_i}{\partial t} = \left.\frac{\delta n_i}{\delta t}\right|_D + \left.\frac{\delta n_i}{\delta t}\right|_A - \vec{V} \cdot \nabla n_i, \tag{I-5}$$

where $(\delta n_i/\delta t)_D$ includes the contribution of all processes other than accretion which lead to development or dissipation of droplets within an air parcel, $(\delta n_i/\delta t)_A$ denotes the loss of fog droplets due to accretion, $\vec{V} \cdot \nabla n_i$ represents changes due to horizontal advection. It is clear from Eqs. (I-4) and (I-5) that

to achieve a specified visual range, the rate of removal of fog droplets $(\delta n_i/\delta t)_A$ must compensate the sum of the rate of production $(\delta n_i/\delta t)_D$ and the rate of increase of droplets due to advection at the required value of n_i. If the apparent relation between rainfall rate and visibility shown in Figs. I-1 through I-5 was indeed due to accretion effects, it would seem that rather modest rainfall rates can compensate for the production of new droplets in fogs associated with rainstorms. In practice, the advection term in Eq. (I-5) presents more serious problems if V is not negligible due to necessary limitations on the areal extent of artificial spray.

Following Rigby et al. [6], we can write the time changes in fog-droplet number as

$$\left.\frac{\delta n_i}{\delta t}\right|_A = -\frac{\bar{E}}{4} n_i \int_0^\infty N_D v \pi D^2 \, dD. \tag{I-6}$$

In Eq. (I-6), the precipitation is specified by the drop-size distribution function N_D, the diameter D and the fall speed v. The quantity $\bar{E}$ represents the collection efficiency averaged over all precipitation drop sizes for the droplet size d_i. On integration,

$$n_t/n_0 = \exp\left(-1115\bar{E}t \int_0^\infty N_D D^{5/2} \, dD\right), \tag{I-7}$$

where use has been made of Spilhaus' [7] relation for terminal velocity ($v = 1420D^{1/2}$ cm sec^{-1}). Combining Eqs. (I-4) and (I-7) yields

$$\frac{V_t}{V_0} = \frac{\sum_i n_{0i} d_i^2}{\sum_i n_{0i} d_i^2 \exp\left(-1115\bar{E}_i t \int_0^\infty N_D D^{5/2} \, dD\right)} \tag{I-8}$$

To apply Eq. (I-8), it is necessary to specify the initial fog-droplet-size-distribution function n_{0i}, the collection efficiency $\bar{E}$ (as a function of droplet size), and the precipitation-drop-size-distribution function N_D. The quantities n_{0i} and $\bar{E}_i$ present the greatest difficulties, for little is known about the contribution of small droplets ($d < 5\mu$) to the restriction of visibility in natural fogs* and about the true variation of $\bar{E}$ with droplet size. As a result of these uncertainties,

*See, for example, the discussion reported by Singleton [8, p. 182].

calculations based on Eq. (I-8) are little more than exercises, and the results must be interpreted with great caution.

Two quite different drop-size distributions, as shown in Table I-1, were used in sample calculations of V_t/V_0. The data in column (a) are based on a smoothed curve of the data presented by aufm Kampe and Weickmann [9 p. 191] for stratus cloud. The data in column (b) were derived from measurements reported by May [10]. Mean values of May's data for two samples (1030 and 1230, Dec. 13, 1960) with very low observed values of visual range and high droplet counts were used in Table I-1. The drop-size spectrum was evaluated from Best's [11] equation, $1 - F = \exp[-(x/a)^n]$, where F is the fraction of the water content accounted for by drops with diameter less than x and where a and n are constants. The values of a and n and the size range indicated in Table 2 of May's [9] paper were used in the calculations.

The visual range according to Eq. (I-3) for column (b) in Table I-1 with $\bar{\epsilon} = 0.02$ and $C_s = 2$ is 134 m. The observed visual range was approximately 80 m.

According to May, the discrepancy between observed and calculated values of visual range could be accounted for by errors in the assumed values of $\bar{E}$ and C_s, by droplet-sampling errors, and by errors in the estimate of visual range by eye. For comparison, the relative drop numbers reported by aufm Kampe and Weickmann [9] were multiplied by a constant factor to give a theoretical visual-range value of 134 m.

For the purpose of calculating values of V_t/V_0, two raindrop-size-distribution functions were used. The equation of Marshall and Palmer [12], $N_D = N_0 \times \exp(-\lambda D)$, with $N_0 = 0.08\ \mathrm{cm}^{-4}$ and $\lambda = 41R^{-0.21}\ \mathrm{cm}^{-1}$, was used to simulate natural precipitation of rate R. Computations were also carried out for monodisperse raindrops with $D = \text{const.} = 400\mu$. Collection efficiencies $\bar{E}$ based on the work of Langmuir [13] were used in all computations. More will be said about the limitations and shortcomings of the calculations later in this section.

Values of V_t/V_0 for selected rainfall rates and times are shown in Figs. I-6 through I-8. The fog-drop-size distribution shown in column (b), Table I-1,

TABLE I-1
OBSERVED FOG-DROP-SIZE DISTRIBUTIONS

Diameter, μ	No. cm^{-3}		Diameter, μ	No. cm^{-3}		Diameter, μ	No. cm^{-3}	
	(a)	(b)		(a)	(b)		(a)	(b)
1	9.1	370	21	0.97	0.59	41	0.18	0.0027
2	8.1	170	22	0.87	0.49	42	0.17	0.0019
3	7.2	95	23	0.84	0.41	43	0.16	0.0014
4	6.4	70	24	0.77	0.34	44	0.15	0.0010
5	5.7	51	25	0.69	0.28	45	0.13	0.0008
6	5.1	37	26	0.64	0.24	46	0.12	-
7	4.5	27	27	0.59	0.20	47	0.12	-
8	4.1	20	28	0.54	0.16	48	0.11	-
9	3.7	15	29	0.50	0.14	49	0.10	-
10	3.4	11	30	0.47	0.11	50	0.094	-
11	3.0	8.2	31	0.42	0.082	51	0.089	-
12	2.6	6.2	32	0.39	0.058	52	0.084	-
13	2.3	4.8	33	0.35	0.041	53	0.081	-
14	2.1	3.6	34	0.33	0.030	54	0.076	-
15	1.9	2.8	35	0.30	0.021	55	0.072	-
16	1.7	2.1	36	0.28	0.015	56	0.067	-
17	1.5	1.6	37	0.26	0.011	57	0.064	-
18	1.3	1.2	38	0.24	0.0076	58	0.060	-
19	1.2	0.93	39	0.22	0.0054	59	0.057	-
20	1.1	0.71	40	0.20	0.0038	60	0.054	-

was used in Figs. I-6 and I-7. The curve for $R = 0.08$ in. hr^{-1} in Fig. I-7 is reproduced in Fig. I-8 for comparison with the effects of the same precipitation on the fog-drop-size distribution shown in column (a), Table I-1. It will be seen that both rainfall rate and fog-drop-size distribution play important roles in determining the effectiveness of accretion. Though not shown here for lack of adequate information, it is likely that the variation of collection efficiency with drop size is also of primary importance.

Although the curves in Figs. I-6 through I-8 suggest the possibility of significant effects of accretion on visual range, they must be considered tentative because of uncertainties in the basic assumptions and parameters required for the computations. Perhaps the most serious uncertainties are associated with the following parameters.

(a) Scattering cross section C_s. For large values of drop size, a portion of the light beam is diffracted within a small angle of the forward direction and is, therefore, not completely lost from the incident beam. Consequently, the value $C_s = 2$, used in the calculations, may be high for large drops. Further information on this question may become available in the future [14 p. 147]. On the other hand, for very small drop sizes, values of C_s between 2 and 4 may be appropriate, depending on the dominant wavelength of the incident light.

(b) Collection efficiency $\bar{E}$. Some of the discrepancies between calculated values of collection efficiency and laboratory or field measurements are well illustrated for large collecting drops in papers by Adderley [15] and Kinzer and Cobb [16]. The need is clear for more reliable estimates of collection efficiencies.

(c) Fog-drop-size-distribution data. More data are needed on the numbers of small drops present in natural fogs of various types and on the importance of the small drops as contributors to the restriction of visual range. Recent papers by May [10] and Eldridge [17] indicate that these questions are by no means settled at present.

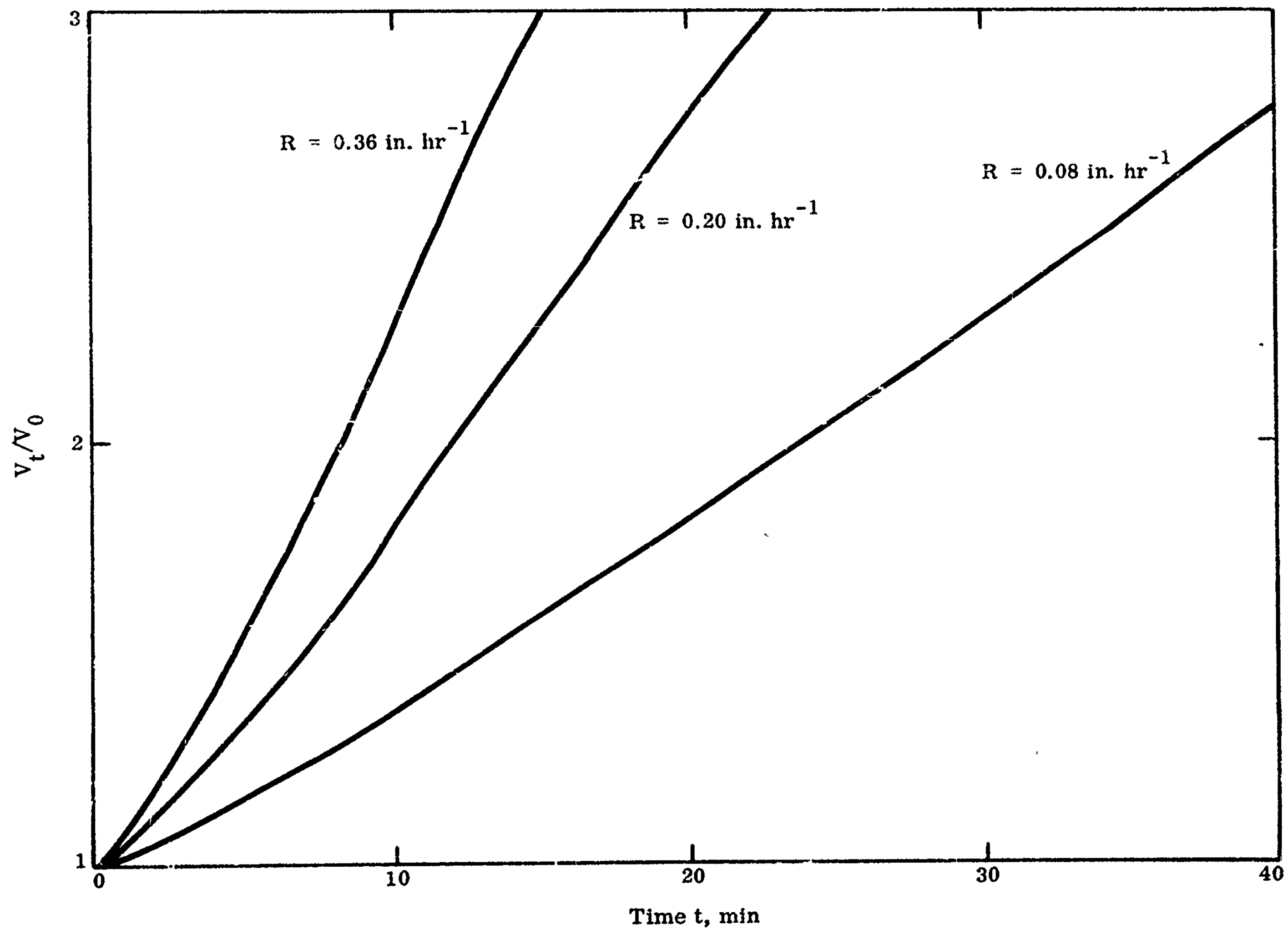

Fig. I-6. Visual range in fog [column (b), Table I-1] as a function of time during accretion by natural rain of rate R, based on collection efficiencies after Langmuir [11].

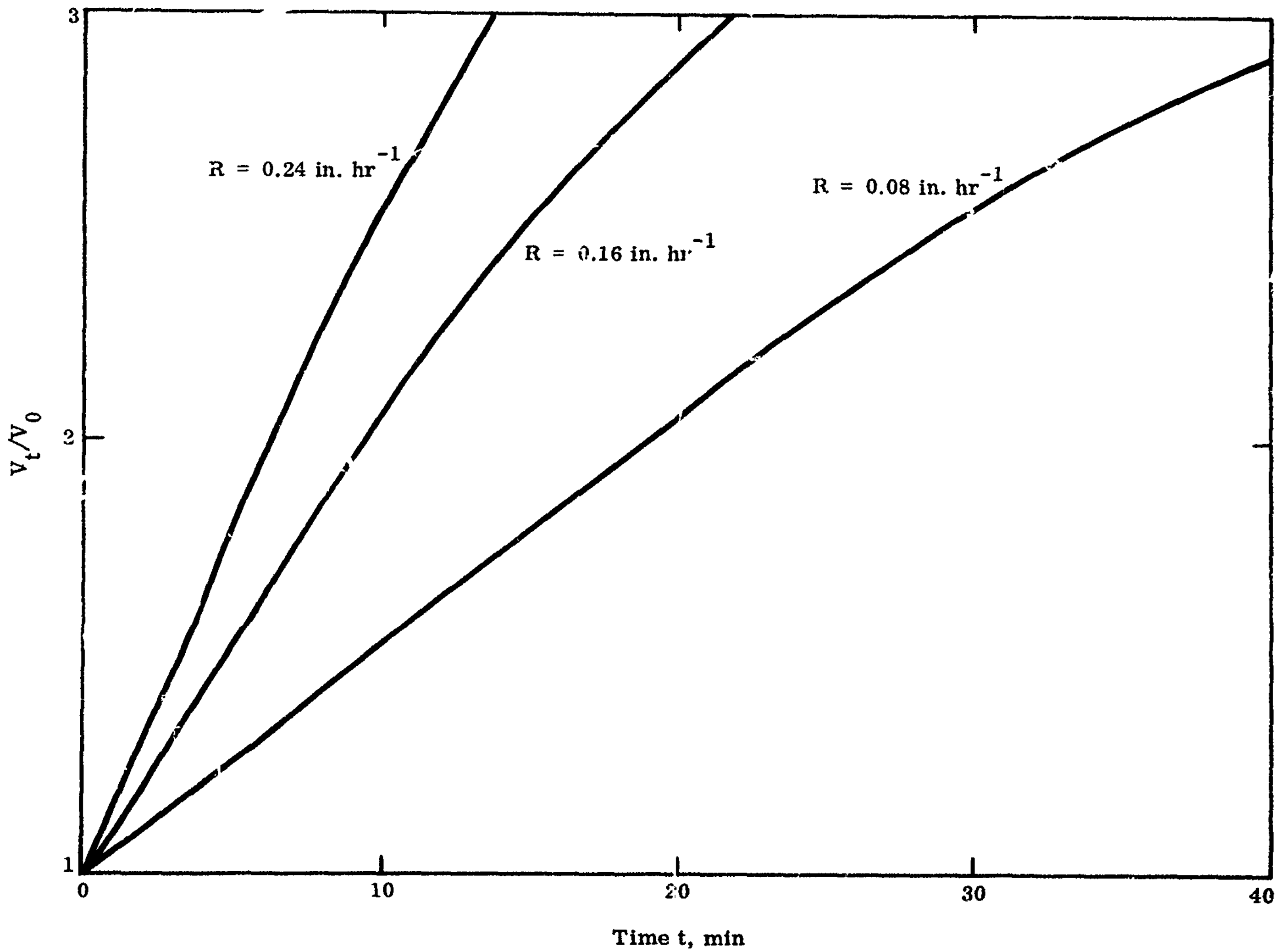

Fig. I-7. Visual range in fog [column (b), Table I-1] as a function of time during accretion by monodisperse rain of rate R (d = 400 μ) based on collection efficiencies after Langmuir [11].

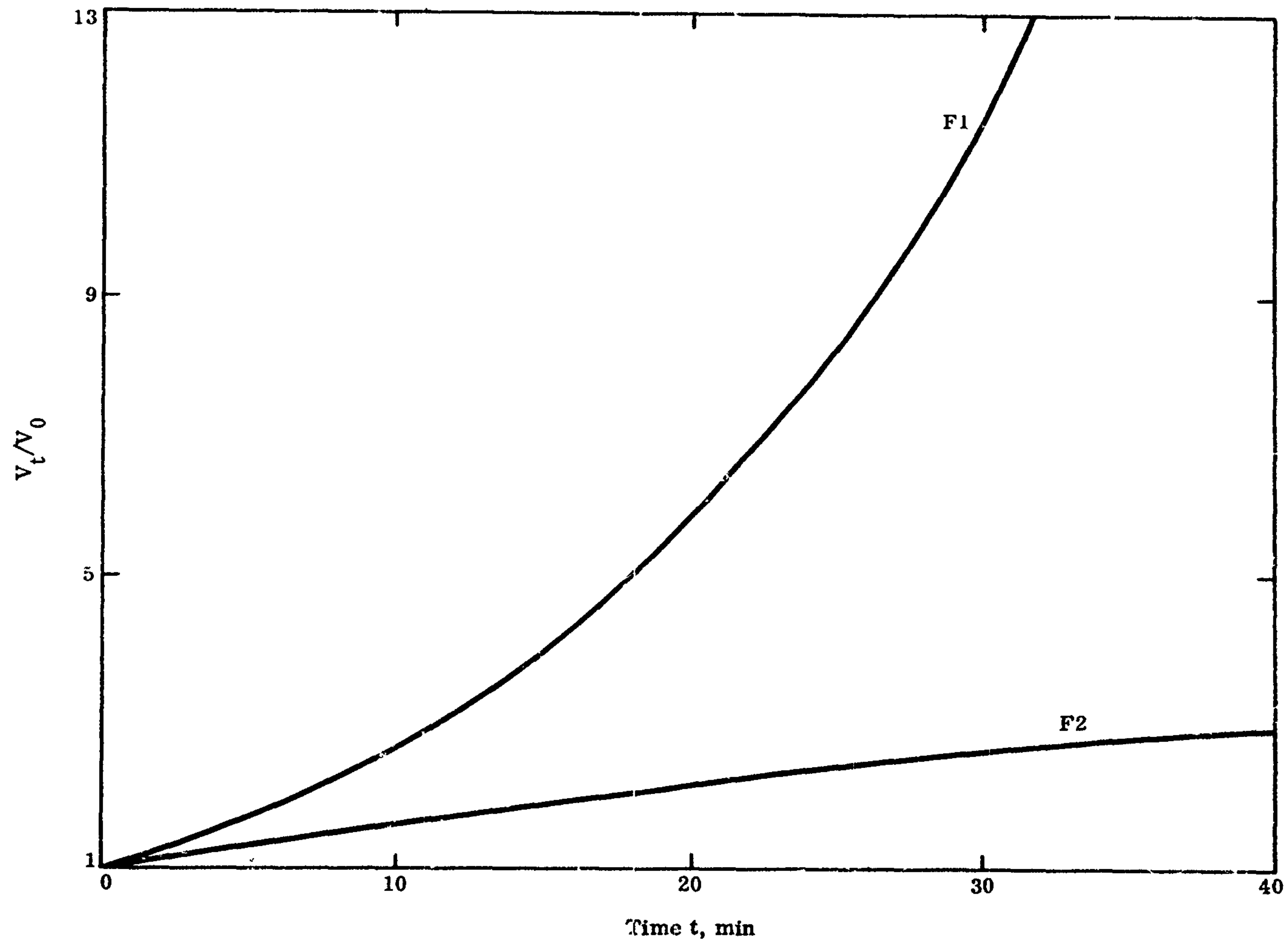

Fig. I-8. Visual range in fog type F1 [column (a), Table I-1] and type F2 [column (b), Table I-1] as a function of time during accretion by monodisperse drops of diameter d = 400 μ and rate R = 0.08 in. hr^{-1}.

I.9.0 PRACTICAL CONSIDERATIONS

Artificial simulation of the accretion process requires elevation of a mass of water to a specified altitude, fractionation of the mass into a certain drop-size distribution, and uniform distribution of the drops over a horizontal area. Rough estimates of water requirements can be derived from Figs I-6 through I-8.

Let d represent the length of a side of a square area to be thinned. The total area A over which the water must be distributed in wind of speed V allowing for wind-direction changes of $\pm\alpha$ degrees is approximately

$$A = d^2 + VT\,(d + VT \tan \alpha), \qquad \text{(I-9)}$$

where T is the time needed for thinning. If A_1 is the area covered by each source, the number n of sources is

$$n = AA_1^{-1}. \qquad \text{(I-10)}$$

The flow rate Q for an equivalent precipitation rate R is Q = AR, and the total volume M of water required to maintain thinning over an area d^2 for time τ is approximately

$$M = AR\,(T + \tau). \qquad \text{(I-11)}$$

Within the range shown in Figs. I-6 and I-7, T is approximately inversely proportional to R, and it is therefore advantageous from the viewpoint of distribution to use a large flow rate under windy conditions in order to minimize T, A, and n. However, for small values of T (T < 1 min, approximately), the inverse relation fails because a finite time is required for the drops to fall from the initial altitude. Computed values of A, n, and Q are shown in Table I-2 for various areas and wind speeds. For these computations, $R = 0.24$ in. hr^{-1}, $A_1 = 10^4$ ft^2, and $\alpha = 30°$. Values of T for each fog type correspond to an increase in visual range by a factor of 2.

The values in Table I-2 indicate major difficulties in the way of practical utilization of the method. The water-volume requirements and the distribution problems are particularly serious in the presence of wind.

During the breakup of sheets or filaments of water, many small droplets of the order of a few microns in diameter are formed. If the water is emitted

TABLE I-2

ESTIMATED SPRAY PARAMETERS FOR DOUBLING THE VISUAL RANGE IN FOG BY WATER-DROP ACCRETION*

Thinned area, ft^2	Wind speed, knots	Fog type F1 (T = 2.5 min)			Fog type F2 (T = 6.5 min)		
		Total spray area A, ft^2	Number n of sources†	Total flow rate Q, gal min^{-1}	Total spray area A, ft^2	Number n of sources†	Total flow rate Q, gal min^{-1}
10^6	0	10^6	10^2	2.5×10^3	10^6	10^2	2.5×10^3
	4	2.6×10^6	2.6×10^2	6.4×10^3	7.6×10^6	7.6×10^2	1.9×10^4
	8	5.4×10^6	5.4×10^2	1.3×10^4	2.2×10^7	2.2×10^3	5.5×10^4
10^7	0	10^7	10^3	2.5×10^4	10^7	10^3	2.5×10^4
	4	1.4×10^7	1.4×10^3	3.5×10^4	2.2×10^7	2.2×10^3	5.5×10^4
	8	1.9×10^7	1.9×10^3	4.7×10^4	4.3×10^7	4.3×10^3	1.0×10^5

*$R = 0.24$ in. hr^{-1}, $A_1 = 10^4$ ft^2, and $\alpha = 30°$.

†Flow rate of each source is 25 gal min^{-1}.

from an airborne vehicle or high towers, these droplets may not present a problem because the majority will remain near the height of emission. However, with ground-based vertical spray under high pressure, the increased production rate of fog droplets by this mechanism may significantly reduce the accretion effect. Detailed nozzle and flow characteristics are required for quantitative estimates of small-droplet production rates. Special nozzles are available for the production of uniform droplets, but it is unlikely that these are suitable for the emission of high-volume, high-kinetic-energy sprays.

I.10.0 SUMMARY AND CONCLUSIONS

The suggestion that the accretion process be simulated artificially as a method for increasing the visual range in fog over land-based airfields has been proposed often [18, 2] and has generally been rejected for the following reasons.

(a) The requirements for large volumes of water are such that an aircraft spray system is impractical in wind speeds that are commonly observed with advection fog.

(b) If towers or other frameworks for the support of spray apparatus are erected over the area to be cleared, they will represent a hazardous interference with the airspace. If they are erected upwind of the area to be cleared, the system will not work in very light winds.

(c) The production of small drops by nozzles in the spray apparatus may be of such magnitude that the process is rendered ineffectual.*

(d) The initial installation costs of towers or other frameworks and water-distribution lines are likely to be high. Land-based installations of this nature cannot be moved easily.

The advantages of the method are as follows.

(a) If water drops are used, the raw material is in many locations abundant and inexpensive. Further, unless salt water is used, the material is nontoxic and noncorrosive, and the method does not involve the production of light, vibrations, or open flames.

(b) If a land- or sea-based system is used, the operating costs are low. Energy is needed only to move the required mass of water through the distribution lines and nozzles against the force of friction and to raise it to the required altitude against the force of gravity. In relatively small volumes of air, the system could be operated continuously over extended periods of time.

It is abundantly clear from Table I-2 that the artificial water-spray technique is not practical for the enhancement of visual range in fog over large areas or in fog that is moving with appreciable speed. At the same time, because of its

*Personal communication from Prof. H. G. Houghton.

advantages, the method may be worthy of further consideration for special purposes or special localities. The advection problem could be substantially reduced at sea by moving the platform of interest with the motion of the fog. The occurrence of fog with extremely light winds is rather common over land in certain sheltered locations, and the method may be useful in the thinning of ground fog and the prevention of deep fog that results from radiative cooling of the top of ground fog in such localities. However, before the method can be seriously considered even for limited application, quantitative studies of the distribution and emission problems, based on up-to-date nozzle and pump technology, are required.

I.11.0 REFERENCES

1. Junge, C. E., Methods of Artificial Fog Dispersal and their Evaluation. AF Surv. in Geophys. 105, Geophys. Res. Dir., AF Cambridge Res. Center, Bedford, Mass., 1958.

2. Plank, V. G., Fog Modification by Cold Water Seeding. Geophys. Res. Paper 31, Geophys. Res. Dir., AF Cambridge Res. Center, Bedford, Mass., 1954.

3. The Travelers Research Center, Inc., Aviation Terminal Weather Prediction. 7072-23, 1962.

4. Atlas, D., "Optical Extinction by Rainfall," J. Meteorol. 10, 486—488, 1953.

5. Johnson, J. C., Physical Meteorology. New York: Technology Press of M.I.T. and John Wiley & Sons, Inc., 1954.

6. Rigby, E. C., J. S. Marshall, and W. Hitschfield, "The Development of the Size Distribution of Raindrops During their Fall," J. Meteorol. 11, 362—372, 1954.

7. Spilhaus, A. F., "Drop Size, Intensity, and Radar Echo of Rain," J. Meteorol. 5, 161—164, 1948.

8. Singleton, F., "Summary of Discussions on a Paper by May (1961)," Weather 17: 181—182, 1962.

9. aufm Kampe, H. J., and Weickmann, "Physics of Clouds," Meteorol. Monogr. 3:18, 182–225, 1957.

10. May, K. R., "Fog-Droplet Sampling Using a Modified Impactor Technique," Quart. J. Roy. Meteorol. Soc. 87, 535–548, 1961.

11. Best, A. C., "Drop-Size Distribution in Cloud and Fog," Quart. J. Roy Meteorol. Soc. 77, 418–426, 1951.

12. Marshall, J. S., and W. McK. Palmer, "The Distribution of Raindrops with Size," J. Meteorol. 5, 165–166, 1948.

13. Langmuir, I., "The Production of Rain by a Chain Reaction in Cumulus Clouds at Temperatures Above Freezing," J. Meteorol. 5, 175–192, 1948.

14. Herman, B. M., "Infra-red Absorption, Scattering, and Total Attenuation Cross-Sections for Water Spheres," Quart. J. Roy. Meteorol. Soc. 88, 143–150, 1962.

15. Adderley, E. E., "The Growth of Raindrops in Cloud," Quart. J. Roy. Meteorol. Soc. 79, 380–388, 1953.

16. Kinzer, G. D., and W. E. Cobb, "Laboratory Measurements of the Growth and Collection Efficiency of Raindrops," J. Meteorol. 13, 195–301, 1956.

17. Eldridge, R. G., "A Few Fog Drop-Size Distributions," J. Meteorol. 18, 671–676, 1961.

18. Houghton, H. G., and W. H. Radford, On the Local Dissipation of Natural Fog. Papers in Phys. Oceanogr. and Meteorol. VI:3, M.I.T. and Woods Hole Oceanogr. Inst., 1938.

APPENDIX J. BOUNDARY LAYER WINDS*

J.1.0 GENERAL DESCRIPTION

J.1.1 Phenomena Types

The winds to be considered are confined to the atmospheric layer in which turbulent viscous forces in the presence of an underlying surface (whether earth or ocean) are dominant.

In general, the wind quantities are assumed to correspond to observations of at least several minutes to, at most, about an hour averaging time. Equivalent space-averaging dimensions are roughly a few hundred meters to a few kilometers in the horizontal, with a vertical averaging dimension of approximately .1 to 1 times the height of the observation above the boundary surface. Smaller scale variations are to be considered turbulence in this context, and are treated in more detail elsewhere in this report.

J.1.2 Characteristic Geographic Extent

Averaged wind velocities of the type considered exhibit characteristic vertical profiles which depend on such parameters (measured on at least the same scale) as horizontal pressure gradient, coriolis forces, aerodynamic roughness characteristics of the underlying surface, and the static stability within the layer (as represented by the Richardson number). The vertical profiles would therefore be uniform over horizontal areas (larger than the space-averaging dimension) in which values of these parameters are uniform. Generally this means that similar vertical profiles of boundary layer wind velocity (comprising a "boundary layer wind system" in this survey) would be expected to extend over areas of about a few tens to a few thousand km on a side.

The upper end of this range would apply over the oceans where horizontal variations in the parameters are weaker, and the lower end over the continents where horizontal inhomogeneities in the parameters are more pronounced. The smallest scale systems will be encountered in the vicinity of horizontal discontinuities in one or more of the parameters, e.g. at coast lines, at ridge-

*By Joseph P. Pandolfo.

valley boundaries, and in air-mass frontal zones.

J.1.3 Characteristic Process and Property Involvement

J.1.3.1 Basic Forces

(a) Horizontal frictional stress at the underlying surface and within the layer

(b) Horizontal pressure gradient forces

(c) Coriolis forces

J.1.3.2 Modifying Factors

(a) Surface roughness

(b) Stability (vertical density structure of layer) which is modified by:

(i) Radiational properties of underlying surface (albedo, long wave emissivity)

(ii) Heat capacity, heat transfer efficiency in underlying layer

(iii) Evaporation at surface

(iv) Cloud effects on surface temperature

(c) Baroclinicity (horizontal density structure of layer)

(d) Large-scale topography of underlying surface

J.1.3.3 Property Transports

(a) Air mass

(b) Air temperature

(c) Water vapor content

(d) Contaminants (dust, smoke, etc.)

J.1.4 Characteristic Life Cycle

There are three predominant time scales evident in the analysis of boundary layer wind systems. The first is the free period of the inertial oscillation given by $T = 2\pi f^{-1}$, where f is the coriolis parameter. At mid-latitudes this would correspond to about 16 hr. The damping effect of the turbulent frictional forces is highly dependent on the stability of the lowest portions of the layer, which undergoes diurnal variations, particularly on clear days and over land. The periods in the diurnal variation here are determined by the daily solar heating cycle. A

thorough analysis of the combined effects of the inertial oscillation and the diurnal variation of eddy viscosity is given by Ooyama [1].

Variations in horizontal pressure gradients occur over periods of 1–5 days with the diurnal period predominant in sea-breeze, mountain valley wind systems, and the synoptic scale period in mid-latitude storm areas. The presence of synoptic periods is much less pronounced over tropical and polar areas.

A linearized analysis of the planetary boundary layer using Eq. (J-3) with non-linear velocity terms neglected, and time-constant pressure gradient and eddy viscosity, gives a damped, quasi-periodic solution for the velocity profile as a function of time, very slowly approaching the classical steady state solution of Ackerblom, given for example in Berry et. al., [2] (the so-called atmospheric Ekman spiral). After three full periods of the inertial oscillation (48 hr in mid-latitudes), the velocity profiles will still oscillate about their steady state value with an amplitude of 10–20% of the steady state values.

The results of this analysis on an extremely simplified model of the boundary layer wind system would appear to indicate that transients dominate the velocity profiles in mid-latitudes, with the lifetime of the boundary layer wind systems determined by the time scale of changes in the free-atmosphere large-scale circulation patterns. Boundary layer systems over subtropical, tropical and polar regions are more long-lived but are definitely oscillatory in nature, with the periods of the inertia oscillation, and/or the diurnal heating cycle, dominant.

J.2.0 ASSESSMENT OF GEOPHYSICAL FORCES

J.2.1 Equation of Horizontal Motion

The general equation for horizontal averaged motion may be written

$$\frac{\partial \vec{V}}{\partial t} = -\frac{1}{\rho}\nabla p - f\vec{k} \times \vec{V} + \frac{1}{\rho}\frac{\partial \vec{\tau}}{\partial z} - w\frac{\partial \vec{V}}{\partial z} - \vec{V}\cdot\nabla\vec{V} + \frac{1}{\rho}\nabla\cdot\vec{\tau} + \nabla\cdot\frac{\mu}{\rho}\nabla\vec{V} + \frac{\partial}{\partial z}\frac{\mu}{\rho}\frac{\partial \vec{V}}{\partial z} \tag{J-1}$$

where

- $\vec{V}$ = horizontal wind vector
- w = vertical component of wind
- f = coriolis parameter
- ρ = air density
- p = pressure
- $\vec{\tau}$ = turbulent (Reynolds') stress tensor
- μ = molecular (laminar) viscosity
- $\vec{k}$ = unit vector in the vertical
- ∇ = horizontal gradient operator.

If it is assumed that the components of the stress tensor may be written as

$$A_z \frac{\partial V}{\partial z},\ A_H \nabla\vec{V},$$

the last six terms on the right hand side may be written

$$[A_z + \frac{\mu}{\rho}]\frac{\partial^2 \vec{V}}{\partial z^2} + [\frac{\partial A_z}{\partial z} - w]\frac{\partial \vec{V}}{\partial z} + [A_H + \frac{\mu}{\rho}]\nabla^2\vec{V} + [\nabla A_H - \vec{V}].\nabla\vec{V}. \tag{J-2}$$

On the basis of order-of-magnitude estimates (see Table J-1) the terms involving the molecular viscosity and A_H and its derivatives may be justifiably neglected. Neglect of the term involving the averaged vertical velocity appears to be indicated, particularly within the lower levels of the boundary layer, where the vertical velocities are presumably small. It should be noted here that A_z is generally not constant with height.

TABLE J-1
ORDER OF MAGNITUDE ESTIMATES OF
VARIOUS TERMS

Terms	Estimated order of magnitude
A_z	~ 10^4 to 10^6 cm^2 sec^{-1}
$\frac{\mu}{\rho}$	~ 10^{-1} cm^2 sec^{-1}
A_H	~ 10^3 to 10^7 cm^2 sec^{-1}
$[\lvert\nabla\vec{v}\rvert]\left[\frac{\partial\vec{v}}{\partial z}\right]^{-1}$	~ 10^{-3}
$[\lvert\nabla^2\vec{v}\rvert]\left[\frac{\partial^2\vec{v}}{\partial z^2}\right]^{-1}$	< 10^{-3}
$\frac{\partial A_z}{\partial z}$	~ 1 to 10^2 cm sec^{-1}
ω	< 1 cm sec^{-1}
$\lvert\nabla A_H\rvert$	~ 1-10 cm sec^{-1}
$\lvert\vec{v}\rvert$	~ 10^2 to 2×10^3 cm sec^{-1}

A simpler horizontal motion equation may now be written as

$$\frac{\partial\vec{V}}{\partial t} + \vec{V}\cdot\nabla\vec{V} = -\frac{1}{\rho}\nabla p - f\vec{k} \times \vec{V} + \frac{\partial}{\partial z}\left[K(R_i, z_0)\frac{\partial\vec{V}}{\partial z}\right] \qquad \text{(J-3)}$$

where K has the dimensions of $\frac{A_z}{\rho}$, (cm^2 sec^{-1}), and z_0 is the roughness parameter of the surface. The following force analysis may be applied for the simplified equation.

The last force (in Table J-2) may be compared in order of magnitude with the advective term $\vec{V}\cdot\nabla\vec{V}$ which is generally less than 10^{-4} cm sec^{-2}; this indicates that neglect of the advective term may be justifiable.

J.2.2 Force Analysis

TABLE J-2
FORCE ANALYSIS

Force	Order of magnitude	Horizontal scale	Vertical scale
Coriolis force			
$-f\vec{k} \times \vec{v}$	10^{-1} to 2 cm sec^{-2}	10^2 to 10^3 km	10^{-1} to 1 km
Horizontal pressure force			
$\frac{1}{\rho} \nabla p$	10^{-1} to 2 cm sec^{-2}	10 to 10^3 km	10^{-1} to 1 km
Turbulent viscous force			
$\frac{\partial}{\partial z} K \frac{\partial \vec{v}}{\partial z}$	10^{-1} to 1 cm sec^{-2}	10^{-1} to 10^3 km	10^{-1} to 1 km

J.2.3 Characteristic Structure

Observations of boundary-layer wind profiles may be classified in the following way. One group consists of wind profiles as measured from fixed towers extending up to less than 100 m height in general [3], although recent observations to 300 have been obtained [4]. A relatively small portion of these observations are obtained over water and all of these are confined to shallow coastal or inland waters [5].

A second group comprises low level (up to 30 m) wind profiles measured from ships and other floating platforms over more open waters [6], with attendant problems in their interpretation because of the response of the wind sensors to platform motions.

A third group of observations, and probably the largest, consists of standard pilot balloon and rawinsonde measurements of wind through the lowest 1–2 km of the atmosphere. Velocity measurements of this type allow less freedom in choice of averaging period or scale, and individual observations will reflect the effects of "turbulence," as defined earlier in this survey.

A valuable group of simultaneous fixed tower and higher level observations over land is available in the results of the Great Plains observational program [7], in which several independent wind-observing systems were used throughout the entire layer of interest. Characteristic wind profile structures shown in these observations may be briefly described as follows:

Through a shallow layer immediately in contact with the earth's surface (about 10 to 100 m thick), variations of the stress with height appear to be relatively small, and the velocity profiles are characterized by a constant direction throughout this layer. Wind speed profiles show an increase with height throughout the layer. The speed profiles are characteristically logarithmic in height, with a form given by Prandtl [8], i.e.,

$$|\vec{V}|\,(z) \;\alpha\; \ln Z. \tag{J-4}$$

Variations in the stability of this layer appear to introduce systematic departures from the logarithmic profile, giving profiles that are well fitted by

$$|\vec{V}|\,(z) = A \ln Z + BZ \tag{J-5}$$

where the coefficients A = A (Z_0, surface stress); B = B (stability, mean temperature, gravity) [9]. In sufficiently unstable conditions power laws seem more appropriate;

$$|\vec{V}|\,(z) \;\alpha Z^{-p} \tag{J-6}$$

where p is a fractional power < 1, [10]. In many applications requiring only empirical fitting of the profiles, power laws may be used, if more convenient, to fit any of the relations above [11].

Above this shallow contact layer the stress variation with height appears considerable. Wind directions show a characteristic turning with height, turning clockwise into the direction of the large scale gradient wind from the ground to the top of the boundary layer in the Northern Hemisphere, and counter-clockwise in the Southern Hemisphere. Maximum deviations in any single profile of wind direction from the gradient direction appear to vary from about 5° to about 30°. The size of the deviation appears to vary systematically with surface roughness, gradient magnitude, latitude, and baroclinicity (horizontal density variation) of the layer [12].

Wind speed profiles in this layer appear roughly to be damped trigonometric functions of height, approaching geostrophic speed at the top of the layer. Speed maxima within the layer are frequently observed and may become very pronounced at heights of a few hundred meters. This phenomenon has been referred to as the "low level jet," and may produce wind shears of 20 m sec^{-1} $(200\ m)^{-1}$ under conditions favorable to its formation, [4].

J.3.0 ASSESSMENT OF GEOPHYSICAL ENERGY

An energy equation has been derived from Eq. (J-3) with the non-linear advective terms neglected. Vertical integration of the equation yields the specific kinetic energy in a vertical column from the surface to any convenient height, D, which represents the top of the layer of interest, in units of ergs cm gm^{-1}. (To obtain vertical average specific kinetic energy, ergs gm^{-1}, divide by D. To obtain vertical average kinetic energy density, ergs cm^{-3}, multiply by air density, $\rho \sim 10^{-3}$.) The energy transformation rates are given in ergs cm gm^{-1} sec^{-1}. Figure J-1 shows the budget represented by the energy equation thus obtained. K, P, and I denote kinetic, potential, and internal energy reservoirs, respectively.

The transformation rate formulas are written so that a negative value denotes transformation from the kinetic energy of the boundary layer wind system, while a positive value denotes transformation to kinetic energy of the boundary wind system. From the definition of τ, it may be seen that the transformation (4) (in Fig. J-1) must always proceed in the direction shown, since the integrand is always positive. The other transformations may proceed in either direction depending on the algebraic signs of the scalar products in the formulas. Normally, for the entire depth of the boundary layer, transformation rate (1) (in Fig. J-1) is relatively small compared to the other rates, (2) is positive, and (3) is either zero or positive, depending on whether the lower boundary is subject to displacement under the action of the wind. Transformation rate (3) for an underlying water surface represents the amount of energy going directly into wind generated waves and/or currents (see Appendixes I, K in [13]).

For order of magnitude estimates of the transformation rates, the simple closed-form solutions for the steady-state atmospheric wind-spirals over land [2] and sea [14] were used to obtain estimate formulas. These formulas are:

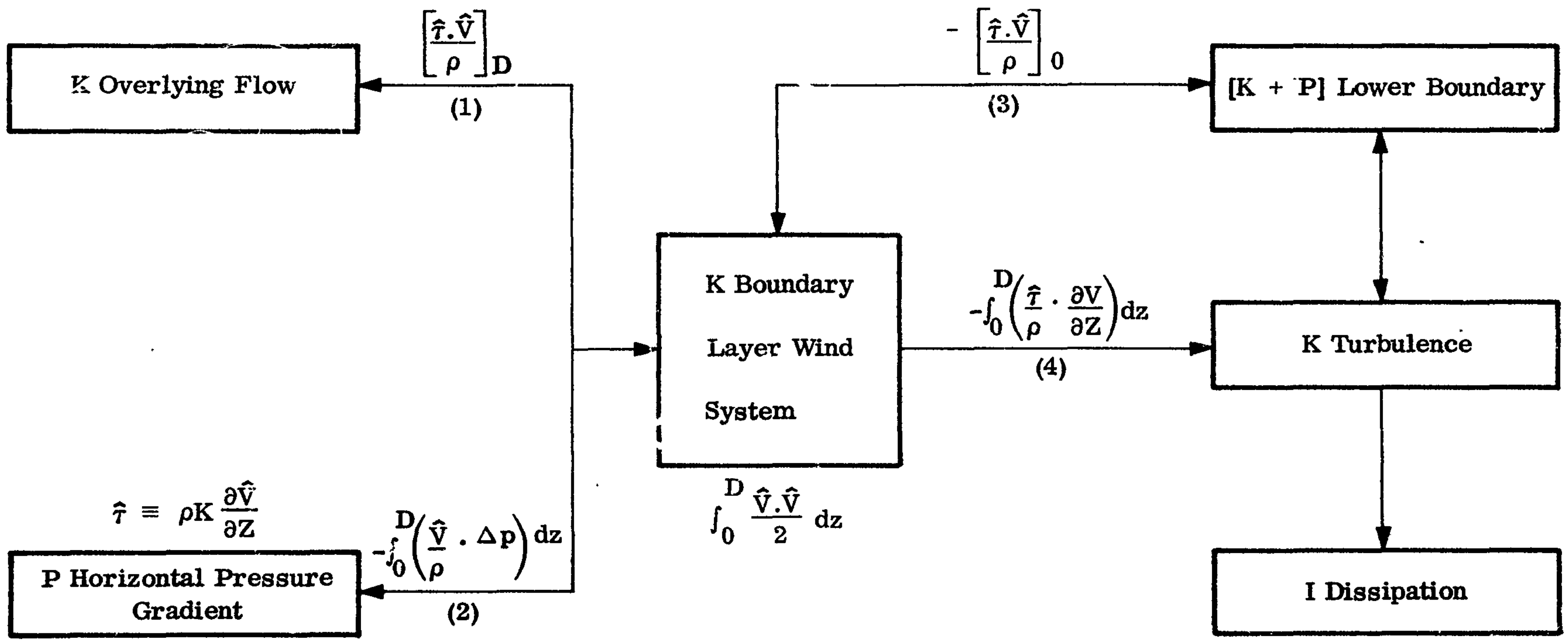

Fig. J-1. Energy budget in boundary layer wind system.

(a) over land

$$1 = -\frac{Kf}{2} u_g^2 \left[\ell^{-\pi} + \ell^{-2\pi}\right]$$

$$2 = \frac{Kf}{2} u_g^2 \left[1 + \ell^{-\pi}\right]$$

$$3 = 0$$

$$4 = -\frac{Kf}{2} u_g^2 \left[1 - \ell^{-2\pi}\right]$$

(b) over water

$$1_w = -\frac{Kf}{2} \frac{u_g^2}{[1 + R]} \quad \ell^{-\pi} + \frac{\ell^{-2\pi}}{[1 + R]}$$

$$2_w = 2 \frac{1}{[1 + R]}$$

$$3_w = -\frac{Kf}{2} \frac{u_g^2}{[1 + R]} \quad 1 - \frac{1}{[1 + R]}$$

$$4_w = -\frac{Kf}{2} \frac{u_g^2}{[1 + R]^2} \left[1 - \ell^{-2\pi}\right]$$

where,

$$u_g \equiv \left| \frac{1}{\rho f} \nabla p \right|$$

$$R \equiv \frac{K\rho^2}{K_w \rho_w^2}$$

K_w is eddy viscosity for the upper layers of the sea.

ρ_w is density of sea water.

Numerical estimates of the transformation rates over land for the entire depth of the Ekman layer are given in Fig. J-2(a). For over-water estimates (1) and (2) are decreased by approximately 1 percent, (4) is decreased by about 2 percent, and (3) becomes about 25 percent of (1). The range of K given for a geostrophic wind speed of 10 m sec^{-1} is from an estimate of the variation in mean K with static stability of the layer. The lowest value would be typical for a stable layer and the highest value for an unstable layer.

The steady state estimates indicate storage to transformation ratios of 10^4 sec, suggesting that changes by relatively small factors in one of the significant transformation rates, while holding the other constant, will lead to significant changes in the storage in about 3 hr. More precise assessments of the time periods and variations would require energy estimates from the transient solutions (as opposed to the steady state solutions), with more realistically modelled height-

(a) Energy estimates for the Ekman boundary layer [$f \approx 10^{-4}$ sec^{-1}]

u_g	Stability	D	K	(1) $\left[\frac{\tau \cdot \hat{V}}{\rho}\right]_D$	(2) $-\int_0^D \frac{\hat{V}}{\rho} \cdot \nabla p dz$	(3) $\left[\frac{\tau \cdot \hat{V}}{\rho}\right]_0$	(4) $-\int_0^D \frac{\tau}{\rho} \cdot \frac{\partial \hat{V}}{\partial z} dz$	Storage $\int_0^D \frac{\hat{V} \cdot \hat{V}}{2} dz$
cm sec^{-1}		cm	cm^2 sec^{-1}	ergs cm sec^{-1} gm^{-1}				erg cm gm^{-1}
10^3	Unstable	1.4×10^5	10^5	-2	2×10^6	0	-2×10^6	3×10^{10}
	Neutral	$.44 \times 10^5$	10^4	.64	6.4×10^6	0	-6.4×10^5	10^{10}
	Stable	$.14 \times 10^5$	10^2	.2	2×10^5	0	-2×10^5	3×10^9

(b) Energy estimates for the "Constant Stress" layer [$D = 5 \times 10^3$ cm]

u_g	Stability	U_{50M}	α*	$\left\lvert\frac{\hat{\tau}}{\rho}\right\rvert$	(1)	(2)	(3)	(4)	Storage
cm sec^{-1}		cm sec^{-1}	deg	cm^2 sec^2	ergs cm sec^{-1} gm^{-1}				erg cm gm^{-1}
10^3	Unstable	5×10^2	65°	5×10^3	25×10^5	$.8 \times 10^5$	0	-25×10^5	1.25×10^9 + ~ 10%
	Neutral		70°	10^3	5×10^5	$.6 \times 10^5$	0	-5×10^5	1.25×10^9
	Stable		85°	10^2	5×10^4	1×10^4	0	-5×10^4	1.25×10^9 - ~ 1%

*Assumed angle between surface wind and $\frac{1}{\rho} \nabla p$

Fig. J-2. Order of magnitude estimates for the energy budget shown in Fig. J-1.

stability-eddy viscosity relationships. While such models have been investigated (see Section J.4.3.0), none of the energy quantities have been computed.

Realistic time variations in the wind speed profiles, however, have been given by numerical solutions of such models. These agree with observations, and also with the inferences drawn above, in showing that significant changes in kinetic energy storage can occur over a few hours, due solely to the abrupt changes in stability (and therefore the eddy viscosity) that occur normally over land surfaces at sunrise and sunset. As the depth of the layer considered approaches that of the so-called "layer of constant stress", (i.e., 10–100 m above the surface), energy transfer at the upper and lower boundaries of the layer becomes more significant than transformation (2). Figure J-2(b) shows some numerical estimates for the lowest 50 m of the atmosphere over a land surface, derived from formulas (4) and (5).

It may be presumed that over water surfaces, transformation (3) becomes comparable in order of magnitude to transformation (1) and may enter in the energy budget with either positive or negative contributions depending on relative wind-wave or wind-current speeds. Realistic time change estimates require stress variations with height within this shallow surface layer to be about 3–10 percent of the stress value itself, at least in neutral and unstable conditions. This magnitude of the stress change with height is normally and justifiably neglected in the derivation of speed-height relations like Eqs. (J-4), (J-5), (J-6); it apparently cannot be neglected in considering the energy budget.

The estimates given in Fig. J-2(b) indicate that this layer is in more precarious balance energetically than the entire boundary layer. Storage to transformation ratios are notably smaller, ranging from about 5×10^2–10^4 sec.

J.4.0 MODIFICATION OR CONTROL FEASIBILITY

J.4.1 Direct Interference

Inspection of the energy budgets, (Figs. J-1, J-2) identifies the parameters which are of importance, aside from wind profile characteristics themselves. These are the horizontal pressure gradient and the vertical coefficient of eddy viscosity.

Direct interference with the horizontal pressure gradient and/or its vertical distribution involves large scale redistribution of atmospheric mass in the horizontal. In most cases this would imply the capability to control synoptic and meso-scale circulation patterns, which is lacking at present.

Direct interference with the vertical mixing process by mechanical means, i.e., the direct artificial production of significant turbulent energy, requires the expenditure of at least 10^8 cal cm sec^{-1} to add one-tenth of the natural turbulent energy production in the planetary boundary layer over an area 1 km on a side (assuming 100 percent efficiency in the expenditure). This is the equivalent to the energy of combustion of 10^{-2} tons of hydrocarbon per second. This energy input would have to be maintained over durations of the order of the storage-transformation ratios estimated in Section J.3.0, i.e., 10^3 — 10^4 sec.

J.4.2 Indirect Interferences

J.4.2.1 Modification of the Stability of the Boundary Layer

Qualitatively, the stability may be represented by the vertical difference in temperature between the bottom and top of the layer considered. The stability may be increased by decreasing the temperature of the lower boundary relative to the temperature at the top of the layer of interest. An increase in stability would result in smaller values of both lower boundary stress and internal eddy viscosity in the absence of other changes. The stability undergoes large diurnal changes over land surfaces, which are accompanied by large-amplitude diurnal variations in boundary layer wind. Over water, because of the character of the underlying layer, diurnal variations in stability are normally much smaller, as are, presumably, diurnal variations in boundary layer wind, though this last effect is not as clearly noted in the literature.

The feasibility of duplicating these naturally observed variations by interference with the thermal exchange budget at the lower boundary is a potentially fruitful area of investigation. This indirect modification procedure might allow significant modification of the energy storage without comparable expenditures of energy.

The largest components in the heat budget of the lower boundary are the radiative exchanges between the interface and the sun, and the interface and upper atmospheric layers (including clouds). Smaller, but considerable, transfers of sensible and latent heat within the lowest atmospheric layers play a role, and these are, to some extent, directly related to the eddy viscosity, and the stability itself. Heat transfer downward from the interface to the underlying material plays a minor role for the land-air interface, and a more significant role for the water-air interface.

Some idea of the differences that might be produced by changing the albedo, emissivity, and moisture of a land surface may be obtained from the report of Estoque and Yee [1[illegible]]. The model integrated by Estoque and Yee was homogeneous in the horizontal. In order to estimate the changes required to alter the characteristics of the boundary layer winds in a more realistic model, the storage-transformation ratios obtained in Section J.3.0 may be used in conjunction with mean wind speed estimates. These indicate that for wind speeds of tens of meters per second, the surface characteristics would have to be changed over upwind fetches of 1–10 km if modification up to levels of 50 m is desired, and over fetches of a few tens to a few hundred km if modification up to gradient levels is desired.

These surface-radiational property changes, if temporary, would have to be maintained for a few hours. Some permanent changes have been investigated in connection with small area modification of precipitation, and cost estimates for permanent blacktopping are given by Black and Tarmy [14] as $48,000 per square kilometer.

J.4.2.2 Modification of Sea Surface Characteristics

The energy budget estimates in Fig. J-2(b) show that the lower boundary transfer rate may become considerable over water surfaces. Modification of the sea state by procedures like those suggested in Appendix I [13] would certainly

result in some modification of the low-level wind profile (up to 10–100 m). A more precise assessment of the amount of modification cannot be made until more precise evaluations of natural transfer rates and the differences between them are available.

J.4.3 Survey of Simulative and Predictive Capabilities

J.4.3.1 Theoretical

The theory of planetary boundary layer winds has developed from the wind-drift ocean current theory of Ekman which was applied to the problem of the atmospheric boundary-layer winds by Akerblom. This theory formulated the turbulent viscous forces in terms of an eddy viscosity coefficient, and then proceeded to derive a solution for the vector wind profile in the steady state, for eddy viscosity, geostrophic wind, and density, all constant with height. Similar solutions were obtained [16] for different lower boundary conditions on the velocity, corresponding to flow over the sea surface.

The resulting solutions were sufficiently realistic to encourage a series of studies of steady-state profiles for more complicated eddy-viscosity height relationships [17], [18], [19], and more recently for a boundary layer in which the geostrophic wind varies with height [12]. Time periodic solutions for the boundary layer wind have been obtained by Ooyama [1] for prescribed eddy viscosity-height-time relationships. These solutions appeared to describe satisfactorily diurnal wind velocity variations.

Time varying solutions for boundary layer winds have been obtained by Estoque [20], for prescribed eddy viscosity - stability - wind shear relationships, thus allowing feedback between the eddy mixing process and the pertinent gradients. For time-constant overlying flow and horizontally homogeneous conditions, very realistic diurnal variations of wind and temperature are exhibited in the solutions. Further development of the model allowed explicit inclusion of thermal exchange processes at the lower boundary [21], and tested the effects of different thermal properties of the lower boundary on boundary layer winds [15]. Similar models designed for applications in short-period forecasting are being studied at The Travelers Research Center, Inc. [18], which include greater

refinement in the modelling of turbulent exchange and thermal heat budget at the surface, and the inclusion of horizontal variations.

Theoretical models of sea breeze circulations have gone through similar stages of development. From steady-state linear theories [22], through time dependent linear models [23, 24], to the non-linear models of Estoque [25], and Fisher [26]. These latest might be considered special cases of the generalized boundary layer models described above, for extreme horizontal variation in the lower boundary conditions.

J.4.3.2 Experimental

Although successful laboratory models have been developed for general circulation studies, and at the other end of the scale for flow around buildings, there appears to be no work in modelling boundary layer flow on the intermediate scales considered in this survey.

J.4.4 Research Required for Further Control or Modification Feasibility Assessment

J.4.4.1 Theoretical

The adequacy of the mixing length concepts underlying the basic formulation given by Eq. (J-2) has been questioned in a recent survey of the subject of atmospheric turbulence [27]. This indicates the ever-present need for alternative concepts in the development of physical models of atmospheric flows.

However, a comprehensive review of present efforts points to a fruitful area of study in the refinement of available non-linear models and their exploitation in determining magnitudes of the important energy transformations, and, furthermore, in preliminary testing of suggested modification procedures on a computer, rather than in the atmosphere. Unfortunately, no alternative physical-mathematical theory has been carried to the point of even crudely simulating or predicting the behavior of the atmosphere, as observable at the present time, on the scales of observation here considered.

J.4.4.2 Observational

Commensurate observational efforts are required to provide tests of physical-mathematical model behavior in the absence of modification procedures.

Particular emphasis on boundary layer wind structure over the open oceans is desirable, as well as further studies of topographic meso-scale wind systems.

J.5.0 REFERENCES

1. Blackadar, A., K. Buajitti, H. Newstein, and K. Ooyama, "Studies of the Wind Structure in the Lower Atmosphere," Final Rpt., Contract AF 19(604)-1368, New York Univ. Coll. of Eng., Res. Div., Dept. of Meteorol. and Oceanogr., 1957.

2. Berry, F. A., E. Bollay, and N. Beers, Handbook of Meteorology, 1068 pp., New York: McGraw-Hill, 1945.

3. Swinbank, W. C., "An Experimental Study of Eddy Transports in the Lower Atmosphere," Div. of Meteorol. Phys., Tech. Paper 2, CSIRO, Melbourne, Austl., 1955.

4. Gerhardt, J. R., "An Example of a Nocturnal, Low Level Jet Stream," J. Atmos. Sci. 19, 116–118, 1962.

5. Kinsman, B., "Surface Waves at Short Fetch and Low Wind Speed - A Field Study," Tech. Rpt. 19, Chesapeak Bay Institute, Johns Hopkins Univ., 1960.

6. Brocks, K., "Ein Neues Gerät Für Störungsfreie Meteorologische Messungen Auf Dem Meer," Arch. Meteorol. Geophys., and Bioklim, Ser. A., Band 11, 227–239, 1959.

7. Lettau, H. H., and B. Davidson. Exploring the Atmosphere's First Mile, New York: Pergamon Press, 2 Vol., 1957.

8. Prandtl, L., "Meteorologische Anwendung der Stromungslehre," Beitr. Phys. fr. Atm., Bjerknes-Festschrift, p. 188, 1932.

9. Monin, A. S., "The Structure of Atmospheric Turbulence," Theory of Probability and its Applications 3, 266–396, 1958

10. Priestley, C. H. B., "Convection from a Large Horizontal Surface," Austral. J. Phys. 7, 176–201, 1954.

11. Sutton, O. G., Micrometeorology, 333 pp., New York. McGraw-Hill, 1953.

12. Blackadar, A. K., "The Vertical Distribution of Wind in a Baroclinic Adiabatic Atmospheric Boundary Layer," Paper presented at the 211th National Meeting of the AMS, 1963.

13. Brooks, D. L., and G. Hilst, "Geophysical Factors in Naval Warfare," 7662-102, The Travelers Research Center, Inc., Hartford, 1963.

14. Black, J. F., and B. Tarmy, "The Use of Asphalt Coatings to Increase Rainfall," J. Appl. Meteorol. 2, 557–564, 1963.

15. Estoque, M., and W. Yee, "Air-Earth Interface Characteristics and the Atmospheric Boundary Layer," Sci. Rpt. 3, Contract AF 19(604)-7484, Univ. of Hawaii, Hawaii Inst. of Geophys., Meteorol. Div., 1963.

16. Bjerknes, V., T. Bjerknes, J. Solberg, and T. Bergeron, Physikalische Hydrodynamik, 797 pp., Berlin: J. Springer, 1963.

17. Blackadar, A. K., "The Vertical Distribution of Wind and Turbulent Exchange in a Neutral Atmosphere," J. Geophys. Res. 67, 3095–3101, 1962.

18. Pandolfo, J., D. Cooley, and E. Newburg, "Preliminary Investigations of Numerical Models for the Short-Period Prediction of Wind, Temperature, and Moisture in the Atmospheric Boundary Layer," 7047-30, The Travelers Research Center, Inc., Hartford, 1963.

19. Rossby, C. G., and R. Montgomery, "The Layer of Frictional Influence in Wind and Ocean Currents," Papers Phys. Oceanogr. Meteorol., M.I.T. and Woods Hole Oceanogr. Inst., 3:3, 101 pp., 1935.

20. Estoque, M., "A Preliminary Report on a Boundary Layer Numerical Experiment," GRD Res. Notes, AFCRC (ARDC) 20, 1959.

21. —, M., "A Numerical Model of the Atmospheric Boundary Layer," J. Geophys. Res. 68, 1103–1113, 1963.

22. Jeffreys, H., "On the Dynamics of Wind," Quart. J. Roy. Meteorol. Soc. 48, 29–47, 1922.

23. Pierson, W. J., "The Effects of Eddy Viscosity, Coriolis Deflection, and Temperature Fluctuation on the Sea Breeze as a Function of Time and Height," Meteorol. Paper, New York Univ. Coll. of Eng., Vol. 1, No. 2, 1950.

24. Haurwitz, B., "A Linear Sea Breeze Model," Quart. Prog. Rpt. No. 3, Contract DA 36-039-Sc-78091, New York Univ. Coll. of Eng., Res. Div., 1959.

25. Estoque, M., "A Theoretical Investigation of the Sea Breeze," Proc. Int. Symp. Num. Weath. Pred. in Tokyo, pp. 523–534, 1960.

26. Fisher, E. L., "Further Studies of Theoretical Sea-Breeze Models," Final Rpt., Contract DA-36-039-Sc-84939, New York Univ. Coll. of Eng., Res. Div., 1961.

27. Malkus, W. V. R., "Atmospheric Turbulence," Trans. A.G.U. 44, 378–379, 1963.

APPENDIX K. ATMOSPHERIC TURBULENCE*

K.1.0 GENERAL DESCRIPTION

K.1.1 Introduction: Atmospheric Turbulence in Relation to Structural Damage

One of the outstanding characteristics of atmospheric turbulence is the extremely wide range of eddy sizes from sub-centimeter dimensions through nine orders of magnitude to the long waves of the general circulation (10^4 km). Within this range, certain groups of well-organized eddies have been identified and studied separately. Among these are the frontal and thunderstorm circulations, coastal, island, mountain, and valley wind systems, the cyclones and anticyclones of middle and high latitudes, and the long waves of the general circulation. Phenomena of this nature are excluded from the present discussion. Within the context of damage to structures by turbulence, the range of eddy sizes can be further restricted by taking into account the dimensions of the structure or vehicle of interest. However, this must be done with caution because of the cumulative effects due to repeated exposure to turbulent stresses. Thus the degree of damage sustained by a structure in strong mechanical turbulence (say of the order of 30 cycles per hour) may be related to the fact that the structure was subjected to a strong frontal gust 12 hr earlier and hence frequencies of the order of 0.1 cycles per hr are significant. The present study will be limited to turbulence frequencies of the order of 0.5 cycles hr^{-1} or more by setting aside the above consideration with the statement that the stress history of the structure or vehicle should be taken into account.

The principal dynamic effects of atmospheric turbulence on structures have been summarized by Davenport [1]. The pressure exerted by the wind on a structure is given approximately by $p = (C/2)\rho V^2$ where C is a shape coefficient, ρ is air density, and V is wind velocity. It will be seen that p depends on the shape and size of the structure and on the duration and magnitude of wind gusts. The damage due to wind pressure will depend on these factors and on the response characteristics of the structure. Structural vibrations may be either self-excited or forced and can be particularly serious if resonance occurs. Examples of self-induced

*By Keith D. Hage.

pressure forces are (a) those which result when the structure moves in response to the wind in such a way as to increase the pressure, and (b) the crosswind pressure forces that occur when air flows around an elongated structure. The spectrum of turbulence is of fundamental importance since it describes the linkage between wind variability and the response function of individual structures.

K.1.2 Types

K.1.2.1 Mechanical Turbulence

The energy of the turbulence is derived from the kinetic energy of the mean flow, and a net transfer of energy from small to large wave numbers takes place through the action of non-linear inertia forces. The energy is ultimately transformed to heat by viscous dissipation at very large wave numbers.

K.1.2.2 Thermal Turbulence

The energy of the turbulence is derived from the release of potential energy by the action of buoyancy forces. The energy at a given wave number of the vertical component can be transferred to other wave numbers by inertial forces or distributed to the horizontal components by pressure forces.

K.1.3 Characteristic Geographical Extent

Mechanical turbulence is most common in the lowest 1000 m of the atmosphere but may occur in association with shear zones at any height in the troposphere and lower stratosphere. Areas of strong vertical wind shear in the boundary layer have characteristic dimensions of the order of the dimensions of cyclones and anticyclones (10^3 km). Above the boundary layer, the shear zones and areas of mechanical turbulence are frequently elongated, with longest dimensions of the order of 10^2–10^3 km and shortest dimensions of the order of 10^{-1}–10^2 km.

The spatial extent of thermal turbulence is similar to that of mechanical turbulence except in the vertical. The characteristic vertical extent of thermal turbulence varies with latitude and from land to sea, but is probably of the order of half the depth of the troposphere.

K.1.4 Characteristic Process and Property Involvement

The characteristic physical processes directly involved in atmospheric turbulence are the horizontal and vertical transport and eddy diffusion of momentum,

kinetic energy, and heat. The magnitudes of these processes are strongly influenced by the environmental properties of roughness, shear of the mean wind, lapse rate, and moisture if condensation takes place. In the lowest several hundred meters of the atmosphere, the scale and energy of the vertical component of turbulence are controlled by height above the surface for specified conditions of roughness, stability, and wind speed. The wave number (n) of maximum energy at height Z is specified rather well by $n = 0.2\, z^{-1}$ on the basis of empirical spectra measured over a variety of uncomplicated terrain (Panofsky and Deland, [2]).

K.2.0 ASSESSMENT OF GEOPHYSICAL FORCES

In their simplest form for an incompressible inhomogeneous fluid the Eulerian equations of motion take the form

$$\dot{\vec{V}} = \frac{\partial \vec{V}}{\partial t} + \vec{V}.\nabla\vec{V} = -\nabla\phi - \alpha\nabla p + \alpha\mu\nabla^2\vec{V} \tag{K-1}$$

where $\vec{V}$ is the fluid velocity vector, ϕ is the gravitational potential, α is specific volume, p is pressure and μ is the coefficient of molecular viscosity. The effect of the earth's rotation has been neglected in Eq. (K-1) because of scale limitations imposed previously. The viscosity has been assumed to be constant. The equation of continuity takes the form

$$\nabla.\vec{V} = 0 \tag{K-2}$$

For air of constant composition with no liquid or solid content the equation of state is $p\alpha = RT$ where T is temperature and R is the appropriate gas constant. The thermodynamical energy equation takes the form

$$\dot{Q} = CpT\,\frac{\dot{\theta}}{\theta} - \alpha\delta \tag{K-3}$$

where $\dot{Q}$ represents the rate of heat exchange per unit mass due to nonadiabatic processes, Cp is the specific heat at constant pressure, θ is potential temperature, and δ is the dissipation, equal and opposite to the internal work of friction. The dissipation is a function of the viscosity coefficient μ and the space derivatives of the velocity field. The six equations listed above represent a complete system for the evaluation of the unknown dependent variables $\vec{V}$, α, p, and T. No solutions to these equations are known except in one or two severely restricted cases of homogeneous turbulence, for which linearization is valid because the turbulent velocities are relatively small, or because the time interval between the disturbance and the time of the solution is so short that inertial effects can be neglected (Batchelor, [3]). A model for the study of the non-linear properties of time-dependent convection processes has been proposed by Saltzman [4].

In order to discuss the forces involved in turbulent motion, it is useful to consider the equation of motion for the vertical component w,

$$\frac{\partial w}{\partial t} + u\,\frac{\partial w}{\partial x} + v\,\frac{\partial w}{\partial y} + w\,\frac{\partial w}{\partial z} = -\alpha\,\frac{\partial p}{\partial z} - g - \alpha\mu\left(\frac{\partial^2 w}{\partial x^2} + \frac{\partial^2 w}{\partial y^2} + \frac{\partial^2 w}{\partial z^2}\right) \tag{K-4}$$

Local vertical accelerations are seen to be the result of the interaction of inertia forces, pressure gradient forces, buoyancy forces, and viscous forces. If U and L are characteristic velocity and length parameters, the ratio of the inertia forces to the viscous force is the Reynolds number Re where

$$Re = \frac{U^2/L}{\alpha\mu \, U/L^2} = \frac{UL}{\mu\alpha} \tag{K-5}$$

If T is a characteristic environmental temperature, and ΔT is a characteristic temperature fluctuation, the buoyancy force is of the order $\frac{g\Delta T}{T}$. The ratio of buoyancy forces to viscous forces is of the order

$$\frac{\Delta T g L^2}{T\alpha\mu U} = \frac{Gr}{Re} \tag{K-6}$$

where Gr is the non-dimensional Grashof number $G_r = \frac{\Delta T g L^3}{\alpha^2\mu^2 T}$. The Grashof number itself represents the ratio of inertia to buoyancy forces.

If the governing equations are written in smoothed form where smoothing is performed over a fluid mass or fluid volume, additional terms appear as a result of nonlinear interactions between the fluctuating components of the dependent variables. In particular, in the equations of motion, the inertia terms yield new quantities capable of transporting momentum in the fluid. These terms are called Reynolds stresses and are formally analogous to the viscous stress terms. In almost all atmospheric applications, the Reynolds stresses greatly exceed the viscous stresses in magnitude, and as a result the Reynolds number as defined in Eq. (K-5) greatly exceeds unity. For order of magnitude estimates of eddy forces, it is useful to introduce the exchange-coefficient hypothesis which postulates that terms of the form $-\rho \overline{X^I u^I}$ representing the eddy transfer of X can be written as the product of an exchange coefficient A and the gradient of $\bar{X}$. If on the basis of empirical findings we neglect viscous transport compared with eddy transport, the previous estimates of the relative importance of viscous, buoyancy, and inertia forces can be adapted to problems in the atmosphere by replacing μ with A in all equations. In fully developed turbulent flow in air layers near the earth's surface, the eddy exchange coefficient for momentum $K_m = A\alpha$

is commonly of the order of 10^3–10^5 cm^2 sec^{-1}, in contrast to a value of 10^{-1} cm^2 sec^{-1} for the kinematic viscosity $2 = \mu\alpha$ (Sutton, [5]).

K.3.0 ASSESSMENT OF GEOPHYSICAL ENERGIES

K.3.1 The Energy Budget

The production and flow of turbulent energy has been described by Stewart [6], who derived the equations below for atmospheric shear flow near the earth's surface. In these equations the x axis is taken in the direction of the mean flow U, and the z axis is vertical. Terms involving redistribution of the fluctuating quantities in space and triple products of velocity fluctuations, specific volume fluctuations, and pressure gradient fluctuations have been neglected. The equations are

$$\frac{-\partial \overline{w^2}}{\partial t} = 2\bar{\alpha}\ \overline{u\frac{\partial p}{\partial x}} + 2\overline{uw}\ \frac{dU}{dz} + M \tag{K-7}$$

$$\frac{-\partial \overline{v^2}}{\partial t} = 2\bar{\alpha}\ \overline{v\frac{\partial p}{\partial y}} + M \tag{K-8}$$

$$\frac{-\partial \overline{w^2}}{\partial t} = 2\bar{\alpha}\ \overline{w\frac{\partial p}{\partial z}} + \frac{2}{\bar{\alpha}}\, g\ \overline{\alpha w} + M \tag{K-9}$$

$$\frac{-\partial \overline{uw}}{\partial t} = \bar{\alpha}\ \left(u\overline{\partial p} + w\frac{\overline{\partial p}}{\partial z} \right) + \frac{g}{\bar{\alpha}}\,\overline{\alpha u} + \overline{w^2}\ \frac{du}{dz} + M \tag{K-10}$$

$$\frac{-\partial \overline{\alpha w}}{\partial t} = \bar{\alpha}\ \frac{\overline{\alpha \partial p}}{\partial z} + \frac{g}{z}\ \overline{\alpha^2} + \overline{w^2}\ \frac{d\bar{\alpha}}{dz} + M \tag{K-11}$$

$$\frac{-\partial \overline{\alpha^2}}{\partial t} = \alpha w\ \frac{d\bar{\alpha}}{dz} + M \tag{K-12}$$

Following Stewart, the effects of wind shear can be described as follows: the existence of $\overline{w^2}$ in a shear flow leads to the production of $\overline{uw}$ which in turn permits the production of $\overline{u^2}$ from the mean flow. In the absence of buoyancy forces suppression of $\overline{w^2}$ will destroy all turbulence. Terms involving the pressure gradient serve to distribute the turbulent energy among the three components. The production of turbulent energy by buoyancy forces occurs only in the $\overline{w^2}$ equation. In the three energy balance equations, the molecular terms M represent energy sinks due to viscosity. The flux Richardson number R_f, equal to

$$R_f = \frac{g/\bar{\alpha}\ \overline{\alpha w}}{\overline{uw}\ du/dz}, \tag{K-13}$$

provides a measure of the relative importance of the production of turbulent

energy by buoyancy forces to that produced by the mean flow. In terms of the exchange coefficient hypothesis

$$
\begin{aligned}
-\overline{uw} &= K_M \, du/dz \\
-\overline{\alpha w} &= K_H \, d\overline{\alpha}/dz
\end{aligned}
\tag{K-14}
$$

where K_H is the eddy exchange coefficient for heat Substituting Eq. (K-14) in Eq. (K-13)

$$
\begin{aligned}
R_f &= \frac{g \, \overline{\alpha} \, d\overline{\alpha}/dz}{(du/dz)^2} \; \frac{K_H}{K_M} \\
&= R_i \; \frac{K_H}{K_M}
\end{aligned}
\tag{K-15}
$$

where R_i is the gradient Richardson number (Priestley, [7], p. 9).

The energy balance equation for the total energy of the turbulence can be obtained by summing Eqs. (K-7), (K-8), and (K-9). By introducing certain hypotheses about the decay rate of turbulent energy, Ellison [8] and Townsend [9] were able to derive expressions for K_H/K_M which provide insight on the critical value of the Richardson number. Ellison's equation took the following form:

$$
\frac{\overline{u^2} + \overline{v^2} + \overline{w^2}}{2T} + \overline{uw} \, \frac{du}{dz} + \overline{w\rho} g = 0 \tag{K-16}
$$

where $1/T$ is the rate of decay of turbulent energy in the absence of production terms. Although Eq. (K-16) provides a basis for a schematic energy budget diagram (Fig. K-1), meaningful numerical estimates of each component will require improved theoretical knowledge of the quantities T, $\overline{uw}$, and $\overline{w\rho}$.

K.3.2 Instabilities

The principal critical point in atmospheric turbulence may be approximately described as the point at which the production of turbulent energy from the mean flow just balances the consumption of turbulent energy by buoyancy and viscous forces. Although many studies of the stability of motion in the presence of a density gradient have been carried out, considerable uncertainty remains. The work of Townsend [9] leads to a critical value of 0.5 for the flux Richardson

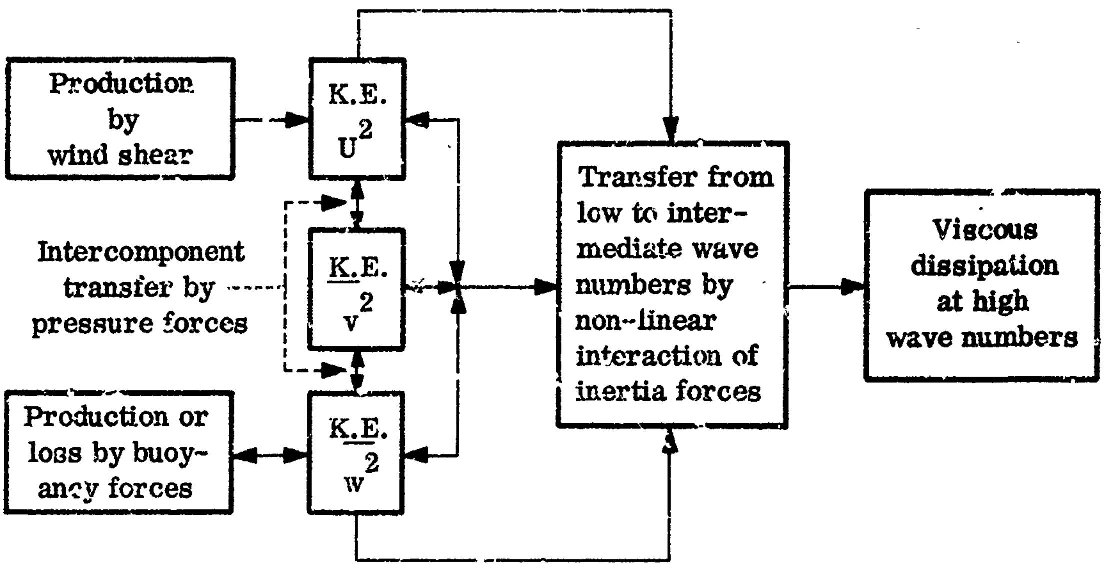

Fig. K-1. Schematic energy budget.

number, while that of Ellison [8] leads to a value of about 0.15. These relatively low values are attributed to the fact that on the average only about 1/6 of the turbulent energy is contained in the vertical component which is the only component directly affected by buoyancy forces [6]. The problem is complicated by the presence of internal gravity waves at large stabilities Batchelor [10].

Experimental measurements of the critical flux Richardson number are not sufficiently precise to check the preceding theoretical predictions. It is possible that some of the observed variations are due to differences in the nature of the surface (Sutton [5]).

K.4.0 MODIFICATION OR CONTROL FEASIBILITY

K.4.1 Suppression of Turbulent Energy

The primary sources of turbulent energy are known to be the kinetic energy of the mean wind and the potential energy released by buoyancy forces. In the context of damage to structures, the atmosphere must be treated as an open system and hence suppression of the mean wind or suppression of buoyancy forces will involve medium- to large-scale weather modification. This is probably the least feasible possibility at the present time.

Since $\overline{w^2}$ normally represents only about 1/6 of the total turbulent energy and yet is essential to the production of turbulent energy in all components either from the mean wind or from buoyancy effects, it would appear reasonable to concentrate on the suppression of this component. Unfortunately, the presence of the structure itself either through its action as a mechanical obstruction or through its action as a heat source tends to enhance $\overline{w^2}$. Such modification does not appear to be feasible except perhaps in limited special cases.

K.4.2 Spectrum Modification

Modification or control possibilities may be approached in two ways through spectrum modification.

(a) Alter the turbulence spectrum in such a way that the pressure forces are minimized for a given structure response function.

(b) Design the structure so that its response function minimizes pressure forces in natural turbulence.

Within the present state of the art, it is not possible to provide a firm estimate of the feasibility of (a) since the relationships between the spectrum of turbulence and parameters such as the size and spacing of structures, structure shape, and the thermal properties of structures are not sufficiently well known. That significant relationships of this nature exist is evident from a comparison of continuous wind records near structures with those at a distance.

Method (b) has been used extensively by aeronautical engineers, but applications to other structures such as bridges, masts, towers, and buildings have lagged.

K.4.3 Research Required for Further Control or Modification Feasibility Assessment

Feasibility assessments would be greatly improved by research leading to parameterization of the turbulent transfer of heat and momentum in terms of the size, shape, spacing and thermal properties of typical flow obstructions. Such information would make possible quantitative estimates of energy transfer and transformation rates and, through numerical or truncated Fourier series solutions to the governing equations, would yield estimates of the spectrum of turbulence for selected structure configurations.

K.5.0 REFERENCES

1. Davenport, A. G., Wind Loads on Structures, Tech. Paper 88, 60 pp., Div. Bldg. Res., National Research Council, Ottawa, 1960.

2. Panofsky, H. A., and R. J. Deland, "One Dimensional Spectra of Atmospheric Turbulence in the Lowest 100 Meters," Advances in Geophys. 6, 41–62, New York: Academic Press, 1959.

3. Batchelor, G. K., "The Theory of Homogeneous Turbulence," 197 pp., Cambridge: The University Press, 1953.

4. Saltzman, B., "A Simplified Model for Studying the Evolution of Finite-Amplitude Convection" 7072-23, pp. 241–250, Aviation Terminal Weather Prediction, The Travelers Research Center, Inc., Hartford, 1962.

5. Sutton, O. G., Micrometeorology 333 pp., New York: McGraw-Hill, 1953.

6. Stewart, R. W., "The Problem of Diffusion in a Stratified Fluid," Advances in Geophys. 6, 303–310, New York: Academic Press, 1959.

7. Priestley, C. H. B., "Turbulent Transfer in the Lower Atmosphere," 130 pp., The University of Chicago Press, 1959.

8. Ellison, T. H., "Turbulent Transport of Heat and Momentum from an Infinite Rough Plane," J. Fluid Mech. 5, p. 456, 1957.

9. Townsend, A. A., "Turbulent Flow in a Stably Stratified Atmosphere," J. Fluid Mech. 5, p. 361, 1958.

10. Batchelor, G. K., "Reflections on Theoretical Problems," Advances in Geophys. 6, 449–452, New York: Academic Press, 1959.

APPENDIX L. CHEMILUMINESCENT REACTIONS IN THE UPPER ATMOSPHERE*

L.1.0 INTRODUCTION

A large reservoir of monatomic oxygen is known to exist at altitudes above about 100 km. Suitable light-emitting reactions using this reservoir might produce significant illumination of the night sky. A promising reaction has been proposed by Harteck and Reeves [1], and used successfully [2, 3] to measure wind properties at these altitudes with small amounts of material. Rough estimates of the amount of material needed to produce significant illumination over sizable areas are to be given in this appendix.

*By Joseph P. Pandolfo.

L.2.0 THE REACTIONS

The general reaction used is the two body reaction*,

$$A + 0 \rightarrow A0^*$$

$$A0^* \rightarrow A0 + h\nu$$

where A is a metallic element. The emitted quantum will be in the form of visible light if the metallic oxide has a dissociation potential in the range of about 3—4 eV at upper atmospheric temperature and pressure.

The reaction proposed in [1] would utilize aluminum as the metallic element. The dissociation energy of Al0 is approximately 3.75 eV, which would give a spectrum peaked at a wave-length of 5000 A with significant emission between about 3800 A and 7000 A. This would lie almost entirely in the visible and near-infrared positions of the electromagnetic spectrum. Furthermore, Harteck and Reeves [1] point out the possibility of cyclical reactions involving aluminum which would increase the total quantum yield per molecule of material used. The reaction suggested would be

1) $Al + 0 \rightarrow Al0 + h\nu$,

then either;

2a) $Al0 + 0 \rightarrow Al + 0_2$

and repetition of 1) until 0 atoms are exhausted, or,

2b) $Al0 + 0 \rightarrow Al0_2 + h\nu$

or possibly,

---

*A theoretical objection to the reaction given is that quantum-mechanical theory requires the presence of a third particle for the reaction to proceed, i.e ,

$$A + 0 + X \rightarrow A0^* + X, \qquad A0^* \rightarrow A0 + h\nu$$

The most probable number of three body collisions (per particle per sec) at a pressure of 10^{-6} atmospheres is of order 5×10^{-7} to 5×10^{-6}. On the other hand, the number of two body collisions is of order 5×10^3 per particle per sec. The results reported in [2] and [3] indicate that the reaction that took place must have involved two particles only, based on the ratio of energy released to material used.

2c) $AlO_2 + O \rightarrow AlO + O_2$

and repetition of 2b) until O atoms are exhausted.

The chain reactions proceeding through 2a) and 2c) would give a longer duration of illuminated sky. If 2c) does not occur under the environmental conditions encountered, the duration of illuminated sky would depend on the relative reaction rates of 2a) and 2b).

For several reasons it is suggested [1] that the metal be introduced into the higher atmosphere in the form of metal-organic compounds, or volatile inorganic compounds. The yield of metallic ions by evaporation from a volatile compound is generally much greater than by evaporation from the bulk metal itself. The experiments reported in [2] and [3] used a small amount of trimethyl aluminum (TMA) as the source of aluminum atoms. This compound has several desirable properties, being an inexpensive volatile liquid which dissociates readily, once vaporized. In [3] it was estimated that about 40% vapor and 60% solid would have been produced upon release from a container at the pre-launch temperature.

L.3.0 THE MONATOMIC OXYGEN RESERVOIR

Assuming an unlimited source of aluminum atoms, the maximum light energy attainable is determined by the amount of monatomic oxygen available in the region of release. An estimate of the reservoir may be obtained by the following calculations.

At 10^{-6} atmospheres, the particle density is about 2.5×10^{13} particles cm^{-3}.

A conservative estimate is that under night-time conditions, 20 per cent of these are oxygen atoms giving a montomic oxygen density of

5×10^{12} atoms cm^{-3}.

For a layer 10 km deep the number of atoms in a unit cross section would then be 5×10^{18} atoms cm^{-2}.

If TMA is the source material for aluminum, the preliminary reaction

$$Al\,[CH_3]_3 \rightarrow Al + 3CO + 4\text{-}1/2\ H_2O$$

must take place for each aluminum atom supplied to the reactions 1) to 2). This means that for each quantum released in reaction 1), 8-1/2 [0] are used; and for each quantum released in reaction 2b), 9-1/2 [0] are needed. Therefore, less than 10 [0] atoms are needed per quantum of light emitted. Assuming sufficient aluminum, the total number of quanta emitted per unit cross section of sky would be of the order of but greater than

$$5 \times 10^{17}\ h\nu\ cm^{-2}.$$

This is the equivalent of about 5 sec at sunlight intensity, or 10 hrs at 500 times full moon intensity from a unit radiating area.

L.4.0 ESTIMATE OF TMS AMOUNTS REQUIRED

The number N of aluminum atoms required at an altitude of 100-120 km to produce P quanta sec^{-1} cm^{-2} from an area of sky L on a side may be estimated as

$$N = 10^{10} P \tau L^2,$$

where τ is the mean interval between light emissions (sec per quantum). τ depends on the rate constant for the light-emitting reaction, and may be roughly estimated at 10^2 sec quantum from the qualitative results reported by Rosenberg et al. [2].

With this estimate for τ, the number of aluminum atoms required to yield 10^{12} quanta per cm^2 sec (i.e., 10 times full moon intensity) from an area of sky 100 km on a side would be

$$N = 10^{28} \text{ Al atoms.}$$

7.2 tons of TMA would contain 6 times this number of aluminum atoms.

L.5.0 FURTHER RESEARCH REQUIRED

The duration of illuminated sky cannot be predicted until more is known about the relative reaction rates of 2a), 2b), and 2c), and the effective rate of the combined reactions at 120 km environmental temperatures and pressures. For example, the reaction 2c) will only occur if the dissociation energy used in the conversion

$$AlO_2 \longrightarrow AlO + O$$

is less than the recombination energy given off by the reaction

$$O + O \longrightarrow O_2\text{, i.e., 117 k cal per gm mol wt.}$$

This is unknown as yet.

If the reaction proceeded directly from 1) to 2b), the illumination produced in the numerical example given above and at the reaction rate quoted would persist for a duration of the order of 100 sec, at a conservative estimate. If either of the cyclical reactions 2a) or 2c) occur to any significant extent, the duration would increase from this minimum to an easily conceivable upper limit of several hours. The dispersal of 10^{-4} times the amount of material quoted in our example over an effective area 5 km on a side produced a photographable cloud at 700 sec after release [3].

L.6.0 ACKNOWLEDGEMENTS

Consultant for this appendix was Professor P. Harteck of Rensselaer Polytechnic Institute, Troy, New York.

L.7.0 REFERENCES

1. Harteck, P. and R. R. Reeves, "Chemiluminescent Reactions of Major Importance for the Upper Atmosphere," Bull. Soc. Chim. Belg., 682-687, 1962.

2. Rosenberg, N. W., D. Golomb, and E. F. Allen, "Chemiluminescent Techniques for Studying Nighttime Winds in the Upper Atmosphere," J. Geophys. Res. 68, 3328-3330, 1963.

3. —, —, —, "Chemiluminescence of Trimethyl Aluminum Released into the Upper Atmosphere," J. Geophys. Res. 68, 5895-5898, 1963.

M.2.2 Factors Influencing Refraction

For moist air the index of refraction n, for wavelengths greater than 2 cm, is given by Batton [1]:

$$(n-1)\,10^6 = N = \frac{79}{T}\left(p - \frac{e}{7} + \frac{4800\,C}{T}\right). \qquad \text{(M–12)}$$

Here p is the atmospheric pressure in millibars, e is the vapor pressure in millibars, and T is the temperature in degrees absolute. Near the earth 's surface, a typical value for n is about 1.0003, and in a standard atmosphere

$$\frac{dn}{dh} \approx -4 \times 10^{-8}\ m^{-1}. \qquad \text{(M–13)}$$

Denoting the angle to the local horizon by ϕ, Appleton [10] has shown that

$$\frac{\phi^2}{2} - \frac{\phi_0^{\ 2}}{2} = \left(\frac{h}{R} + n\right) - \left(\frac{h_0}{R} + n_0\right) = (M - M_0)\,10^6 . \qquad \text{(M–14)}$$

Here ϕ_0 is the angle of the transmitted signal to the local horizon at the source (i.e., at the radar) at a height h_0, and ϕ is the angle the beam makes with the horizon when at a height h above the ground. The quantity $M = [\frac{h}{R} + (n - 1)]\,10^6$, where R is the radius of the earth, is called the modified index of refraction. The path followed by a given beam depends upon the variation of M with height through Eq. (M–14). A concave bending of the beam will occur for $M<M_0$, as in this case ϕ will be less than ϕ_0. In these cases, rays starting out at sufficiently small angles to the horizon will be bent back down to the earth. In such a case, part of the waves are trapped and a duct is said to exist. Within the confines of a ducting layer, the radio waves are stronger than in adjacent regions.

For any given distribution of M with height, there exists a maximum value of ϕ_0 for which trapping may occur. This is obtained by setting $\phi = 0$ in Eq. (M–14), giving

$$(\phi_0)_{max} = [2(M_0 - M_{min})10^{-6}]^{1/2} \qquad \text{(M-15)}$$

A typical value of $(\phi_0)_{max}$ is approximately 0.2°.

Ducts are most commonly produced by the following meteorological conditions:

depending upon the size of the particles and the wavelengths being considered, be small-particle Rayleigh scattering, or large-particle Mie scattering. Certain combinations of particle size and wavelength are possible (and indeed quite common) such as to throw that portion of the scattering into the realm of geometrical optics. The scattering of visible and near infrared radiation by precipitation particles falls into this category. Special conditions giving rise to aurora and airglow within specific atmospheric layers result in spectral emissions negligible within the troposphere. Lightning flashes result in abnormal emissions within the troposphere. Absorption bands, particularly in the ultraviolet region, are present in the high atmosphere above about 20 km, but because of differences in the physical structure of the atmosphere, are absent in lower levels. Similarly, the behavior of microwaves and radio waves within or impinging upon the ionospheric regions is quite different from the behavior of waves propagating through lower levels.

It is therefore quite obvious that a discussion of the many and varied problems of electromagnetic propagation is a subject for a complete study in itself. For this reason the remainder of this report will be limited to certain aspects of microwave propagation through the troposphere. The geophysical phenomenon will be considered to be the atmospheric environment through which the waves are propagating.

M.1.1.5 Characteristic Geographical Extent

Microwaves are normally used over ranges from about 10–500 km Those environmental properties of importance, discussed in the next section, may extend over all or part of this distance.

M.1.2 Characteristic Process and Property Involvement

M.1.2.1 Emission

Emission of microwaves by the atmosphere is completely negligible, the source for such waves being man-made in all cases. Therefore, atmospheric factors effecting the emission of such waves will not be considered.

M.1.2.2 Absorption

Microwaves are absorbed principally by precipitation and cloud particles, water vapor, and oxygen The amount of absorption is temperature dependent as well as wavelength dependent. Further, the amount of absorption is strongly dependent upon the size distribution, number, and physical state (liquid or frozen) of cloud and precipitation particles.

M.1.2.3 Scattering

Other than refractive effects described below, cloud and precipitation particles are responsible for most microwave scattering. Heavy concentrations of atmospheric contaminants (such as in dust storms) may at times cause appreciable scattering.

M.1.2.4 Refraction

Molecular scattering by dry air and water vapor gives rise to refraction effects which may be of considerable importance in discussing the propagation of microwaves The amount of refractive bending is a function of atmospheric pressure, temperature, and water vapor content.

M.2.0 ASSESSMENT OF METEOROLOGICAL FACTORS

M.2.1 Factors Influencing Absorption and Scattering

Following Battan [1], the returned or back-scattered power, P_r, from a target at a distance r, is given to a high degree of approximation by

$$P_r = P_{ro} e^{-2\int_o^r K_T \, dr} \qquad \text{(M-1)}$$

where P_{ro} is the power which would be received in the absence of attenuation, and K_T is the total volume attenuation coefficient. For a given radar set, P_{ro} is a function of the range r, and the back-scattering or reflecting properties of the target. Target properties will not be considered here. Equation (M-1) may be re-written as

$$10 \log \frac{P_r}{P_{ro}} = -2 \times 4.343 \int_o^r K_T \, dr \; . \qquad \text{(M-2)}$$

The lefthand side of Eq. (M-2) expresses the reduction of P_r in decibels and the volume attenuation coefficient is expressed in decibels per unit length. The attenuation coefficient K_T may be written as

$$K_T = K_a + \sum_i n_i \, Q_{Ti} \qquad \text{(M-3)}$$

where K_a is the volume absorption coefficient of the active atmospheric gases (oxygen and water vapor), and n_i is the number of particles of radius i, and total attenuation cross-section Q_{Ti} is for a unit volume. The summation is carried out over a unit volume.

M.2.1.1 The K_a Term

Water vapor has a resonance absorption line centered at about $\lambda = 1.3$ cm. This line is considerably broadened at atmospheric pressures and, further, is temperature dependent. Oxygen has several lines which give rise to peak absorptions somewhat below $\lambda = 1$ cm, and which decrease rapidly at first, and then more slowly throughout the cm wavelength region. Theoretical studies of the attenuation coefficients by Van Vleck [2, 3] show that for T = 20°C,

$$K_T \text{ (oxygen)} \approx 0.02 \text{ db km}^{-1} \qquad \text{(M-4)}$$

as an average volue over the cm range. Attenuation by water vapor, besides being strongly wavelength dependent, varies with the water vapor content of the atmosphere. Values computed by Van Vleck [2, 3] for 7.5 gm m^{-3} of water vapor and T = 20°C are as follows:

$$\lambda = 1.3 \text{ cm}; \quad K_T \text{ (}H_2O\text{ vapor)} \approx 0.2 \text{ db km}^{-1}$$
$$\lambda = 2.0 \text{ cm}; \quad K_T \text{ (}H_2O\text{ vapor)} \approx 0.01 \text{ db km}^{-1} \qquad \text{(M-5)}$$
$$\lambda = 4.0 \text{ cm}; \quad K_T \text{ (}H_2O\text{ vapor)} \approx 0.001 \text{ db km}^{-1}$$

These values are somewhat temperature dependent. According to Ryde [4], they will be increased by about 60 percent at T = -40°C and decreased by about 12 percent at T = 40°C. These results indicate that, for most purposes, the effect of attenuation by atmospheric gases is negligible at wavelengths longer than about 2.0 cm. For this reason, most radar sets in operation today are at wavelengths 3.0 cm or greater.

M.2.?.2 The $\sum_i n_i Q_{Ti}$ Term

This term arises from the presence of cl[illegible] precipitation particles. As such, it is highly variable in both time and space. Assuming these particles to be spherical, Q_T may be computed from the Rayleigh or Mie scattering equations, depending upon the ratio of sphere circumference to wavelength of incident radiation. The results are dependent upon wavelength, drop radius (a), and the complex index of refraction which is itself a function of wavelength and temperature.

The total attenuation cross-section, Q_T is given by

$$Q_T = Q_A + Q_S \qquad \text{(M-6)}$$

where Q_A and Q_S are the absorption and scattering cross-sections, respectively For values of α (= $\frac{2\pi a}{\lambda}$) less than about 0.3, the Rayleigh laws hold to a high degree of approximation, and

$$Q_S = \frac{128}{3} \frac{\pi^5 a^6}{\lambda^4} \left| \frac{m^2 - 1}{m^2 + 2} \right|^2 \qquad \text{(M-7)}$$

and

$$Q_A = \frac{8\pi^2 a^3}{\lambda} \; I_m \left(- \frac{m^2 - 1}{m^2 + 2} \right) \tag{M-8}$$

where m is the complex index of refraction of the particle. Over the microwave region cloud particles and most precipitation particles are small enough for these formulas to apply. Further, it has been demonstrated by Atlas, Kerker, and Hitschfeld [5] that the shape factor for small frozen particles is relatively unimportant and therefore Eqs. (M–7) and (M–8) are reasonably accurate. For larger particles, the more complex Mie equations must be used. These equations are functions of the same variables that appear in Eqs. (M–7) and (M–8), but the dependencies are much more complex.

It is evident from these equations that for $\alpha << 1$, $Q_A >> Q_S$. This condition is met for cloud droplets, and

$$Q_T \approx Q_A \tag{M-9}$$

Therefore,

$$\sum_i n_i \; Q_{Ti} \approx \left[\frac{6\pi}{\rho\lambda} \; I_m \left(- \frac{m^2 - 1}{m^2 + 2} \right) \right] \; M \tag{M-10}$$

where $M = \frac{4}{3} \pi \rho \sum_i n_i \; a_i^3$, and ρ is the density of the droplet substance (i.e., water or ice). Thus, for cloud particles, the attenuation is a function of the total water or ice content M and not of the drop size distribution per se. Some values of the term $4.343 \sum_i n_i \, Q_{T\,i}$, computed by Gunn and East [6], are given in Table M–1, in units of db km^{-1} gm^{-1} M^{-3}.

The decrease in attenuation with increasing wavelength is such that for wavelengths greater than 5 cm, attenuation by clouds is negligible.

The simplified expressions, Eqs. (M–7) and (M–8), are not valid for the larger size particles associated with precipitation, and the complete Mie equations must be used. Figure M–1 shows results for the normalized total attenuation cross-section σ_T $\left(= \frac{Q_T}{2\pi a}\right)$ as a function of α. The curve for ice was taken from Herman and Battan [7] while the curve for water is from Herman, Browning, and Battan [8]. These curves show that the attenuation from the larger size

TABLE M-1

ATTENUATION COEFFICIENT IN CLOUDS IN Db Km^{-1} Gm^{-1} M^{-3}

Temperature °C		Wavelength (cm) 1.24	3.2
Water Cloud	20	0.311	0.0483
	0	0.532	0.0858
	-8	0.684	0.112
Ice	0	6.35×10^{-3}	2.46×10^{-3}
Cloud	-20	1.34×10^{-3}	5.63×10^{-4}

(large α) particles is a rather complicated function. Nevertheless, Hitschfeld and Bordon [9] have shown empirically that the attenuation from rain may be expressed simply as

$$K_p = K_2 R^{\gamma} \quad \text{(M-11)}$$

where K_p is the attenuation in db km^{-1} and R is the rainfall rate expressed in mm hr^{-1}. Values of K_2 and γ have been determined by Gunn and East [6]. These are given in Table M-2.

TABLE M-2

VALUES OF K_2 AND γ WHEN R IS IN mm hr^{-1} AND RANGE IS IN km

	Wavelength (cm) 0.9	3.2	10
K_2	0.22	0.0074	0.0003
γ	1.00	1.31	1.00

The decrease of K_2 with increasing wavelength is a result of shifting the entire drop size distribution toward smaller values of α. From Fig. M-1, it can be seen that for values of $\alpha < 1.0$ (for water drops), the normalized attenuation coefficient drops rather rapidly. The values of σ_T for ice would be applicable for attenuation through hail, sleet, freezing rain, and possibly such relatively rare precipitation forms as graupel snow pellets, etc. Little is known about attenuation by snow, and it will not be considered here.

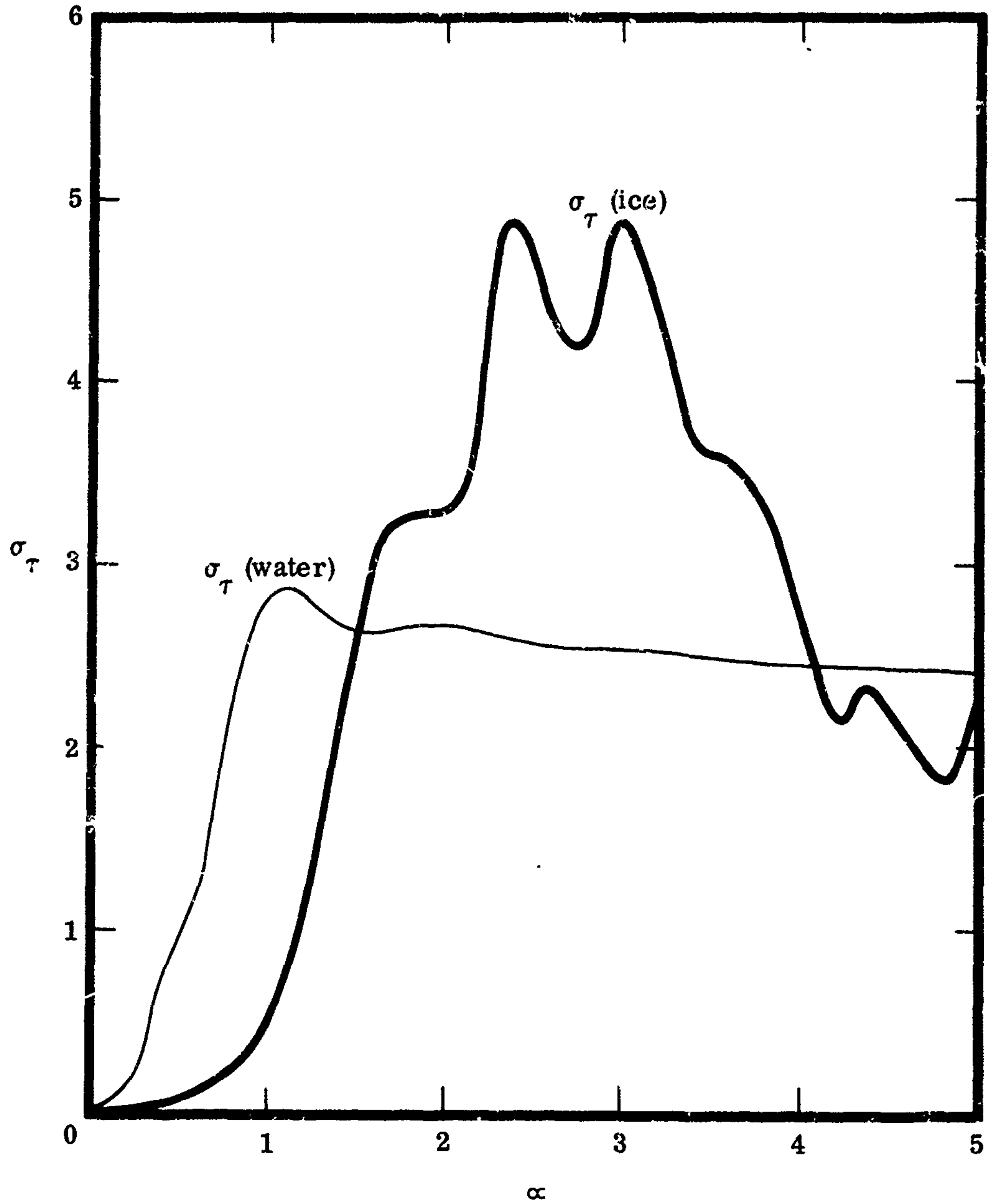

Fig. M-1. Normalized total attenuation cross-section for water and ice.

M.2.2 Factors Influencing Refraction

For moist air the index of refraction n, for wavelengths greater than 2 cm, is given by Batton [1]:

$$(n-1)\,10^6 = N = \frac{79}{T}\left(p - \frac{e}{7} + \frac{4800\,C}{T}\right). \qquad \text{(M–12)}$$

Here p is the atmospheric pressure in millibars, e is the vapor pressure in millibars, and T is the temperature in degrees absolute. Near the earth's surface, a typical value for n is about 1.0003, and in a standard atmosphere

$$\frac{dn}{dh} \approx -4 \times 10^{-8}\ m^{-1}. \qquad \text{(M–13)}$$

Denoting the angle to the local horizon by ϕ, Appleton [10] has shown that

$$\frac{\phi^2}{2} - \frac{\phi_0^{\,2}}{2} = \left(\frac{h}{R} + n\right) - \left(\frac{h_0}{R} + n_0\right) = (M - M_0)\,10^6 \,. \qquad \text{(M–14)}$$

Here ϕ_0 is the angle of the transmitted signal to the local horizon at the source (i.e., at the radar) at a height h_0, and ϕ is the angle the beam makes with the horizon when at a height h above the ground. The quantity $M = \left[\frac{h}{R} + (n-1)\right] 10^6$, where R is the radius of the earth, is called the modified index of refraction. The path followed by a given beam depends upon the variation of M with height through Eq. (M–14). A concave bending of the beam will occur for $M<M_0$, as in this case ϕ will be less than ϕ_0. In these cases, rays starting out at sufficiently small angles to the horizon will be bent back down to the earth. In such a case, part of the waves are trapped and a duct is said to exist. Within the confines of a ducting layer, the radio waves are stronger than in adjacent regions.

For any given distribution of M with height, there exists a maximum value of ϕ_0 for which trapping may occur. This is obtained by setting $\phi = 0$ in Eq. (M–14), giving

$$(\phi_0)_{max} = \left[2(M_0 - M_{min})10^{-6}\right]^{1/2} \qquad \text{(M-15)}$$

A typical value of $(\phi_0)_{max}$ is approximately 0.2°.

Ducts are most commonly produced by the following meteorological conditions:

a. Nocturnal radiation on clear, calm nights, particularly with a sharp decrease in moisture with height.

b. Advection of warm, dry air over cooler water causing increased moisture and a decreased temperature of surface layers.

c. Subsidence extending to near ground level. Ducts are a primary cause of propagation beyond the optical horizon.

Table M-3 summarizes the preceeding discussions.

TABLE M-3
METEOROLOGICAL FACTORS OF IMPORTANCE FOR THE GIVEN PROPAGATION CHARACTERISTICS

Propagation characteristic	Of primary importance	Of secondary importance
Absorption by atmospheric gases	Quantity of O_2 and H_2O vapor present	Temperature, pressure
Particle attenuation (a) small particles	Physical state of H_2O content (i.e., liquid or solid); total amount of liquid or solid H_2O.	Temperature, density of particle substance
(b) large particles	Physical state of precipitation (note propagational characteristics of frozen precipitation not adequately known): rainfall rate (or drop-size distribution)	Temperature
Refraction	Temperature and moisture distribution with height	Pressure change with height

Factors of importance such as wavelength, emitted power, etc., which are of obvious importance, but which are not subject to meteorological control, have not been listed in Table M-3.

The preceeding discussion, and the discussion to follow, are concerned primarily with cm wavelengths. At shorter wavelengths, absorption by oxygen and water vapor become more intense as does attenuation by cloud and precipitation particles. At longer wavelengths, the primary factor controlling propagation is refractive index variations, and the discussions presented here dealing

with this factor are applicable. Atmospheric conditions giving rise to the so-called "angels" over all wavelengths are not understood sufficiently and will not be discussed.

M.3.0 MODIFICATION, OR CONTROL FEASIBILITY

We will consider the meteorological factors listed as of primary importance in Table M-3 for each of the propagation characteristics.

M.3.1 Direct Control or Modification

M.3.1.1 Absorption by Atmospheric Gases

The most likely approach here would seem to be modification of water vapor content in the lowest levels of the atmosphere. Experiments have been performed which demonstrate that some degree of control over evaporation from water surfaces may be achieved by the spreading of films of various substances over the surface. Presumably a reduction in evaporation rate would lower the vapor content of the lowest levels of the atmosphere. Obviously over oceanic areas such techniques could be effective only under calm, or nearly calm conditions. A reduction of vapor content along the microwave path could significantly lower attenuation of the shorter wavelengths (i.e., $\lambda < 2.0$ cm).

M.3.1.2 Small Particle Attenuation

The most important factor to consider here is the physical state of the attenuating fog or cloud particles. For the shorter (cm) wavelengths, Table M-1 shows attenuation (in db) to be two to three orders of magnitude less in ice clouds than in water clouds. The rather normal occurrence of sub-cooled clouds and fogs at below freezing temperatures suggests the feasibility of conversion to ice by introducing freezing nuclei such as dry ice or silver iodide. The research on this subject need not be reviewed here.

M.3.1.3 Large Particle Attenuation

This attenuation is primarily caused by precipitation particles, and large effects might be accomplished by changing the physical state of the particles. However, this requires relatively large changes in temperature over enormous volumes of the atmosphere and is not considered feasible at this time.

Relatively large effects may be realized by altering rainfall rates along the range by virtue of Eq. (M-11). The possibilities for cloud seeding on this phase are quite evident and again, need not be re-evaluated. The actual effects

produced by seeding are still subject to considerable controversy and so cannot be accurately evaluated at this time.

M.3.1.4 Refraction

Ducts may be generated by causing decreasing values of M with height, as shown by Eqs. (M–14) and (M–15). Increasing temperature, or decreasing vapor pressure with height, are the means of accomplishing this as shown by Eq. (M–12). Ducts are, conversely, destroyed by the reverse of the above processes. Large scale direct modifications of the vertical distribution of T and C over sufficient depths do not appear possible at present.

M.3.2 Indirect Control

The temperature and moisture content of the lowest atmospheric levels over oceanic areas are strongly dependent upon sea surface temperatures. Possible methods of control over this latter parameter may justify future investigation. The spreading of high albedo or low albedo films over the ocean surface could alter the absorption of radiation, both long- and short-wave, by the oceanic surface with a consequent change of surface temperature. These films may alter evaporation rates also, resulting in changes in evaporative heat losses.

M.3.3 Predictive Capabilities

Most of the meteorological factors which have been listed as affecting propagation are routinely predicted by meteorologists. Therefore their predictive capabilities are quite well-known and will not be considered further here.

M.4.0 RESEARCH REQUIRED FOR FURTHER CONTROL OR MODIFICATION FEASIBILITY ASSESSMENT

M.4.1 Theoretical

The effect of changes in the drop-size distribution of rain on attenuation is a subject which requires additional work. The necessary data for the theoretical calculations are available, thus these calculations could be made. However, better values of actual drop-size distributions are needed, as well as an understanding of how these distributions may be altered by processes such as seeding.

Studies on the effect of modification of the radiational and evaporative characteristics of the sea surface on the temperature and moisture distribution of the atmosphere are required. Such studies will be valuable in determining the feasibility of modifying ducting conditions.

Little is known of the attenuating properties of snow, or other non-spherical particles. Conditions giving rise to "angels" are poorly understood and also in need of further work. "Angel" phenomena are at times capable of causing considerable effect on propagational characteristics.

M.4.2 Experimental

Experimental evaluation of the overall effects of seeding techniques is currently being conducted by a large number of organizations. Results of these studies will be of significance for the present work. Experiments could be performed for the purpose of evaluating possible modifying effects of surface films as described earlier.

M.5.0 REFERENCES

1. Battan, L.J., Radar Meteorology, Chicago: University of Chicago Press, 1959.

2. Van Vleck, J.H., Radiation Laboratory Report, No. 43-2, Mass. Inst. of Tech., 1942.

3. ———, Radiation Laboratory Report, No. 664, Mass. Inst. of Tech., 1945.

4. Ryde, J.W., "Attenuation and Radar Echoes Produced at Centimetre Wavelengths," Meteorological Factors in Radio-Wave Propagation. London: The Physical Society, 1946.

5. Atlas, D., M. Kerker, and W. Hitschfeld, "Scattering and Attenuation by Non-spherical Atmospheric Particles," J. Atm. Terr. Phys. III, 108-119, 1953.

6. Gunn, K.L.S., and T.W.R. East, "The Micro-wave Properties of Precipitation Particles," Quart. J. Roy. Met. Soc. LXXX, 522-545, 1954.

7. Herman, B.M., and L.J. Battan, "Calculations of the Total Attenuation and Angular Scatter of Ice Spheres," International Conference on Electromagnetic Scattering. London: Pergamon Press, 1963.

8. ———, ———, and S.R. Browning, "Tables of Radar Cross-Sections of Water Spheres," Tech. Rpt. 9, Inst. of Atmos. Physics, Univ. of Arizona, 1961.

9. Hitschfeld, W., and J. Bordan, "Errors Inherent in the Radar Measurement of Rainfall at Attenuating Wavelengths," J. Meteorol. XI, 58-67, 1964.

10. Appleton, E., "The Influence of Tropospheric Conditions on Ultra-Short-Wave Propagation," Meteorological Factors in Radio-Wave Propagation. London: The Physical Society, 1946.

APPENDIX N. SEA SURFACE STATE*

N.1.0 GENERAL DESCRIPTION

N.1.1 Types

(a) Ripples ("cat's paw"). The energy input from the wind field presumably occurs over too short a duration and/or fetch to allow resonant or unstable wavelengths to develop by nonlinear transfer of wave energy from the initial wavelengths generated. Because the initial wavelengths are extremely short, the rate of viscous dissipation soon approaches, and may even exceed, the rate of energy input in the area of the generating wind field.

(b) Growing sea. The energy input from the wind field occurs over a long enough fetch and/or duration for resonant or unstable wavelengths to develop. Interaction of these wavelengths with the wind field then increases the rate of energy input. The shorter wavelengths reach saturation first [1]. In this state, the interaction of these wavelengths reach saturation first [1]. In this state, the combined dissipative effects of viscous dissipation and nonlinear wave breaking are not enough to balance the rate of energy input, although they do set an upper limit on the maximum wave energy at a given wavelength.

(c) Fully developed sea. Long enough wavelengths are generated so that the rate of dissipation due to breaking (and, to a much lesser extent, to viscosity) balances the rate of energy input at a given wind speed. The wave spectrum remains constant in time. Empirically useful equilibrium spectra have been tabulated for various wind speeds, fetches, and durations [2].

(d) Swell. The rate of energy input decreases following the wave group, either because of horizontal movement of the waves out of the generating area or a decrease in the wind. Dispersion and preferential dissipation of shorter wavelengths tend to produce a line spectrum near the wavelength of maximum energy density in the fully developed spectrum.

(e) Surf. The sea or swell enters an area where solid boundary effects become significant. The waves take on the characteristics of shallow-water waves, and breaking becomes the dominant energy-transfer process. Reflection of wave energy from lateral boundaries back out of the area may also become significant.

---

*By Joseph P. Pandolfo.

N.1.2 Characteristic Geographical Extent

The five types of sea state vary considerably in geographical extent:

(a) Fields of ripples that do not develop into growing sea are generally of from one to hundreds of meters in extent.

(b) The extent of growing sea is limited to areas of lesser extent than the fetch required for full development, at a given wind speed. Empirically, this would mean about 300 miles for a 30-knot wind [2].

(c) Fully developed seas require longer fetch and duration and are to be found in long-lived large-scale wind systems like mid-latitude winter storms and the trade winds. They may extend over distances of a few hundred to a few thousand miles.

(d) Swell may extend for several thousand miles. It is generally more evident as it travels through large areas of relatively light wind in the subtropical and equatorial latitudes.

(e) Surf associated with boundary effects will be confined to shallow-water areas, with depths of from 12 to 25 m in areas of gradual bottom slope and with depths of up to 200 m in areas where sharp bottom slopes are evident [3, p. 125].

N.1.3 Characteristic Process and Property Involvement

The basic forces acting in each of the five types of sea state may be classified as driving forces, restoring forces, and dissipating forces, for all the types are quasi-periodic. The typical primary forces that act on each type of sea state are listed in Table N-1.

Because the driving forces are generally estimated in terms of mean wind speeds, an important modifying factor to be considered is the thermal stratification of the atmospheric layer in contact with the water surface. The magnitudes of both the turbulent shearing stress and the turbulent pressure may vary widely with stability at a given wind speed. The eddy structure of the turbulent surface wind is also dependent on the stability of the atmospheric surface layer.

Although capillary forces are not significant restoring forces in types (b), (c), and (e), they are important modifying factors. This is because the magnitude of the driving and dissipative forces is significantly dependent on the presence and

TABLE N-1
PRIMARY FORCES OF SEA STATES

Sea state	Driving force	Restoring force	Dissipative force
(a) Ripples	Turbulent wind pressures normal to the horizontal surface	Surface tension, gravity	Viscosity
(b) Growing sea	Turbulent wind pressures normal to the wave surface	Gravity	Nonlinear breaking, viscosity
(c) Fully developed sea	Same as (b)	Same as (b)	Nonlinear breaking
(d) Swell	Quasi-periodic water pressure	Same as (b)	Wind pressure
(e) Surf	Same as (b) and/or (d)	Same as (b)	Same as (c)

form of the shortest waves composing the sea state, although these waves contain an insignificant portion of the total wave energy.

Viscous forces are not listed as primary dissipative forces in types (b) through (e); and they do not appear to be significant in general. However, the presence of floating solid contaminants appears to enhance the dissipative mechanism significantly [3, p. 139].

The nonlinear forces leading to breaking in type (e) appear to come into play primarily through the depth of the water. However, as already indicated, the bottom configuration—as opposed to the absolute depth—is observed to be a modifying factor in promoting the generation of surf. Finally, mean surface currents, and the shears in these currents, have been observed to play an important role in modifying the sea state.

All sea states transport potential energy and periodic kinetic energy over large horizontal distances. They are also effective, particularly in their turbulent or breaking phases, in the vertical transport across the interfaces of momentum, heat, salinity, water substance, and other atmospheric and oceanic constituents.

N.1.4 Characteristic Life Cycles

Ripple fields generated by isolated eddies are characterized by lifetimes of from 1 to 10 min.

The lifetime of a growing sea might be defined as the duration required for

full development at a given wind speed and unlimited fetch. This would be about 30 hr for a 30-knot wind and a fetch greater than 300 naut mi [2].

Fully developed seas would be limited in characteristic life cycle only by the lifetime of the generating wind field.

The lifetime of swell would also be limited only by the relative magnitudes of the energy-dissipation rate and the wave energy—or the travel time to the coast, whichever is smaller.

N.2.0 ASSESSMENT OF GEOPHYSICAL FORCES

Real wind-driven waves are neither irrotational nor of infinitesimal amplitude. However, the equations of motion derived under these assumptions are useful for order-of-magnitude force estimates.

For some interior point in the fluid, an equation of motion may be written

$$\frac{\partial \phi}{\partial t} + \frac{p}{\rho} + gz = F(t), \tag{N-1}$$

where ϕ is velocity potential, p is pressure, ρ is density, and gz is the geopotential. The continuity equation is

$$\nabla^2 \phi = 0. \tag{N-2}$$

At the interface $z = \xi \approx 0$ (ξ being the vertical surface displacement), the equation takes the form

$$\left.\frac{\partial \phi}{\partial t}\right|_{z=0} = \frac{p}{\rho} - \frac{T}{\rho}\left(\frac{\partial^2 \xi}{\partial x^2} + \frac{\partial^2 \xi}{\partial y^2}\right) + g\xi, \tag{N-3}$$

and, by definition,

$$\left.\frac{\partial \phi}{\partial t}\right|_{z=0} = \frac{d\xi}{dt}, \tag{N-4}$$

where T is the surface tension. Equation (N-1) will have periodic solutions if the boundary conditions are Eq. (N-3) and $\nabla\phi \to 0$ as $z \to \infty$. Solutions for ξ are of the form

$$\xi(\vec{n}, t) = \xi(t)\sum_k \cos k\vec{n} \qquad (\vec{n} = \vec{i}x + \vec{j}y). \tag{N-5}$$

To assess the forces acting at the interface, appeal must be made to somewhat speculative theories of wave generation, maintenance, and growth. The latest of these theories are the most encouraging, in that they have been least fully tested against observation.

For ripples, the order-of-magnitude estimate of the mean-square pressure fluctuation is given by Phillips [4]:

$$\bar{p}^2 = 9 \times 10^{-8}\, U^4. \tag{N-6}$$

where p represents the pressure forces acting per unit area of sea surface. The

standard-deviation pressure fluctuation would be

$$\sigma_p = 3 \times 10^{-4} U^2, \tag{N-7}$$

where U is approximately the anemometer-level wind. Thus, for a wind of 2 m sec^{-1},

$$\sigma_p \approx 12 \text{ dynes cm}^{-2}. \tag{N-8}$$

The order of magnitude of the combined restoring forces, $\rho g \xi - T(\partial^2 \xi/\partial \bar{n}^2)$, is highly dependent on the wave form, which is not too well known. If the waves are assumed to be sinusoidal, extremely unrealistic estimates of the magnitudes of these forces are obtained. Sinusoidal waves of greater than 0.1-cm amplitude could not be generated until the wind reached 6 or 7 m sec^{-1} [5, p. 523]. Obviously the spectrum of even the initially formed waves must have enough components to produce far from sinusoidal wave forms with much smaller restoring forces if waves of realistic height are to be generated with wind-pressure forces as estimated above.

However, an estimate of the relative magnitudes of the restoring forces may be obtained quite simply from Eqs. (N-3) and (N-5) because

$$\frac{\rho g \xi}{T(\partial^2 \xi/\partial \bar{n}^2)} \propto \frac{\rho g}{Tk^2} \tag{N-9}$$

and because

$$T \approx 10^2 \text{ dynes cm}^{-2} \qquad g \approx 10^3 \text{ cm sec}^{-2}, \qquad \rho \approx 1 \text{ gm cm}^{-3},$$

$$\begin{aligned} \rho g \xi &= 0.1\ T(\partial^2 \xi/\partial \bar{n}^2) \text{ for } k = 10 \text{ cm}^{-1}, \\ \rho g \xi &= 1\ T(\partial^2 \xi/\partial \bar{n}^2) \text{ for } k = 3 \text{ cm}^{-1}, \\ \rho g \xi &= 10\ T(\partial^2 \xi/\partial \bar{n}^2) \text{ for } k = 1 \text{ cm}^{-1}. \end{aligned} \tag{N-10}$$

It is obvious that for wave numbers smaller than 1 in 10 cm, the surface tension is insignificant if considered purely as a restoring force.

For growing and fully developed seas, containing larger waves, the wind-pressure forces per unit area of sea surface, as estimated by Stewart [6] from the wave observations tabulated by Groen and Dorrstein, are approximately equal to those given by Eq. (N-7).

Equation (N-7) would give wind pressures per unit area of sea surface as

$$\sigma_\rho \approx 2 \times 10^3 \text{ dynes cm}^{-2} \quad \text{at} \quad U = 20 \text{ m sec}^{-1}. \tag{N-11}$$

Swell is characterized by more purely sinusoidal wave forms than those appropriate to ripples, growing sea, and fully developed sea. The periodic gravitational restoring forces existing in swell may be estimated on a root-mean-square basis. A typical long-crested swell might be represented for order-of-magnitude estimates by

$$\xi = \frac{H}{2} \cos \frac{2\pi}{L} x; \qquad \begin{array}{l} H = 350 \text{ cm}, \\ L = 8800 \text{ cm}. \end{array} \tag{N-12}$$

Then the rms gravitational restoring forces would be given by

$$\sigma_F = \rho g \left[\frac{1}{\pi} \int_0^\pi \frac{H^2}{4} \cos^2 \frac{2\pi x}{L} \, d\left(\frac{2\pi x}{L}\right)\right]^{1/2}$$

$$\approx \frac{\rho g H}{2\sqrt{2}} \approx 5 \times 10^5 \text{ dynes cm}^{-2}. \tag{N-13}$$

Order-of-magnitude force estimates for breaking surf are difficult to obtain on an average basis. Measured values of shock pressures of surf on vertical walls [3, p. 134] show values of the order of 10^3 dynes cm^{-2} per wave.

N.3.0 ASSESSMENT OF GEOPHYSICAL ENERGIES

N.3.1 Energy Budgets

The energy budgets presented in Fig. N-1 are for wave groups comprising the sea state, except for (e) surf, where the figure represents the energy budget for a fixed shallow-water area. (Figure N-2 gives numerical estimates for three selected sea states.)

Energy-storage rates are given by the formulas under the box labeled "Wave energy per unit area." Energy-transformation and -dissipation rates in wave energy per unit time and unit area are shown under the arrows and are given by formulas involving measurable or known quantities where possible. References for the formulas are given in the figure.

The energy-transfer rates to the waves shown for growing sea, fully developed sea, and swell are maximal estimates based on the assumption that all the energy transferred downward through the anemometer level goes directly into wave energy at the sea surface and only indirectly into mean currents. Stewart [6] gives plausible arguments based on empirical data that these maximal estimates are too large by at most a factor of 5.

The downward energy flux through anemometer level is

$$F_E = \tau U, \tag{N-14}$$

where τ is the turbulent shearing stress and U is the mean wind speed. The stress τ may be estimated from

$$\tau = \rho_A C_D U^2, \tag{N-15}$$

where C_D is given empirically as approximately 10^{-3}.

N.3.2 Instabilities

We may list three critical points in the life cycle of a sea state, which involve more or less abrupt changes in the nature and rate of energy transfer, and consequently in the trend of energy-storage amounts.

One such critical point is identified in nature in the transition from ripples to growing sea. In the linear resonance theory of Phillips [4], this would correspond to a change from time-constant wave energy to wave energy linearly

(a) Ripples.

Work done by normal pressures $\longrightarrow$ Wave energy per unit area $\longrightarrow$ Viscous dissipation

$$(2 \sin n_2 t - \sin 2n_2 t) \int_0^\infty \frac{k^2 p(k)}{(gk + Tk^3 \rho^{-1})^{3/2}} \, dk$$

$$n_2 \equiv (gk + Tk^3 \rho^{-1})^{1/2} \quad [7]$$

$$\left\{ \begin{aligned} &\rho \int_0^\infty k^2 C^2(k) S(k)\, dk \\ &+ T \int_0^\infty k^2 S(k)\, dk \\ &+ \rho g \int_0^\infty S(k)\, dk \quad [8] \end{aligned} \right\}$$

$$4\mu \, [g \int_0^\infty k^2 S(k)\, dk + T\rho^{-1} \int_0^\infty k^4 S(k)\, dk \quad [9]$$

(b) Growing sea.

Work done by normal pressures + Work done by wave drag $\longrightarrow$ Wave energy per unit area $\longrightarrow$ Viscous dissipation + Breaking

$$I \equiv \rho_A C_D U^3 \quad [6]$$

$$\underbrace{\begin{aligned} &4\rho g \int_0^\infty I(\omega)\, d\omega \\ &\omega_\mu = \omega_\mu(T, F) \quad [10, 2] \\ &I(\omega) = \alpha g^2 \omega^{-5} \quad [4] \\ &\alpha = 7.4 \times 10^{-3} \quad [11] \end{aligned}}_{\Delta \approx \rho_A (0.12 \approx 0.18) C_D U^3}$$

$$I - \Delta$$

(c) Fully developed sea. Same as (b), but with $\Delta = 0$ and $\omega_\mu \neq \omega_\mu(T, F)$.

(d) Swell.

Form drag $\rightleftarrows$ Wave energy per unit area $\longrightarrow$ Viscous dissipation

$\rho_A C_D (U_v - v)^2$

v = phase velocity

$8^{-1} \rho g H^2$ [2]

$16 \mu g H^2 \pi^2 L^{-2}$ [9]

(e) Surf (for a fixed location).

Horizontal transport of wave energy $\rightleftarrows$ Wave energy per unit area $\longrightarrow$ Breaking

Fig. N-1. Sea-state energy budgets.

(b)

Wind speed, cm sec^{-1}	Duration, hr	Storage, ergs cm^{-2}	$\Delta \cdot$ duration, ergs cm^{-2}
10^3	18	$\approx 6 \times 10^6$	$\approx 8 \times 10^6$
2×10^3	18	$\approx 6 \times 10^7$	$\approx 6.5 \times 10^7$
10^3	9	$\approx 3 \times 10^6$	$\approx 4 \times 10^6$ (check against storage)

(c)

Assume that $\omega_\mu \approx Ug^{-1}$

Wind speed, cm sec^{-1}	Storage, ergs cm^{-2}	Production, dissipation, ergs cm^{-2} sec^{-1}
10^3	7.4×10^6	10^3
2×10^3	1.2×10^8	8×10^3
5×10^2	4.6×10^5	1.25×10^2

(d)

Wind speed, component in v-direction, cm sec^{-1}	L, cm	H, cm	v, cm sec^{-1}	Storage, ergs cm^{-2}	Viscous dissipation, ergs cm^{-2} sec^{-1}	Drag
0	10^4	4×10^2	13×10^2	2×10^7	-2.56	-1.7
10^3	10^4	4×10^2	13×10^2	2×10^7	-2.56	-0.4
-10^3	10^4	4×10^2	13×10^2	2×10^7	-2.56	-3.0

Fig. N-2. Numerical estimates for selected sea states.

increasing in time for a given spectrum of turbulent atmospheric-pressure fluctuations. Ripples would correspond to a system of forced waves generated by any turbulent pressure distribution, and the transition to growing sea would occur only if turbulent pressure fluctuations exist whose wavelengths and translation speeds closely correspond to the wavelengths and translation speeds of free gravity waves. This theory must be complemented by a linear instability theory of Miles [7] to obtain realistic rates of growth of growing seas. When some wave components have grown linearly in time (by resonance) to an amplitude at which sheltering effects (form drag) can become effective, there is a transition in the combined theory from a linear growth rate to an exponential growth rate. This transition is not as easily identifiable in nature, but its existence is required to give any correspondence between the combined linear theories and the observed behavior of sea states, since the sheltering mechanism would take too long to initiate waves, whereas the resonance mechanism would have them grow too slowly once they are initiated.

A third, more gradual, transition is required to a state in which nonlinear energy transfers become important enough to halt the exponential growth of initially generated short waves and allow progressively longer waves to develop. This state is called "saturation" by Phillips [4], who has derived the saturation spectrum on the basis of dimensional arguments.

N.4.0 MODIFICATION OR CONTROL FEASIBILITY

N.4.1 Energy Interference

N.4.1.1 Direct

(a) Interference through wind speed or wind structure. The energy-budget charts suggest some direct interferences, of varying feasibility. The most obvious, and perhaps the least feasible, is to change the rate of energy transfer to the sea surface by changing the wind speed through large-scale weather modification.

For ripples, however, small-scale local modification of the turbulent pressure spectrum is feasible. Such small-scale modification may be observed in the generation of ripple fields to the lee of obstacles in the wind flow. The wavelength distribution of the turbulent pressure fields over small areas (of the order of from 50 to 500 m) could be grossly controlled by the nature of the obstacles.

(b) Interference through surface-tension modification. The contamination of the sea surface by oil films appears to interfere either with the energy-transfer rates to the wave or with the dissipation rates of the wave energy, or with both. In any case, the calming effect is definitely established, according to Defant [3, p. 139].

Applications of an oil film have resulted in a measured reduction of the mean-square wave slope in a sea state by a factor of 2 or 3 [11]. Since the shortest waves in the spectrum contribute most to the mean-square slope, the measured reduction is interpreted to indicate that the slick selectively eliminates the shortest waves immediately.

The reason for this elimination, according to Defant, is that the calming contaminants have less surface tension than sea water does. This property causes the oil to spread rapidly into a very thin film. For sufficiently thin films, the surface tension becomes a function of the film thickness, and the surface opposes any motion that tends to make the film thinner. Thus, wave motions in the underlying water are subjected to tangential drag by the resisting film, and dissipation of the particle kinetic energy is increased.

In addition, it is plausible that the drag coefficient of the surface with respect

to the wind depends to some extent on the mean-square slope of the sea state, although the degree of dependence has yet to be definitely established observationally. The energy-budget diagrams for growing sea show that the portion of the energy transfer from the wind that goes into increasing the wave energy amounts to at least about 10% of the total. A 10% decrease in drag coefficient in a growing sea would therefore eliminate this surplus over the dissipation rate, even were the dissipation rate to remain constant upon application of the film.

On the basis of this explanation, we would not expect a contaminant that reduces the surface tension without forming a film (e g., a detergent) to be effective in calming seas. This is borne out by observations [3]. Whether this type of contaminant would have any effect on sea state—and what the effect might be—remains an open question.

(c) Interference through modification of dissipation rate. Defant notes that such solid contaminants as mud, ice, and seaweed may either prevent wave development or cause waves to decay rapidly. This effect is presumably due to the increased viscous drag of orbital motion against solid bodies in suspension. Later estimates of the increased dissipation may be possible.

(d) Interference through prevention of horizontal transport of wave energy into restricted areas. The traditional method for exercising control of surf over local areas has been to construct breakwaters. Use of modern materials and techniques may make temporary artificial breakwaters for restricted areas feasible, particularly if the barrier effect can be combined with an increased frictional drag as described previously. Materials like the recently developed foam plastics come to mind as being suitable.

(e) Interference through superposition of mechanically generated turbulent motions on the wave field. This would obviously be restricted to local areas. The development of a theoretical basis for a prediction of interaction effects between organized small- and large-scale motions and random small-scale motions is formidable.

It might be noted that the essence of this problem is contained in the problem of understanding the natural degeneration of waves by breaking.

N.4.1.2 Indirect

The boundary-layer turbulent wind structure and stress are obviously affected by the thermal stratification in this layer. Theories successfully describing the variations of these parameters with stability over land surfaces have been developed recently. It is problematical as yet whether such theories apply to overwater boundary layers in view of possibly significant differences in the nature of the underlying surface.

The line of attack on this approach would be to investigate methods for modifying the surface-water temperature by interference with the surface-heat balance. This interference could affect the net radiation, evaporation, and/or advective and turbulent transports of heat.

N.4.2 Survey of Simulation and Predictive Capabilities

N.4.2.1 Theoretical

In the previous sections, an idealized equilibrium spectrum [1] has been used to obtain the gross energy estimates desired for this preliminary study. It is believed that this spectrum, obtained without detailed consideration of nonlinear effects and on purely dimensional grounds, does not differ in order-of-magnitude total energy from other empirically tabulated spectra [2] or from the averages of recently observed spectra [12, 13].

Other important features of wind-wave spectra, such as the peak frequency (or frequencies) at various stages of development cannot be explained theoretically without detailed consideration of nonlinear effects. Recent nonlinear theoretical gravity-wave models [14, 15] offer differing predictions about preferred wavelengths in developing spectra.

A few observed spectra that have been reported agree in some ways with the results of both models [16].

Thus, the theoretical simulation of wave spectra by linear models may be described as having achieved some success in predicting the total amount of wave energy at any stage of development, and, perhaps, the directional distribution of wave energy relative to the generating wind [17].

Nonlinear models that have been considered are capable of predicting pre-

ferred frequencies or wavelengths in the spectrum, but these have not yet been fully checked out against observations. The possibility of theoretically simulating sea states with realistic statistics of 0th or high order (e.g., distributions of wave height, slope, and curvature) must await the development of such models. The statistics of integral properties (e.g., total energy and directional energy distributions) are satisfactorily simulated by linear models to the accuracy desired in this study.

N.4.2.2 Synoptic-empirical

Practical techniques for obtaining sea-state forecasts have been available for several years [e.g., 2]. The forecasts have produced operationally useful prior estimates of such sea-state properties as total wave energy, significant height, and dominant wavelength in routine practice [18]. Subsequent applications of these techniques include the specification of optimum ship routes [19] and the development of numerical forecasting techniques [20].

Improvement of these techniques requires, in addition to the theoretical developments described above, improvement in the specification of initial and predicted wind fields over the oceans, as well as the availability of many more observations of wave spectra, particularly at high wind speeds.

N.4.2.3 Experimental

Observations made in wind-tunnel tanks and wave channels [17, 21] are, obviously, severely restricted in their capability to simulate nature sea states.

However, it is certain that relevant experiments concerned with contamination effects on viscous damping and on capillary--small gravity-wave profiles could be designed for such facilities.

N.4.3 Research Required for Further Control or Modification Feasibility Assessment

This section emphasizes problem areas that, in a recent survey of research [21] in this field, appear to be relatively neglected.

Several important questions raised in Stewart's [6] speculative discussion of the wave-generation problem deserve further investigation. Preliminary field observational studies relevant to one of these questions have been described by

Stewart [22].

Basically, the wave-generation and -maintenance problem, as considered by Stewart, can be cast in the following form for a growing sea. Given two turbulent layers of fluid of different densities with a bounding interface. The upper fluid layer contains a source of mean momentum or kinetic energy. The important quantities to be determined are the rate of turbulent transport of mean kinetic energy downward into the interface, and the rate of viscous dissipation of kinetic energy within the uppermost portions of the lower layer plus the turbulent transport downward from these uppermost portions into deeper portions of the lower fluid.

With proper parameterization of the turbulent viscosity of the two fluids, a theoretical approach to the problem is possible.

A further step would lead to a 3-layer model consisting of two (turbulently) viscous layers separated by a thin fluid film, if a formulation of the combined turbulent-thin film mechanics is possible. This theoretical problem, if solvable, might shed further light on the calming effect of surface slicks.

An increase in effective viscosity of the lower fluid layer might adequately parameterize the effects of floating solid particles for theoretical investigation of another proposed modification technique.

The class of theoretical models proposed assumes that the growth of a sea state in nature is adequately represented by an accumulation of mean kinetic energy in the vicinity of the interface in the models. Although the models are extremely simplified, their formulation is far from a trivial problem. A key aspect of the problem is the formulation of appropriate boundary conditions at the interface(s).

Experimental and field observational studies directed toward the evaluation of the turbulent fluxes and dissipation rates in the vicinity of the interface(s) would be very useful in the formulation of the type of theoretical model outlined above.

N.5.0 REFERENCES

1. Phillips, O. M., "The Equilibrium Range in the Spectrum of Wind Generated Waves," J. Fluid Mech. 4, 426–434, 1958.

2. Pierson, W. J., Jr., G. Neumann, and R. W. James, Practical Methods for Observing the Forecasting Ocean Waves. Washington, D.C.: Hydrogr. Ofc., U.S. Navy, 1960.

3. Defant, A., Physical Oceanography, vol. 2. New York: Pergamon Press, 1961.

4. Phillips, O. M., "On the Generation of Waves by a Turbulent Wind," J. Fluid Mech. 2, 417–445, 1957.

5. Sverdrup, H., M. Johnson, and R. Fleming, The Oceans. New York: Prentice-Hall, 1942.

6. Stewart, R. W., "The Wave Drag of Wind over Water," J. Fluid Mech. 10, 189–194, 1961.

7. Miles, J. W., "On the Generation of Waves by Shear Flows," J. Fluid Mech. 3, 185–204, 1957.

8. Cox, C., and W. Munk, "Slopes of the Sea Surface Deduced from Photographs of Sun Glitter," Bull. Scripps Inst. Oceanogr. 6:9, 401, 1956.

9. Charnock, H., "Wind Generated Water Waves," Sci. Progress 44:183, 487–501, 1958.

10. Phillips, O. M., and E. J. Katz, "The Low Frequency Components of the Spectrum of Wind-generated Waves," J. Marine Res. 19:2, 57–69, 1961.

11. Lamb, H., Hydrodynamics. New York: Dover Publications, 1932.

12. Burling, R. W., Wind Generation of Waves on Water. Ph.D. dissertation, Imperial Col., Univ. of London, 1955.

13. Pierson, W. J., Jr. (Ed.), "The Directional Spectrum of a Wind Generated Sea as Determined from Data Obtained by the Stereo Wave Observation Project," Meteorol. Papers (Col. Eng., New York Univ.) 2:6, 1960.

14. Phillips, O. M., "On the Dynamics of Finite-amplitude Unsteady Gravity Waves. 1. The Elementary Interactions," J. Fluid Mech. 9, 193–217, 1960.

15. Tick, L. J., "A Non-linear Random Model of Gravity Waves," J. Math. and Mech. 8:5, 1959.

16. Kinsman, B., "Some Evidence on the Effect of Nonlinearity on the Position of the Equilibrium Range in Wind-Wave Spectra," J. Geophys. Res. 66:8, 2411–2415, 1961.

17. Phillips, O. M., "Recent Developments in the Theory of Wave Generation by Wind," J. Geophys. Res. 67, 3135, 1962.

18. Neumann, G., and W. J. Pierson, Jr., "A Detailed Comparison of Theoretical Wave Spectra and Wave Forecasting Methods," Sond. Deut. Hydro. Zeit. 10:3, 73–146, 1957.

19. James, R. W., "Wave Forecasting," in Ocean Wave Spectra. New York: Prentice-Hall, 1963.

20. Baer, L., An Experiment in Numerical Forecasting of Deep Water Ocean Waves. Ph.D. thesis, Dept. of Meteorol. Oceanogr., New York Univ., 1962.

21. Pierson, W. J., Jr., "Gravity Waves," Trans. Am. Geophys. Un. 44:2, 485–488, 1963.

22. —, and H. L. Grant, "Determination of the Rate of Dissipation of Turbulent Energy near the Sea Surface in the Presence of Waves," J. Geophys. Res. 67, 3177, 1962.

APPENDIX O. SURFACE OCEAN CURRENTS*

O.1.0 GENERAL DESCRIPTION

O.1.1 Phenomenon Types

Here, we shall consider the surface wind-driven currents only; surface currents associated with tides, surges, and tsunamis are not considered.

O.1.2 Characteristic Geographic Extent

The surface wind-driven ocean currents are responsible for the bulk of the observed large-scale circulation of the world's surface ocean waters, e.g., the gyral systems associated with the Gulf Stream, Kuroshio, etc., and the equatorial current regimes. In the open ocean, these currents' intensity decreases with depth and is generally negligible below about 500 m.

O.1.3 Characteristic Process and Property Involvement

O.1.3.1 Basic Forces

Horizontal frictional stress of wind on water's surface.

O.1.3.2 Modifying Factors

(a) Wind speed
(b) wind direction
(c) water depth
(d) eddy viscosity of water
(e) earth's rotation rate
(f) coastal configuration
(g) wind duration
(h) sea-surface tension
(i) lateral diffusion
(j) air pressure
(k) sea-surface state (roughness).

O.1.3.3 Property Transports

(a) Water mass
(b) water temperature (heat).

---

*By W. Lawrence Gates.

O.1.4 Characteristic Variations (Life Cycle)

In shallow or coastal waters, the wind-driven current responds to wind variations of the order of hours, and often is in a transient state of growth or decay. In deep water, say of depth greater than 100 m, the wind driven currents are more fully developed, and respond to the longer-period wind variations of the order of days, weeks, or months. The major oceanic surface circulations show relatively small variations (c. 10%) on these same time periods, and evidently also have a seasonal variation (autumn minimum) of the order of 20%. No life cycle as such occurs for the surface wind-driven currents, once the wind-stress action has been acting for longer than one-half pendulum day [1].

O.2.0 ASSESSMENT OF GEOPHYSICAL FORCES

O.2.1 Basic Physical Equations

(a) Equation of horizontal motion:

$$\frac{d\vec{v}}{dt} = -f\vec{k} \times \vec{v} - \frac{1}{\rho}\nabla p + \frac{1}{\rho}\frac{\partial \vec{\tau}}{\partial t} + A\nabla^2\vec{v}. \qquad \text{(O-1)}$$

(b) Continuity equation:

$$\frac{d\rho}{dt} = -\nabla \cdot \rho\vec{v} - \frac{\partial \rho w}{\partial z}. \qquad \text{(O-2)}$$

(c) Hydrostatic equation:

$$\frac{\partial p}{\partial z} = -\rho g. \qquad \text{(O-3)}$$

Here, the symbols are defined as follows:

$\vec{v}$ = horizontal current vector

w = vertical current

f = $2\Omega \sin \varphi$, coriolis parameter

ρ = water density

p = water pressure

$\vec{\tau}$ = vertical component of horizontal wind stress on water surface

A = horizontal eddy viscosity

g = gravitational acceleration

z = vertical coordinate (upward)

$\vec{k}$ = vertical unit vector.

O.2.2 Force Analysis

TABLE O-1
ESTIMATED FORCE MAGNITUDE AND SCALE

Term	Order of magnitude	Horizontal scale	Vertical scale
Coriolis force ($-f\vec{k} \times \vec{v}$)	10^{-3} to 2×10^{-2} cm sec^{-2}	10^2 to 10^3 km	10^{-1} to 1 km
Horizontal pressure force ($-\rho^{-1} \nabla p$)	10^{-3} to 2×10^{-2} cm sec^{-2}	10^2 to 10^3 km	10^{-1} to 1 km
Vertical frictional force [$\rho^{-1}(\partial\vec{\tau}/\partial z)$]	3×10^{-5} cm sec^{-2}	10^2 to 10^3 km	500 m
Horizontal frictional force ($A \nabla^2 \vec{v}$)	10^{-6} to 10^{-4} cm sec^{-2}	10^2 km	10^2 to 10^3 m
Horizontal mass divergence ($\nabla \cdot \rho\vec{v}$)	10^{-9} gm cm^{-3} sec^{-1}	10^2 to 10^3 km	500 m
Vertical mass divergence ($\partial \rho w/\partial z$)	10^{-9} gm cm^{-3} sec^{-1}	10^2 to 10^3 km	500 m
Vertical pressure gradient ($\partial p/\partial z$)	10^3 gm cm^{-2} sec^{-2}	-	-

O.2.3 Characteristic Structure

Wind-driven currents are found in all the oceans and constitute the dominant surface circulation. Their speed is greatest at or just beneath the surface and is of the order of 0.5 m sec^{-1}, with maximum speeds of about 2 m sec^{-1} occurring in the western ocean boundary currents (e.g., Gulf Stream). The current speeds decrease with depth in the ocean, with the velocity vector showing a spiral-like (cum sole) variation. At several hundred meters' depth, the wind-driven currents have virtually disappeared. In the open sea, the surface current deviates approximately 45° to the right of the wind.

The net water transported by the wind-driven current is to the right of the

wind (in the Northern Hemisphere), and if the wind's stress action continues long enough, a piling up of surface waters may occur, especially near a coast. A geostrophic slope current may thus appear directed parallel to the wind, with the consequent modification of the total water flow. In a fully developed or steady-state current, the surface-water slope may be of the order of 10^{-5}, corresponding to an internal horizontal pressure gradient of 1 mb km^{-1}.

The semipermanent large-scale surface-wind distribution of the lower and middle latitudes gives rise to a system of large-scale oceanic gyres (circulation cells), with the gyral boundaries occurring in the regions of maximum and minimum wind stress. The total circulation within each gyre depends upon the magnitude of the vertical component of curl $\vec{\tau}$, with the poleward meridional flow generally increasing westward across the ocean and leading to an intense current at the western boundary. Total water transported by these wind-driven circulations are of the order of 3×10^{14} gm sec^{-1}, divided among six major ocean gyral circulations. The magnitude of $\vec{\tau}$ is of the order of 1 dyne cm^{-2}.

Smaller-scale and/or shorter-period winds also produce surface currents of smaller extent and of a less permanent nature. These transient wind currents do not extend to great depth.

O.3.0 ASSESSMENT OF GEOPHYSICAL ENERGY

O.3.1 Energy Budget

Let a boxed symbol denote an energy intrinsic to the wind-driven surface current, and a circled symbol denote an energy related to the intrinsic ones by

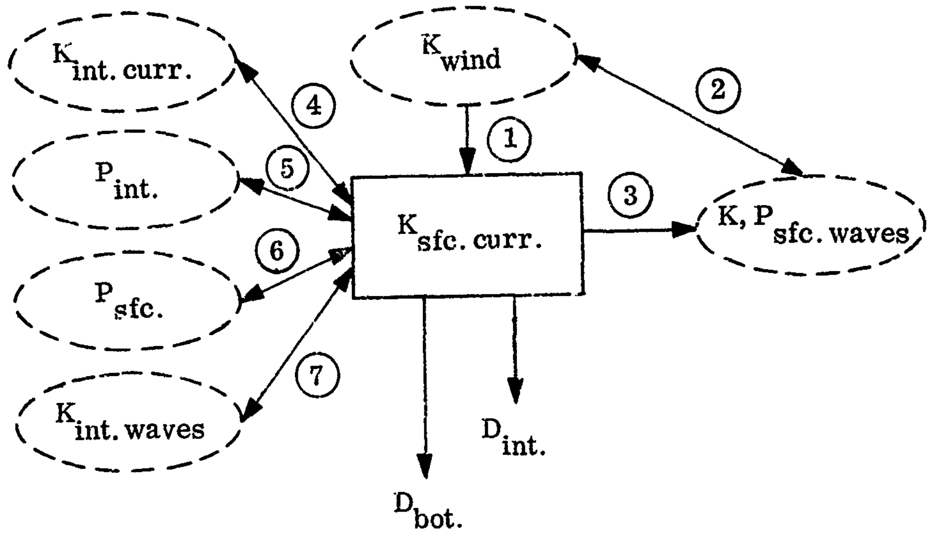

Fig. O-1. Energy budget.

an energy-transformation process. Let us also denote a dissipation of energy by the symbol D. The kinetic-energy budget of the surface ocean currents may now be represented by the accompanying diagram, to which the following discussions refer.

O.3.1.1 Storage Estimates

(a) $K_{sfc.\ curr.}$ = kinetic energy of wind-driven surface currents

$$= 0.5\rho \cdot |\vec{v}|^2 \text{ area} \cdot \text{depth}$$

$$\approx 0.5 \left(\frac{1\ \text{gm}}{\text{cm}^3}\right)\left(\frac{50\ \text{cm}}{\text{sec}}\right)^2 \cdot 3 \times 10^{18}\ \text{cm}^{2*} \cdot 200\ \text{m};$$

$$K_{sfc.\ curr.} = 1.5 \times 10^{17}\ \text{cal.} \qquad \text{(O-4)}$$

This energy corresponds to approximately 0.05 cal cm^{-2} of sea surface. Note that about 75% of this total energy is probably contained in the assumed upper 50 m.

*The area 3×10^{18} cm^2 represents approximately the world's major ocean surface area; the total water-covered area is 3.61×10^{18} cm^2.

(b) $K_{\text{int. curr.}}$ = kinetic energy of internal ocean currents. This may include both the familiar internal geostrophic or dynamic currents, turbidity currents, as well as the system of undercurrents now coming to light. We may estimate the dynamic currents' kinetic energy as $0.5\rho\,|\vec{v}|^2$ area · depth; assuming that $|\vec{v}|$ = 5 cm $\sec^{-1}$ over a depth of 3000 m and an area of 3×10^{18} cm^2, we find the estimate

$$K_{\text{int. curr. (1)}} = 2.2 \times 10^{16} \text{ cal.} \tag{O-5}$$

The deep currents underlying the Gulf Stream system, for example, probably have a kinetic energy comparable to this figure.

The kinetic energy of the equatorial undercurrents may be estimated [2] from their apparent depth of 100 m, length of 10^4 km (at the equator), width of 200 km, and a mean speed of about 2 knots. Hence, we find

$$K_{\text{int. curr. (2)}} = 2.5 \times 10^{16} \text{ cal.} \tag{O-6}$$

The kinetic energy of a turbidity current may be estimated [3] from an average speed of 20 m $\sec^{-1}$, a width of 1 km, a depth of 10^2 m, and an estimated length of 10^3 km. Thus, we find

$$K_{\text{int. curr. (3)}} = 1 \times 10^{14} \text{ cal.} \tag{O-7}$$

This energy appears negligible, even for a moderate frequency of occurrence of such currents.

(c) $P_{\text{int.}}$ = potential and internal energy of internal baroclinic ocean structure. Assuming geostrophic equilibrium for the internal currents, we may estimate $P_{\text{int.}} \approx K_{\text{int. curr.}}$, i.e.,

$$P_{\text{int.}} = 2.2 \times 10^{16} \text{ cal.} \tag{O-8}$$

(d) $P_{\text{sfc.}}$ = potential energy of large-scale sea-surface elevation:

$$P_{sfc.} = \rho g(\bar{h}^2) * \cdot \text{area}$$

$$\approx \frac{1\ \text{gm}}{\text{cm}^3} \frac{10\ \text{m}}{\text{sec}^2} (750\ \text{cm}^2) \cdot 1.5 \times 10^{18}\ \text{cm}^2;$$

$$P_{sfc.} = 2.3 \times 10^{16}\ \text{cal.}\dagger \qquad \text{(O-9)}$$

(e) $K_{int.\ waves}$ = kinetic energy of internal waves:

$$\frac{\text{wave energy}}{\text{unit area}} = \frac{\rho g H^2}{8} \text{ for sinusoidal waves of height H;}$$

$$K_{int.\ waves} = \frac{1}{8} \frac{1\ \text{gm}}{\text{cm}^3} \frac{10\ \text{m}}{\text{sec}^2} (2\ \text{m})^2 \cdot \underbrace{3 \times 10^{17}\ \text{cm}^2}_{\text{10\% of seas' surface}};$$

$$K_{int.\ waves} = 3.8 \times 10^{16}\ \text{cal.} \qquad \text{(O-10)}$$

(f) $K, P_{sfc.\ waves}$ = kinetic and potential energy of sea-surface waves:

$$K + P_{sfc.\ waves} = \frac{\rho g H^2}{8} \cdot \text{area} \qquad (H = 1\ \text{m}) \quad \text{(for sinusoidal waves);}$$

$$K, P_{sfc.\ waves} = 9.5 \times 10^{16}\ \text{cal.} \qquad \text{(O-11)}$$

O.3.1.2 Transformation-rate Estimates

(a) (1) = energy-transmission rate from low-level wind to ocean via tangential wind stress $\vec{\tau}$ on water. Assuming that $\vec{\tau}$ (ocean) = 1 dyne cm^{-2}, $\vec{\tau}$ (land) = 10 dynes cm^{-2}, then the ocean stress accounts for about 25% of the total wind-energy dissipation, which may be estimated [4] at 10^{13} cal sec^{-1}. Hence,

$$(1) = 2.5 \times 10^{12}\ \text{cal sec}^{-1}. \qquad \text{(O-12)}$$

(b) (2) = energy-transmission rate from wind to sea-surface waves. This is evidently accomplished by turbulent air-pressure variations, resonance, and by aerodynamic pressure effects of the wave shape [5]. The latter mechanism's

---

*$(\bar{h}^2)$ = mean-square height = $\alpha^2 L^2/3$, where α is slope, and L is distance. Assuming that $\alpha = 1.6 \times 10^{-7}$, giving 50 cm rise over 3000 km, $(\bar{h}^2) = 750\ \text{cm}^2$.

†The atmospheric pressure effect (1 mb ≈ 1 cm ocean-level variation) contributes an energy estimated at 2×10^{15} cal.

energy-flux rate may be taken [6] proportional to the expression

$$\rho_{air}\left(\frac{h}{L}\right)^2 (v - c)^2, \quad \text{(O-13)}$$

where h is the wave height, L is the wavelength, c is the wave speed, and v is the wind speed. Measurements [7] indicate an average value of 0.1 watt m^{-2}, or

$$(2)_1 = 7.5 \times 10^{12} \text{ cal sec}^{-1} \quad \text{(O-14)}$$

for the entire earth's ocean surface. This transmission rate may also be estimated by assuming that essentially all of the wind's stress action goes into the surface waves [8]. This rate is $\vec{\tau} \cdot c$, where c is an average wave speed relative to the wind. Hence,

$$\vec{\tau} \cdot c \cdot \text{area} = \frac{1 \text{ dyne}}{\text{cm}^2} \cdot \frac{3 \text{ m}}{\text{sec}} \cdot 3 \times 10^{18} \text{ cm}^2 \quad \text{(O-15)}$$

or

$$(2)_2 = 2.2 \times 10^{13} \text{ cal sec}^{-1}. \quad \text{(O-16)}$$

This estimate is an order of magnitude larger than (1), we note, and is in relatively good agreement with $(2)_1$.

(c) (3) = energy-exchange rate between surface waves and surface current. No estimate available; the water particles in a surface-wave motion are usually considered to move in circular orbits, with no net translation of their own making. Some energy transfer seems likely, however, probably in the direction of $K_{sfc.\ curr.}$ from P, $K_{sfc.\ waves}$.

(d) (4) = energy-exchange rate between surface current and internal currents. This exchange depends on the vertical energy flux, either by organized vertical currents or by vertical turbulent diffusion. The convergence in the wind-driven surface or Ekman layer results in a downward water motion at the layer's base at about 500 m depth. This speed, w_e, may be estimated at 5×10^{-5} cm sec^{-1}. Assuming sinking to occur over half of the world's oceans, and taking a kinetic energy at this level for a speed of 5 cm sec^{-1} relative to a surface speed of 50 cm sec^{-1}, we may estimate the vertical kinetic energy advection $w_e(\partial k/\partial z)$. Assuming now a correlation between the sinking motion and the

stronger oceanic surface currents (the dominant anticyclonic gyres), we may estimate the net downward kinetic-energy flux as $0.1\,w_e(\partial k/\partial z)$. Thus we find that

$$④ = 0.6 \times 10^{12} \text{ cal sec}^{-1}. \qquad \text{(O-17)}$$

The role of vertical diffusion of kinetic energy from the upper to the lower ocean layers is not known as a separate phenomenon, and no estimate is available. It seems probable, however, that this effect also proceeds in the direction $K_{\text{sfc. curr.}}$ to $K_{\text{int. curr.}}$, and may be masked in the above estimate.

(e) ⑤ = energy-exchange rate between surface current and the internal oceanic potential energy. No direct estimate available. Assuming the development of a geostrophic balance, however, we may make an indirect estimate dependent on the storage estimate $P_{\text{int.}}$. Ekman [9] estimates that geostrophic equilibrium is established over a distance of 10^2 km from a coast in about 1 day. For an average ocean "radius" of 3000 km, about 30 days is thus required. Hence,

$$⑤ = \frac{\rho_{\text{int.}}}{30 \text{ days}} = 8.4 \times 10^{9} \text{ cal sec}^{-1}. \qquad \text{(O-18)}$$

(f) ⑥ = energy-exchange rate between surface current and the potential energy of the sea-surface slope. No direct estimate available. By the method of (e) above, however, we may estimate that

$$⑥ = \frac{\rho_{\text{sfc.}}}{30 \text{ days}} = 8.8 \times 10^{9} \text{ cal sec}^{-1}. \qquad \text{(O-19)}$$

(g) ⑦ = energy-transmission rate between surface currents and the kinetic energy of internal waves. No direct estimate available. It would appear probable, however, that the energy propagation is in the direction $K_{\text{sfc. curr.}}$ to $K_{\text{int. waves}}$.

O.3.1.3 Dissipation-rate Estimates

(a) $\dot{D}_{\text{bot.}}$ = frictional dissipation at sea bottom. Assuming the bottom stress to be proportional to ρv^2 and taking $\rho_{\text{water}} = 10^3\,\rho_{\text{air}}$ and $v_{\text{water}} = 10^{-3}\,v_{\text{air}}$, we find that $\tau_{\text{water}} = 10^{-3}\,\tau_{\text{air}}$. Thus, from the transformation rate

estimate (1), we may estimate that

$$D_{bot.(1)} = 2.5 \times 10^{9} \text{ cal sec}^{-1}. \tag{O-20}$$

This estimate is appropriate to the apparent mean deep-sea currents with speeds of the order of 1 cm sec^{-1}. There is increasing evidence of large and variable currents in the deep and bottom water of the ocean [2]; the effective dissipation of these currents, with $v \approx 10$ cm sec^{-1}, may be 10^2 times that estimated above. Hence, we may estimate as an upper value

$$D_{bot.(2)} = 2 \times 10^{11} \text{ cal sec}^{-1}. \tag{O-21}$$

This higher dissipation rate is also in better agreement with the estimate [5] that the bottom stress is approximately 0.03 times the surface stress.

(b) $D_{int.}$ = energy dissipation in the ocean's interior due to turbulent viscosity. Assuming first that this dissipation is represented mainly by <u>lateral</u> eddy diffusion, we may consider it to be proportional to the transformation (1), i.e.,

$$D_{int.} = (1)\, \rho A \nabla^2 \bar{v}\, \tau^{-1}_{sfc.}, \tag{O-22}$$

where $\bar{v}$ is the vertically integrated horizontal current speed, and A is the coefficient of lateral eddy diffusion. Taking $\tau_{sfc.} = 1$ dyne cm^{-2}, $\rho = 1$ gm cm^{-3}, and $A = 10^8$ cm^2 sec^{-1} and estimating $\nabla^2\bar{v}$ for the whole ocean* as 2×10^{17} cm^{-1} sec^{-1} (times 4000 m depth), we have (using (1) that

$$D_{int.(1)} = 2.0 \times 10^{9} \text{ cal sec}^{-1}. \tag{O-23}$$

An independent estimate of $D_{int.}$ may be made from the estimate [12] that 12 yr would be required to dissipate the ocean's kinetic energy by internal (lateral) eddy friction. Thus, from $K_{sfc.\ curr.} + K_{int.\ curr.} + K_{int.\ waves} = 1.4 \times 10^{17}$ cal, we have that

$$D_{int.(2)} = 3.8 \times 10^{9} \text{ cal sec}^{-1} \tag{O-24}$$

It has also been estimated [12] that bottom frictional dissipation proceeds at

---

*In the narrow western boundary currents, e.g., the Gulf Stream, the value of $\nabla^2\bar{v}$ may easily be 10^2 times this value. The present estimate may be regarded as a dissipation by these boundary currents occupying 1% of the ocean.

about 4 times the rate of $D_{int.}$. Hence, from $D_{bot.}$, we may estimate $D_{int.}$ to be about 0.6×10^9 cal sec^{-1}; this estimate, however, appears somewhat low and is not felt to be sufficiently reliable.

Assuming that the internal dissipation of the surface-current energy takes place by means of small-scale turbulence, we may use the recently measured [8] value of the dissipation of order of 0.1 erg cm^{-2} sec^{-1} per meter's depth found at 15 m as representing this mechanism. Over 100 m depth and for all the world's oceans, we thus find the estimate

$$D_{int.(3)} = 0.8 \times 10^{12} \text{ cal sec}^{-1}. \qquad \text{(O-25)}$$

We note that this estimate is considerably greater than the previous two estimates and does not appear physically unreasonable.

O.3.2 Instabilities

The wind-driven surface ocean currents appear to be relatively stable and permanent features of the large-scale oceanic circulation. No instabilities on a large scale have been reported, although—as noted earlier—there are both regular and irregular variations in certain features of the circulation. On a smaller scale, there are the more shallow and localized transients due to moving wind systems and local winds. These also appear to display no instabilities.

Recently, the meanders [13] of the intense western boundary currents (e.g., Gulf Stream) have received considerable attention and may be regarded as a kind of instability of the surface current. These eddies are of a few hundred kilometers' dimension and appear to have a lifetime of several weeks, at least. Although their cause is not fully known, it would appear that they occur in connection with bottom-topography variations when the current leaves the continental shelves for deeper water [14]. The meanders' form and structure also appear to be related to the nonlinear nature of the boundary current [15].

O.4.0 MODIFICATION OR CONTROL FEASIBILITY

O.4.1 Force and/or Energy Interference

As a preliminary to the consideration of energetic interference, it is instructive to examine first a summary of the energy budget, given below. Here, the energy transformations and dissipations are in units of 10^{12} cal sec^{-1}. If we assume a steady state of current and wave development, it appears that there may be a significant energy transfer from $K, P_{sfc.\ waves}$ to $K_{sfc.\ curr.}$ of the order of 10^{12} cal sec^{-1}. It also appears that the transfer $K_{sfc.\ curr.}$ to $K_{int.\ curr.}$ is significant, and may well be accompanied by further transformations (indicated

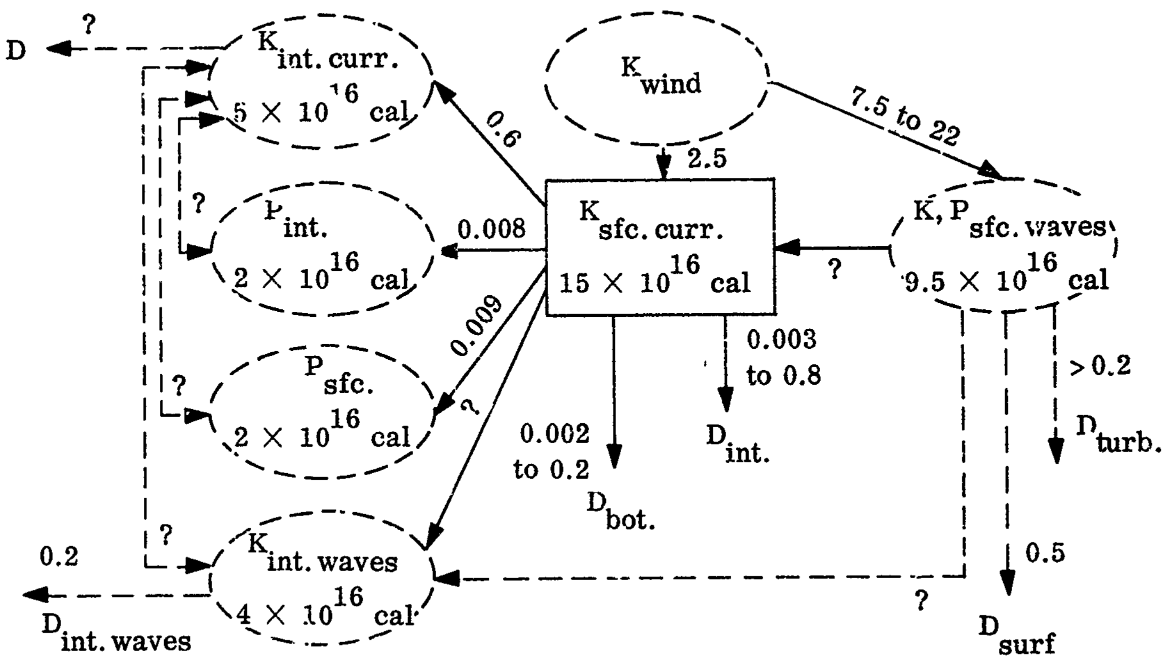

Fig. O-2. Energy budget summary.

by dashed lines) with $P_{int.}$, $P_{sfc.}$, and $K_{int.\ waves}$. The possibility of direct transfer between $K_{sfc.\ curr.}$ and $K_{int.\ waves}$, and between $K_{int.\ waves}$ and $K, P_{sfc.\ waves}$ is also suggested; the magnitudes of these may have a critical bearing on the overall energy budget of the surface currents.

In view of the relatively prominent energetic role of the surface waves, some further consideration of the dissipations by internal friction and coastal surf are of interest. Considering D_{surf} first, we have, from $K, P_{sfc.\ waves}$, wave energy =

$8^{-1} \rho g H^2$. If we assume a wave period of 10 sec, giving a group velocity of 7.8 m sec^{-1}, the wave-energy transmission rate is approximately 4×10^9 ergs sec^{-1} per centimeter of coast. Assuming $5 \times 10^{0.4}$ km of surf coastline, we have

$$D_{surf} = 0.5 \times 10^{12} \text{ cal sec}^{-1}. \tag{O-26}$$

This dissipation rate is small compared with the wave-energy input rate from the wind (2).

The internal frictional dissipation $D_{int.}$ of the surface waves is difficult to estimate because of the evidently strong dependence on wind speed and wave height. For wave heights less than 1 m, the turbulent dissipation in the layer 1 m beneath the waves' troughs may be estimated [16] at 3 ergs cm^{-2} sec^{-1}, or

$$D_{turb.} = 0.2 \times 10^{12} \text{ cal sec}^{-1}. \tag{O-27}$$

The internal turbulent dissipation due to the waves decreases rapidly with depth and may be considered negligible below 10 m.

This estimate of $D_{turb.}$ is no doubt a significant underestimate; most of the waves' energy dissipation probably occurs very near the sea surface (< 1 m) [8]. Even allowing for a tenfold increase, neither this estimate nor that of D_{surf} accounts for a significant part of the estimated rate of energy input to the surface waves from the wind. The possible significance of an energy transfer from the surface waves to the surface current is again indicated.

It may also be of interest to record an estimate of the dissipation rate of the energy of internal waves, in view of these waves' possible close energetic relation to the surface-current energy. Using the estimated energy of $K_{int.\ waves}$, and an estimated dissipation rate of 24-hr period waves (of length 110 km) [16], we find that

$$D_{int.\ waves} = 0.2 \times 10^{12} \text{ cal sec}^{-1}. \tag{O-28}$$

In view of the apparent omnipresence of internal waves, this estimate may be low, although the longer waves' energy is much greater than that of the shorter waves. If there is a significant downward propagation of energy from the surface waves to internal waves, then this dissipation may assume a critical role in the overall energy balance.

0.4.1.1 Direct

From the total energy storage in the surface currents, of the order of 10^{17} cal, it is clear that a direct energy confrontation intended to destroy or drastically alter these currents is not feasible.* Moreover, the current energy is here present in an organized, large-scale phenomenon, and presumably only a comparable organization of energy could be effective in a direct interference scheme.

Interference with or successful modification of the large-scale surface ocean currents would immediately call into play the other significant energy transfers in which these currents play a role, particularly at the sea-air boundary. Dominant here is the energy flux to the atmosphere in the form of latent heat, which may be estimated [4] to average 200 cal cm^{-2} day^{-1}. Over the world's oceans, this represents an energy transfer of 7×10^{15} cal sec^{-1}, a very much greater flux than those directly associated with the surface current per se. Associated with this latent-heat flux is a flux of sensible heat of approximately 10^{15} cal sec^{-1}, a current-heat transport of about 10^{15} cal sec^{-1}, and a turbulent-energy dissipation of the wind of the order of 10^{13} cal sec^{-1}. It is only this last and relatively small energy flux that evidently is directly responsible for the surface currents themselves.

0.4.1.2 Indirect

From the variety of energy transfers discussed above, a number of indirect mechanisms for surface-current interference might be suggested. Even the least ambitious of these, however, involves a rate of energy expenditure that is a considerable fraction of the total rate of electric energy production in the U.S., which has been estimated [4] at 10^{10} cal sec^{-1}. Modification of the surface currents on a more local scale, say by the alteration of the surface-wind stress or of the local submarine topography, would produce correspondingly local effects, which might well be only temporary. Suppression of surface-wind waves by films [17] has reportedly been successful over areas as large as 3×10^4 m^2 in 1 hr, although the effects on surface currents are not known.

---

*We may recall here that the energy released in a 10-kiloton atomic bomb is of the order of 10^{15} cal.

In general, it may be concluded that even indirect interference with surface currents is not feasible, a conclusion furthered by the unknown energetic interactions in the surface currents' energy budget.

O.4.2 Promotion or Suppression of Critical Conditions

The only conditions or processes that appear critical or vital to the surface currents, on the basis of present knowledge, are the atmospheric stress and the relations with internal currents.

O.4.2.1 Atmospheric Wind Stress

The reduction of wind stress by oil or acid films effectively suppresses ripples and evidently inhibits the formation of the longer surface-gravity wave [18]. If these films could be maintained over large areas of the subtropical oceans, an overall reduction in the surface-current system's intensity might result. The film's interference with evaporation and sensible-heat flux to the atmosphere,* however, would very likely substantially alter the surface currents in other (and presently unknown) ways through a change in the atmospheric circulation itself.

O.4.2.2 Internal Current Energy

The modification of the surface current by changes of the bottom and/or coastal configuration would have uncertain effects until the energetic transfers between surface and internal currents are known. Submarine topographic modification might well shift a surface current laterally, but might at the same time divert it downward. Related to this problem are the local phenomena of sediment transport, upwelling, and thermal heat balance. Such "side effects" of changes of bottom topography (and hence internal-current energy changes) might well overshadow an intended result.

*The latent-heat flux to the atmosphere from the ocean may be estimated at 7×10^{10} cal sec^{-1}; note the enormity of this flux as compared with those in the surface-current energy balance (Section O.4.1).

O.4.3 Survey of Simulation and Predictive Capabilities

O.4.3.1 Theoretical

The theory of surface ocean currents has received considerable attention during the past 10 to 15 years. This research may be broadly grouped into

(a) studies of the more local wind-driven surface currents, following the general pattern of the classic study of Ekman [9] and

(b) studies of the general surface circulation of the world's oceans, following the pioneer studies of Sverdrup [19].

In the present state of development [20], the theory of wind-driven local surface currents can account for the growth and structure of such currents in homogeneous water and can satisfactorily describe the effects of limited water depth and coasts. Given the atmospheric wind field, its variation and the stress, methods exist [21] for the satisfactory prediction of storm surges and the associated wind-driven currents. On a local basis, these methods may be considered to constitute the first oceanographic forecast schemes (other than for tidal phenomena).

The theory of the large-scale or general oceanographic circulation, on the other hand, is somewhat less satisfactorily developed. As first shown by Munk [22], the broad general circulation pattern may be found from a knowledge of the wind stress and consideration of lateral frictional dissipation. Subsequent theory has concentrated on the more detailed structure of the western boundary current, and on the role of the vertical ocean-temperature structure. The theory of subsurface currents is not well developed, and the role of the thermohaline currents in the overall circulation has only begun to be studied. A predictive capability cannot be said to exist at present.

O.4.3.2 Experimental

The general wind-driven ocean circulation has been successfully modeled [23, 24] under a variety of conditions approximating those in nature, including realistic ocean boundaries. In rotating fluid experiments, dye tracers have revealed a striking resemblance to the Gulf Stream system, for example. The capability for conducting a wide variety of model tests exists, and at least a qualitative view of oceanic behavior might thereby be obtained.

O.4.4 Research Required for Further Control or Modification Feasibility Assessment

O.4.4.1 Theoretical

Before an adequate assessment of the feasibility of the control or modification of surface ocean currents can be made, much further theoretical research appears necessary. In particular, the effects of bottom topography, the role of nonlinear effects in momentum transport, and the dynamics of internal thermal and dynamic currents all must be clarified before the surface currents can be better understood. The testing of dynamic ocean models on modern computers and, in particular, the study of the time-dependent current evolution promise to provide a particularly fruitful avenue of attack. Ultimately, the thermohaline circulations in the ocean must be coupled with the wind-driven currents, and the outlines of a combined dynamic theory constructed. Such a step appears necessary before significant progress can be made on the very important problem of the atmosphere-ocean interaction; reliable considerations of ocean-current control must consider this coupling.

O.4.4.2 Experimental

The effects of bottom topography and the effects of barriers could easily be studied in rotating model apparatus. Techniques for the measurement of the model fluid's velocity and temperature in something approaching synoptic detail should be refined. The relative roles of thermal and wind-driven currents would also appear amenable to experimental attack. In suitable wave tanks (nonrotating), the transfer of wave energy to surface currents and to interior currents and/or internal waves might also be studied. Quantitative estimates of these processes would aid greatly in the control-feasibility assessments.

O.4.4.3 Observational

The testing of theoretical models and the interpretation of model experiments both require adequate observations from the world's oceans, not to mention the much more stringent observational requirements for oceanic prediction in a synoptic sense. The presently available data (largely from hydrographic stations and bathythermographs) are inadequate in both time and space for either of

these roles. Methods for observing oceanic variables—and, in particular, the currents—from aircraft, from buoys or nets of buoys, and from satellites should be investigated.

O.5.0 REFERENCES

1. Veronis, G., "Partition of Energy Between Geostrophic and Non-Geostrophic Oceanic Motions," Deep-Sea Res. 3, 157–177, 1956.

2. Montgomery, R. B., and E. D. Stroup, Equatorial Waters and Currents at 150°W in July–August, 1952. Baltimore: Johns Hopkins Press, 1962.

3. Plapp, J. E., and J. P. Mitchell, "A Hydrodynamic Theory of Turbidity Currents," J. Geophys. Res. 65, 983–992, 1960.

4. Malkus, J. S., "Large-Scale Interactions," pp. 88–294 of The Sea. New York: Interscience, 1962.

5. Phillips, O. M., "Recent Developments in the Theory of Wave Generation by Wind," J. Geophys. Res. 67, 3135–3141, 1962.

6. Ivanov, R. N., "On the Mechanism of the Transfer of Wind Energy to Currents," Izv. Akad. Nauk S.S.S.R. ser. Geofiz., no. 5, 673–677, 1958.

7. Kolesnikov, A. G., and G. E. Kononkova, "Instrumental Determination of Energy Transmitted by Normal Wind Pressure to the Surface of Sea Waves," Izv. Akad. Nauk S.S.S.R. ser. Geofiz., no. 10, 1551–1559, 1961.

8. Stewart, R. W., and H. L. Grant, "Determination of the Rate of Dissipation of Turbulent Energy Near the Sea Surface in the Presence of Waves," J. Geophys. Res. 67, 3177–3180, 1962.

9. Ekman, V. W., "On the Influence of the Earth's Rotation on Ocean-Currents," Arkiv Mat. Astr. Fysik 2:11, 1905.

10. Crease, J., "Velocity Measurements in the Deep Water of the Western North Atlantic; Summary," J. Geophys. Res. 67, 3173–3176, 1962.

11. Francis, J. R. D., "A Note on the Velocity Distribution and Bottom Stress in a Wind-driven Water Current-System," J. Marine Res. 12:1, 1953.

12. Veronis, G., and H. Stommel, "The Action of Variable Wind Stress on a Stratified Ocean," J. Marine Res. 15, 43–75, 1956.

13. Fuglister, F. C., and L. V. Worthington, "Some Results of a Multiple Ship Survey of the Gulf Stream," Tellus 3, 1–14, 1951.

14. Warren, B. A., Topographic Influences on the Path of the Gulf Stream. Ph.D. thesis, Dept. Geol. Sci., M.I.T., 1962.

15. Bryan, K., "A Numerical Investigation of a Nonlinear Model of a Wind-driven Ocean," 41 pp. Unpubl. MS (1963).

16. Rattray, M., Jr., "Propagation and Dissipation of Long Internal Waves," Trans. Am. Geophys. Un. 38, 495–500, 1957.

17. Shuleikin, V. V., "Forty Years of Soviet Ocean Physics," Izv. Akad. Nauk S.S.S.R. ser. Geofiz., no. 11, 1366–1383, 1957.

18. Vines, R. G., "The Damping of Water Waves by Surface Films," Australian J. Phys. 13, 43–51, 1960.

19. Sverdrup, H. U., "Wind-driven Currents in a Baroclinic Ocean; With Application to the Equatorial Currents of the Eastern Pacific," Proc. Natl. Acad. Sci. U.S. 33, 318–326, 1947.

20. Fofonoff, N. P., "Dynamics of Ocean Currents," pp. 323–395 of The Sea. New York: Interscience, 1962.

21. Welander, P., "Numerican Prediction of Storm Surges," Advances in Geophys. 8, 316–379, 1961.

22. Munk, W. H., "On the Wind-driven Ocean Circulation," J. Meteorol. 7, 79–93, 1950.

23. Stommel, H., A. B. Arons, and A. J. Faller, "Some Examples of Stationary Planetary Flow Patterns in Bounded Basins," Tellus 10, 179–187, 1958.

24. von Arx, W. S., "Some Techniques for Laboratory Study of the Primary Ocean Circulation," Proc. 1st Symp. on Use of Models in Geophys. Fluid Dynamics (Ofc. of Nav. Res.), pp. 89–99, Sep. 1953.

APPENDIX P. INTERNAL OCEAN WAVES*

P.1.0 INTRODUCTION

This appendix assesses the phenomena of internal waves in the ocean from the standpoint of possible operational benefits to be gained from their modification, control, or prediction. Such an assessment is inhibited from the outset by three factors:

(a) Observational data on such waves are extremely sparse, far too few to allow any reasonably exact empirical determination of their characteristics in time and space within extensive geographical areas. The existence of such wave forms must in most cases be inferred from observational data on fluctuations of other oceanographic parameters, e.g., sea temperature, salinity, and currents.

(b) Investigations into the basic causes of such waves are still in the early stages of development, again due primarily to the lack of sufficient observational data.

(c) The theoretical background for describing the dynamical and physical processes involved in internal waves has not yet been developed to a point at which general and complete systems of equations, suitable for operational use with observable parameters, are available. Here again, the lack of observational data hampers any empirical evaluation of mathematically complex dynamical models.

The subsequent discussion is, as a result of these inhibiting factors, primarily descriptive. It is an attempt to assess characteristics that have been indicated with some degree of assurance by sparse observational data or that can reasonably be inferred from basic theoretical considerations.

*By Russell G. Harris.

P.2.0 GENERAL DESCRIPTION

This assessment of internal waves from an operational-use standpoint is based primarily on the information contained in the references listed in The Bibliography (see Section P.6.0). The interest in the structure and causes of internal waves has grown at an accelerating rate, particularly during the past few years. Much investigative work has been and is being done, from both the theoretical and the empirical standpoints. Empirical work has consisted of observations both in nature and in controlled laboratory (wave-tank) experiments. No doubt these current studies will alleviate some of the lack of knowledge noted here when their results are more complete and generally available.

Internal waves are usually discussed in terms of two primary physical models:

(a) internal waves occurring at the boundary of a desnity-discontinuity surface in the ocean and

(b) internal waves occurring in water in which multiple layers are present or in which the density is a continuous function of depth.

The following description will be oriented in the same fashion. It should be emphasized that observations of internal waves, and hence their characteristics, are primarily inferences made from observations of other oceanographic parameters. Consequently, they can often be questioned as to whether the observed fluctuations stem from wave action or from undetermined advective processes.

P.2.1 Internal Waves at a Boundary Surface of Density Discontinuity (2-layer Model)

The observed density structure in the ocean frequently is such that it can be represented reasonably well by a 2-layer model. For example, near-shore waters may be made up primarily of a relatively shallow layer of fresh water (e.g., river runoff) superposed on denser, more saline water. Another example is found in water with a well-defined thermocline of sharply decreasing temperature (and increasing density) beneath a well-mixed isothermal layer extending to the surface. The bottom of the mixed layer in this case serves as a density "discontinuity."

Wave action is believed to occur along the interface of such discontinuities. The waves can, to some extent, be described mathematically in much the same manner as waves at the ocean surface or in the atmosphere. The waves are described as having their maximum amplitude at the surface of discontinuity, with vertical displacements decreasing with distance both above and below the density discontinuity. The presence of internal waves is not necessarily related

to the existence of waves at the ocean surface. When occurring in relatively shallow depths, the internal wave action causes alternate zones of convergence and divergence at the ocean surface. This process has been observed to cause alternate bands of ripples and slicks—and distinguishable bands of compacted biological organisms at the surface of the ocean under which the wave action is occurring. The length and periods of internal waves span a range representing multiple orders of magnitude and are commonly treated as "short" or "long" waves according to whether or not the wavelength is small with respect to the thickness of the superposed layers. Wavelengths range from a few meters to hundreds of kilometers, periods from a few minutes to a matter of days. The wave motions need not be, and usually are not, related in any simple fashion to wave motion at the ocean surface.

The amplitudes of the internal waves can be much larger than those of waves on the surface. The density difference across the discontinuity is usually very small; hence, the potential energy required for the formation of internal waves is relatively small. The speed of wave propagation, however, is much less than for waves of equal length on the surface. (One investigator calculated the ratio to be about 1/30 for long waves of tidal period.) The inertia of such waves shows a corresponding increase. The usual mathematical treatment of these internal waves indicates that the direction of the water movement reverses across the interface. Calculations on internal waves having the characteristic of "long" waves of moderate amplitude show horizontal water velocities connected with wave passage to range from 0.1 to 0.5 knot.

By far the greatest number of investigators of waves of this type have delineated internal waves of longer periods, particularly of tidal periods.

P.2.2 Internal Waves in Multilayer Systems or Where Density is a Continuous Function of Depth

A more complex mathematical treatment has been developed to describe internal waves, which may be formed either at multiple surfaces of density discontinuity or in water in which the density is a continuous function of depth. The solutions of the dynamical equations admit the possibility of families of waves with different periods. The number of waves possible is a function of the number

of layers defined. When the density is considered as a continuous function of depth, the number of possible waves becomes infinite. Most investigators seeking to substantiate the models with observational data utilize harmonic and spectrum analyses to delineate the predominant periods. Here again, the most frequently observed waves are those of long period, usually clustered near semidiurnal or diurnal tidal periods. The lengths of these long-period waves are short, however, in comparison with the length of the surface tides. Amplitudes are large in comparison with surface tides and commonly range to 100 ft or more. The amplitudes apparently vary inversely with the vertical density gradients. In some regions, these waves have been observed to be oscillatory, rather than progressive. Investigative work done in coastal waters (and in model tank experiments) indicates that, in areas of the ocean over sloping continental shelves, the internal waves of tidal character may become standing waves as a result of bottom topographical effects. Under assumed realistic conditions, such internal tides would be of the order of from 15 to 20 ft in deeper water, but could theoretically increase to more than 100 ft nearer shore. The currents associated with such waves have been estimated to range up to 0.5 knot.

The possibility of "submarine surf," i.e., breaking internal waves in regions of mechanical instability, has been indicated both from a theoretical standpoint and from observational data obtained in the open ocean and in model wave-tank experiments. Such submarine surf would, however, be much less active than similar phenomena at the ocean surface. Wave velocities would be much lower, with relatively small amounts of energy involved.

Although most investigations with observational data have been concerned with "long" waves, theoretical considerations of internal waves with "short-wave" characteristics suggest the existence in the ocean of "cells" in which regular oscillations of fixed period occur, as if between fixed walls. The cells would be of definite extent and shape, with the period dependent on the density structure within the cell and the size and shape of the cell itself. Many of the short temperature fluctuations observed in the ocean -and previously ascribed to turbulence effects—are now felt to be probably the effects of such cellular systems.

P.3.0 CAUSES OF INTERNAL WAVES

P.3.1 Forces of Tidal Period

That most investigators of internal waves have delineated waves with periods at or near tidal periods would seem to suggest that the usual tidal forces would be related in a mathematically simple fashion to the occurrence of internal tides. This is not the case, and the absence of any simple connection has been substantiated from both theoretical and observational standpoints. Refinement of the dynamical models to include the effects of the earth's rotation, however, provide a more definite description of resonance conditions favorable for the generation of oscillations at internal discontinuity surfaces by tidal forces. The rotation factor further enhances the indications for internal waves with amplitudes much greater than those of the surface tides.

P.3.2 Aperiodic Forces

P.3.2.1 Meteorological

The effect of meteorological forces on the generation of internal waves is highly important. Because the amounts of energy needed for the generation of internal waves are usually small, such waves can be formed by the passage of relatively mild meteorological disturbances. One series of observations on waves formed by a passing moderate storm showed internal waves with a period of near 6 hr, wavelength of about 40 km, wave velocity between 3 and 4 knots, and maximum amplitude of 180 ft. Other investigative work conducted on the occurrence of internal waves at the mixed-layer depth and bottom of the thermocline has shown the effects of meteorological disturbances. Internal waves with large amplitudes were usually associated with the slow passage at the surface of strong weather systems. The divergence in surface waters resulting from the passage of low-pressure systems, or air-mass fronts, is considered to be a "trigger" mechanism for initiating the internal waves. The meteorological systems, however, frequently move out ahead of the slower-moving internal wave. In such cases, the wave has been found to oscillate for days before settling back into the usual tidal pattern. Active air-mass fronts that dissipate over the ocean can produce the same effect.

P.3.2.2 Changes in Bottom Topography

The effect of bottom topography on the generation of internal waves and in changing their characteristic has been mentioned previously. Evidence indicates that internal waves may be formed in stratified water flowing over bottom-topography "obstructions." In particular, the effect of a sloping continental shelf results in standing waves near shore and progressive waves offshore, moving seaward. Other investigations support the existence of internal surf in 2-layer systems in which the differences in current velocities across the interface is as low as from 1 to 3 knots. Such phenomena would, however, be of a much less violent character than breakers and surf at the surface.

P.3.2.3 Sudden Changes in Surface and/or Subsurface Currents

It has been suggested that sudden appearances of strong surface currents may initiate internal waves on subsurface interfaces. Submarine tidal currents themselves may also generate such waves. Indeed, it is entirely possible that many of the fluctuations interpreted as internal waves may well be a reflection not of true wave motion but of advective processes associated with the ebb and flow of tidal currents at depth.

In general, the causes of internal waves in the open ocean, other than theoretically possible relations with tidal resonance, are to a large extent unknown. There is much evidence to support the conclusion that they probably exist over most oceanic areas, but all too few data are available to form the bases for observationally supported, operational working hypotheses.

P.4.0 IMPLICATIONS FOR OPERATIONAL USE

P.4.1 Prediction

The most profitable activity to be pursued initially would seem to be one of attempting to devise methods for predicting the existence and characteristics of internal waves as they presently occur. The term prediction is used here in the sense of diagnosis of their appearance at a given time and place in the future. Such prediction techniques would serve both short- and long-term purposes. In the short view, prediction and diagnosis of internal waves, particularly those occurring at the mixed-layer depth, would have an immediate payoff in permitting

more accurate definition of the thermal and acoustical structure of the ocean, particularly in operationally significant areas. The means to be used in devising the prediction methods would not be overly complex, and would involve primarily the acquisition and interpretation of proper and sufficient meteorological and oceanographic observational data in specified regions. The methods of interpretation can initially be empirically straightforward. In the long view, the predictions would provide a basis for closer consideration of control and modification possibilities. A reasonably satisfactory method for predicting the future state of such disturbances in time and space obviously would be vital to the success and safety of such attempts.

P.4.2 Interference or Control

That internal wave action is generally considered to involve relatively small amounts of energy implies that internal waves of considerable magnitude might be generated mechanically. Particular operational procedures suitable for the purpose are unknown, nor are there enough observational data yet available for a reasonably precise assessment. Presumably, however, any force capable of creating an initial disturbance in the existing temperature structure of the water within a restricted region, e.g., heating at the bottom or explosions by conventional means, could possibly produce not only an initial progressive internal wave, but a resultant oscillatory wave for some time into the future. This would correspond to previously mentioned meteorological effects.

Once such procedures for generating internal waves were available, however, these low-energy, artificially stimulated phenomena could conceivably be used to good advantage, should disturbance of the existing thermal, density, or acoustical structure of the ocean be desired for short periods over restricted areas. At least one investigator has suggested, moreover, that internal waves reinforced by strong meteorological forces and tidal currents—under optimum conditions—could become high-energy phenomena. Neither theoretical nor empirical knowledge of internal waves is sufficient, however, at present, for adequate assessment of this possibility.

P.5.0 RESEARCH REQUIRED

P.5.1 Theoretical

Continuing research into the basic structure and dynamics is vital, if control and/or modification is to be considered. This is particularly important in obtaining operationally useful working hypotheses of the structure and causes of internal waves over the open ocean. More exact definition of the relations among coexisting currents, state of the sea surface, and internal waves of both the "long" (tidal) and "short" (cellular) types previously described is badly needed.

P.5.2 Operational

Research along empirical lines would seem to offer the most immediate payoff, especially in the areas of prediction and diagnosis. The models tested for the prediction techniques would probably be most useful from an operational standpoint if they were devised with empirical methods. The science to be dealt with is semiexact because of obvious observational difficulties. All data that can be expected to be available for operational use would be subject to unavoidable and, to a large extent, uncorrectable errors. These facts imply that operational prediction models should be developed primarily by averaging procedures, e.g., statistical methods. Such models could be expected to provide more operationally useful products than those based primarily on differential processes sensitive to an unrealistic degree to unavoidable random errors in routine observational data.

P.6.0 BIBLIOGRAPHY

1. Cox, C. S., "Internal Waves," Trans. Am. Geophys. Un. 44:2, 488–489, Jun. 1963.

2. Defant, A., "On the Origin of Internal Tidal Waves in the Open Sea," J. Marine Res. IX:2, 111–119, Oct. 1950.

3. —, Physical Oceanography, vol. 2. New York: Pergamon Press, 1961.

4. Eckart, C., Hydrodynamics of Oceans and Atmospheres. New York: Pergamon Press, 1960.

5. Ewing, G., "Slicks, Surface Films and Internal Waves," J. Marine Res. IX:3, 161–187, Dec. 1950.

6. Fjeldstad, J. E., "Internal Waves," Geofys. Publ 10:6, 1–35, 1935; transl. by M. C. Stonor, Dir. Sci. Info. Svcs., DRB Canada, May 1961.

7. Gaul, R. D., The Occurrence and Velocity Distribution of Short-Term Internal Temperature Variations Near Texas Tower No. 4. ASWEPS Rpt. 1, U.S. Navy Hydrogr. Ofc., Washington, D.C., May 1961.

8. Lamb, H., Hydrodynamics, 6th ed., p. 370. London: Cambridge Univ. Press, 1932.

9. Mazeika, P. A., Prediction of the Thermocline Depth. ASWEPS Rpt. 5, U.S. Navy Hydrogr. Ofc., Washington, D.C., Jun. 1960.

10. Power Spectrum Analysis of Internal Waves from Operation Standstill. Tech. Rpt., Appl. Oceanogr. Br., Div. Climatol., U.S. Navy Hydrogr. Ofc., Washington, D.C., 1955.

11. Proudman, J., Dynamical Oceanography. New York: John Wiley & Sons, 1953.

12. Rattray, M., "Propagation and Dissipation of Long Internal Waves," Trans. Am. Geophys. Un. 38:4, 495–500, Aug. 1957.

13. —, "On the Coastal Generation of Internal Tides," Tellus 12:1, 54–62, Feb. 1960.

14. Reid, J. L., "Observations of Internal Tides in October 1950," Trans. Am. Geophys. Un. 37:3, 278–28?, Jun. 1956.

15. —, "Observations of Inertial Rotation and Internal Waves," Deep Sea Res. 9, 283–290, Jul.–Oct. 1962.

16. Rudnick, P., and J. D. Cochrane, "Diurnal Fluctuations in Bathythermograms," J. Marine Res. X:3, 247–256, Dec. 1951.

17. Schule, J. J., Jr., et al., The Effects of Weather Upon the Thermal Structure of the Ocean. H.O. Misc. 15360. U.S. Navy Hydrogr. Ofc., Washington, D.C., 1952.

18. Sverdrup, H. U., M. W. Johnson, and R. H. Fleming, The Oceans. New York: Prentice-Hall, Inc., 1949.

APPENDIX Q. INTERNAL OCEAN CURRENTS*

Q.1.0 GENERAL DESCRIPTION

Q.1.1 Phenomena Types

Here we shall consider the purely internal modes of oceanic circulation–the so-called thermohaline currents–and the systems of undercurrents in both middle-latitude and equatorial regions.

Q.1.2 Characteristic Geographic Extent

An organized system of internal ocean currents appears to be present in most of the oceans' bulk, although generally less intense than the familiar surface currents. These internal currents appear to reach their maximum development near the continental boundaries in deep water.

Q.1.3 Characteristic Process and Property Involvement

Q.1.3.1 Basic Forces

The downward transfer of (horizontal) momentum and heat through the ocean surface (Ekman) boundary layer.

Q.1.3.2 Modifying Factors

surface wind stress
surface ocean temperature
ocean basin configuration
eddy viscosity of water
earth's rotation rate
coriolis parameter variability
vertical thermal stability
water buoyancy
eddy thermal diffusion

Q.1.3.3 Property Transports

water mass
water temperature (heat)
water momentum

---

*By W. Lawrence Gates.

Q.1.4 Characteristic Variations (Life-cycle)

In the bulk of the oceans' interior, the internal currents appear to be very steady and relatively slow; no direct evidence of a life-cycle is available. The development of such an internal circulation mode has been estimated [1] to require a period of the order of $1-10^2$ years, assuming that it is excited by processes at the ocean surface.

Q.2.0 ASSESSMENT OF GEOPHYSICAL FORCES

Q.2.1 Basic Physical Equations

(a) Equation of horizontal motion:

$$\frac{d\vec{V}}{dt} = - f\vec{k} \times \vec{V} - \frac{1}{\rho} \nabla p + Av \frac{\partial^2 \vec{V}}{\partial z^2} \tag{Q-1}$$

(b) Continuity equation:

$$\frac{d\rho}{dt} = - \rho \left(\frac{\partial u}{\partial x} + \frac{\partial v}{\partial y} + \frac{\partial w}{\partial z} \right) \tag{Q-2}$$

(c) Hydrostatic equation:

$$\frac{\partial p}{\partial z} = - g\rho \tag{Q-3}$$

(d) Equation of state:

$$\rho = \rho_0 (1 - \alpha T) \tag{Q-4}$$

(e) Thermal energy equation:

$$\frac{dT}{dt} = \kappa \frac{\partial^2 T}{\partial z^2} \tag{Q-5}$$

Here the symbols are defined as follows:

$\vec{V}$ = horizontal current vector

f = coriolis parameter

$\vec{k}$ = vertical unit vector

ρ = density (mean value, ρ_0)

p = pressure

Av = vertical eddy diffusivity (momentum)

z = vertical coordinate (upward)

u = eastward current component

v = northward current component

w = upward current component

α = thermal expansion coefficient (water)

T = temperature

κ = vertical eddy diffusivity (heat)

Q.2.2 Force Analysis

TABLE Q-1
ESTIMATED FORCE MAGNITUDE AND SCALE

Force	Order of magnitude	Horizontal scale	Vertical scale
Coriolis force $(-f\vec{k} \times \vec{V})$	10^{-3} - 10^{-5} cm sec^{-2}	10^3 km	1 km
Horizontal pressure force $(-\frac{1}{\rho} \nabla p)$	10^{-3} - 10^{-5} cm sec^{-2}	10^3 km	1 km
Vertical mixing frictional force $(A_v\, \partial^2\vec{V}/\partial z^2)$	10^{-5} - 10^{-7} cm sec^{-2}	10^3 km	0.1 km
Horizontal divergence $(\partial u/\partial x + \partial v/\partial y)$	10^{-9} sec^{-1}	10^3 km	0.1-1 km
Vertical divergence $(\partial w/\partial z)$	10^{-9} sec^{-1}	10^3 km	0.1-1 km
Vertical pressure gradient $(-\rho g)$	10^3 gm^{-2} sec^{-2}	--	--
Thermal expansion $(-\alpha T)$	10^{-3}	--	--
Vertical heat diffusion $(\kappa \partial^2 T/\partial z^2)$	10^{-9} deg sec^{-1}	10^3 km	1 km

Q.2.3 Characteristic Structure

Internal currents are generally less strong than the surface currents, although they extend through a much greater volume of water. The maximum speed of internal or thermohaline currents is usually found close to the continents' western shores, where speeds of the order of 10 cm sec^{-1} have been reported at about 3000 m depth [2]. In the central portions of the open oceans, speeds of 1 cm sec^{-1} are more common. In overall pattern, these currents are thought to consist of an intense western boundary current and a much weaker poleward flow over the bulk of the ocean basin, coupled with a general rising motion of the order of 1 cm day^{-1}. This overall circulation is apparently driven by an intense surface cooling and consequent sinking in the North Atlantic and in the Weddel Sea. The total water transported by these thermohaline currents has been estimated to be of the order of $10\text{–}40 \times 10^6$ m^3 sec^{-1} [3,4], which is comparable to that of the major surface currents. The direct observational evidence of the internal currents is at present still quite limited, and the above broad description is dictated as much by physically-reasonable theory as by actual measurement.

Q.3.0 ASSESSMENT OF GEOPHYSICAL ENERGY

Q.3.1 Energy Budget

Denoting kinetic energy by K, internal (plus potential) energy by I, and an energy dissipation process by D, the energy budget of the internal ocean currents may be sketched as below.

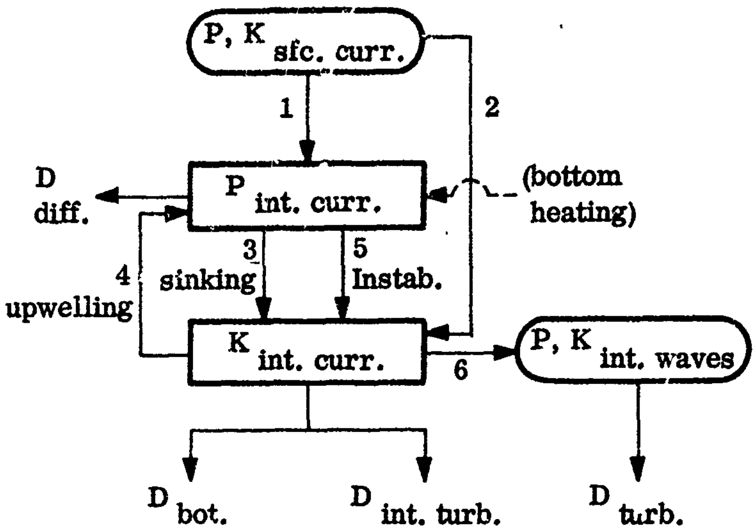

Fig. Q-1. Schematic energy budget.

Q.3.1.1 Storage Estimates

(a) $P_{int.\ curr.}$ = potential (plus internal) energy of internal currents. Assuming that the internal currents are in approximate geostrophic equilibrium (except in the western boundary regions), we may estimate that the potential and kinetic energies are of the same order of magnitude. The potential energy appears in the equilibrium configuration of the internal temperature field, of which only a crude estimate can be made. Assuming a characteristic density difference across the main thermocline (separating surface waters from deep water) $\Delta\rho \simeq 10^{-3}\ \rho_0$, where ρ_0 is an average value, we have

$$P_{int.\ curr.} \simeq \rho_0\ (g\ \frac{\Delta\rho}{\rho_0})\ (h^2).$$

$$\text{Area} = \frac{1\text{g}}{\text{cm}^3} \left(\frac{1\ \text{cm}}{\text{sec}^2}\right) (10^4\ \text{m}^2) \cdot 3 \times 10^8\ \text{km}^2;$$

$$P_{\text{int. curr.}} = 7.5 \times 10^{16}\ \text{cal.}$$

Here we have assumed a root-mean-square perturbation of 10 m for the density interface, and taken the area as that at the 2000 m level in the world's oceans.

(b) $K_{\text{int. curr.}}$ = kinetic energy of internal currents. We may assume that the kinetic energy of the strong internal currents at the oceans' western boundaries is approximately equal to that of the slower (geostrophic) internal currents over the remainder of the oceans' bulk. Selecting the latter for estimation, we have

$K_{\text{int. curr.}} = 1/2\ \rho_0\ |\vec{V}|^2 \cdot \text{Area} \cdot \text{depth}$; assuming $\rho_0 = 1\ \text{g cm}^{-3}$, $|\vec{V}| = 5\ \text{cm sec}^{-1}$ over a depth of 4000 m and an area of $3 \times 10^{18}\ \text{cm}^2$ (2000 m area), we find the estimate

$$K_{\text{int. curr.}} = 5.8 \times 10^{16}\ \text{cal.}\ ^*$$

(c) $P, K_{\text{sfc. curr.}}$ = kinetic and potential (plus internal) energy of the surface currents. Assuming $|\vec{V}| = 50\ \text{cm sec}^{-1}$ over a depth of 200 m and an area of $3 \times 10^{18}\ \text{cm}^2$, we have the estimate

$$P, K_{\text{sfc. curr.}} = 4.5 \times 10^{17}\ \text{cal.}$$

This estimate assumes equipartition between the kinetic and potential (plus internal) energy, appropriate to geostrophic surface currents; the potential energy here represented is, of course, the available potential energy. The contribution of the western surface boundary currents and of the near-surface equatorial undercurrents is one-third of the total figure given.

*If the kinetic energy of the equatorial undercurrents (whose velocity maximum, however, occurs at about 100 m depth and hence are more properly "surface" currents) is included, this estimate is raised by about 50%.

(d) $P, K_{int.\ waves}$ = potential and kinetic energy of internal waves. This energy would be indistinguishable from that of the internal currents on a local scale, and is doubtless more variable in both space and time. Assuming equipartition between the potential and kinetic energy, we may estimate a density difference $\Delta\rho = 10^{-4}\ \rho_0$, a mean-square wave height $(\overline{h^2}) = 10^{+2}\ m^2$, and an effective area of 10% of the oceans' 2000 m area. Hence,

$$P, K_{int.\ waves} = 1.5 \times 10^{13}\ cal.$$

Q.3.1.2 Transformation Rate Estimates

(a) ① = energy transmission rate due to the downward diffusion of thermal energy from the surface layer. Under equilibrium conditions, we may estimate this rate as $\rho c \times$ Area $\times$ Depth $\times\ \partial^2 T/\partial Z^2$. Assuming $\partial^2 T/\partial Z^2 \simeq 1$ deg $(km)^{-2}$ as a value appropriate in the main thermocline beneath the surface layer, assuming the specific heat $c = 1$ cal g^{-1} deg^{-1}, and taking an effective ocean area of $3 \times 10^{17}\ cm^2$ and a depth of 1 km for the transmission process, we have

$$① = \frac{1 g}{cm^3} \times \frac{1\ cal}{g\ deg} \times 3 \times 10^{17}\ cm^2 \times 1\ km \times \frac{1\ cm^2}{sec}\ \frac{1\ deg}{km^2};$$

$$① = 3 \times 10^{12}\ cal\ sec^{-1}$$

Here we have also assumed a value $x = 1\ cm^2\ sec^{-1}$, according to recent studies [5].

(b) ② = energy transmission rate due to the wind-induced convergence in the surface Ekman layer. Assuming a downward vertical motion $w_e = 10^{-5}$ cm sec^{-1} at the base of the Ekman layer [3, 5, 6] as characteristic of, say 50% of the oceans' area, we may estimate 2 from the downward vertical advection of kinetic energy $w_e\ \partial K/\partial Z$ as ② = $1/2\ \rho$ Area $\times\ w_e \times \Delta|\vec{V}|^2$, where $|\vec{V}|^2$ is the change of squared speed through the surface layer $\simeq |\vec{V}|^2$ sfc. Hence, taking $\vec{V}_{sfc.} = 50$ cm sec^{-1}, we find

$$② = 4.7 \times 10^{8}\ cal\ sec^{-1}$$

This vertical advection of kinetic energy is evidently an important process for the kinetic energy of the internal currents, and bypasses the intermediate stage of potential and internal energy.

(c) (3) = energy transformation rate due to the sinking of upper water masses to the deep ocean, through the combined action of surface cooling due to radiation and heat conduction to a cold overlying atmosphere. This formation of dense bottom water is believed to occur principally in a restricted region of the North Atlantic and in the Weddell Sea off Antarctica [3]. We may estimate the energy transformation rate of this process as

$$(3) \doteq 1/2\, \rho_0\ (\text{sinking volume transport})^3 \times (\text{area})^{-2}.$$

Assuming a total sinking transport of $20 \times 10^6\ m^3\ sec^{-1}$ [3] over an area of 0.01% ($30{,}000\ km^2$) of the oceans' 2000 m area, we find the estimate

$$(3) \doteq 4.5 \times 10^3\ \text{cal sec}^{-1}$$

This process is thought to represent the major driving force of the oceans' abyssal circulation [3, 7], and the above estimate is compatible with an average sinking speed of $0.1\ cm\ sec^{-1}$.

(d) (4) = energy transformation rate of the general upwelling motion of the large-scale internal currents. This process occurs over the bulk of the oceans, and is the compensation to the volume transport of the intense localized sinking of (3) above. From the estimate for (3) , we may here estimate

$$(4) = 4.3 \times 10^{-5}\ \text{cal sec}^{-1}$$

This is evidently an exceedingly weak link in the kinetic energy balance process, due to the participation of so large a volume of water. The general rising vertical motion associated with this process is of the order of $10^{-5}\ cm\ sec^{-1}$.

(e) (5) = energy transformation between the kinetic energy of internal currents and the potential (plus internal) energy of the internal stratification. This transformation is analogous to that accompanying baroclinic instability in the atmosphere, and is accomplished by the systematic rising of the warmer

fluid Relatively little study has been given to the possible presence or role of such internal oceanic disturbances, although there is mounting evidence of marked spatial and time variability of the interior ocean currents [8]. No direct estimate is available for this transformation, although we might make an estimate by analogy with the atmosphere. Assuming that the ratio between the rate of potential-to-kinetic energy transformation in the atmosphere and ocean is approximately equal to the corresponding ratio between the total kinetic energies (involving the implicit assumption that the present transformation is a major source of the kinetic energy), we may write

$$⑤ = ⑤_{\text{atmos.}} \left(\frac{\text{mass ocean}}{\text{mass atmos.}}\right) \frac{|\vec{V}\ \text{ocean}|^2}{|\vec{V}\ \text{atmos.}|^2}.$$

Assuming the ratio of masses is about 300, and taking $\vec{V}$ ocean = 10 cm sec^{-1}, $\vec{V}$ atmos. = 10 m sec^{-1}, and using the value $⑤_{\text{atmos.}} = 10^{14}$ cal sec^{-1}, [9], we find

$$⑤ = 3 \times 10^{12} \text{ cal sec}^{-1}$$

(f) ⑥ = energy transformation rate between the kinetic energy of internal currents and the energy of internal waves. No direct estimate is available, although it would appear reasonable that there is an energy flux to the internal waves. This process may be viewed as a form of energy dissipation with respect to the internal currents, although it seems likely that it plays a relatively minor role in the total dissipation of the internal currents' kinetic energy.

Q.3.1.3 Dissipation Rate Estimates

a) $D_{\text{bot.}}$ = frictional dissipation at the sea bottom. We may estimate this dissipation from the general recognition that the bottom stress is about 0.03 times that at the sea surface [10]. Hence, we may take $\vec{\tau}_{\text{bot.}} \simeq 0.03$ dyne cm^{-2}, and write $D_{\text{bot.}} = |\vec{V}|\ \vec{\tau}_{\text{bot.}} \times$ Area, or

$$D_{\text{bot.}} = 1.5 \times 10^{9} \text{ cal sec}^{-1}$$

Here we have used the estimates $|\bar{V}|_{bot.} = 2$ cm sec^{-1}, and taken the area as 10^{18} cm^2.

b) $D_{int. turb.}$ = kinetic energy dissipation by internal turbulence. Probably the most reasonable estimate available is that obtainable from the statement that $D_{int. turb.}$ is responsible for about one-fourth the dissipation of kinetic energy as is $D_{bot.}$ [1]. Hence, we have the estimate

$$D_{int. turb.} = 3.8 \times 10^8 \text{ cal sec}^{-1}$$

This estimate is compatible with a value of the lateral eddy viscosity coefficient $A = 6 \times 10^7$ cm^2 sec^{-1} in the formula $D_{int. turb.} = \text{volume} \cdot \rho \cdot A \nabla^2 v \cdot \bar{v}$ when $\nabla^2 v = 10^{-16}$ cm^{-1} sec^{-1} and $\bar{v} = 2$ cm sec^{-1}. This is within the usually reported range of 10^6–10^8 cm^2 sec^{-1} [11].

c) $D_{diff.}$ = dissipation of internal (thermal) energy associated with internal currents by turbulent diffusion. Although no very precise estimate is available, we may proceed as in transformation (1): and write

$$D_{diff.} = \rho c \cdot \text{volume} \quad \kappa \frac{\partial^2 T}{\partial Z^2},$$

where ρ = density, and c = specific heat. Assuming $\rho = 1$ gcm^{-3}, c = 1 cal g^{-1} deg^{-1}, $\kappa = 0.1$ cm^2 sec^{-1}, $\partial^2 T/\partial Z^2 = 0.1$ deg km^{-2}, and taking the oceanic volume as 1.2×10^{24} cm^3, we find the estimate

$$D_{diff.} = 1.2 \times 10^{12} \text{ cal sec}^{-1}$$

This diffusive heat loss may be compared with the heat addition at the sea bottom, which is of the order of 0.09 cal cm^{-2} day^{-1} [12]. For an oceanic bottom area of 10^{18} cm^2, this represents an energy input of approximately 10^{12} cal sec^{-1}.

d) $D_{turb.}$ = turbulent dissipation of internal wave energy. Since there is relatively little direct evidence of the structure and amplitude of internal waves in the deep sea, it is difficult to estimate their rate of dissipation. From the

decay estimate of long internal waves relatively near the surface [13], we may form the estimate

$$D_{turb.} \doteq 7.5 \times 10^{7} \text{ cal sec}^{-1}$$

Here we have used the previously estimated total internal wave energy $(P, K_{int. waves})$. This estimate is compatible with a dissipation of all internal wave energy in about 2.3 days, if no wave-producing mechanisms operated.

Q.3.2 Instabilities

The internal ocean currents have been investigated in only a very small portion of the oceans' bulk, and no doubt an increasingly complex picture will come to light as exploration continues. On the basis of those few deep current measurements now available (almost all of which are in the western North Atlantic), it appears safe to estimate that a large-scale system of such bottom and intermediate-depth currents exists in the world's oceans. From the present measurements [8], these deep currents appear to be just as variable in space and time as are the more familiar surface currents. Whether or not these variations are actual instabilities or the result of wave disturbance propagation or other effects is not known. There has been a general tendency, however, to regard the internal currents as a relatively stable phenomenon of primarily thermal origin, with a time constant or response time of many years [3, 14].

Q.4.0 MODIFICATION OR CONTROL FEASIBILITY

Q.4.1 Force and/or Energy Interference

As a preliminary to consideration of energetic interference, let us first examine a summary of the energy budget of the internal currents and closely related effects. In the diagram below, the energy transformations and dissipations are in units of 10^9 cal sec^{-1}.

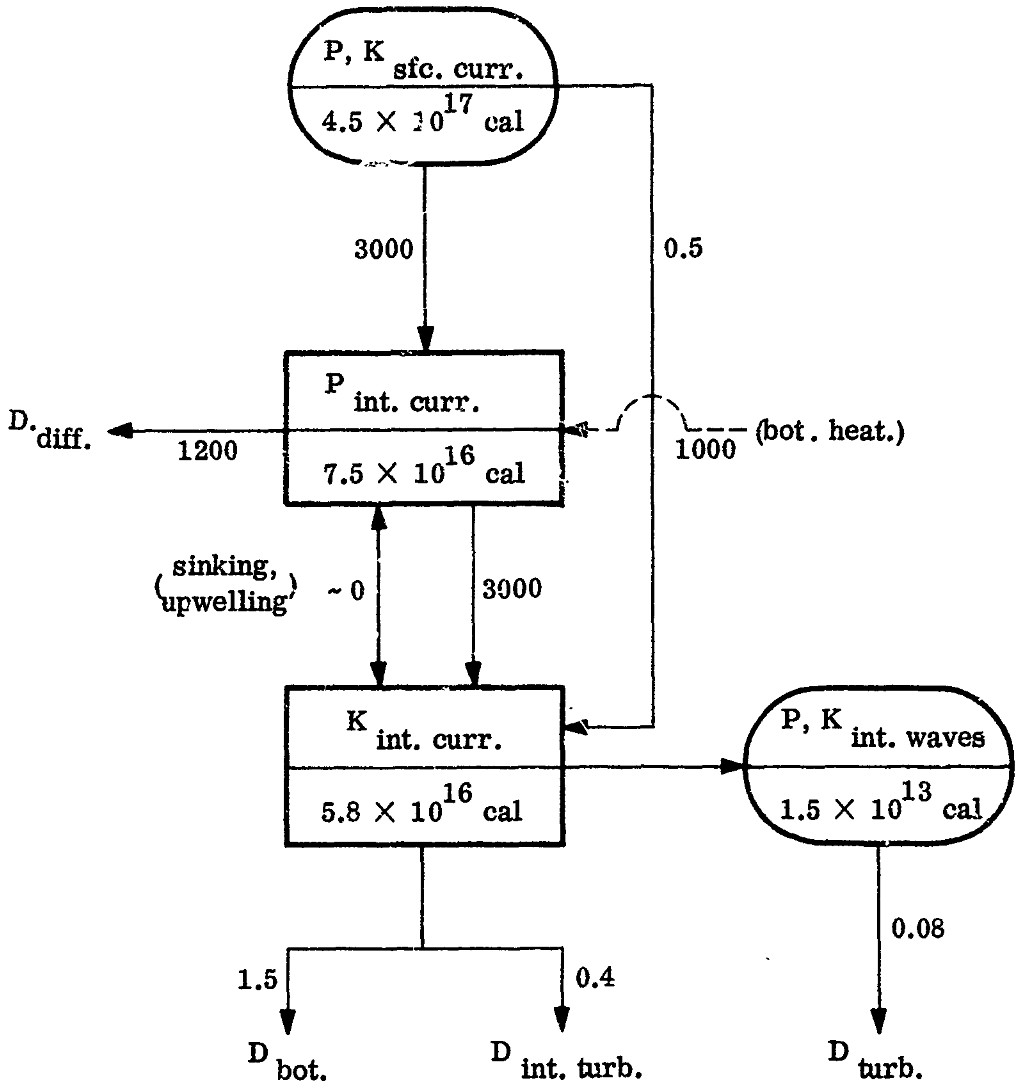

Fig. Q-2. Summary of energy budget.

Q.4.1.1 Direct Interference

A direct energetic interference with the internal currents does not appear feasible for at least three reasons: the relatively large magnitude of the currents' energy, the organization of this energy in a world-wide pattern, and the uncertainty surrounding the distribution and behavior of these currents. The cost and difficulty of the erection of deep sea barriers, for example, appear more than sufficient to rule such schemes out of practical consideration. Direct interference schemes in general here appear to be particularly impractical in view of the very slow and sluggish behavior of the internal currents.

Q.4.1.2 Indirect Interference

From the energy budget summarized above, it is apparent that the energy source for the internal currents is within the surface water layers, so that any alteration of the surface properties might be expected to have repercussions in the interior. The deep ocean currents appear to be driven or pumped primarily by the thermal energy source of the relatively warm upper mixed layer, and the accompaying downward diffusion of heat and momentum [3, 4]. The overall pattern of deep and bottom currents appears, moreoever, to be driven by intense sinking in two relatively small areas: one in the North Atlantic and one in the Weddell Sea. Although this mechanism evidently carries little energy, it accounts for the bulk of the deep water later set in motion as internal currents. It is thus conceivable that control or alteration of these cold bottom water source regions would alter the deep current pattern. At the same time, however, it is also evident that bottom water will always be formed somewhere, and new surface source areas would hence be called into play, with possibly only a negligible influence on the internal currents [5]. It may be concluded that even indirect alteration of the internal currents is not feasible.

Q.4.2 Promotion or Suppression of Critical Conditions

So little is known concerning the overall dynamics of internal currents that it is difficult even to identify conditions critical to their existence and/or behavior. Probably one could cite the existence and structure of the main oceanic thermocline itself as critical to the thermodynamic basis of the internal currents. The

removal or major alteration of this feature would require a fundamental overhaul of the ocean's heat balance and probably of the atmosphere's as well. The strength of the internal currents and of the all-important associated vertical motion can be shown, on a steady state linear basis at least, to be quite sensitive to the strength of the assumed vertical turbulent mixing through the thermocline [15].

A more specific process which may be considered critical to the internal currents is the evidently major energetic role played by internal baroclinic instability. Again, however, this phenomenon rests in the large-scale thermal structure of the oceans, and alteration is not immediately suggested. A major portion of the large-scale internal currents appear to be governed by advective thermal processes [16], and it is just the non-linear character of this effect which makes speculation on critical conditions so difficult.

Q.4.3 Survey of Simulation and Predictive Capabilities

Q.4.3.1 Theoretical

The systematic theoretical study of internal currents may be regarded as having begun with studies of the oceanic thermocline [17], and the associated field of vertical motions required to maintain it. This is generally viewed as an upward current in the open ocean, balancing the generally downward motion induced by the convergent Ekman layer [18]. By coupling a prescribed (although realistic) distribution of such vertical motion beneath the thermocline to the world-wide deep ocean currents, a schematic distribution of internal currents may be constructed [3, 6, 7]. Viewed as driven by concentrated high-latitude sources, these currents display an intense western boundary flow, southward in the North and South Atlantic and northward in the Pacific to the latitude of Japan. Some recent observational evidence supports these speculations [2], although they are based upon the hypothesis of steady frictionless currents. The present theory can account quantitatively for only the gross picture of the vertical motions associated with the internal currents [19]; the distribution of horizontal currents is at present largely qualitative, although shrewdly designed to correspond to known simple theoretical current systems on a sphere [20]. All of the theoretical studies of the internal currents to date have been made for linearized steady

conditions, and are consequently not applicable to the study of possible transient or instability effects. A predictive capability cannot be said to exist.

Q.4.3.2 Experimental

The overall circulation pattern of deep and bottom currents has been modeled in an oceanic sector of uniform depth through the proper arrangement of (homogeneous) water sources and sinks [21]. The results are qualitative, but they do support the general notion of a deep western boundary current (controlled by the β-effect), and show a more-or-less large-scale return drift in the interior. More precise simulation of the oceanic case is made difficult by the prominence of the bottom Ekman frictional layer in the experiments, and a quantitative predictive capability cannot now be said to exist.

Q.4.4 Research Required for Further Control or Modification Feasibility Assessment

Q.4.4.1 Theoretical

Much further theoretical research is needed on every aspect of internal currents; in general, they are on a much less secure theoretical basis than are the surface or wind-driven currents. The removal of the common assumptions of steady, linearized and generally frictionless motion is needed, and consideration should also be given to the effects of bottom topography and to the deep water effects of sea-surface slope. The details of the deep-water thermal structure are also virtually unstudied. A major need is the direct dynamic coupling of the internal (thermohaline) currents with the purely wind-driven currents. This interaction appears to be an essentially non-linear process, and the solution of appropriate models on high-speed computers should prove a fruitful approach.

Q.4.4.2 Experimental

The experimental simulation of internal ocean currents has thus far been confined to highly idealized geometry and the use of homogeneous fluid; removal of these approximations would certainly represent a significant step toward a greater simulative capability. Experimental studies should also be directed to the problem of inducing appropriate thermal circulations in the laboratory, and to the problem of bottom topography. Of particular interest would be an

experimental verification of the gross structure of the oceanic thermocline in view of its evident close relation to the internal currents. In all of these investigations, a system of quantitative measurements of the internal temperature and velocity field would be of great value.

Q.4.4.3 Observational

The direct observation of the internal currents in the ocean has barely begun, and it is quite essential that much further observational work be carried out in all the world's oceans. It would appear particularly important to verify further the hypothesized system of deep countercurrents, and to determine the actual flow over entire ocean basins. The use of deep floating buoys may be suitable for such work [22, 23]. If effort were focused on a single ocean basin, for example, the North Atlantic, an adequate documentation of the larger-scale features of the deeper currents might be obtained with a coordinated multiple-ship survey such as that employed for surveys of the surface Gulf Stream [24].

Q.5.0 REFERENCES

1. Veronis, G., and H. Stommel, "The Action of Variable Wind Stresses on a Stratified Ocean," J. Mar. Res. 15, 43-75, 1956.

2. Swallow, J. C., and L. V. Worthington, "An Observation of a Deep Countercurrent in the Western North Atlantic," Deep-Sea Res. 8, 1-19, 1961.

3. Stommel, H., and A. B. Arons, "On the Abyssal Circulation of the World Ocean - II. An Idealized Model of the Circulation Pattern and Amplitude in Oceanic Basins," Deep-Sea Res. 6,217-233, 1960.

4. Wyrtki, K., "The Thermohaline Circulation in Relation to the General Circulation in the Oceans," Deep-Sea Res. 8, 39-64, 1961.

5. Robinson, A., and H. Stommel, "The Oceanic Thermocline and the Associated Thermohaline Circulation," Tellus 11, 295-308, 1959.

6. Stommel, H., "The Abyssal Circulation," Deep-Sea Res. 5, 80-82, 1958.

7. ——, and A. B. Arons, "On the Abyssal Circulation of the World Ocean - I. Stationary Planetary Flow Patterns on a Sphere," Deep-Sea Res. 6, 140-154, 1960.

8. Crease, J., "Velocity Measurements in the Deep Water of the Western North Atlantic; Summary," J. Geophys. Res. 67, 3173-3176, 1962.

9. Saltzman, B., and A. Fleisher, "Spectrum of Kinetic Energy Transfer Due to Large-scale Horizontal Reynolds Stresses," Tellus 12, 110-111, 1960.

10. Francis, J. R. D., "A Note on the Velocity Distribution and Bottom Stress in a Wind-driven Water Current-system," J. Mar. Res., 12, 1, 1953.

11. Fofonoff, N. P., "Dynamics of Ocean Currents," The Sea, pp. 323-395, New York: Interscience. 1962.

12. Bullard, E. C., "The Flow of Heat Through the Floor of the Atlantic Ocean," Proc. Roy. Soc. A 222, 1954.

13. Rattray, M., Jr., "Propagation and Dissipation of Long Internal Waves," Trans. Am. Geophys. Un. 38, 495-500, 1957.

14. Stommel, H., "A Survey of Ocean Current Theory," Deep-Sea Res. 4, 149-184, 1957.

15. Tareev, B. A., "Contribution to a Theory of Convectional Circulation in Oceanic Deeps," Izv. Akad. Nauk. S.S.S.R., ser. geofiz., 7, 1022-1029, 1960.

16. Welander, P., "An Advective Model of the Ocean Thermocline," Tellus 11, 309-318, 1959.

17. Lineikin, P. S., "On the Determination of the Thickness of the Baroclinic Layer in the Sea," Doklady, Akad. Nauk. S.S.S.R. 101, 461-464, 1955.

18. Stommel, H., and G. Veronic, "Steady Convective Motion in a Horizontal Layer of Fluid Heated Uniformly from Above and Cooled Non-uniformly from Below," Tellus 9, 401-407, 1957.

19. Lineikin, P. S., "Wind and Thermal Circulation in the Ocean," Doklady, Akad. Nauk. S.S.S.R. 138, 1341-1344, 1961.

20. Goldsbrough, G. R., "Ocean Currents Produced by Evaporation and Precipitation," Proc. Roy. Soc. A 141, 512-517, 1933.

21. Stommel, H., A. B. Arons, and A. J. Faller, "Some Examples of Stationary Flow Patterns in Bounded Basins," Tellus 10, 179-187, 1958.

22. Swallow, J. C., "A Neutral-buoyancy Float for Measuring Deep Currents," Deep-Sea Res. 3, 74-81, 1955.

23. —, "Some Further Deep Current Measurements Using Neutrally-buoyant Floats," Deep-Sea Res. 4, 93-104, 1957.

24. Fuglister, F. C., and L. V. Worthington, "Some Results of a Multiple Ship Survey of the Gulf Stream," Tellus 3, 1-14, 1951.

APPENDIX R. TSUNAMI*

R.1.0 GENERAL DESCRIPTION

R.1.1 Phenomena Types

Tsunami are long waves in the ocean excited by sudden disturbances in the earth's crust caused by earthquakes, landslides, or submarine volcanic eruptions [1,2,3]. They are distinguished from surges by their much shorter period and by the fact that the latter are of atmospheric (wind) origin.

R.1.2 Characteristic Geographical Extent

Tsunami may occur in any of the world's oceans, but are most common in the Pacific. This is no doubt a result of the relatively great submarine volcanic and earthquake activity in this ocean. Some tsunami move across the entire ocean from the region of their origin, and on suitably exposed coasts may manifest themselves as an abnormally high and possibly destructive coastal wave (the popular "tidal wave").

R.1.3 Characteristic Process and Property Involvement

R.1.3.1 Basic Forces

Sudden faulting or slumping action on the sea floor associated with an earthquake or submarine volcanic eruption.

R.1.3.2 Modifying Factors

(a) water depth

(b) coastal configuration

(c) ocean basin shape

R.1.3.3 Property Transports

(a) coastal sediments

(b) surface kinetic energy

---

*By W. Lawrence Gates.

R.1.4 Characteristic Variations (life-cycle)

From their point or region of origin, tsunami spread rapidly outward across the ocean, and may even be reflected by the submarine continental boundaries. In the open sea, their height is usually small ($\sim$1 ft), but on exposed beaches or coasts, the tsunami wave height often reaches 30 ft. The first few waves are the largest, with periods of a few minutes, and are followed by lesser waves for several hours or even days [4]. The initial wave train is the result of the slight dispersion of the tsunami, while the later waves are probably due to refraction and/or reflection [5].

R.2.0 ASSESSMENT OF GEOPHYSICAL FORCES

R.2.1 Basic Physical Equations

(a) Equation of horizontal motion:

$$\frac{d\vec{V}}{dt} = - \frac{1}{\rho} \nabla p + \frac{1}{\rho} \frac{\partial \vec{\tau}}{\partial t} \qquad \text{(R-1)}$$

(b) Continuity equation:

$$\frac{d\rho}{dt} = - \rho \nabla . \vec{V} \qquad \text{(R-2)}$$

Here the symbols are defined as follows:

$\vec{V}$ = current velocity

ρ = water density

p = water pressure

$\vec{\tau}$ = frictional stress

z = vertical coordinate (upward)

R.2.2 Force Analysis

TABLE R-1
ESTIMATED FORCE MAGNITUDE AND SCALE

Force	Order-of-magnitude	Horizontal scale	Vertical scale
Pressure force $(-\frac{1}{\rho} \nabla p)$	$10^{-2} - 10^{-1}$ cm sec^{-2}	$10^2 - 10^4$ km	1 m – 4 km
Frictional force $(-\frac{1}{\rho} \frac{\partial \vec{\tau}}{\partial z})$	10^{-5} cm sec^{-2}	10^2 km	1 m – 4 km
Divergence $(\nabla \cdot \vec{V})$	~ 0	—	—
Density (ρ)	1 g cm^{-3}	10^4 km	4 km

R.2.3 Characteristic Structure

Tsunami are fast surface waves moving out from a point or line source, usually a faulting or slumping action in a submarine trench or trough [5, 6, 7, 8]. These impulsively generated waves behave as though the ocean were incompressible, and move with a speed of approximately 500 mph. Their wavelength is about 100 mi, so that tsunami behave as "shallow water" waves even in the open ocean. The amplitude of tsunami at sea is usually undetected and is of the order of 1 ft. Upon approaching shallow water at a coast, the tsunami waves are markedly slowed, inasmuch as their forward speed is given very nearly by $\sqrt{gh}$, where g is gravity and h is the water depth. This slowing results in a large amplitude increase as the waves crowd together and break, waves of over 100 ft height have been reported [8]. The local wave height is very strongly influenced by the local submarine topography, with the higher waves generally found near submarine ridges extending seaward perpendicular to the approaching tsunami wavefronts. A series of lesser waves usually follows the initially highest waves within a few hours, although some waves continue to be observed for days [4]. No net transports appear to be accomplished by tsunami except at the shore, where modification of the beach may be substantial [2].

R.3.0 ASSESSMENT OF GEOPHYSICAL ENERGY

R.3.1 Energy Budget

We may sketch the overall energy budget of tsunami as shown below.

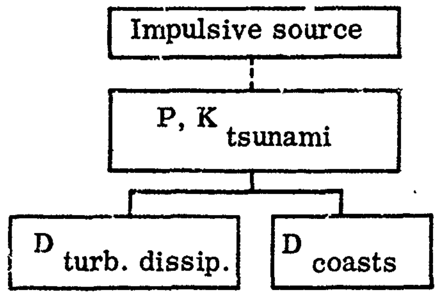

Figure R-1. Schematic energy budget.

R.3.1.1 Storage Estimates

$P, K_{tsunami}$ = total potential and kinetic energy of the tsunami wave train. Here both the potential and kinetic energy are considered together, as it may be assumed that the energy is approximately equally partitioned between them as in ordinary surface waves. Although there is no doubt great variation in total tsunami energy, estimates have been made for several of the better-documented occurrences. For the Alaskan tsunami of 9 March 1957, a total wave train energy of 2.5×10^{22} ergs has been estimated, while 7.5×10^{23} ergs has been given for the Chilean tsunami of 22–23 May 1960 [9]. Hence, we may take as an energy estimate for a major tsunami, the figure

$$\boxed{P, K_{tsunami} = 2 \times 10^{15} \text{ cal.}}$$

The energy of the parent crustal disturbance is quite difficult to estimate, although a figure of 10^{23} ergs has been suggested for the 9 March 1957 event [9].

R.3.1.2 Transformation Rate Estimates

None. The wave energy is continually being transferred between potential and kinetic energy at the surface as the wave progresses.

R.3.1.3 Dissipation Rate Estimates

(a) $D_{turb.\ dissip.}$ = the energy dissipation by means of internal and bottom turbulence. Tsunami often traverse the entire Pacific ocean with as much apparent energy as near the source region, and there is relatively little dispersive loss from the wave train in the deep ocean [8]. No direct evidence of tsunami-induced motion near the sea-bottom is available for deep water. Moreover, it seems unlikely that bottom friction would have much importance in this connection, in view of the likely decay of wave particle orbital speeds with depth and the small mid-ocean tsunami amplitudes. The progressive amplitude decrease of repeatedly reflected tsunami, however, provides a means for estimating the internal energy dissipation rate. Munk [4], for example, has shown that the tsunami wave energy decreases by approximately e^{-1} each 12 hr. Hence, we may form the estimate

$$\boxed{D_{turb.\ dissip.} = 2 \times 10^{10}\ \text{cal sec}^{-1}}$$

This energy loss rate also applies to the time interval between the originating disturbance and the tsunami's first coastal detection.

(b) D_{coasts} = tsunami energy dissipation on coasts. This dissipation accounts for the bulk of the energy of the wave train. If we assume that some of the tsunami wave energy is reflected from coasts [5], and hence accounting for the persistence of the wave train over several days on occasion, we may form an estimate of the minimum energy dissipation rate by coastal surf. Thus, assuming P, $K_{tsunami}$ is totally dissipated in, say, 10 hours on the average, we have

$$\boxed{D_{coasts} = 6 \times 10^{10}\ \text{cal sec}^{-1}}$$

Since most of the tsunami wave energy is often locally dissipated in the first few hours, the local rate of dissipation may be an order of magnitude greater than the above estimate. The above dissipation rate may also be considered to include an allowance for average trans-ocean travel time [10] at the nearly

constant group velocity $\sqrt{gh}$, where g is gravity and h the water depth.

R.3.2 Instabilities

Tsunami are the ocean's natural response to a sudden disturbance of the earth's crust, and as such they are a mechanism for the dispersal of the concentrated energy released by the earthquake, volcano or landslide. While certain factors favor their local enhancement, their dynamics display no geophysical instabilities.

R.4.0 MODIFICATION OR CONTROL FEASIBILITY

R.4.1 Force and/or Energy Interference

R.4.1.1 Direct Interference

Summarizing the tsunami energy budget as shown below, we may note that the total tsunami

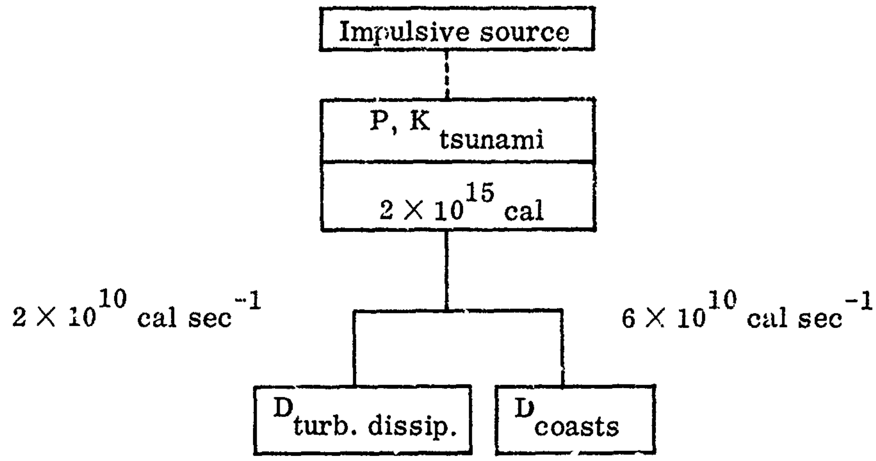

Figure R-2. Summary of tsunami energy budget.

energy is comparable to that available in atomic explosives (10 Kton bomb ~ 10^{15} cal). Hence, it is quite feasible to directly cause a tsunami by a suitably placed atomic or nuclear explosive in the ocean [11]. Once a tsunami, whether natural or artificial, has been initiated, there appears little that can be done on a direct basis to control it, other than minimizing its destructive coastal effects. The tsunami strength probably bears a direct relation to the intensity of the initial impulsive water displacement and to its geographical arrangement. Most natural tsunami appear to have line or areal sources along active fault zones or slumping regions [6, 7]. An artificial explosively-generated tsunami would be a point source of energy, and hence would have a different pattern of initial wave ray paths, and possibly a different regime of absorption and reflection.

R.4.1.2 Indirect Interference

The only apparent means of indirectly modifying a tsunami is through alteration of the local submarine topography. The height of the wave on shore, and hence its destructive power, is very much dependent upon the geometry of the local bottom contours over areas of the order of just a few kilometers. On a large scale (ocean-wide) glancing incidence of the tsunami wave train on the coast results in generally lower wave heights [8], while normal incidence is somewhat more favorable for higher waves. These general effects, however, may be very much modified by the refraction of waves around barriers and by their focussing onto specific shore locations. Observed coastal tsunami wave heights are highest near submarine ridges extending seaward, and lowest in bays [8]. The presence of off-shore reefs greatly reduces the wave height on the coast itself. Indirect interference with tsunami waves by appropriate design of shore barriers and harbor facilities is certainly feasible, as is the deliberate creation of tsunami by undersea explosions in areas close to vulnerable shore facilities.

R.4.2 Promotion or Suppression of Critical Conditions

There are no critical physical conditions associated with tsunami, other than the effects of water depth on tsunami wave propagation and height. See discussion under Section R.4.1.2 above.

R.4.3 Survey of Simulation and Predictive Capabilities

R.4.3.1 Theoretical

The theory of tsunami is reasonably well developed as is that of surface long (or shallow-water) waves in general. Once the tsunami wave train is excited, its movement can be predicted with reasonable accuracy: the waves' energy moves at the speed $\sqrt{gh}$ to within a few percent, where h is the water depth [10].

Following the tsunami of April 1946 in Hawaii, the U.S. Coast and Geodetic Survey established a tsunami warning service, by which vulnerable coastal areas are alerted following the detection of a severe earthquake in the Pacific seismic troughs. Unfortunately, of earthquakes of apparently identical seismic

intensity, only a portion actually give rise to tsunami [12]. Hence tsunami occurrence warnings from seismic evidence alone are often more precautionary than actually predictive. The U.S.C.G.S. Pacific warning system now depends upon recorded wave heights [13] at a number of ocean stations. The local tsunami wave height, however, is so highly dependent upon the local water depth pattern as well as upon the incidence angle of the oncoming wave train that it can be predicted with only moderate accuracy.

R.4.3.2 Experimental

Aside from the capability of creating artificial tsunami, an experimental simulation of tsunami behavior using electronic networks has recently been developed [14]. At the present time, however, such experimental studies are preliminary, and cannot be said to offer increased predictive ability.

R.4.4 Research Required for Further Control or Modification Feasibility Assessment

R.4.4.1 Theoretical

Further theoretical work is needed on the mechanisms of tsunami origin on the ocean floor, on the problem of the dissipation and absorption of tsunami wave energy, and on the details of the wave refraction and breaking in shallow water. The possible effects of the thermal stratification of the oceans on tsunami behavior also should be examined.

R.4.4.2 Experimental

Laboratory studies on tsunami causative mechanisms are needed, together with model studies in realistically shaped ocean basins. Such studies now assume even greater significance in view of the recent prohibition of underwater nuclear explosions. Since most of the tsunami energy is in wave periods of a few minutes, serious modeling problems may be encountered in simulation with fluid tanks. Further work with electric network simulation should also be pursued.

R.4.4.3 Observational

The tsunami recording network should be extended to greater parts of the world's oceans, both to increase the reliability of the tsunami warning system and to provide more data for research analysis. Stations both in the deep ocean and at ciritical off-shore locations should be considered.

R.5.0 REFERENCES

1. Miller, D. J., "The Alaska Earthquake of July 10, 1958: Giant Wave in Lituya Bay," Bull. Seism. Soc. Am. 50, 253–266, 1960.

2. Shepard, F. P., G. A. MacDonald, and D. C. Cox, "The Tsunami of April 1, 1946," Bull. Scripps Inst. Oceanog. Univ. Calif. 5, 391–528, 1950.

3. Unoki, S., and M. Nakano, "On the Cauchy–Poisson Waves Caused by the Eruption of a Submarine Volcano," Papers Meteorol. Geophys. 4, 139–150, 1953.

4. Munk, W. H., "Some Comments Regarding Diffusion and Absorption of Tsunamis," Bull. I. U. G. G., 1961.

5. Cochrane, J. D., and R. S. Arthur, "Reflection of Tsunamis," J. Mar. Res. 8, 239–251, 1948.

6. Gutenberg, B., "Tsunamis and Earthquakes," Bull. Seism. Soc. Am. 29, 517–526, 1939.

7. Houtz, R. W., "The 1953 Suva Earthquake and Tsunamis," Geol. Surv. Dept. Fiji Rep. No. 61, 1960.

8. Shepard, F. P., Submarine Geology, 2nd Ed., 557 pp., New York: Harper and Row, 1963.

9. van Dorn, W. G., and W. L. Donn, "Long Waves," Ann. I.G.U., 10:5, 1960.

10. Zetler, B. D., "Travel Times of Seismic Sea Waves to Honolulu," Pacific Sci. 1, 185–188, 1947.

11. Nakano, M., "Atomic Energy and the Oscillation of Sea Level," Res. in the Effects and Influences of the Nuclear Bomb Test Explosions, 401-407, 1955.

12. Ewing, M., I. Tolstoy, and F. Press, "Proposed Use of the T Phase in Tsunami Warning Systems," Bull. Seism. Soc. Am. 50, 253–266, 1950.

13. van Dorn, W. G., "A Portable Tsunami Recorder," Trans. Am. Geophys. Un. 37, 27–30, 1956.

14. Ishiguro, S., "A Method of Analysis for Long-wave Phenomena in the Ocean Using Electronic Networks Models. I. The Earth's Rotation Ignored," Phil. Trans. Roy. Soc. Lond. A251, 303–340, 1959.

APPENDIX S. OCEANIC VORTICES AND TURBULENCE*

S.1.0 GENERAL DESCRIPTION

S.1.1 Phenomena Types

Oceanic vortices of one type or another evidently exist on a very wide scale in the ocean, extending from the ocean-wide gyres of the wind-driven circulation to the very small scale eddies. On certain scales within this broad spectrum, the vortices may display a recognizable organization or coherence and be recognizable as individual phenomena, while these same disturbances may play the role of "turbulent eddies" with respect to larger-scale vortices.

S.1.2 Characteristic Geographic Extent

Oceanic vortices occur in all the oceans, although certain types appear to be more common in some locations. Below are summarized the characteristic space scale and characteristic geographical location of the identifiable oceanic vortices.

TABLE S-1
CHARACTERISTIC SPACE SCALE AND GEOGRAPHICAL LOCATION OF IDENTIFIABLE OCEANIC VORTICES

Vortex phenomenon	Characteristic space scale	Characteristic location
1. Large-scale wind-driven gyres	10^3–10^4 km	all oceans
2. Large-scale convective eddies	10^3–10^4 km	all oceans
3. Surface current meanders [1, 2, 3, 4, 5, 6]	10–10^3 km	all oceans but especially western portions
4. Internal current meanders	10^2 km	all oceans
5. Surface topographic eddies	1–10^2 km	coasts and convergence regions
6. Submarine topographic eddies	1–10^2 km	all oceans
7. Tidal current vortices	1–10^2 km	all, but especially coasts
8. Inertial current vortices	1–10^2 km	all oceans except equatorial regions

*By W. Lawrence Gates.

Vortex phenomenon		Characteristic space scale	Characteristic location
9.	Internal wave vortices	10m–10 km	all oceans
10.	Small-scale convective eddies	10m–1 km	all oceans
11.	Sea surface wave eddies	1–10 m	all oceans
12.	Finer grain turbulence	1 m	all oceans

S.1.3 Characteristic Process and Property Involvement

S.1.3.1 Basic Forces

The basic forces responsible for oceanic vortices and turbulence are those dynamic and thermal forces causing oceanic motion in general, on all scales.

S.1.3.2 Modifying Factors

All dynamic, thermal and geographic factors at play in the oceans may be considered modifying factors for vortex and turbulence production. Of particular significance are the effects of water depth, coastal configuration, variable wind stress, and variable surface thermal energy balance.

S.1.3.3 Property Transports

All properties of and suspended materials in the oceans are in some way transported by oceanic vortices and turbulence. Of particular importance are the transports of heat, mass, momentum, salt and dissolved oxygen.

S.1.4 Characteristic Variations (life-cycle)

Oceanic vortices display a wide spectrum of time variation or period, as well as a variation in their relative frequency of occurrence. These properties are summarized below for the vortex phenomena previously identified.

TABLE S-2
CHARACTERISTIC TIME SCALE AND
OCCURRENCE ESTIMATES

	Vortex phenomenon	Characteristic time scale	Characteristic occurrence
1.	Large-scale wind-driven gyres	1 mo–1 yr	continuous
2.	Large-scale convective eddies	$1-10^2$ yr	continuous
3.	Surface current meanders [1, 4]	10 days	continuous
4.	Internal current meanders [7, 8]	$10-10^2$ days	continuous
5.	Surface topographic eddies	$1-10^2$ days	continuous
6.	Submarine topographic eddies [9]	10 days	continuous
7.	Tidal current vortices	10 hr	diurnal or semi-diurnal
8.	Inertial current vortices	10 hr	occasional
9.	Internal wave vortices [10]	$1-10^3$ min	frequent
10.	Small-scale convective eddies	$10-10^3$ min	frequent
11.	Sea surface wave eddies	1–10 sec	continous
12.	Finer grain turbulence	1 sec	continuous

S.2.0 ASSESSMENT OF GEOPHYSICAL FORCES

S.2.1 Basic Physical Equations

The equations basic to the formation and behavior of oceanic vortices and the process of turbulent dissipation include all the fundamental equations for the general and total description of the oceans. Hence, we may list the equations of motion, the continuity equation, the thermodynamic energy equation and an equation of state. Included in these formulations are the appropriate turbulent and frictional forces.

S.2.2 Force Analysis

All of the forces in the general dynamic equations may be regarded as important for vortex and turbulence production on some scale, and the magnitudes of these forces will show the same wide variations over many orders of magnitude as do the turbulent vortices themselves.

S.2.3 Characteristic Structure

Perhaps the simplest summary of the force-related structure of oceanic vortices is to estimate the size of the characteristic eddy diffusion coefficient. This term represents in a bulk fashion the frictional or turbulent forces, although here again we should expect a wide variation.

TABLE S-3
CHARACTERISTIC HORIZONTAL EDDY DIFFUSION COEFFICIENTS

Vortex phenomenon	Characteristic horizontal eddy diffusion coefficient ($cm^2\ sec^{-1}$)
1. Large-scale wind-driven gyres [11, 12, 13, 14]	10^6-10^{10}
2. Large-scale convective eddies	10^6-10^8
3. Surface current meanders [15, 12, 14]	10^5-10^8
4. Internal current meanders	10^5-10^6
5. Surface topographic eddies	10^5
6. Submarine topographic eddies	10^5
7. Tidal current vortices	10^5
8. Inertial current vortices	10^5
9. Internal wave vortices	10^3-10^4
10. Small-scale convective eddies	10^3
11. Sea surface wave eddies	10
12. Finer grain turbulence	< 1

In these estimates it has been assumed that the horizontal eddy diffusion coefficient is related to the characteristic space scale L of the vortex or turbulent phenomenon according to $L^{4/3}$, as would be the case if there were a statistically steady cascade of energy down the spectrum to the final dissipation by the fine grain turbulence. This relationship has specifically been used to estimate the coefficient for the vortex phenomena (see Table 5-2; 2. and 4.-12.). It has been suggested that this "$L^{4/3}$ law" applies to oceanic turbulence scales of 1 cm–1 m [16] and to those in the range 1–10 m [17]. More recently, it has been

suggested that such a relationship applies to the entire range of eddy scales from 10 cm to 1000 km [18].

For some of the organized oceanic vortices above, important turbulent eddy processes operate in the vertical direction. This is particularly the case for those phenomena whose characteristic horizontal dimensions are small compared to their vertical dimension. Estimates in these cases of the characteristic vertical eddy diffusion coefficient are given below.

TABLE S–4
CHARACTERISTIC VERTICAL EDDY DIFFUSION COEFFICIENTS

Vortex phenomenon		Characteristic vertical eddy diffusion coefficient ($cm^2\ sec^{-1}$)
9.	Internal wave vortices [15, 19]	1–30
10.	Small-scale convective eddies	10^2
11.	Sea surface wave eddies [20]	500–6000
12.	Finer grain trubulence	< 10

Here there is no apparent relationship of the eddy coefficient to scale size, and the values are strongly influenced by friction at the ocean surface and ocean bottom, as well as by the characteristic vertical structure of the ocean.

S.3.0 ASSESSMENT OF GEOPHYSICAL ENERGY

S.3.1 Energy Budget

S.3.1.1 Storage Estimates

In the case of those vortex phenomena which possess a characteristic structure, estimates of the total energy are given below.

If we assume that the energy of the turbulent vortices is distributed in a (statistically) steady fashion culminating in the final degradation into heat, the energy could be expected to be distributed over the various scale phenomena according to $L^{5/3}$, where L is the characteristic wavelength of the turbulent process [17, 23]. From these characteristic energy estimates, it appears that there are significant direct energy inputs to the vortex phenomena selected, with only an overall tendency for more turbulent energy to exist on the larger scales of flow.

TABLE S-5
CHARACTERISTIC STRUCTURE OF OCEANIC VORTEX PHENOMENA

Vortex phenomenon	Characteristic energy (cal)
1. Large-scale wind-driven gyres	10^{18}
2. Large-scale convective eddies	10^{17}
3. Surface current meanders	10^{17}
4. Internal current meanders	10^{17}
5. Surface topographic eddies [21]	10^{16}
6. Submarine topographic eddies	10^{16}
7. Tidal current vortices	10^{17}
8. Inertial current vortices	?
9. Internal wave vortices [22]	$10^{13}-10^{16}$
10. Small-scale convective eddies	?
11. Sea surface wave eddies	10^{16}
12. Finer grain turbulence [16]	10^{16}

S.3.1.2 Transformation Rate Estimates

None.

S.3.1.3 Dissipation Rate Estimates

According to the view taken above of the distribution of the eddy diffusion coefficient and the turbulent energy with respect to characteristic eddy scale, we may here assume that the apparent dissipations for one vortex phenomenon are the energy input for another of smaller scale. Hence, the total net energy dissipation by friction in oceanic vortices is estimated as [7].

$$\text{Net dissipation} = 10^{12} \text{ cal sec}^{-1}.$$

It should be again emphasized, however, that some of the identifiable vortex phenomena receive a direct input of energy without its passage down the spectral scale [23]. For example, the local wind field may excite local surface current patterns, or intense local surface cooling may initiate a convective overturning. The above estimate accounts

for only the purely frictional turbulent dissipation in such specific vortex phenomena, and is probably an underestimate.

S.3.2 Instabilities

Each of the considered oceanic vortex phenomena is the result of certain dynamical and physical conditions, and are not generally regarded as themselves displaying instability. The vortices, in fact, may be regarded as the result of an instability of a parent or superposed current or oceanic state.

S.4.0 MODIFICATION OR CONTROL FEASIBILITY

S.4.1 Force and/or Energy Interference

Because of the close energetic relations among the various classes and scales of vortex phenomena, direct or indirect interference with one particular phenomenon would have effects on others as well. For this reason, in addition to the rather large amounts of energy involved, modification of oceanic vortex and turbulent phenomena is not in general considered feasible. In a number of instances, certain interference measures suggest themselves, however. Here we may mention the possible erection of surface and/or submarine barriers to deflect surface and/or internal currents, the forced vertical mixing of water to alter the density and/or temperature stratification supporting internal waves and convective eddies, and the reduction of the sea surface stress to suppress surface wind waves. On a local scale and for limited periods of time, it is possible that interference with phenomena of corresponding scales could be successfully accomplished, but the broader-scale effects of so doing cannot be now estimated.

S.4.2 Promotion or Suppression of Critical Conditions

See Section S.4.1.

S.4.3 Survey of Simulation and Predictive Capabilities

A theoretical and experimental basis for a number of the oceanic vortex phenomena now exists or is under development (see Table S–6).

The only phenomena (of Table S–6) for which an adequate predictive capability could be said to exist are the tidal current eddies (entailing the prediction of the tidal current itself), and the sea surface wave eddies (depending upon prediction of the surface wind). The term "adequate" in other cases indicates that the

TABLE S-6
STATUS OF THEORETICAL AND EXPERIMENTAL PREDICTIVE CAPABILITIES FOR OCEANIC VORTEX PHENOMENA

	Vortex phenomenon	Theoretical basis	Experimental basis
1.	Large-scale wind-driven gyres	Adequate [13]	Adequate [24]
2.	Large-scale convective eddies	Tentative [25]	-
3.	Surface current meanders	Tentative [6]	Tentative [24]
4.	Internal current meanders	-	-
5.	Surface topographic eddies	Tentative [6]	Tentative [24]
6.	Submarine topographic eddies	Tentative [6]	-
7.	Tidal current eddies	Adequate	Adequate [24]
8.	Inertial current eddies	Adequate	-
9.	Internal wave vortices	Tentative [22]	-
10.	Sea surface wave eddies	Adequate [26]	-
11.	Finer grain turbulence	Tentative [15]	-

general pattern of the vortex phenomenon is well depicted by theory or experiment, while "tentative" indicates only a beginning in this direction. No significant simulation by either theory or experiment is indicated by a dash.

S.4.4 Research Required for Further Control or Modification Feasibility Assessment

S.4.4.1 Theoretical and Experimental

The above survey of the simulation and predictive capability for oceanic vortex phenomena serves as a convenient guide to those areas where further theoretical and experimental research is needed. We may note particularly the lack of suitable experimental capability for most phenomena, and a general need for further theoretical research on a number of scales. In particular, those phenomena related to the interior or deep ocean are inadequately understood, and the thermal-dynamic interactions in all phenomena need further attention.

S.4.4.2 Observational

Perhaps the greatest hindrance to a more adequate modification or control assessment is the general paucity of suitable observations for most of the oceanic

vortex phenomena. This is particularly true for the internal oceanic vortices and those in the deep sea. The relatively few observations available suggest a marked variability, with significant and widespread departures from a supposed mean state [21, 27]. Observational programs, moreover, have to be rather carefully designed to resolve adequately the scale of the phenomena sought, and should not be expected or interpreted to apply to other vortex scales. The question of the energetic relationships in the spectrum of oceanic vortices and their roles as turbulent phenomena is fundamentally involved here, and observational programs must be designed accordingly [28, 29].

S.5.0 REFERENCES

1. (Anonymous), "Oceanic Eddies," Commercial Fisheries Review, Bur. Comm. Fish., Washington, D.C., August, 1963.

2. (Anonymous), "Changes in Kuroshio Current," Ocean Science News 5:23, p. 1, Washington, D.C.: Nautilus Press, 16 August 1963.

3. Fuglister, F.C., "Alternative Analyses of Current Surveys," Deep-Sea Res. 2:213-229, 1955.

4. ——, and L.V. Worthington, "Some Results of a Multiple Ship Survey of the Gulf Stream," Tellus 3, 1–14, 1951.

5. von Arx, W.S., D.F. Bumpus, and W.S. Richardson, "On the Fine-Structure of the Gulf Stream Front," Deep-Sea Res. 3:46-65, 1955.

6. Warren, B.A., "Topographic Influences on the Path of the Gulf Stream," Tellus 15:167-183, 1963.

7. Dietrich, G., General Oceanography, p. 154, 588pp., New York: Interscience, 1957.

8. Swallow, J.C., and B.V. Hamon, "Some Measurements of Deep Currents in the Eastern North Atlantic," Deep-Sea Res. 6:155-168, 1960.

9. Robinson, A., and H. Stommel, "Amplification of Transient Response of the Ocean to Storms by the Effect of Bottom Topography," Deep-Sea Res. 5:312-314, 1959.

10. Mosby, H., "Bottom Current Fluctuations in the Open Sea," Assoc. Ocean. Phys. Proc. Verb. 5:195, 1951.

11. Hidaka, K., and M. Tsuchiya, "On the Antarctic Circumpolar Current," J. Mar. Res. 12, 214–222, 1953.

12. Ichiye, T., "A Note on the Horizontal Eddy Viscosity in the Kuroshio," Rec. Oceanogr. Works Japan 3:16-25, 1957.

13. Munk, W.H., "On the Wind Driven Ocean Circulation," J. Meteorol. 7:79-93, 1950.

14. ——, "Lateral Eddy Diffusivity in the Gulf Stream System," Deep-Sea Res. 3:88-90, 1955.

15. Bowden, K.F., "Turbulence," The Sea, pp. 802-825, New York: Interscience, 1962.

16. Patterson, A.M., Development of Hot-wire Instrument for Ocean Turbulence Measurements, Tech. Mem. 57-2, Pacific Nav. Lab., 1957.

17. Ozmidov, R.V., "Experimental Investigation of Horizontal Turbulent Diffusion in the Sea and in A Shallow Artificial Reservoir," Izv. Akad. Nauk SSSR, Ser. Geofiz. 6:756-764, 1957.

18. Olson, F.C.W., and T. Ichiye, "Horizontal Diffusion," Science 130,1255, 1959.

19. Wüst, G., "Stromgeschwindigkeiten im Tiefen-und Bodenwasser des Atlantischen Ozeans auf Grund dynamischer Berechnung der Meteor—Profile der Deutschen Atlantischen Expedition 1925-27," Deep-Sea Res. Supp. to 3:373-397, 1955.

20. Kitaigorodskii, S.A., "The Coefficient of Vertical Turbulent Exchange in the Sea," Izv. Akad. Nauk SSSR, Ser. Geofiz. No. 9, 1118-1132, 1957.

21. Crease, J., "Velocity Measurements in the Deep Water of the Western North Atlantic; Summary," J. Geophys. Res. 67:3173-3176, 1962.

22. Cox, C.S., "Internal Waves," The Sea pp. 752-763, New York: Interscience, 1962.

23. Stommel, H., "Horizontal Diffusion Due to Oceanic Turbulence," J. Mar. Res. 8:199-225, 1949.

24. von Arx, W.S., "An Experimental Approach to Problems in Physical Oceanography," Physics and Chemistry of the Earth, vol. 2, pp. 1–29, New York: Pergamon, 1957.

25. ———, "A Survey of Ocean Current Theory," Deep-Sea Res. 4:149-184, 1957.

26. Pierson, W.J., Jr., Practical Methods for Observing and Forecasting Ocean Waves by Means of Wave Spectra and Statistics, H.O. Publ. 603, U.S. Navy, Washington, D.C., 1955.

27. Swallow, J.C., "Some Further Deep Current Measurements Using Neutrally-Buoyant Floats," Deep-Sea Res. 4:93-104, 1957.

28. Blackburn, M., "Unmanned Moored Station Systems for Oceanography and Meteorology," Trans. Am. Geophys. Un. 44:595-598, 1963.

29. ———, "Varieties of Oceanographic Experience," Science 139:572-576, 1963.

APPENDIX T. SOIL TRAFFICABILITY*

T.1.0 Discussion

The ability of wheeled or tracked vehicles to traverse land surface (off-road) is of considerable importance in military operations and is a matter in which there are numerous considerations. Generally speaking, the performance capability of a given vehicle depends on its mechanical features and the land features—terrain, surface conditions (e.g., vegetation), and the soil's physical characteristics. Herein, consideration shall be given primarily to the soil's physical characteristics as they relate to trafficability and in turn to geophysical processes or factors. It will be assumed that the soil surface geometry (terrain) and surface conditions are constant and that the vehicle mechanical design features are specified, the aim being to consider means of altering soil physical properties to enhance its capability to support vehicular traffic.

Bekker [1] has proposed that a statistical value of soil trafficability (ST) may be determined with the following expression:

$$(ST) = f(\gamma, C, \phi, k, n, K_1, K_2, h_w, l_d, l_w, h) . \qquad \text{(T-1)}$$

where γ, ϕ, and C express specific gravity, friction, and cohesion, respectively; k, n, K_1, and K_2 are soil structural constants; and the last four (h_w, l_d, l_w, and h) specify the terrain roughness. Actually, this expression serves as a definition of that portion of trafficability which depends on the soil's physical properties. The difficulty of translating these independent variables into a form which would permit evaluation of a change of soil properties on (ST) is obvious. This results from the fact that the structural constants (k, n, K_1, and K_2) are empirical and have no apparent physical significance.

*By Roger M. Jorden.

An alternative approach to evaluating the trafficability of a given soil has been developed by the Corps of Engineers. With this method, the trafficability can be estimated on the basis of a single soil strength index, "soil cone index". This index is obtained by field measurement of the force required to move a "cone penetrometer" through the soil at a given depth. This method has been criticized [1] but has proven to be quite functional for many military purposes. As with the former soil-trafficability relationship, this approach does not provide a basis for delineating the effect of various soil properties on trafficability. To circumvent this difficulty, studies have been conducted on specific soils to demonstrate the relationship between cone index and such properties as soil moisture content and density [2]. Bearing in mind that the objective is to consider ways of improving a soil's trafficability rather than vehicle design, it appears that theoretically, there are two basic approaches; one is to alter or control the soil's environment, and the second is to directly treat the soil (e.g., mechanically or with additives). The environmental approach will be considered first.

Theoretically, if the rates and factors of soil formation were known and were predictable, and soil's physical and chemical properties could be related to trafficability, it would be possible to modify a soil to one's own advantage. Even though we have limited knowledge of the latter relationship, it would seem justifiable to consider our present knowledge of soil formation or genesis in an attempt to assess the feasibility of this approach.

Our present knowledge of soil genesis is at a more-or-less descriptive stage and is sufficient only to the extent that it may enable one to understand in a general way why broad soil types have formed. Generally speaking, soil genesis consists of two simultaneous processes. They are the accumulation of the parent materials and differentiation of the soil horizons in the profile. The latter has been broken down into changes caused by addition, removal, transfer and transformation on or within the soil profile. It may be that any of these processes or any combination of them may be going on simultaneously to either differentiate or homogenize the soil. It is the balance of these individual processes that dictates the particular physical

and chemical state that a soil profile possesses at a given time.

Jenny [3] in attempting to evaluate the formation of soils listed five factors which he felt were effective: climate, organisms, topography, parent material and time. The climate characteristics considered were precipitation (intensity, total, time, and distribution), and temperature (average and variations), with due consideration given to micro- and paleo-climatology. The three types of organisms that have been considered are microorganisms, flora and fauna. The types of parent material considered are: unconsolidated, consolidated, organic material, and mature soils. For some of these factors, general relationships have been developed for certain physical or chemical properties. To mention a few: yearly precipitation vs. % clay content in the upper six inches of soil, general climate vs. type of exchange cations, yearly precipitation vs. depth to zone of lime accumulation, general climate and soil type vs. number of microorganisms per mass of soil (broken down into bacteria, actinomycetes, and fungi), and van't Hoff's rule has generally been found to be applicable to soil chemical reactions (for every $10^{o}C$ rise in temperature, the rate of a chemical reaction increases by a factor of two or three).

In addition, descriptions of soil forming processes have been developed for some of the general soil categories (e.g., Podzols and Laterites). These descriptions normally specify the general climatic conditions and, sometimes, vegetation, whereas for some soil types the climate and vegetation are not specified but the type of parent material and topography are. For most of these categories, theories have been developed that adequately account for the chemical environment, and how this relates to the translocation of such things as iron, aluminum, silica, and clay within the soil horizon.

There are some specific examples that may indicate the magnitude of the minimum time necessary for soil development. In 1699, the Kamenetz Fortress in the Ukraine (20 in. precipitation annually) was abandoned. In 1930, 231 years later, it was found that 12 inches of soil had developed on the limestone buildings. The soil was remarkable similar to the surrounding soil which had also developed on limestone. The 1883 explosion of Krakatoa deposited some 100 feet of volcanic ash on

the island of Lang Eiland. Twenty years later, a fertile soil had developed

From this general description of our present knowledge of the process of soil development as it relates to the geophysical environment, several things become apparent. First of all, these concepts would not allow one to predict local soil conditions even to the extent of our present knowledge (e.g., Table A-VIII, [4]), and especially in terms of soil physical characteristics which may be related to comparative trafficability. In addition, these concepts would prove of little use in predicting the effect of geophysical modification (e.g., climate) on soil trafficability, other than such advantages as the reduction or control of precipitation to maintain natural soil stability, and the modification of temperature to control permafrost conditions. To date, the only approach to improving a soil's trafficability, other than by compaction, has been with (a) the addition of compounds to solidify or stabilize soils, and (b) the application of dustproofing or waterproofing compounds to modify soil moisture. Soil stabilization is not considered here.

The philosophy underlying efforts to improve trafficability by waterproofing a soil surface results from the fact that even moderate changes of soil moisture content significantly alter the trafficability of a given soil. It is reasoned that most naturally-occurring fine-grained soils, when compacted sufficiently at an appropriate water content, will provide a medium that will meet most military off-road requirements. Infiltration of water from even moderate amounts of precipitation may render such a soil untrafficable. A very useful material then would be one that could be readily applied in moderate amounts to the soil surface and be capable of preventing the ingress of moisture in order to retain the natural stability of a soil, and thus make that soil trafficable during wet weather. Since 1954, the U.S. Army Engineer Waterways Experiment Station has been conducting research on soil waterproofing materials [6, 7]. Recently, soil stability requirements have been established that would prove useful in evaluating such materials [5]. Some selected materials have been tested in the field and in the laboratory on a variety of soil types under a variety of conditions.

The latest testing program [7] was a two-phase laboratory study in which the primary objectives were: (a) to determine the waterproofing ability of an aniline-furfural resin, a MCO cutback asphalt, a siliconate salt, a quanternary ammonium chloride, and a commercial road oil on five soils of different origins ranging from a silt to a plastic clay, and (b) to conduct preliminary evaluations of the soil waterproofing ability of new and untested materials. The most significant conclusion was that the aniline-furfural resin was the superior additive, and was found to be a highly effective and versatile waterproofer of soils. In addition, some of the new materials showed sufficient promise to justify further field and laboratory testing.

T.2.0 References

1. Bekker, M.G., Theory of Land Locomotion, Ann Arbor: Univ. of Michigan Press, 1962.

2. U.S. Army, "Laboratory Test to Determine Effects of Moisture Content and Density Variations," Trafficability of Soils, First Supplement, Tech. Memo 3-240, Corps of Engineers, Waterways Experiment Station, 1948.

3. Jenny, H., Factors of Soil Formation, New York: McGraw-Hill, Inc., 1941.

4. Marine Corps Logistics Systems Study, Vol. II, Final Report, AD 329-415, SR1/NWRC.

5. U.S. Army, Soil Stabilization Requirements for Military Roads and Airfields in the Theater of Operations, Misc. Paper 3-605, Corps of Engineers, Waterways Experiment Station, 1963.

6. U.S. Army, Review of Materials and Methods for Dustproofing and Waterproofing Soils, Misc. Paper 3-176, Corps of Engineers, Waterways Experiment Station, 1956.

7. U.S. Army, Dustproofing and Waterproofing of Soils, Report No. 1: Field and Laboratory Investigations of Selected Materials, 1959. Report No. 2: Laboratory Studies of Soil Waterproofing Materials, 1963. Tech. Report 3-530, Corps of Engineers Waterways Experiment Station.

APPENDIX U. HYDROLOGY*

U.1.0 EVAPORATION MODIFICATION

Essentially all of the work to date on retardation of evaporation by monolayers has been conducted over fresh or non-saline waters. Since the evaporation retardation efficiency of a given compound is effected by the chemistry of the water, contaminants which may be incorporated in the monolayer, bacterial action, and more important wind and wave action, it would seem that results of studies on relatively small bodies of fresh water should be extrapolated to oceanic evaporation retardation with caution. The implied intent is to utilize monolayers to retard evaporation from large areas of the oceans to accomplish weather modification. Nevertheless, the more recent results from fresh water studies shall be reviewed along with work relating to saline waters since they may shed light on the general nature of the phenomenon as well as indicate some of the problem areas that need further research.

The only piece of literature found that pertained to saline water described some laboratory studies [1], using a synthetic sea water in which the effect of wind was not investigated. One of the more pertinent conclusions reached was "... that the dissolved particles from the salts in solution interfere with the effectiveness of the monomolecular film in retarding water evaporation." It was suggested that the "... ions physically interfere with true orientation (i.e., canting of the vertical aligned molecules) of the monolayer molecules and thus leaves openings through which water molecules may escape." In fact, it was found in applying an octadecanal (C_{18}) and hexadecanal (C_{16}) mixture to a solution in which NaCl concentration was varied from 0 to 20% (by weight) that the maximum evaporation rate occurred at a NaCl concentration of 3.5% (the equivalent total dissolved solid concentration of sea water). With no film, the evaporation rate continuously decreased as the salt concentration increased from 0 to 20%.

*By Roger M. Jo~den.

Also some of the studies on fresh water indicate that serious problems may be encountered in reducing evaporation from sea water. The most apparent serious problem is the detrimental effect of wind. For example, it has been concluded from the Bureau of Reclamation studies [2,3] that it is impractical if not impossible to maintain any appreciable monomolecular film coverage when winds reach 15 to 20 mph. Also their large scale field tests indicate that for a given situation (i.e., climate and water temperature) specific methods of application of compounds of unique specifications may be required for optimum results. Moreover, for large fresh water lakes, the films must be replenished daily. Thus large quantities of material may be required to continuously modify evaporation in a given region, since the apparent rates of application are of the order of 0.2 to 0.4 lb/ac/day.

Obviously, for a monolayer to retard evaporation, it should provide complete and continuous coverage of a surface. Wave action tends to rupture a monolayer surface. Therefore, the property of "self healing" after rupture by wave action is an important characteristic. Barnes and LaMer [4] have found that liquid monolayers of C_{16} (stearyl) alcohols spread spontaneously or are good "self healers" whereas the C_{18} (cetyl) alcohols are superior retardants but do not spread spontaneously. Thus these laboratory studies indicate that a mixture of these two compounds should prove to be the superior retardant for field use.

It seems apparent that the studies cited indicate that some serious problems may be encountered in evaporation retardation from the oceans by the application of monolayers. The major problem is that winds tend to break up and laterally transport a monolayer and make it ineffective when speeds reach 15-20 mph. Also, there appears to be a "chemical effect" that reduces the evaporation reduction efficiency of a monolayer. The minimum reduction of evaporation due to the "chemical effect" appears to be near the total dissolved concentration of sea water.

If serious consideration is being given to the use of monolayers on the ocean surface to attempt weather modification, then a need for additional research is clearly indicated. This should conceivably take the form of research that has

been directed toward use of monolayers on fresh water. Laboratory studies should be conducted to select the more promising compounds or mixtures and methods of application, as well as examining some specific deleterious effects (e.g., chemical, bacteriological, photochemical, or temperature). Results from this work should then be utilized to design field experiments, if conditions so warrant. It should be pointed out that difficulties may be encountered in actually determining evaporation reduction in the field.

Basically there are two ways of determining evaporation reduction: water budget and energy budget methods. It has been found [5] that significantly different results are obtained when different methods of analysis are applied in fresh water lake studies (where they have somewhat of a confined system for determining the water budget).

U.2.0 WATER TABLE MODIFICATION

Because of the fact that depth to a water table has an influence on a local economy (e.g., flooding or, conversely a lack of water due to great depth), geophysical warfare connotations are implied. The three controls to accomplish modification of water table depth are evaporation, precipitation, and runoff.

Construction or subversive control of existing dams and channels are the principal means of establishing runoff control for geophysical warfare (GW) purposes. These might be accomplished by espionage agents giving deliberately erroneous hydrologic advice to a "naive" nation, or control of waters originating outside a nation being attacked. Runoff control is not considered further because of the unreasonable nature of any of the mentioned approaches (with the possible exception of the last, which poses no threat to the U.S.). Insidious evaporation and precipitation modification techniques are within the state of the art, and are considered elsewhere in this report.

U.3.0 SOIL PERMEABILITY MODIFICATION

Several U.S. government agencies have been interested in methods of altering the permeability of the ground surface for various reasons. In general, the efforts have been to increase permeability in some cases and decrease it in others.

Clay bearing soils with a high sodium content can be made more permeable by the addition of flocculating agents. The application of gypsum at a rate of 100 pounds per 1000 square feet has been found effective in increasing the permeability of some such soils. This method is inexpensive but does not compare in efficiency with the more expensive commercial soil conditioners which function as chelating agents. There has been some success but relatively little work on the use of electric fields to increase permeability.

The main efforts for reducing permeability have been directed to the problem of reducing seepage from reservoirs. Addition of bentonite-type clays has been found to be effective as a lining agent in addition to such materials as Portland cements, asphaltic cements, vinyl plastics, and various emulsified asphaltic compounds.

The implied problems relating to the logistics necessary for utilizing such techniques essentially rule out permeability modification from further consideration. Furthermore, the impact on a national economy by modifying permeability is thought to be relatively small. The most reasonable approach that appears is that of giving deliberately erroneous advice to a "naive" nation. It is conceivable that this might be effective against a small nation having little technical know-how, but not against the U.S.

U.4.0 HYDROLOGIC FACTORS

In Man's efforts to modify his environment to his own advantage, it has been found, in certain cases, that geophysical processes are initiated which may be detrimental. Some such cause and effect relationships are worth examining in light of their GW implications.

The development of oil deposits and/or the withdrawal of ground water at a rate that exceeds natural replenishment has in cases resulted in earth subsidence. One school of thought is that subsidence occurs where a decrease of hydrostatic head has resulted in the dewatering of clays or clay bearing strata. The area of subsidence generally corresponds to the area of pressure decline and the two are often separated by a considerable time lag. The magnitude of subsidence ranges to as high as 20 feet (Long Beach, California). The effects generally are characterized by the cracking of structures [6,7] or may result in land submergence at high tide [8]. The recent failure of Los Angeles' Baldwin Hills Dam (estimated $50 million damage) has been attributed by some to earth subsidence due to ground water and oil withdrawals [9].

Most of the documented cases of water-level-induced subsidence are related to pumping withdrawals. Presumably subsidence could be fostered by decreasing natural ground water recharge (e.g., decreasing infiltration or precipitation), assuming this would cause a sufficient lowering of hydrostatic head. Precipitation modification might produce such a side effect in addition to altering total water supply.

The obvious difficulty of execution, control, and prediction of subsidence compared with the GW effectiveness apparently excludes this phenomenon from serious consideration as a GW alternative. However, this effect should be recognized when evaluating the many effects of weather modification.

Another geophysical consideration of weather modification relates to variations of loading the earth's surface. Assuming that significant changes in continental moisture distribution could be accomplished through weather modification, several geophysical responses might occur. For example, Munk and MacDonald [10, p. 238] have suggested that changes in ground water storage due to man's activities produce an observable motion of the earth's poles. Also, it is possible that storage

changes, (ground water and surface water) may contribute to crustal deformation. It seems that these factors should be mentioned even though they do not represent promising GW alternatives.

Diversion of the flow of a large river system may have a serious effect on port utility, and especially inland navigation. A means of accomplishing this is through induced "stream piracy". The lower Mississippi River is a classic example of this phenomenon. Anancient stream meander of the Mississippi River, called Old River, constitutes a six-mile-long connection between the Mississippi and Atchafalaya Rivers and is located 320 and 120 river miles from the respective mouths. Dredging operations for navigation and flood reduction purposes were responsible for inhancing the diversion of the Mississippi River flow to the Atchafalaya. In 1944, the diversion amounted to 17% of the Mississippi River flow and 25% in 1954. It was estimated that when the diversion reached 40%, siltation would make New Orleans and Baton Rouge unnavigable. In addition, bridge approaches and towns along the lower Atchafalaya would experience flooding as the river channel widened and deepened to compensate the additional flow. This would constitute a serious threat to shipping, commerce, and property. To correct this situation, at $75 million dike, lock, and channeling program was recommended [11,12].

Detailed evaluation of topographic maps could establish the vulnerability of the world's major river systems to such a GW method. Presumably, it might be possible to activate such a process by blasting a small section of the land barrier between streams whose channels are at different elevations.

U.5.0 References

1. Cheeves, F. A., R. G. Dressler, and W. G. McGavock, "Evaporation Suppression of Monolayers on Saline Solutions" (in press). Address: Dr. R. G. Dressler, Chem. Dept., Trinity Univ., San Antonio.

2. Timblin, L. O., Jr., Q. L. Florey, and W. U. Garstka, "Laboratory and Field Reservoir Evaporation Reduction Investigations Being Performed by the Bureau of Reclamation. Reduction of Evaporation by Monolayers: Transport Process, La Mer, V. K. (ed), New York: Academic Press, 1962.

3. Water Loss Investigations - Lake Cachuma; Evaporation Reduction Investigations, Chem. Eng. Lab. Dept. No. SJ-33, Denver Div. of Eng. Labs., U. S. Bur. of Reclamation, Washington, D.C., 1962.

4. Barnes, G. T. and V. K. La Mer, "The Evaporation Resistance of Monolayers of Long-Chain Acids and Alcohols and Their Mixtures." Reduction of Evaporation by Monolayers: Transport Process, La Mer, V. K. (ed), New York: Academic Press, 1962.

5. "Survey of Methods for Evaporation Control," J. Am. Water Works Assoc. 55:2, 157-163, Feb., 1963.

6. Loehnberg, A., "Aspects of the Sinking of Mexico City and Proposed Countermeasures," J. Am. Water Works Assoc. 50:3, 432, March, 1958.

7. Mamrelli, E. S., "Distribution Problems in Areas of Unstable Ground," J. Am. Water Works Assoc. 51:3, 379, March, 1959.

8. Gilluly, J. and U. S. Grant, "Subsidence in the Long Beach Harbor Area," Bull. Geo. Soc. Am. 60:3, 461, 1949.

9. "Multiple Probes Station Dam Failure," Engr. News-Record, p. 15, Jan. 2, 1964.

10. Munk, W. H. and G. F. MacDonald, The Rotation of the Earth, London: Cambridge Press, 1960.

11. Fisk, H. N., "Mississippi River Valley Geology - Relation to River Regime." Am. Soc. Civil Engrs. Prov. 78, Separate D-80, May, 1952.

12. Baum, A. W., "Will New Orleans Lose the Mississippi?" Sat. Eve. Post 277:22, July 31, 1954.

APPENDIX V. EARTHQUAKE PHENOMENA*

V.1.0 DISCUSSION

An earthquake is characterized by a train of vibrations of material at or beneath the earth's surface and is generally thought to result from the sudden release of gradually accumulated tectonic strain in a region of the earth's crust. The magnitude of energy release is generally from 10^{12} to 10^{28} ergs.

A conceivable means for utilizing this phenomenon as a warfare alternative may be to trigger the release of accumulated strain with underground nuclear detonations. From data based on some of the AEC Nevada tests, it has been tentatively concluded [1] that release of tectonic strain did occur along with the Ranier explosion (1.7-kt TNT equiv.) but that the magnitude of this release was too small to affect the character of seismograms. However, experiments have been suggested [1] which should conclusively prove or disprove this hypothesis.

Inherent in such a scheme would be the detection of areas in which tectonic strain is accumulating. To date, two possible detective methods have been suggested. One requires on-site instrumentation and is based on the fact that gradual crustal movement occurs as strain is accumulating. The other, suggested by Dr. Keilis-Borok (Institute of the Physics of the Earth, Moscow) at the IGY review meeting at UCLA, August 1963, is based on the fact that shear waves are apparently impeded by material under great strain. As a prediction technique, this is reported to be only in the developmental stage.

It appears that the preparation and hardware needed to harness earthquakes would limit their use to defensive warfare. Their use for offensive warfare seems impractical because the apparent energy needed to trigger the release of tectonic strain (the equivalent of tens of kilotons of TNT) is so great that direct use of the energy may prove more advantageous.

V.2.0 REFERENCE

1. Press, F., and C. Archambeau, "Release of Tectonic Strain by Underground Nuclear Explosions," J. Geophys. Res. 67:1, 337, 1962.

*By Roger M. Jorden

UNCLASSIFIED
Security Classification

DOCUMENT CONTROL DATA - R&D

(Security classification of title, body of abstract and indexing annotation must be entered when the overall report is classified)

1. ORIGINATING ACTIVITY *(Corporate author)*
The Travelers Research Center, Inc.
250 Constitution Plaza
Hartford, Connecticut 06103

2a. REPORT SECURITY CLASSIFICATION
[redacted] UNCLASSIFIED

2b. GROUP
[redacted]

3. REPORT TITLE
Geophysics In Warfare, Report II
ANALYSES OF GEOPHYSICAL PHENOMENA

4. DESCRIPTIVE NOTES *(Type of report and inclusive dates)*
Final Report, May 1963—May 1964

5. AUTHOR(S) *(Last name, first name, initial)*
Brooks, Douglas L.
Hilst, Glenn R.
Milly, George H.

6. REPORT DATE	7a. TOTAL NO. OF PAGES	7b. NO. OF REFS
May 1964	405	165

8a. CONTRACT OR GRANT NO.
Nonr 4112(00)

b. PROJECT NO.

c.

d.

9a. ORIGINATOR'S REPORT NUMBER(S)
TRC-7662-119C

9b. OTHER REPORT NO(S) *(Any other numbers that may be assigned this report)*

10. AVAILABILITY/LIMITATION NOTICES
U.S. military agencies may obtain copies of this report directly from DDC. Other qualified users shall request through the Office of Naval Research, Code 493.

11. SUPPLEMENTARY NOTES

12. SPONSORING MILITARY ACTIVITY
Office of Naval Research, Department of the Navy, Code 493, Washington 25, D. C.

13. ABSTRACT

This report presents the results of a scientific analysis conducted as part of a one-year survey of geophysics in naval warfare conducted for the Office of Naval Research by The Travelers Research Center, Inc. In the main study, reported separately and entitled Geophysics in Warfare, Report I—Geophysical Factors in Naval Warfare (U), the scientific feasibility and military significance to the Navy and Marine Corps of exploiting a large range of possibilities for either geophysical prediction or control are systematically explored and recommendations for the most fruitful follow-on programs are provided. In this report, (Report II), details of the scientific analysis of feasibility of control of a number of geophysical phenomena are presented. In addition, there are presented the theoretical aspects of evaluating the utility of prediction and control in operations affected.

DD FORM 1 JAN 64 1473

UNCLASSIFIED
Security Classification

UNCLASSIFIED
Security Classification

14. KEY WORDS	LINK A		LINK B		LINK C	
	ROLE	WT	ROLE	WT	ROLE	WT
Survey of scientific feasibility						
Selected geophysical phenomena						
Prediction						
Control						

INSTRUCTIONS

1. ORIGINATING ACTIVITY: Enter the name and address of the contractor, subcontractor, grantee, Department of Defense activity or other organization *(corporate author)* issuing the report.

2a. REPORT SECURITY CLASSIFICATION: Enter the overall security classification of the report. Indicate whether "Restricted Data" is included. Marking is to be in accordance with appropriate security regulations.

2b. GROUP: Automatic downgrading is specified in DoD Directive 5200.10 and Armed Forces Industrial Manual. Enter the group number. Also, when applicable, show that optional markings have been used for Group 3 and Group 4 as authorized.

3. REPORT TITLE: Enter the complete report title in all capital letters. Titles in all cases should be unclassified. If a meaningful title cannot be selected without classification, show title classification in all capitals in parenthesis immediately following the title.

4. DESCRIPTIVE NOTES: If appropriate, enter the type of report, e.g., interim, progress, summary, annual, or final. Give the inclusive dates when a specific reporting period is covered.

5. AUTHOR(S): Enter the name(s) of author(s) as shown on or in the report. Enter last name, first name, middle initial. If military, show rank and branch of service. The name of the principal author is an absolute minimum requirement.

6. REPORT DATE: Enter the date of the report as day, month, year; or month, year. If more than one date appears on the report, use date of publication.

7a. TOTAL NUMBER OF PAGES: The total page count should follow normal pagination procedures, i.e., enter the number of pages containing information.

7b. NUMBER OF REFERENCES: Enter the total number of references cited in the report.

8a. CONTRACT OR GRANT NUMBER: If appropriate, enter the applicable number of the contract or grant under which the report was written.

8b, 8c, & 8d. PROJECT NUMBER: Enter the appropriate military department identification, such as project number, subproject number, system numbers, task number, etc.

9a. ORIGINATOR'S REPORT NUMBER(S): Enter the official report number by which the document will be identified and controlled by the originating activity. This number must be unique to this report.

9b. OTHER REPORT NUMBER(S): If the report has been assigned any other report numbers *(either by the originator or by the sponsor)*, also enter this number(s).

10. AVAILABILITY/LIMITATION NOTICES: Enter any limitations on further dissemination of the report, other than those imposed by security classification, using standard statements such as:

(1) "Qualified requesters may obtain copies of this report from DDC."

(2) "Foreign announcement and dissemination of this report by DDC is not authorized."

(3) "U. S. Government agencies may obtain copies of this report directly from DDC. Other qualified DDC users shall request through ___________."

(4) "U. S. military agencies may obtain copies of this report directly from DDC. Other qualified users shall request through ___________."

(5) "All distribution of this report is controlled. Qualified DDC users shall request through ___________."

If the report has been furnished to the Office of Technical Services, Department of Commerce, for sale to the public, indicate this fact and enter the price, if known.

11. SUPPLEMENTARY NOTES: Use for additional explanatory notes.

12. SPONSORING MILITARY ACTIVITY: Enter the name of the departmental project office or laboratory sponsoring *(paying for)* the research and development. Include address.

13. ABSTRACT: Enter an abstract giving a brief and factual summary of the document indicative of the report, even though it may also appear elsewhere in the body of the technical report. If additional space is required, a continuation sheet shall be attached.

It is highly desirable that the abstract of classified reports be unclassified. Each paragraph of the abstract shall end with an indication of the military security classification of the information in the paragraph, represented as *(TS), (S), (C), or (U)*.

There is no limitation on the length of the abstract. However, the suggested length is from 150 to 225 words.

14. KEY WORDS: Key words are technically meaningful terms or short phrases that characterize a report and may be used as index entries for cataloging the report. Key words must be selected so that no security classification is required. Identifiers, such as equipment model designation, trade name, military project code name, geographic location, may be used as key words but will be followed by an indication of technical context. The assignment of links, roles, and weights is optional.

UNCLASSIFIED
Security Classification